

https://dspace.org/

The induction of KLF4 expression by coupled epigenetic therapies: potential association with the WNT signalling pathway in colorectal cancer cells

Moodley, Natanya

2014-02-06
http://hdl.handle.net10539/13682

Downloaded from a DSpace repository. https://dspace.org/

THE INDUCTION OF KLF4 EXPRESSION BY COUPLED EPIGENETIC THERAPIES; POTENTIAL ASSOCIATION WITH THE WNT SIGNALLING PATHWAY IN COLORECTAL CANCER CELLS

NATANYA MOODLEY

A dissertation submitted to the Faculty of Heath Sciences, University of the Witwatersrand, in fulfilment of the requirements for the degree of Master of Science

Supervisor:

Dr. Clem Penny
Department of Internal Medicine, University of the Witwatersrand, South Africa

Johannesburg, 2013

DECLARATION

I, Natanya Moodley, declare that this dissertation is my own unaided work. It has being submitted for the degree of Master of Science in the Faculty of Health Sciences in the University of the Witwatersrand, Johannesburg. It has not been submitted before for any degree or examination at this or any other University.

_____

Natanya Moodley

This _____ day of _____20_____

RESEARCH OUTPUTS

Conference posters:

The effects of epigenetic modulation on the expression of pluripotent stem cell markers in colon cancer cells.

N. Moodley, V. E. Gibbon, C. B. Penny, P. Ruff

Presented at:

- *Wits Faculty of Health Sciences Research Day* (2010) University of the Witwatersrand, Johannesburg.
- *Molecular Biosciences Research Thrust* (2010) Wits – Professional Development Hub, Johannesburg.
- *SASCRO SASMO Congress* (2011) Sun City.

ABSTRACT

Epithelial cancers such as colorectal cancers are highly predominant in the Southern African population, and are attributable to a number of factors, including genomic instability due to histone modifications and aberrant DNA methylation of gene promoters, as well as the inactivation of tumour-suppressor genes or the activation of oncogene pathways. The Wnt/β-catenin pathway plays a vital role in the regulation of intestinal epithelial cells, and is aberrantly activated in colon neoplasms. Krüppel-like factor 4 (KLF4) is a tumour suppressor gene that is hypermethylated at its promoter region and therefore down-regulated in colon cancer cells. This zinc finger transcription factor is crucial in colon cancer cells, where its induction has been proposed to regulate tumourigenesis. Over recent years, epigenetic modulators such as histone deacetylase (HDAC) inhibitors and DNA methyltransferase (DNMT) inhibitors have been investigated with regards to their potential anticancer activities. The following study assessed the in vitro effects of the HDAC inhibitor Valproic acid and DNMT inhibitor Zebularine on the expression of KLF4 in early (SW480) and late stage (DLD-1) colon cancer, and breast (MCF-7) cancer cells. At the onset, bioinformatics tools were utilised to predict and assess the methylation status and to examine methylation patterns within the KLF4 and CTNNB1 (β-catenin) genes. In association with this, methylated DNA within early and late stage colon cancer cells was quantified. Here, the 5' untranslated region of KLF4 was highly methylated, while CTNNB1 displayed a low frequency of methylation. Following drug treatments, with Valproic acid and Zebularine respectively, gene expression profiles showed that high dosages increased the expression of KLF4 relative to low doses in early stage cancer cells; however the greatest induction of KLF4 was observed in late stage cancer cells in response to a high dose combination treatment with Valproic acid and Zebularine. CTNNB1 was antagonistically regulated relative to KLF4, wherein its expression was down-regulated post-treatment. Breast cancer cells surprisingly exhibited opposing results, with both KLF4 and CTNNB1 being up-regulated following high dose treatments, and the low dose treatments displaying the greatest anti-tumourigenic activities. Confocal microscopy results illustrated that KLF4 was localised in the nucleus and nuclear periphery, where it could associate directly with β-catenin. Thus in response to epigenetic therapy, KLF4 was differentially expressed in early and late stage colon cancer cells as a tumour suppressor. The down-regulation of β-catenin in colon cancer cells resulted in the suppression of the Wnt signalling pathway, thereby exerting anti-tumourigenic and anti-proliferative properties on the cells. Therefore, this study concludes that Valproic acid and Zebularine may serve as potential anti-cancer agents in the pursuit of an epigeneic therapy for colorectal cancer.

DEDICATION

This thesis is dedicated with love and respect to my parents,
Vasan and Lutchmee Moodley,
for their endless support and encouragement.

ACKNOWLEDGEMENTS

I would first like to express my heart-felt gratitude to my parents to whom this thesis is dedicated to, Vasan and Lutchmee Moodley, and my sister, Irushka Moodley, and her husband Andre Dowley, for their unconditional love and support throughout this journey. Their constant strength and sacrifice have aided and encouraged me through this endeavour.

To my Supervisor, Dr. Clem Penny, for his endless support, advice, and pain-staking efforts in the execution of this work and the writing of this thesis, I am deeply grateful. His patience and guidance has helped me overcome many challenging situations and aided in the completion of this work. I would also like to thank Prof. Paul Ruff for his insightful thoughts and comments, as well as meeting with us regularly to encourage us.

To my colleagues, Drishna Govan, Brenda Milner, Alexander Hsiao, Andrea Papadopoulos, I would like to express sincere gratitude for your help and advice throughout my Masters. Also tremendous appreciation goes to all the lab technicians for all their assistance.

To my family, my aunts and uncles, Gonum Pillay, Seelan Moodley, Shiela Moodley, Vanie Pillay, Pragashnee Govender, Malcolm Govender, Anand Moodley, Joyce Moodley, and cousins, Natasha Pillay, Kamani Pillay, Ireshen Pillay, Shiran Moodley, Shimona Moodley, Kammy Govender, Keegan Govender, Reece Govender, Sharesce Ramiah, Teshlin Akaloo, Thirres Arumugam, Sivi Arumugam, Tiyara Arumugam, Shaylin Arumugam, Karuna Pillay, Kesree Pillay, thank you for your continuous support during this endeavour.

To my inspiration Shivaan Cooppan, your love and positive attitude has motivated me to set my standards high and reach for the stars. I am forever thankful.

To my friends, my alternative family, Kavitha Nundkwar, Kovanya Moodley, Yashodan Naidoo, Narushka Pillay, Sambarthan Cooppan, Derusha Frank, Andre Govender, Chantal Koomcaran, Priyen Naidu, Kiren Pillay, Taygan Pillay, Vino Pillay, Ameena Wadee, Janine Carim, Firdaus Nabeemeeah, Ashmeetha Manillal, thank you for being a part of my life during this venture.

Final gratitude goes to the National Research Foundation and the Faculty Research Committee for financial support, and the University of the Witwatersrand.

TABLE OF CONTENTS

CHAPTER 1: AN OVERVIEW OF GENE REGULATION IN COLON CANCER 1

1.1 Colorectal Cancer 1
1.2. Colon Cancer Stem Cells (CSCs) 2
1.3 Biology of Colonic Epithelium 3
1.4 Importance of Eliminating CSCs in Therapy/Therapeutic Implications of CRC-SC 4
1.5 Gene Regulation in Colon Cancer 6
1.5.1 Oncogenes and tumour suppressors 6
1.5.2 Krüppel-like factors 6
1.5.3 Krüppel-like factor 4 9
1.5.4 Cancer signalling pathways 11
1.5.5 β-catenin 12
1.5.6 Cross talk 15
1.6 Stem Cells and Epigenetics 16
1.6.1 An “epic-genetic” overview 16
1.6.2 The evolution of epigenetics 16
1.6.3 Histone modifications 16
1.6.3.4 Histone deacetylase inhibitors: Valproic acid 17
1.6.4 DNA methylation 17
1.6.4.1 DNA methyltransferase inhibitors: Zebularine 17
1.7 Study Aims 18

CHAPTER 2: MATERIALS USED AND METHODS IMPLEMENTED IN THIS STUDY 19

2.1 Cell Culture 19
2.1.1 Thawing 19
2.1.2 Passaging/subculturing 20
2.1.3 Cyropreservation 20
2.1.4 Harvesting cells 20
2.1.5 Cell viability assay 20
2.2 Drug Treatments 21
2.2.1 Valproic acid 21
2.2.2 Zebularine 21
2.2.3 Combination treatments 21
2.3 Total RNA Isolation 22
2.3.1 RNeasy plus mini kit 22
2.3.2 Nucleospin® RNA II kit 23
2.3.3 RNA quantification 24
2.4 Total DNA Isolation 24
2.4.1 QIAamp DNA micro kit 24

2.5 Methylated DNA Quantification 25
2.5.1 MethylFlash™ methylated DNA quantification kit (colorimetric) 25
2.5.2 MethylFlash™ hydroxymethylated DNA quantification kit (colorimetric) 27
2.6 Primer Design 28
2.7 Reverse Transcription 29
2.8 PCR Optimisation 30
2.8.1 Conventional PCR 30
2.8.2 Real-time (RT) – PCR 31
2.9 Microscopy 32
2.9.1 Seeding cells onto coverslips 32
2.9.2 Fixing cells to the coverslips 32
2.9.3 Immunofluorescence 32
2.9.3.2 Incubation of cells with secondary antibody 33
2.9.3.3 Fluorescent staining of the actin cytoskeleton and nucleus 33

CHAPTER 3: HISTONE MODIFICATIONS 35

3.1 Introduction 35
3.1.1 An overview of histone modifications 35
3.1.1.1 The structure and organisation of chromatin 35
3.1.1.2 Histone acetylation and deacetylation 36
3.1.1.3 Characterisation of histone deacetylases 36
3.1.1.4 Histone deacetylases in cancer 37
3.1.2 Epigenetic therapy by histone deacetylase inhibitors 38
3.1.2.1 Classification of HDAC inhibitors 38
3.1.3 Valproic acid as a histone deacetylase inhibitor 39
3.1.4 Experimental approach 39
3.2 Results 40
3.2.1 Relative Quantification of gene expression 40
3.2.1.1 The effects of Valproic acid treatment on early stage colorectal adenocarcinoma cells (SW480) 40
3.2.1.2 The effects of Valproic acid on late stage colorectal adenocarcinoma cells (DLD-1) 43
3.2.1.3 The effects of Valproic acid on breast adenocarcinoma cells (MCF-7) 46
3.3 Discussion 49
3.3.1 The effect of Valproic acid on cell viability 50
3.3.2 Valproic acid on gene expression in colorectal cancer cells 50
3.3.3 The effects of Valproic acid on gene expression in breast cancer cells 51
3.3.4 Histone deacetylase inhibition by Valproic acid 52

CHAPTER 4: DNA METHYLATION 54

4.1 Introduction 54
4.1.1 An overview on DNA methylation 54
4.1.1.1 DNA methyltranferases (DNMTs) 54
4.1.1.2 CpG island methylation 55
4.1.1.3 DNA methylation and gene silencing 57
4.1.1.4 Gene silencing and cancer 58
4.1.1.5 Hydroxymethylated DNA 58
4.1.2 Epigenetic therapy mediated by DNA methyltransferase inhibitors 59
4.1.3 Zebularine as a demethylating agent 60
4.1.4 Experimental approach 61
4.2 Results 62
4.2.1 Bioinformatics 62
4.2.1.1 CpG Island Searcher 62
4.2.1.2 MethyCancer 64
4.2.1.3 Methylator 66
4.2.2 Global methylated DNA quantification 68
4.2.2.1 Quantification of methylated DNA in the SW480 and DLD-1 cell lines 68
4.2.3 Relative quantification of gene expression 70
4.2.3.1 The effects of Zebularine on early stage colorectal adenocarcinoma cells (SW480) 70
4.2.3.2 The effects of Zebularine on late stage colorectal adenocarcinoma cells (DLD-1) 73
4.2.3.3 The effects of Zebularine on MCF7 breast adenocarcinoma cells 76
4.3 Discussion 79
4.3.1 Analysis and quantification of methylation patterns 80
4.3.2 The effect of Zebularine on cell viability 81
4.3.3 The effects of Zebularine on gene expression in colorectal cancer cells 81
4.3.4 The effect of Zebularine on gene expression in breast cancer cells 84
4.3.5 DNA methyltransferase inhibition by Zebularine 85

CHAPTER 5: COMBINATION THERAPY 87

5.1 Introduction 87
5.1.1 Synergistic activity of HDAC inhibitors and demethylating agents 87
5.1.2 Combination therapy in clinical practice 88
5.1.3 Experimental approach 88
5.2 Results 89
5.2.1 Relative quantification of gene expression 89
5.2.1.1 The effects of low and high dose synergistic treatments on early stage colorectal adenocarcinoma cells (SW480) 89
5.2.1.2 The effects of low and high dose synergistic treatments on late stage colorectal adenocarcinoma cells (DLD-1) 92

5.3 Discussion 95
5.3.1 The effect of combination therapies on cell viability 96
5.3.2 Combination therapy on gene expression in colorectal cancer cells 96
5.3.3 Epigenetic modulation through combination therapies 97

CHAPTER 6: GENERAL DISCUSSION 100

6.1 KLF4/β-catenin cross-talk and its involvement in the Wnt pathway 101
6.2 The effect of KLF4 on the regulation of cell proliferation in colon cancer cells 103
6.3 KLF4 expression in breast cancer cells 104
6.4 Valproic acid and Zebularine in clinical trials 106

CHAPTER 7: CONCLUDING REMARKS AND FUTURE DEVELOPMENTS 107

7.1 Concluding remarks 107
7.2 Future developments 107

REFERENCES 109

APPENDIX 139

A1 Exonic sequence with mapped primers for KLF4 139
A2 Exonic sequence with mapped primers for CTNNB1 141
A3 List of reagents and ingredients 145
A4 Drug information 146
A5 The $2^{-\Delta\Delta Ct}$ method 147
A6 Microscopy control images 148
A7 Methylator results for *KLF4* (Red indicates methylated cytosines) 150
A8 Methylator results for *CTNNB1* (Red indicates methylated cytosines) 152
A9 Standard curve for MethylFlash™ methylated DNA quantification kit (colorimetric) 154
A10 Standard curve for MethylFlash™ hydroxymethylated DNA quantification kit (colorimetric) 155
A11 Ethics Waiver 156

LIST OF FIGURES

CHAPTER 1: INTRODUCTION

Figure 1.1 A schematic model of the hierarchical organisation of cancer stem cells.....2
Figure 1.2 Progression of colon cancer as a result of cancer stem cells.....4
Figure 1.3 Schematic diagram showing different approaches in CRC therapy.....5
Figure 1.4 Schematic view of a zinc finger protein.....9
Figure 1.5 Structural view of the *KLF4* gene and its protein product.....10
Figure 1.6 Representation of the tumour suppressor role of *KLF4* leading to cell cycle arrest and thus reduced proliferation in colon cancer cells.....11
Figure 1.7 The Wnt/ β-catenin pathway.....12
Figure 1.8 Structural view of the *CTNNB1* gene and its β-catenin protein product.....14
Figure 1.9 Various pools of β-catenin following separate fates.....15

CHAPTER 2: MATERIALS USED AND METHODS IMPLEMENTED

Figure 2.1 Schematic illustration of results demonstraing colour development associated with methylation (5-mC) patterns.....27
Figure 2.2 Schematic illustration of results showing colour development associated patterns with hydroxymethylation (5-hmC) patterns.....28

CHAPTER 3: HISTONE MODIFICATIONS

Figure 3.1 Schematic view of a nucleosome.....36
Figure 3.2 Schematic view of Zn^{+2} dependent Class I, II and IV HDACs (Class III HDACs being sirtuins), illustrating their varying lengths and localisation.....37
Figure 3.3 Mechanism of action of HDACs and HATs.....38
Figure 3.4 Chemical structure of VPA (2-propylpentanoic acid), an eight branched short-chain fatty acid.....39
Figure 3.5 SW480 cell susceptibility to HDACi.....41
Figure 3.6 The effect of VPA on KLF4 expression in SW480 cells.....42
Figure 3.7 The effect of VPA on CTNNB1 expression in SW480 cells.....43
Figure 3.8 DLD-1 cell susceptibility to HDACi.....44
Figure 3.9 The effect of VPAon KLF4 expression in DLD-1 cells.....45
Figure 3.10 The effect of VPA on CTNNB1 expression in DLD-1 cells.....46
Figure 3.11 MCF-7 cell susceptibility to HDACi.....47
Figure 3.12 The effect of VPA on KLF4 expression in MCF-7 cells.....48
Figure 3.13 The effect of VPA on CTNNB1 expression in MCF-7 cells.....49

CHAPTER 4: DNA METHYLATION

Figure 4.1 Structural analysis of three DNA methyltransferase (DNMT) families.....55

Figure 4.2 Schematic view of DNMT adding a methyl group to the 5th carbon of cytosine forming 5-methylcytosine....56
Figure 4.3 Schematic illustration of DNA methylation in normal and tumourigenic cells....57
Figure 4.4 Differences in chemical structure of methylated DNA....59
Figure 4.5 Structural differences between cytosine and 5-methylcytosine, and cytidine and its analogues....61
Figure 4.6 The CpG island extraction algorithm....63
Figure 4.7 ChroView on human chromosome 9 focusing on position 9q31.2 illustrating the location of gene *KLF4*....65
Figure 4.8 ChroView on human chromosome 3 focusing on position 3p22.1 illustrating the location of gene *CTNNB1*....66
Figure 4.9 Graph displaying the threshold value and specificity of results are directly proportional to each other....68
Figure 4.10 Graph exhibiting the difference between global 5-mC and 5-hmC in SW480 and DLD-1 cell lines....70
Figure 4.11 SW480 cell susceptibility to HDACi....71
Figure 4.12 The effect of ZEB on KLF4 expression in SW480 cells....72
Figure 4.13 The effect of ZEB on CTNNB1 expression in SW480 cells....73
Figure 4.14 DLD-1 cell susceptibility to HDACi....74
Figure 4.15 The effect of ZEB on KLF4 expression in DLD-1 cells....75
Figure 4.16 The effect of ZEB on CTNNB1 expression in DLD-1 cells....76
Figure 4.17 DLD-1 cell susceptibility to HDACi....77
Figure 4.18 The effect of ZEB on KLF4 expression in MCF-7 cells....78
Figure 4.19 The effect of ZEB on CTNNB1 expression in MCF-7 cells....79

CHAPTER 5: COMBINATION THERAPY

Figure 5.1 Schematic diagram illustrating the effects of HDAC inhibitors on DNA methylation....88
Figure 5.2 SW480 cell susceptibility to HDACi....90
Figure 5.3 The synergistic effect of VPA and ZEB on KLF4 expression in SW480 cells....91
Figure 5.4 The synergistic effect of VPA and ZEB on CTNNB1 expression in SW480 cells....92
Figure 5.5 DLD-1 cell susceptibility to HDACi....93
Figure 5.6 The synergistic effect of VPA and ZEB on KLF4 expression in DLD-1 cells....94
Figure 5.7 The synergistic effect of VPA and ZEB on CTNNB1 expression in DLD-1 cells....95

CHAPTER 6: GENERAL DISCUSSION

Figure 6.1 Linking the biology of colonic epithelium with the expression of KLF4 and CTNNB1.....102
Figure 6.2 Schematic diagram illustrating the association of KLF4 protein with β-catenin....102
Figure 6.3 Schematic diagram demonstrating the nuclear association of KLF4 and β-catenin with TCF4.....103
Figure 6.4 KLF4 in cell cycle regulation and tumour suppression.....104
Figure 6.5 KLF4 is involved in the regulation of p53 through its association with MUC1.....105

CHAPTER 7: CONCLUDING REMARKS AND FUTURE DEVELOPMENTS

Figure 7.1 The anti-tumourigenic effects of epigenetic treatments with Valproic acid and Zebularine.....107

APPENDIX

Figure A6.1 Microscopy images of untreated SW480 cells representing protein localisation for [A] KLF4 (63x) and [B] β-catenin (63x).....148
Figure A6.2 Microscopy images of untreated DLD-1 cells representing protein localisation for [A] KLF4 (60x) and [B] β-catenin (60x).....148
Figure A6.3 Microscopy images of untreated MCF-7 cells representing protein localisation for [A] KLF4 (63x) and [B] β-catenin (63x).....149
Figure A6.4 Fluorescent images depicting negative control DLD-1 cells in which secondary antibody was omitted.....149
Figure A9.1 Standard curve of OD 450nm values versus the amount of ME4 buffer at each concentration point.....153
Figure A10.1 Standard curve of OD 450nm values versus the amount of HC5 buffer at each concentration point.....154

LIST OF TABLES

CHAPTER 1: INTRODUCTION

Table 1.1 List of FDA-approved drugs and combination regimens.....5
Table 1.2 Expression patterns of Krüppel-like factors.....8
Table 1.3 List of target genes of β-catenin signalling in the Wnt pathway.....13

CHAPTER 2: MATERIALS USED AND METHODS IMPLEMENTED

Table 2.1 Standard curve preparation using five different concentrations of ME4 buffer after diluted to 10ng/µl.....26
Table 2.2 Standard curve preparation using five different concentrations of HC5 buffer after diluted to 10 ng/µL.....27
Table 2.3 Primer sequences, melting temperatures, amplicon sizes and gene accession numbers for the various genes used in this study.....29
Table 2.4 Reverse transcription reagents and volumes.....30
Table 2.5 PCR core kit master mix.....30
Table 2.6 SYBR Green master mix.....31

CHAPTER 4: DNA METHYLATION

Table 4.1 CpG Island Searcher results.....63
Table 4.2 CpGi130 results.....64
Table 4.3 Global DNA methylation status of two colorectal cancer cell lines.....69
Table 4.4 Global DNA hydroxymethylation status of two colorectal cancer cell lines.....69

LIST OF EQUATIONS

CHAPTER 2: MATERIALS USED AND METHODS IMPLEMENTED

Equation 2.1 Concentration of primers.....29

Equation 2.2 Molecular weight of primers.....29

Equation 2.3 Melting temperature of primers.....29

CHAPTER 4: DNA METHYLATION

Equation 4.1 The O/E ratio for CpG islands.....57

Equation 4.2 Assigning an *x* value to each fragment during training by SVM.....67

APPENDIX

Equation A5.1 Normalising the C_t of the target gene to that of the reference gene for the test sample.....147

Equation A5.2 Normalising the C_t of the target gene to that of the reference gene for the calibrator sample.....147

Equation A5.3 Normalising the C_t of the test sample to that of the calibrator sample.....147

Equation A5.4 Normalised expression ratio.....147

Equation A9.1 Absolute amount of methylated DNA.....153

Equation A9.2 Absolute percentage of methylated DNA.....153

Equation A10.1 Absolute amount of hydroxymethylated DNA.....154

Equation A10.2 Absolute percentage of hydroxymethylated DNA.....154

5-aza-CdR	5-aza-2'-deoxycytidine
5-aza-CR	5-azacytidine
5-FU	5-fluorouricil
5-hmC	5-hydroxymethylcytosine
5-mC	5-methylcytosine
A	adenine
AOE	2-amino-8-oxo-9,10-epoxy-decanoyl
APC	adenomatous polyposis coli
ARM	armadillo
Bak	Bcl-2 homologous antagonist killer
Bax	Bcl-2–associated X
Bcl-2	B-cell lymphoma 2
$BclX_L$	B-cell lymphoma-extra large
BKLF	basic Krüppel-like factor
BMP	bone morphogenetic protein
BSA	bovine serum albumin
BTEB	basic transcription element binding-protein
C	cytosine
CDK	cyclin-dependent kinase
CDKN1A	cyclin-dependent kinase inhibitor 1A
cDNA	complementary DNA
CGI	CpG island
CO_2	carbon dioxide
Cox-2	cyclooxygenase-2
CPBP	core promoter binding protein
CpG	cytosine-phosphodiester bond-guanine
CRC	colorectal cancer
CRC-SC	colorectal cancer stem cells
CSC	cancer stem cells
CT	conventional therapy
C_t	cycle threshold
C-terminus	carboxyl-terminus
CTNNB1	catenin beta-1
Cys	cysteine
DAPI	4',6-diamidino-2-phenylindole
DAPK	death-associated protein kinase
DMEM:F-12	Dulbecco's Modified Eagle medium:Nutrient mixture F-12
DMSO	dimethyl sulfoxide

DNA	deoxyribonucleic acid
DNMT	DNA methyltransferase
dNTP	deoxyribonucleotide triphosphate
Drg-1	developmentally-regulated GTP-binding protein 1
DRP-1	DAPK-related protein kinase-1
DRRF	dopamine receptor regulating factor
Dsh	dishevelled
EGRα	early growth response alpha
EKLF	erythroid Krüppel-like factor
ER	endoplasmic reticulum
ER-α	estrogen receptor alpha
ESCs	embryonic stem cells
FBS	foetal bovine serum
Frz	frizzled
FWD	forward
G	guanine
G0	G zero/resting phase
G1	Gap 1 phase
GBF	GC-rich sites binding factor
gDNA	genomic DNA
GKLF	gut-enriched Krüppel-like factor
GSK-3β	glycogen synthase kinase-3-beta
H_2O	water
HATs	histone acetyltransferases
Hda1	homologous to DnaA-1
HDACi	histone deacetylase inhibitor
HDACs	histone deacetylases
HeLa	Hela cells from Henrietta Lacks
HEPA	high-efficiency particulate arresting
HESCs	human embryonic stem cells
HMG	high mobility group
ICM	inner cell mass
IKLF	intestinal Krüppel-like factor
iPS cells	induced pluripotent stem cells
K	lysine
KLF	Krüppel-like factor
LEF	lymphoid enhancer factor
LKLF	lung Krüppel-like factor
M	mean

MAPK/ERK	mitogen-activated protein kinase/extracellular signal-regulated kinases
MDB	membrane desalting buffer
MeCP-1	methyl cytosine binding protein 1
MeCP-2	methyl cytosine binding protein 2
$MgCl_2$	magnesium chloride
miRNA	microRNA
MLH1	mutL homolog 1
mRNA	messenger RNA
MUC1	mucin-1
M.w.	molecular weight
NAD^+	nicotinamide adenine dinucleotide
NIH	National Institute of Health
NLS	nuclear localisation signal
NSAID	non-steroidal anti-inflammatory drug
N-terminus	amino-terminus
O/E	observed/expected ratio
OCT4	octamer-binding transcription factor 4
OD	optical density
ORF	open reading frame
p	probability
p53	tumour protein 53
Pax-5	paired box protein 5
PBS	phosphate buffered solution
PCR	polymerase chain reaction
PE21	21-bp element
PI3-K/Akt	phosphoinositide 3-kinase/protein kinase B
Rb1	retinoblastoma protein
RCAS1	receptor binding cancer antigen expressed on SiSo cells
RLT	RNeasy lysis buffer
RNA	ribonucleic acid
RT	reverse transcription
RT-PCR	real-time PCR
RVS	reverse
SAH	S-adenosylhomocytsteine
SAHA	Vorinostat
SAM	S-adenosylmethionine
SD	standard deviation
Ser	serine
SIRT	surtuins

SOX2/9	SRY (sex determining region Y)-box 2/9
S-phase	synthesis phase
SVM	support vector machine
SYN1	synergistic 1 (Valproic acid 1.5mM + Zebularine 0.1mM)
SYN2	synergistic 2 (Valproic acid 5mM + Zebularine 0.3mM)
T	thymine
Taq	Thermus aquaticus
TCF	T-cell specific factor
Tet	tetracycline
TGF-β	transforming growth factor beta
TGN	trans-Golgi network
Thr	threonine
TIEG	transforming growth factor-β-inducible early gene
T_m	melting temperature
tRNA	transfer RNA
TSA	Trichostatin A
TT	targeted therapy
UKLF	ubiquitous Krüppel-like factor
UTR	untranslated region
UV	ultraviolet
VEGF	vascular endothelial growth factor (VEGF)
VPA	Valproic acid
Wnt	wingless
Y	tyrosine
ZEB	Zebularine
Zn^{2+}	zinc
β-catenin	beta-catenin
β-ME	β-mercaptoethanol

%	percentage
~	approximately
°C	degree celsuis
µg	micrograms
µl	microlitres
µM	micromolars
bp	basepairs
cm^3	centimetre cubed
da	daltons
g	grams
g/mol	gram/mol (molar mass)
kb	kilo basepairs
L	litres
M	Molar
mg	milligrams
ml	millilitres
mM	millimolars
ng	nanograms
nm	nanometres
rpm	revolutions per minute
α	alpha
β	beta
ε	epsilon

CHAPTER 1

AN OVERVIEW OF GENE REGULATION IN COLON CANCER

Cancer has earned the title as a major public health concern, not just in Africa but also internationally. In the United States of America alone, it has been found that one in four deaths is caused by cancer which is responsible for approximately 7.6 million deaths worldwide (Jemal *et al.*, 2009; Globocan, 2008). The World Health Organisation (WHO) estimates that more than 10 million people are diagnosed with cancer globally every year, and projects that these cases will increase to more than eleven million by the year 2030 (WHO, 2011). At a molecular level, cancer is fundamentally a genomic disease as well as an epigenetic disease, and is comprised of a diverse population of cells which may vary in several essential factors, including cell morphology, the ability of cells to proliferate, tumorigenicity, and the expression of characteristic biological markers. This assortment may be justified by variations in genetics and the micro-environment, in addition to the rate of differentiation of discrete cells (Vermeulen *et al.*, 2008).

All types of cancers have undergone the process of Darwinian evolution, and according to Nowell (1976) this is based on the incorporation of sequential mutations within the genome leading to genetic variability and consequential natural selection of highly proliferative cells that out survive their benign acquaintances (Stratton *et al.*, 2009). Such proliferative cells giving rise to the growth of tumours is highly dependent on the formation of new blood vessels known as angiogenesis (Folkman, 1990). This results in the migration of cells from a tumour to other isolated tissues via the blood stream or lymphatic system leading to their invasion, thereby becoming metastatic (Ramaswamy *et al.*, 2003).

1.1 Colorectal Cancer

Epithelial cancers such as colorectal cancers (CRCs) are highly predominant in the Southern African population. The latest National Cancer Registry (NCR) report states that 1 in 97 males and 1 in 162 females suffer from colorectal cancer in South Africa (CANSA, 2010). Although CRC is the second most common cancer in the world, its therapy has been dramatically improved over the past few decades (Jemal *et al*., 2009). The high incidence of colorectal cancers is tightly associated with aging, leading to the occurrence of both malignant and benign neoplasms. It has been identified that aging correlates with an increased proliferation and apoptosis in colon mucosal linings thus increasing cancer susceptibility (Patel *et al.*, 2009).

The development and progression of colorectal cancer may be a result of a number of factors with the most common being genomic instability, this includes the instability of chromosomes, DNA repair defects and aberrant DNA methylation. The inactivation of tumour-suppressor genes or the activation of oncogene pathways may also increase the incidence of cancer (Markowitz and Bertagnolli, 2009).

1.2. Colon Cancer Stem Cells (CSCs)

Solid tumours are comprised of heterogeneous cell populations displaying hierarchies of various phenotypes according to their exclusive morphologies and ancestral markers (Rich and Bao, 2007). Bulk tumours are mainly composed of non-tumourigenic cells that display differentiating properties, as well as a minor subset of tumour-initiating cells known as cancer stem cells (CSCs). Cancer stem cells were initially documented in acute myeloid leukaemia (Lapidot *et al.*, 1994), and their existence and participation has been found in other cancers, including that of the breast (Dick, 2003). Cancer stem cells have some similarities to embryonic and adult stem cells, since there is an ability for (uncontrolled) extended self-renewal, as well as their likelihood to differentiate into a progeny of differentiated cell types (Figure 1.1) (Zhang and Wang, 2008). In contrast, under homeostatic conditions, embryonic and adult stem cell populations are highly regulated, allowing for lineages of differentiated cells and the repair of damaged tissues (Rich and Bao, 2007; Ailles and Weissman, 2007; Konisch *et al.*, 2008).

It has been found that a small proportion of cells within a tumour are capable of self-renewal, this predetermined population that possess the “cancer stem cell” phenotype plays a role in tumour progression whereas other cells of that tumour are unable to self-renew and instead lead to cell differentiation (Houghton *et al*., 2007). This observation has led to the “cancer stem cell hypothesis” which claims that, as stated above, a small fraction of cells within the tumour displays unrestrained proliferative ability thereby contributing to the growth of tumours (Houghton *et al*., 2007).

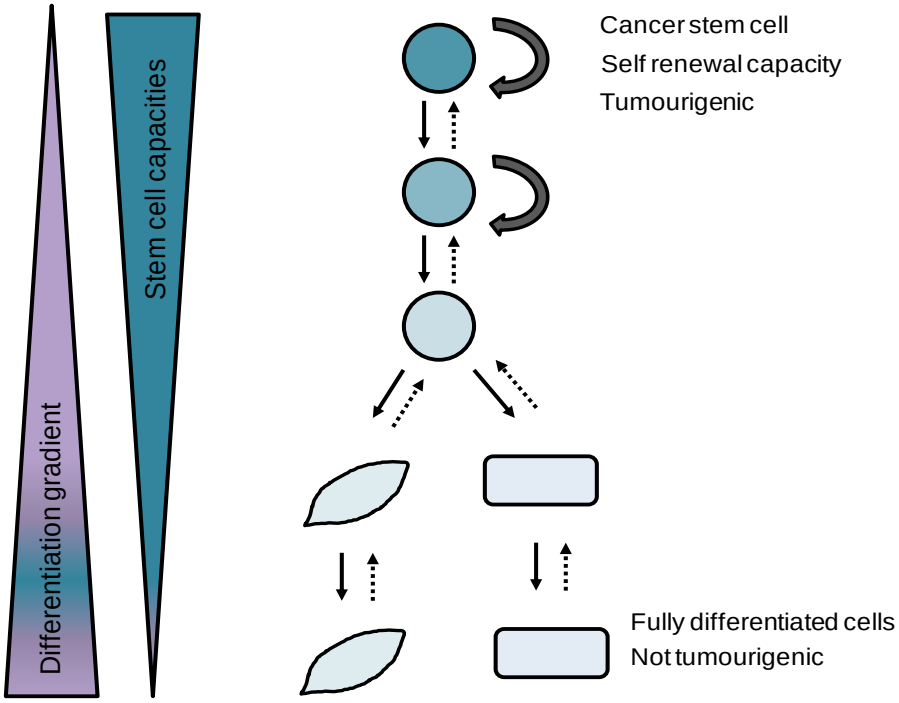


Figure 1.1 A schematic model of the hierarchical organisation of cancer stem cells. This illustration, sourced from Vermeulen *et al.*, (2008) demonstrates that cancer stem cells, like normal stem cells, retain the ability to self renew by dividing to allow the production of more cancer stem cells, as well as to induce a diverse collection of differentiated cells present in a particular malignancy.

Essentially, these properties of stem cells allow for their application in the fields of biotechnology as well as regenerative medicine and tissue development. However, the impairment of these abilities may lead to their uncontrolled proliferation, thereby resulting in tumourigenic mutant stem cells that are capable of causing cancer. The development of CSCs may be attributable to microenviromental variations of stem cells within a tissue, metabolic and cell cycle modifications as well as alterations in signalling pathways due to mutations, and the expansion of cell populations with a mutant phenotype resulting in primary tumours which may lead to metastasis (Klonisch *et al.*, 2008).

It is thought that cancer stem cells may be responsible for relapse following chemotherapy, particularly in regions deficient of ample drug delivery, which may be a result of impaired angiogenesis and inadequate blood supply in such tumour areas. Thus, instead of destroying these bulk cancer cells through certain signalling pathways, the lack of drug delivery is proposed to lead to their conversion to stem cells (Yang *et al.*, 2009), possibly through epigenetic modifications, so altering the chromatin status of these cells. Such non-heritable modifications of DNA may include alterations in histones (deacetylation and phosphorylation) and DNA methylation levels, leading to the activation or repression of gene transcription as seen below. Studies have shown the importance of epigenetic profiles that retain significant pluripotent stem cell markers in a repressed state which can subsequently be activated by drug treatment (Spivakov and Fisher, 2007). Thus, novel therapies involving the epigenetic modification of genes through drug treatment has shown to be a valuable pursuit.

1.3 Biology of Colonic Epithelium

Colonic epithelium replaces itself every five days, making it the fastest tissue in the human body to self-renew (Potten *et al.*, 1992). It contains invaginations of columnar cells known as the crypts of Lieberkuhn, each of which is maintained by stem cells located at the floor of the crypts (Brittan and Wright, 2002). These stem cells produce epithelial cells which follow one of three lineages, namely enterocytes which display absorptive properties, goblet cells that secret mucous and migrating enteroendocrine cells which journey up the crypt to renew the colon (Chandler and Lagasse, 2010). It may be apparent that the high incidence of colon cancer is attributable to the excessive degree of cell renewal taking place in the colon, however comparatively, the small intestine produces epithelium exhibiting similar rates of renewal but with a lower incidence of cancer, therefore this is probably not likely (Boman and Huang, 2008).

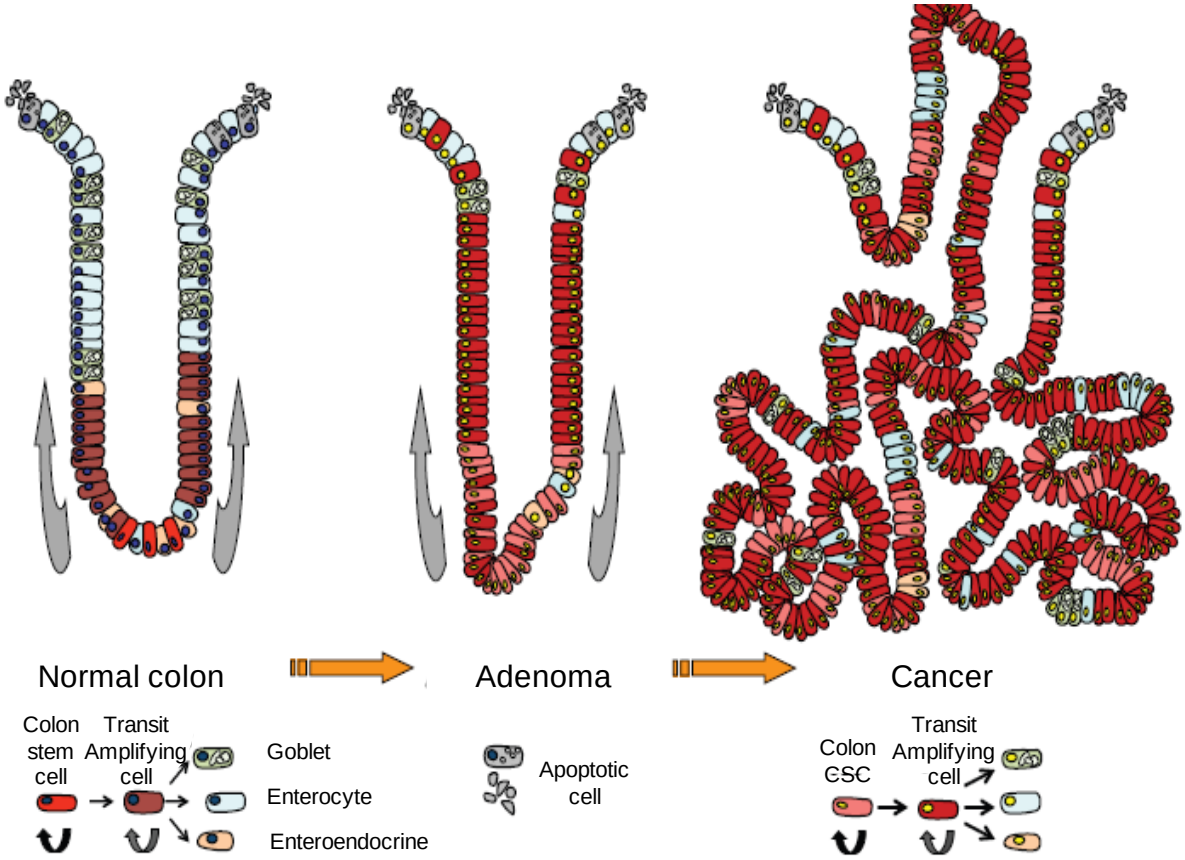


Figure 1.2 Progression of colon cancer as a result of cancer stem cells. These stem cells produce epithelial cells which follow one of three lineages, namely enterocytes, goblet cells enteroendocrine cells (sourced from Chandler and Lagasse, 2010).

1.4 The Importance of Eliminating CSCs in Therapy/Therapeutic Implications of CRC-SC

Efforts to reduce the mortality rate of colorectal cancer patients around the world include the steps involved in preventing bowel cancer, which entails educating the public about changing their dietary and lifestyle habits and frequent colonoscopies, thereby diagnosing the cancer at an earlier stage, preventing recurrence by primary therapy as well as treating the disease if it recurs (August *et al.*, 1984).

Strategies associated with the ablation of colorectal cancer may be categorised as conventional or targeted therapies and are represented in Figure 1.3. Conventional therapy, such as chemotherapy, may spare the minor subset of CSCs within a tumour, resulting in relapse (Torado *et al.*, 2010). As most chemotherapeutic agents generally target the more actively dividing cells, CSCs are protected due to their quiescent nature (Fabrizi *et al.*, 2010). These cells also express high levels of multidrug transporter genes leading to a greater outflow of chemotherapeutic drugs and thus resulting in multidrug resistance (Hirschmann-Jax *et al.*, 2004). Targeted therapies however involve the use of drugs to selectively target and destroy CSCs resulting in complete tumour regression (Ortega *et al.*, 2010). This is executed by pathway inhibitors, as well as differentiation-inducing and cytotoxic agents (Torado *et al.*, 2010).

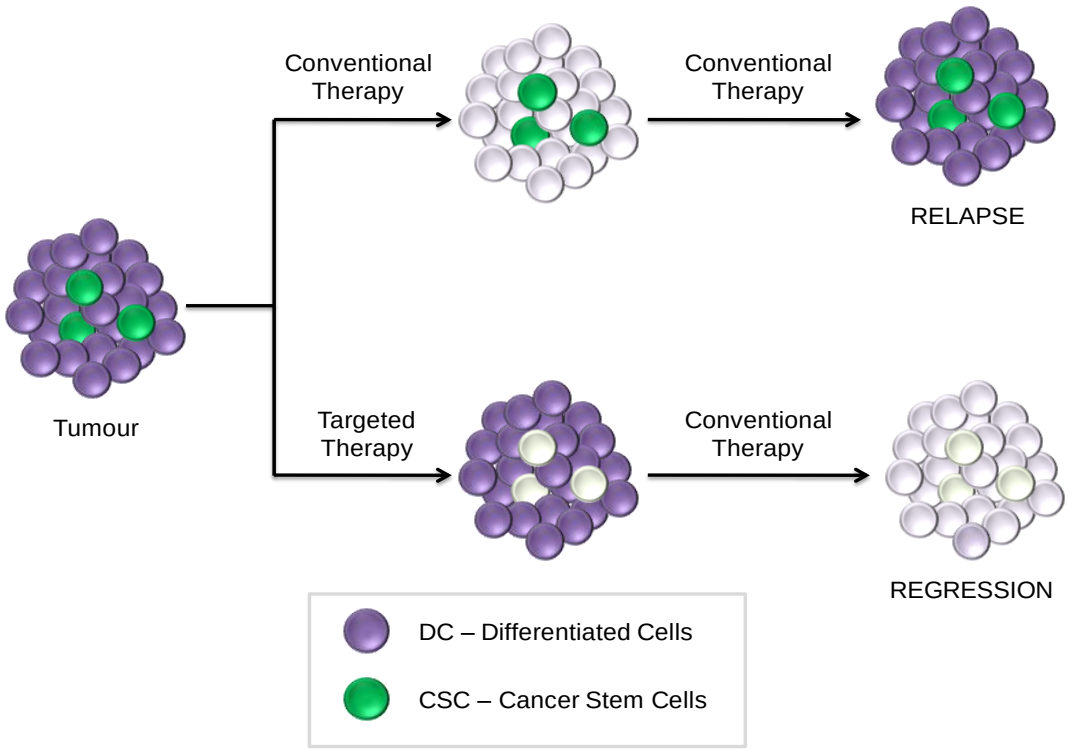


Figure 1.3 Schematic diagram showing different approaches in CRC therapy. CSC target therapy is highly specific and results in complete tumour regression, whilst CSCs are salvaged by conventional therapies leading to tumour relapse (modified from Torado *et al.*, 2010).

The first-line treatment for metastatic CRC is a combination regimen of 5-fluorouricil (5-FU), leucovorin and irinotecan (FOLFIRI), and is involved in inhibiting DNA replication by blocking the synthesis of thymine, due to the fact that 5-FU is a thymidylate synthase inhibitor (Longley *et al.*, 2003). Leucovorin and irinotecan work synergistically with 5-FU, by strengthening the affinity of 5-FU to its target and enhancing cellular cytotoxicity respectively (Zhang *et al.*, 1992; Iyer and Ratain, 1998). Table 1.1 displays other first-line and second-line drug combinations utilised in the treatment of CRC. Targeted therapies involve the use of drugs such as Cetuximab and Bevacizumab (Meyerhardt and Mayer, 2005).

Table 1.1 List of FDA-approved drugs and combination regimens (Longley *et al.*, 2003; Zhang *et al.*, 1992; Iyer and Ratain, 1998; Meyerhardt and Mayer, 2005)

FDA-approved combination drugs	FDA-approved drugs					
	Fluoro-uricil (CT)	Cape-citabine (Xeloda) (CT)	Irino-tecan (Camp-tosar) (CT)	Oxali-platin (Eloxatin) (CT)	Cetux-imab (Erbitux) (TT)	Beva-cizumab (Avastin) (TT)
IFL*	X		X			
FOLFIRI*	X		X			
FOLFOX*	X			X		

*All combination regimes include Leucovorin which has not yet gained FDA-approval.
CT – Conventional Therapy
TT – Targeted Therapy

The accelerated development of this field has allowed for the discovery of novel stem cell markers, which have played an immense role in the pursuit of a successful cancer treatment by targeting CSCs. The advancement of tools permitting the controlled expression of CSCs as well as an enhanced perception of the processes influencing the growth, differentiation and migration of cells contribute to the development of drugs leading to the transformation of therapeutic approaches for the treatment of cancer (Klonisch *et al.*, 2008).

1.5 Gene Regulation in Colon Cancer

1.5.1 Oncogenes and tumour suppressors

Cancer is instigated by genetic change, which may be familial or may result from a collection of abnormalities over time in the same cell. Such abnormalities include the activation or repression of certain genes which may influence tumour formation, either positively or negatively, therefore damage may be dominant or recessive (Klein, 1988; Bishop, 1991). Proto-oncogenes are targets of dominant damage and are involved in the regulation of normal cellular processes and growth; once mutations are introduced to these genes, they form oncogenes resulting in a gain-of-function (Bishop, 1991). The transformed oncogenes promote the uncontrolled growth of normal cells into malignant cells. Several known oncogenes fall into the categories of growth factors, growth factor receptors, protein kinases, signal transducers and transcription factors (Klein, 1988).

On the other hand, targets for recessive damage are known as tumour suppressor genes and require the inactivation of both alleles (Comings, 1973). These genes are capable of neutralising the effect of the activated oncogenes and result in a loss-of-function once mutated, leading to the emergence of tumours (Bishop, 1991; Klein, 1988). One of the earliest lines of evidence of tumour suppressor genes dates back to Knudson's research on retinoblastomas. He demonstrated that in familial retinoblastoma, the first mutation or "hit" in the Rb1 gene succeeded through the DNA and the second "hit" occurred in somatic cells. However, in non-inherited retinoblastoma, both mutations took place in somatic cells leading to tumourigenesis (Knudson, 1971). It has been argued that there is a possibility that the tumourigenic properties of a cell may be reversed following the manipulation of a tumour suppressor gene to reinstate its active role in a particular cell, creating a model for an anticancer therapy (Sherr, 2004).

1.5.2 Krüppel-like factors

In this study, a potential tumour suppressor gene of interest is Krüppel-like factor-4 (KLF4 or GKLF4), of which its product displays homology to the protein Krüppel isolated from *Drosophila melanogaster*. KLF4 belongs to a family of transcription factors, as demonstrated in Table 1.2, that are involved in the regulation of growth and development, cell proliferation, differentiation, apoptosis and evidently transcription (Dang *et al.*, 2000, Ghaleb and Yang, 2008). The classification of transcription factors are based mainly on the DNA-binding motifs that they contain, where the zinc finger domain is highly conserved in Krüppel-like factors (Yang, 1998). A zinc

finger, as displayed in Figure 1.4, is a small structural domain which arranges an array of cysteine and histidine residues to tetrahedrally coordinate the zinc atom forming the common Cys_2His_2 conformation (Laity *et al.*, 2001). Zinc stabilises an α-helix and a β-sheet and forms a vital piece of the puzzle within the DNA-binding region creating a protrusion resembling a finger that is in close proximity to the DNA (Yang, 1998).

Table 1.2 Expression patterns of Krüppel-like factors

Gene Name	Associated Gene Names	Area of protein expression
KLF1	EKLF (Erythroid Krüppel-like factor)	Cells of the erythroid lineage
KLF2	LKLF (Lung Krüppel-like factor)	Lung, spleen, high levels in heart
KLF3	BKLF (Basic Krüppel-like factor)	Liver, lung, muscle, brain, hematopoietic tissues
KLF4	GKLF (Gut-enriched Krüppel-like factor)	Lung, testis, skin, thymus, vascular endothelial cells, epithelial cells of gut and skin
KLF5	IKLF/BTEB2 (Intestinal-enriched Krüppel-like factor/Basic Transcription Element-Binding protein 2)	Gastrointestinal epithelium (toward proliferating zone of crypt cells)
KLF6	CPBP/GBF/Zf9 (Core Promoter Binding Protein/GC-rich sites Binding Factor)	Placenta, lung, heart, liver, pancreas
KLF7	UKLF (Ubiquitous Krüppel-like factor)	Initially identified in endothelial cells, later discovered in almost all tissues
KLF8	BKLF3/ZNF741 (Basic Krüppel-like factor 3)	Kidney, heart and placenta
KLF9*	BTEB (Basic Transcription Element-Binding protein)	Liver, endometrial epithelium
KLF10	EGRα/TIEG1 (Early Growth Response α/Transforming growth factor-β-Inducible Early Gene 1)	Keratinocytes, epithelial cells of placenta, breast and uterus, osteoblasts and skeletal muscle
KLF11	TIEG2 (Transforming growth factor-β-Inducible Early Gene 2)	Expressed in all tissues, with higher levels in pancreas, skeletal muscle and erythroid cells
KLF12	AP-2rep (Transcriptional repressor of AP-2α gene)	Mouse kidney, liver, lung
KLF13	RFLAT-1 (activator of RANTES)	Ubiquitous expression with high levels in peripheral blood lymphocytes and thymus
KLF14	N/A	Ubiquitous expression with high levels in placenta and fetal heart, liver, lung and colon
KLF15	N/A	Liver, kidneys, heart and skeletal muscle
KLF16	DRRF (Dopamine Receptor Regulating Factor)	Mouse brain, heart, spleen, lung, liver, kidney, testis
KLF17	N/A	Low levels in brain, testis and bone

*KLF9/BTEB was the first Krüppel-like factor identified.
(Sourced from Dang *et al.*, 2000; Nagai *et al.*, 2009)

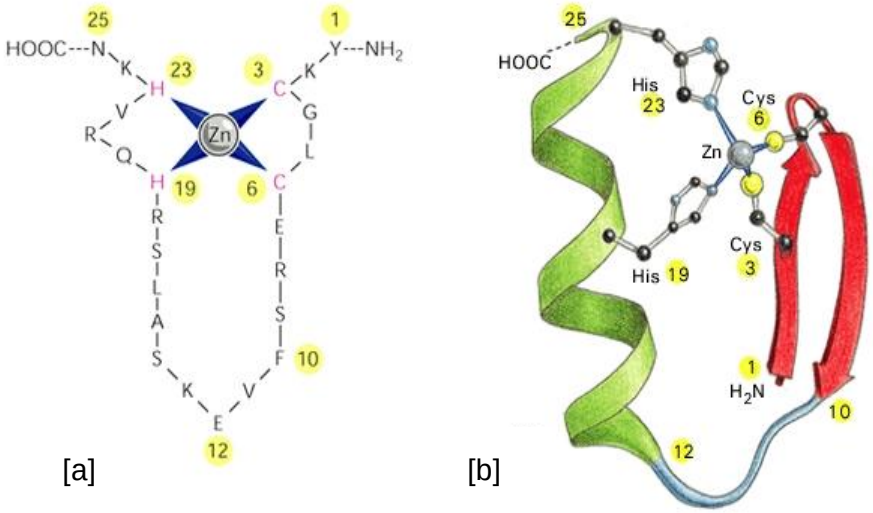


Figure 1.4 Schematic view of a zinc finger protein. [a] A two-dimensional overview of a finger showing the single zinc atom which forms an essential part of the protein motif. [b] A three-dimensional view displaying an antiparallel β-sheet pursued by an α-helix (sourced from Alberts *et al.*, 1994).

1.5.3 Krüppel-like factor 4

The human *KLF4* gene locus demonstrated in Figure 1.5 is located on chromosome 9 at position 9q31.2 and spans over 5.6kb in distance. The gene contains five exons with a transcript length of 2813bp, and the KLF4 cDNA encodes a protein of 479 amino acid residues with an average residue weight of 106.631g/mol and a molecular weight of 51076.240g/mol. The gene sequence as well as protein sequence is listed in Appendix 1 (Ensembl, 2011). As a transcription factor, KLF4 binds to CACCC elements or GC-rich regions of target genes leading to their activation or repression (Yet *et al.*, 2008; Philipsen and Suske, 1999).

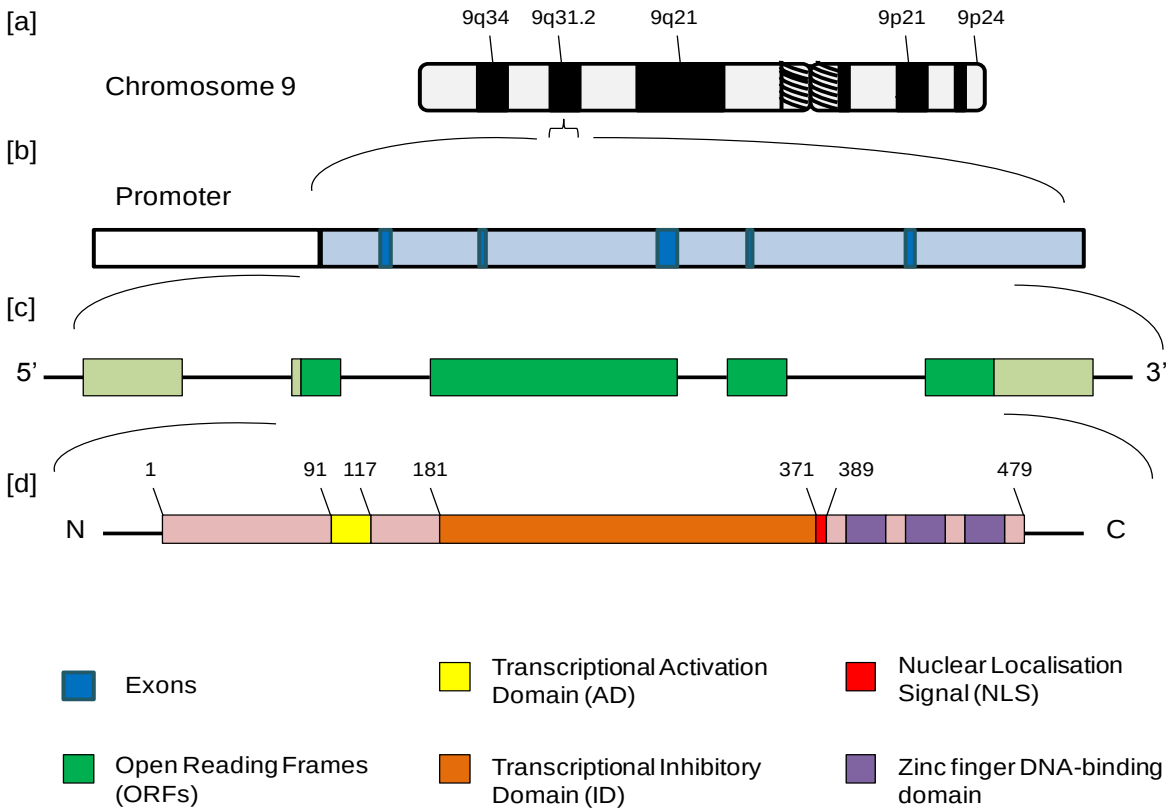


Figure 1.5 Structural view of the *KLF4* gene and its protein product. [a] KLF4 is located on chromosome 9 at position 9q31.2. [b] The blue areas represent the five exons of the gene sequence. [c] Five boxes indicate the five exons, and the green denotes the ORF which encodes for [d] the KLF4 protein of 479 amino acids, including a number of functional domains, namely the transcriptional activation domain (AD) transcriptional inhibitory domain (ID), the three zinc finger binding domains and the nuclear localisation signals (one controlled by the three zinc fingers which is not shown) (Modified from Wei *et al.*, 2006).

The initial isolation of KLF4 was achieved by Shields from an NIH 3T3 cDNA library screening with a probe that encodes the zinc finger segment of the gene product zif/268 by low stringency hybridisation (Shields *et al.*, 1996). Shields also proved that KLF4 is a nuclear protein controlling two strong and independent nuclear localisation signals (NLSs), one contained by the three zinc fingers and the other within a cluster of amino acids directly contiguous to the first zinc finger, as demonstrated in Figure 1.5 (Shields and Yang, 1997). Both these signals are identified in KLF1, KLF2 and KLF4, which are closely related Krüppel proteins belonging to a small subfamily (Shields and Yang, 1997). Shields pragmatically determined the consensus binding sequence for KLF4 in a target detection assay using highly purified recombinant protein (Shields and Yang, 1998). It was found that the sequence 5'-$^{G}/_{A}{}^{G}/_{A}$GG$^{C}/_{T}$G$^{C}/_{T}$-3' was present in the promoters of several genes such as the CACCC element and the basic transcription element (BTE) which commonly interacts with a number of transcription factors (Shields and Yang, 1998).

As displayed in Table 1.2, KLF4 is expressed in a number of tissues such as the lung, skin, testis and thymus, with the highest levels present in the gut epithelium (Dang, Pevsner and Yang, 2000). The expression of KLF4 has been well characterised in gastrointestinal tissue. Chen and colleagues established that the induced expression of KLF4 lead to a reduced rate of proliferation, which was a possible result of cell cycle arrest preventing G1/S progression and is thus a potent inhibitor of DNA synthesis (Chen *et al.*, 2001; Shields *et al.*, 1996). It does so by acting directly on

the promoter of p53 (a tumour suppressor involved in preventing cancer by regulating the cell cycle) thereby repressing it and consequently inducing the expression of $p21^{CIP1}$ as is displayed in Figure 1.6 (Rowland *et al.*, 2005). Inhibition of KLF4 expression in cultured breast cancer cells may lead to apoptosis due to the restoration of the tumour suppressor p53 (Rowland *et al.*, 2005).

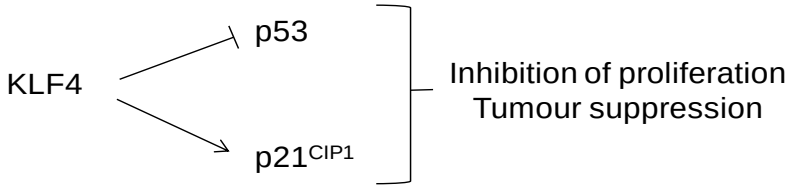


Figure 1.6 Representation of the tumour suppressor role of KLF4 leading to cell cycle arrest and thus reduced proliferation in colon cancer cells (Rowland, *et al*., 2005).

KLF4, along with three other transcription factors OCT4, SOX2 and C-MYC, have been found to transform dermal fibroblasts into inducible pluripotent stem cells (iPS cells) when ectopically expressed; these transcription factors were initially experimented on mouse embryonic and adult fibroblasts (Lowry *et al.*, 2008; Takahashi and Yamanaka, 2006). These are known to resemble human embryonic stem cells (HESCs) which are pluripotent and are isolated from the inner cell mass (ICM) of blastocysts (Martin, 1981; Evans and Kaufman, 1981). The above mentioned pluripotent markers work synergistically to promote the expression of "stemness" genes and inhibit that of genes associated with differentiation in ES cells (Takahashi *et al*., 2007). It is considered that OCT4 and SOX2 are capable of binding to their gene targets once C-MYC and KLF4 epigenetically modify the chromatin structure by interacting with proteins involved in the acetylation of histones (Yamanaka, 2007; Evans *et al*., 2007). The development of iPS cells could also be achieved using the pluripotent gene party OCT4, SOX2, NANOG and LIN28 (Yu *et al*., 2007).

1.5.4 Cancer signalling pathways

Studies done on the homeostatic regulation of adult intestinal epithelium show that there are several chief participants involved, namely the major signalling pathways Wnt, TGF-β, BMP, Notch, MAPK/ERk and PI3-K/Akt; furthermore defects in several of these pathways may lead to cancer (Sancho *et al.*, 2004). This is characterised by increased proliferation that is mediated by growth factor stimulated pathways such as the Wnt pathway as well as MAPK, acting as a complex process involving a succession of protein kinase cascades (Zhang and Lui, 2002). Others players include the pro-survival pathway PI3-K/Akt that may lead to decreased cell death or apoptosis (Yap *et al.*, 2008). Most protein components of these pathways have become targets for cancer therapy, consequently in the following study, the protein target of interest is β-catenin which is a key component of the Wnt pathway.

The Wnt/β-catenin signalling pathway is evidently crucial in the self-renewal of human embryonic stem cells, as well as intestinal epithelial stem cells and skin stem cells, as a result of its direct link to the central transcriptional regulatory circuitry of embryonic stem cell pluripotency (Dravid *et al.*,

2005). Loss of regulatory ability leads to carcinogenesis and is frequently associated with colorectal cancer (Clevers, 2006).

When the Wnt receptors are unoccupied, the newly-synthesised cytoplasmic protein β-catenin associates with various proteins, namely adenomatous polyposis coli (APC), glycogen synthase kinase-3β (GSK-3β) and axin to form the destruction complex (Lustig and Behrens, 2003; He *et al.*, 2003). A set of conserved Ser and Thr residues in the amino terminus of β-catenin is phosphorylated and subsequently ubiquinated, thereby targeting it for proteosomal degradation. However, induction of the pathway by the binding of Wnt to its surface receptor Frizzled (Frz) leads to the activation of the protein Dishevelled (Dsh), therefore inhibiting the destruction complex (Lustig and Behrens, 2003; He *et al.*, 2003). β-catenin thus accumulates in the cytoplasm followed by its translocation to the nucleus where it interacts with and transiently converts T-cell factor (TCF)/Lymphoid enhancer factor (LEF) into transcriptional activators (Lustig and Behrens, 2003; He *et al.*, 2003). In the absence of a Wnt signal, TCF/LEF proteins directly associate with co-repressors, such as Groucho, leading to the suppression of their target genes (Lustig and Behrens, 2003, He *et al.*, 2003; Reya and Clevers, 2005).

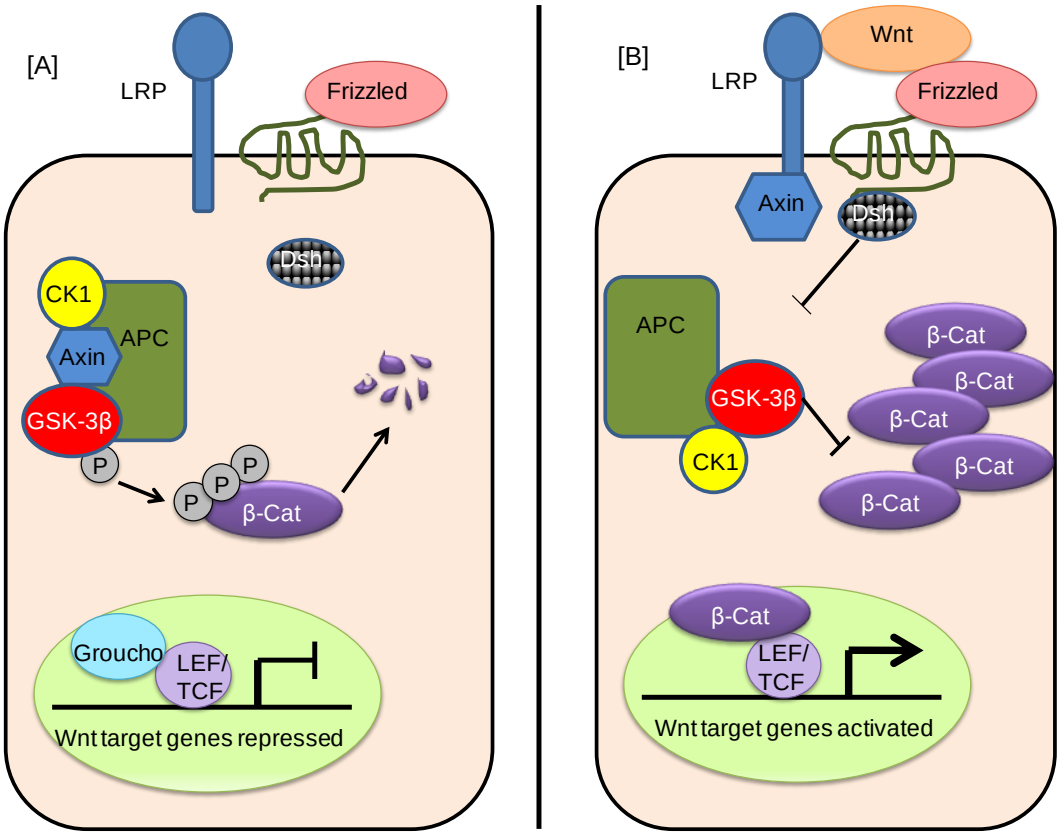


Figure 1.7 The Wnt/β-catenin pathway. [A] The absence of the Wnt ligand results in the ubiquitination and degradation of β-catenin. [B] In the presence of the Wnt ligand, Dishevelled is recruited to Frizzled leading to the inhibition of the destruction complex, thus β-catenin accumulates resulting in the transcriptional activation of TCF/LEF in human ESCs (Modified from Pinto and Clevers, 2005).

1.5.5 β-catenin

β-catenin is a well known transcription factor encoded by the gene *CTNNB1,* and is defined as an oncogene in colon cancer (UniProtKB, 2011; Polakis, 1999). As demonstrated in the Wnt pathway,

β-catenin is up-regulated by Wnt-1 and suppressed by APC, axin and GSK-3β contributing to its oncogenicity (Polakis, 1999). β-catenin signalling may lead to the constitutive activation of several gene targets in cancer, such as the proto-oncogene c-myc, by delivering perpetual signals dominating cell growth regulation (Polarkis, 1999). Table 1.3 displays the many gene targets of β-catenin in colon cancer and other biological systems.

Table 1.3 List of target genes of β-catenin signalling in the Wnt pathway

Gene	Organism	System	Upstream/Downstream	REF
c-myc	Human	Colon cancer	Upstream	He, 1998
Cyclin D	Human	Colon cancer	Upstream	Tetsu, 1999
				Shtutman, 1999
Tcf-1	Human	Colon cancer	Upstream	Roose, 1999
LEF1	Human	Colon cancer	Upstream	Hovanes, 2001
				Filali, 2002
Axin-2	Human	Colon cancer	Upstream	Yan, 2001
				Lustig, 2002
				Jho, 2002
Gastrin	Human	Colon cancer	Upstream	Koh, 2000
BMP4	Human	Colon cancer	Upstream	Kim, 2002
CD44	Human	Colon cancer	Upstream	Wielenga, 1999
VEGF	Human	Colon cancer	Upstream	Zhang, 2001
Survinin	Human	Colon cancer	Upstream	Zhang, 2001
Sox9	Human	Intestine	Upstream	Blache, 2004
Sox2	Xenopus	Retina	Upstream	Vaan Raay, 2005
Nanog	Human	ES	Upstream	Pereira, 2006
				Cole, 2008
Oct4	Human	ES	Upstream	Cole, 2008
Frizzled	Human	EC cells	Upstream	Willert, 2002

The human *CTNNB1* gene locus is situated on chromosome 3 at position 3p22.1 and spans over 23.2kb of DNA (Nollet, 1996; Kraus, 1994). The transcript encompasses a length of 3356bp and contains sixteen exons, of which the first is non-coding and the sixteenth undergoes alternative splicing, shortening the 3' untranslated region (UTR) by 159bp (Ensembl, 2011; Nollet *et al.*, 1996). A TATA box was found to be contained within the promoter region and was discovered to be GC rich (Nollet *et al.*, 1996). The cDNA encodes a protein of 781 amino acid residues with an average residue weight of 109.470g/mol and a molecular weight of 85496.350g/mol (Ensembl, 2011). The gene sequence as well as the protein sequence for CTNNB1 and β-catenin is listed in Appendix 2 (Ensembl, 2011; Nollet *et al.*, 1996).

β-catenin is composed of an NH_2 terminal of approximately 130 amino acids containing a GSK-3β phosphorylation site and a COOH terminal of about 100 amino acids containing a transactivation

domain, both these regions flank the armadillo (ARM) repeat region of 550 amino acids containing twelve repeats of 42 amino acids (Peifer *et al.*, 1994; Huber *et al.*, 1997). Alpha helices are organised in pairs within each armadillo repeat to form small hairpin structures (Huber *et al.*, 1997). CTNNB1 was initially identified as a segment polarity gene in *Drosophila* embryogenesis wherein mutations in the armadillo gene lead to the production of anterior structures in the posterior regions of the fly (Riggleman *et al.*, 1989). As displayed in Figure 1.8, the armadillo repeat region is the chief binding site for major interactive proteins, depending on the functional fate of β-catenin. In its involvement in adhesion, E-Cadherin would bind to this region, however in the Wnt signalling pathway this is a critical binding zone for Axin and APC of the destruction complex, as well as TCF (Harris and Peifer, 2005).

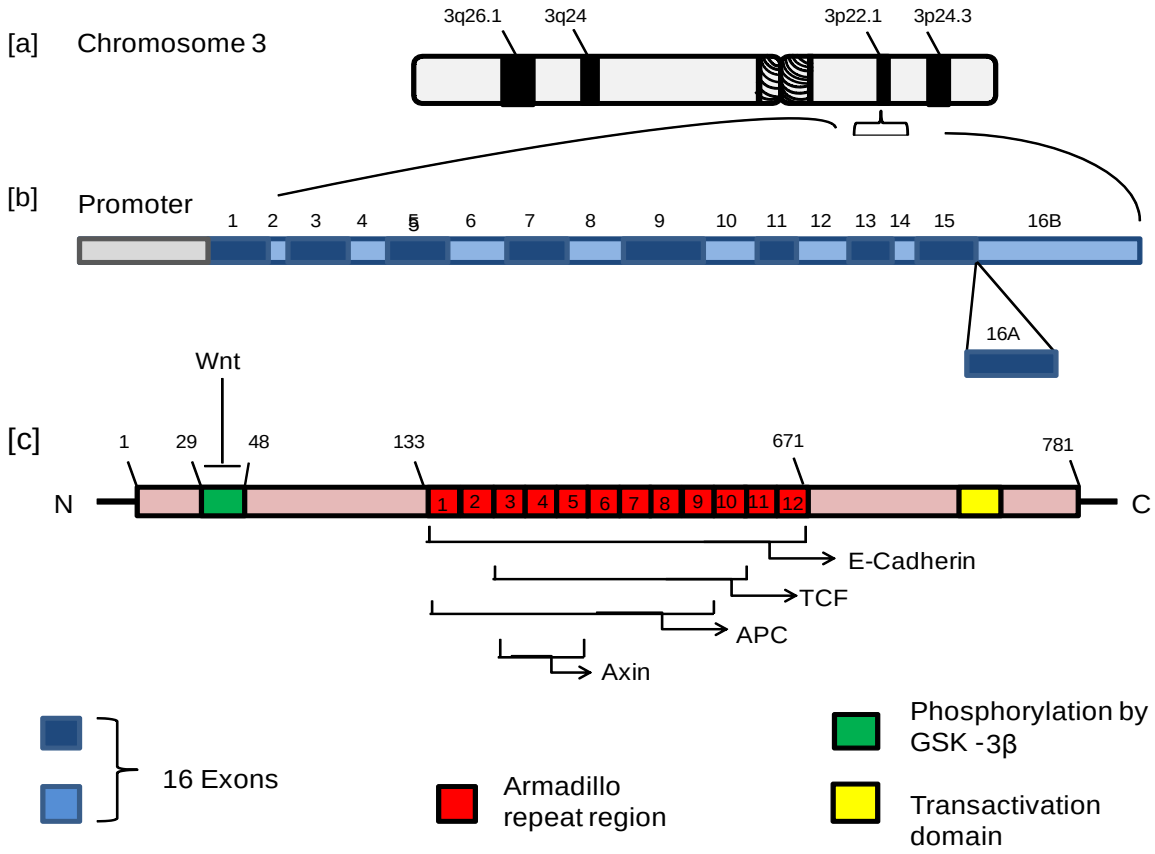


Figure 1.8 Structural view of the *CTNNB1* gene and its β-catenin protein product. (a) CTNNB1 is located on chromosome 3 at position 3p22.1. (b) The light and dark blue regions represent the sixteen exons of the gene sequence. The 5' portion of exon 16 (16A) is often removed as a result of alternative splicing, reducing the mRNA length by 159bp. (c) The β-catenin protein product contains 781 amino acids and includes twelve copies of a 42 amino acid sequence motif known as the armadillo repeat, a phosphorylation site by GSK-3β as well as a transactivation domain. Binding sites for Wnt signalling as well as adhesion are displayed by TCF (ARM repeat 3-10), APC (ARM repeat 1-9), Axin (ARM repeat 3-5) and E-Cadherin (ARM repeat 1-12) respectively (Ensembl, 2011; Nollet *et al.*, 1996; Huber *et al.*, 1997; Harris and Peifer, 2005).

As discussed, β-catenin is involved in the Wnt pathway as a transcriptional activator of LEF/TCF and other target genes. Prior to this finding, β-catenin was found to be involved in cell adhesion by linking E-cadherin receptors to α-catenin, thereby linking β-catenin to the actin cytoskeleton by adherens junction molecules (Kelmer, 2003; Gottardi and Gumbiner, 2001). The functional switch between these two roles is controlled by the phosphorylation of tyrosine residues of β-catenin. The phosphorylation of Y654 localised within the twelfth armadillo repeat prevents its binding to E-

cadherin (Roura *et al.*, 1999; Piedra *et al.*, 2001). Another vital residue located in the first armadillo repeat is Y142; this residue was found to inhibit the binding of β-catenin to α-catenin when phosphorylated (Piedra *et al.*, 2003). This regulatory mechanism executed by tyrosine kinases promotes the transcriptional activation of β-catenin. The involvement of β-catenin in adhesion as a tumour suppressor and in transcription as an oncogene is crucial for normal cellular functioning, although a loss of equilibrium in this system by phosphorylation instigates a heightened transcriptional activity and repressed adhesive functionality, paving the way for malignancies such as cancer (Brembeck *et al.*, 2006).

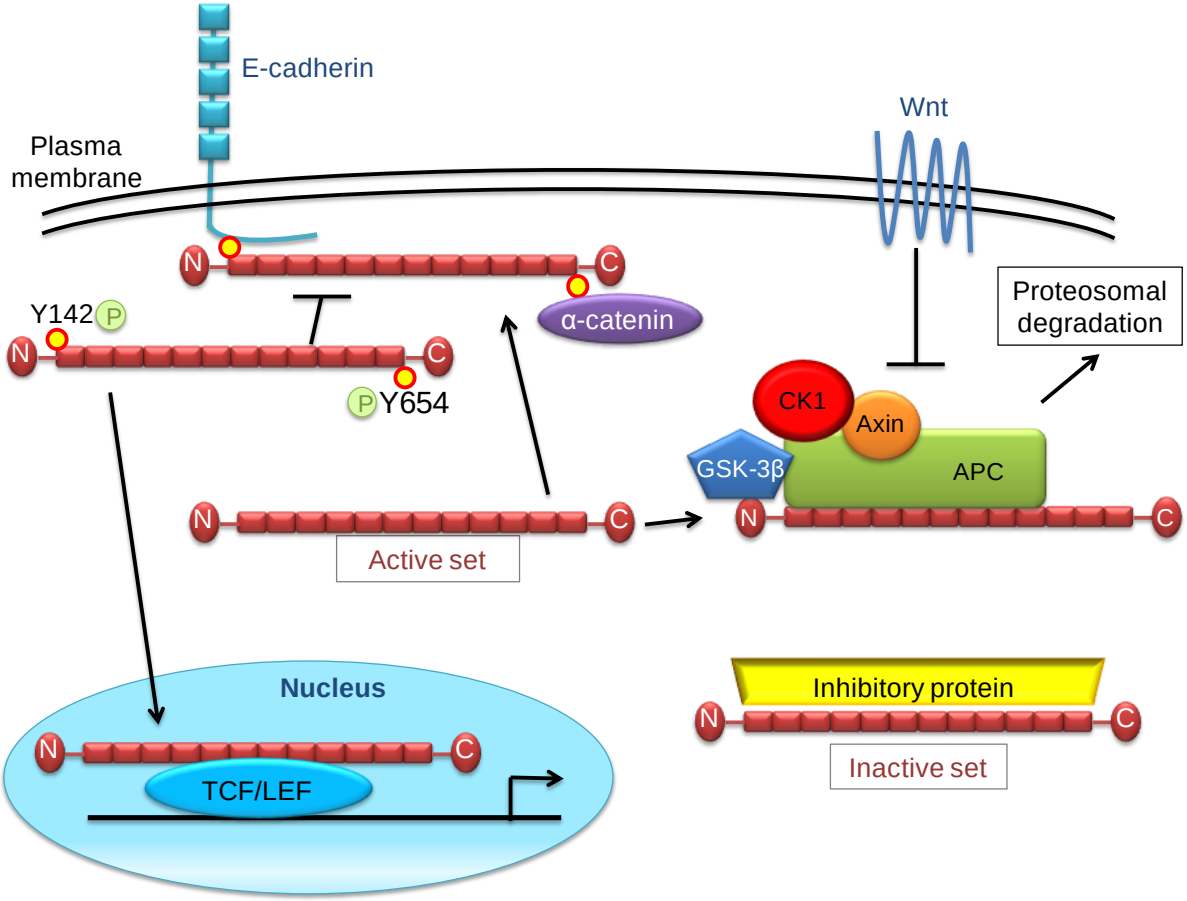


Figure 1.9 Various pools of β-catenin following separate fates. The active set are found to bind to the cytoplasmic portion of E-cadherin aiding in adhesion. Other active pools may bind to the destruction complex in the absence of a Wnt signal, however when a signal is present β-catenin binds to and activates TCF/LEF in the nucleus. Phosphorylation sites are also displayed, these aiding in the functional switch between adhesion and transcription leading to oncogenic activity. An inactive pool of β-catenin could be a consequence of their association with inhibitory proteins (yellow) or from post-translational modification of the protein (Gottardi and Gumbiner, 2001; Brembeck *et al.*, 2006).

1.5.6 Cross talk

In the present study, the induced expression of the pluripotent stem cell marker KLF4 was considered together with its interactions with β-catenin, a key transcription factor of the Wnt signalling pathway. As discussed, Krüppel-like factor 4 (KLF4) or GKLF is a zinc-finger transcription factor which acts as a tumour suppressor in colorectal cancer cells. The induced expression of KLF4 in cultured cell lines results in the inhibition of DNA synthesis thereby inhibiting cell proliferation (Ghaleb and Yang, 2008). It has been established that cross talk between KLF4

and β-catenin plays an important role in homeostasis of intestinal epithelium as well as in driving tumorigenesis of colon cancers. β-catenin mediates Wnt signalling, and KLF4 interacts with the transcriptional activation domain of β-catenin leading to its inhibition, thus stalling the Wnt pathway (Zhang *et al.*, 2006).

1.6 Stem Cells and Epigenetics

1.6.1 An "epic-genetic" overview

The term epigenetics in the literal sense means "out" or "outside conventional genetics" and was established by C. H. Waddington in the early 1940's to describe the lack of variation in phenotype when influenced genetically that was later found to be a result of environmental changes (Jaenisch and Bird, 2003; Waddington, 1942). The birth of epigenetics took place while uncovering embryonic development and has since become one of the fastest growing fields of this age (Waddington, 1942). Epigenetic changes through the modification of chromatin structure and function by posttranslational modifications may lead to an up-regulation or down-regulation of gene expression, bringing about variations in cellular activities (Ellis *et al.*, 2009). It is possible that such alterations could stimulate tumourigenic activity influenced by behavioural changes in the cell (Pollock and Richon, 2009). Cancer therapies are being revolutionised with the exciting advent of epigenetic treatments coming to the fore (Ellis *et al.*, 2009). Epigenetic modifications are classified into several different categories, namely DNA methylation, histone acetylation or deacetylation and chromatin remodelling amongst others. The present study assesses the modulation of DNA methylation and histone acetylation in colon cancer cells (Gal-Yam *et al.*, 2008).

1.6.2 The evolution of epigenetics

It is possible that new mutations may be induced in the germline of ova or sperm through epigenetic manipulation, thereby influencing the DNA passed on between generations; thus it is safe to say that epigenetics may play a role in the evolutionary process. Opposing the neo-Darwinian approach, which is the marriage of natural selection and Mendelian genetics, it was determined that the interaction between the epigenetic system and the environment is the cause of variations that is non-random and drives change in evolution (Ho, 1979). Epigenetic regulation and evolution is a result of several contributing factors. There is evidence that the inception of these variations may have been a result of a natural mechanism of defending the DNA structure from viruses or parasites, wherein stimuli such as diet or aging may have played a vital role in these alterations (Matzke *et al.*, 1999; Jaenisch and Bird, 2003).

1.6.3 Histone modifications

Chromatin complexity and its epigenetic regulation of gene expression have been revealed in eukaryotes for some time now, and modifications such as acetylation and deacetylation are involved in these regulatory processes (Shankar and Srivastavar, 2008; Grunstein, 1997). The acetylation of histones involves the transfer of acetyl groups to the highly conserved and positively

charged ε-amino group of lysine residues by histone acetyltransferases (HATs), whereas deacetylation leads to the removal of acetyl groups from lysine side chains via histone deacetylases (HDACs) thus restoring the positive charge of histones (Shankar and Srivastavar, 2008; De Ruiter *et al.*, 2003). Both HATs and HDACs are involved in the regulation of malignancies through the control of cell proliferation, differentiation and apoptosis, and it was found that histone hyperacetylation through HATs is associated with the activation of genes while deacetylation leads to the condensation of chromatin and thus the silencing of the targeted gene (Kouzarides, 1999; Johnstone and Licht, 2003; Strahl and Allis, 2000).

1.6.3.4 *Histone deacetylase inhibitors: Valproic acid*

HDACs play a vital role in the regulation of gene expression, and inhibitors thereof display anti-tumour activity influencing cellular processes such as growth arrest, cellular differentiation, inhibition of angiogenesis, cytotoxicity as well as cell death, through the activation of apoptotic pathways which leads to the prevention of cancer cell proliferation. These changes are a result of restored acetylation of histones which may alter the expression of downstream genes (De Ruiter *et al.*, 2003). There are several histone deacetylase inhibitors (HDAC inhibitors) that have exhibited therapeutic improvements on cellular behaviour, one in particular that is considered in this study is Valproic acid (VPA). This drug, originally exploited for its antiepileptic benefits, was found to be highly stable at room temperature (25°C) and soluble in a variety of solvents including water (Gottlicher *et al.*, 2001; Duenas-Gonzales *et al.*, 2008). VPA has been found to induce cell differentiation in transformed haematopoietic cells as well as other carcinoma cell types and thus could be valuable in the eradication of cancer (Gottlicher *et al.*, 2001; Kramer *et al.*, 2001).

1.6.4 DNA methylation

Methylation of DNA segments is fast becoming a frequent occurrence in eukaryotes, and its association with cancer as well as its reversible nature makes it a potential candidate in the therapy of several types of malignancies (Das and Singal, 2004). Cancer cells are known to display two main types of methylation, namely hypomethylation occurring on a genome-wide scale as well as hypermethylation of promoter regions exhibiting a high frequency of CpG islands (Esteller, 2008). Hypomethylation activity is commonly localised at repeat regions of the DNA sequence and is associated with the overexpression of proteins involved in tumourigenesis and thus an increased risk of colon cancer (Feinberg and Tycko, 2004; Kaneda and Feinberg, 2005). The following study will focus on hypermethylation through the addition of methyl groups to the fifth cytosine poitision of CpG island dinucleotides via catalyst enzymes known as DNA methyltransferases (DNMTs) (Momparler *et al.*, 2000; Robertson, 2001).

1.6.4.1 *DNA methyltransferase inhibitors: Zebularine*

Inhibitors of DMNTs range in their usefulness in terms of their stability and half-life in solvents. They operate in the prevention of DNMT activity by binding to these enzymes after relocating to the

nucleus, resulting in their exhaustion and thus a reduction in their numbers (Jutterman *et al.*, 1994; Bouchard and Momparler, 1983; Santi *et al.*, 1983). This leads to demethylation of the DNA segments in question and potentially to apoptosis as a result of a block in DNA synthesis (Jutterman *et al.*, 1994; Bouchard and Momparler, 1983; Santi *et al.*, 1983). Demethylating agents are capable of reversing the effects of methylation in certain sites of the DNA thus leading to an enhanced expression of suppressed genes and ultimately the differentiation of cells (Bender *et al.*, 1998; Attadia, 1993). There are several DNMT inhibitors that have been employed in this sense, two highly potent drugs are 5-aza-2'-deoxycytidine (5-aza-CdR) and 5-azacytidine (5-aza-CR). These drugs however have been found to be highly toxic and highly unstable as well as lacking in target specificity and therefore may lead to tumorigenic activity instead of preventing it (Constantinides *et al.*, 1977; Worm and Guldberg; 2002). One other DNMT inhibitor that displays much more favourable properties, including low toxicity and high stability, is the cytidine analogue Zebularine (ZEB) (Cheng *et al.*, 2003). This therapeutic agent is also capable of being administered at a lower dose for a long time period due to its less toxic nature (Cheng *et al.*, 2004). The following study demonstrates the effects of this drug on various cancer cell lines.

1.7 Study Aims

In view of the association of stem cell pluripotentiality factors with cancer stem cells, in particular KLF4, the following hypothesis was proposed:

The induction of KLF4 signalling in colon cancer cells regulates tumourigenesis.

This was specifically investigated under the following objectives:

1. To determine whether early stage colon cancer cells express the pluripotent stem cell marker KLF4
2. To determine whether KLF4 expression is induced by epigenetic modifications through drug treatment in late stage colon cancer cells
3. To compare the effect of epigenetic modulations by DNA methyltransferase inhibitors with histone deacetylase inhibitors on the induction of KLF4
4. To establish the effects of a synergistic treatment with both DNA methyltransferase inhibitors and histone deacetylase inhibitors on early and late stage colon cancer cells
5. To determine a possibility of a link between KLF4 and the Wnt signalling pathway (β-catenin)

CHAPTER 2

MATERIALS USED AND METHODS IMPLEMENTED IN THIS STUDY

All materials and methods described in this chapter were implemented in the subsequent chapters, unless otherwise stated. All reagents and materials are listed in Appendix 3.

2.1 Cell Culture

All cell culture procedures were performed by the implementation of aseptic techniques and good cell culturing practice to prevent contamination from bacteria, fungi and mycoplasma as well as cross contamination with other cell lines. This included the use of personal protective equipment, such as gloves and lab coats at all times.

The following general cell culture procedures were executed in the cell culture room under a laminar flow cabinet. A UV-C germicidal lamp was used to sterilise the cabinet when it was not in use and was switched off during use, and the fluorescent light and the fan were turned on, drawing air in through a HEPA filter. The flow hood was sanitised with 70%$^{v}/_{v}$ ethanol before commencing with work and gloves were sanitised with 70%$^{v}/_{v}$ ethanol periodically when handling different equipment. All materials (including 50mL media bottles, culture flasks, 10mL pipettes) including the surface of the flow hood were sterilised with 70%$^{v}/_{v}$ ethanol.

Three cell lines were used, an early colorectal cancer cell line SW480 (Dukes' type B colorectal adenocarcinoma) (Health Science Research Resources Bank, Japan), a late colorectal cancer cell line DLD-1 (Dukes' type C colorectal adenocarcinoma) (Health Science Research Resources Bank, Japan) and MCF-7 (human breast adenocarcinoma) (ATCC Cell Biology Collection, USA). These cell lines were cultured in Dulbecco's modified eagle medium: Nutrient mixture F-12 (DMEM/F-12) (Invitrogen) supplemented with heat-inactivated foetal bovine serum (FBS) (Invitrogen) prepared to a 50mL volume, at a 10%$^{v}/_{v}$ FBS/DMEM:F12, containing 100µL penicillin/streptomycin stock solution (Lonza BioWhittaker®) was added.

2.1.1 Thawing

Frozen cell lines were resuscitated by thawing after storage at -70°C and were washed in approximately 5mL of 10%$^{v}/_{v}$ culture medium. Cells were centrifuged at 800rpm for 3 minutes to remove dimethyl sulfoxide (DMSO), which is a cyroprotectant that is toxic above 4°C; therefore it is crucial that cells were thawed quickly and diluted in culture medium to reduce toxicity. The supernatant was removed and the pellet was resuspended in 10mL culture medium and mixed thoroughly by pipetting. The resuspended pellet was subsequently spilt into two small (50mL/25cm^3) culture flasks. Cells were visualised using an inverted phase contrast microscope. Cells were cultured in a 37°C incubator, providing an atmosphere of 5% CO_2 and 90% humidity. Cells were examined daily to observe the degree of confluency as well as examining for fungal or bacterial contamination.

2.1.2 Passaging/subculturing

The confluency of cells was examined, and once cells developed a complete cell sheet (80%-90% confluency) with few spaces they were ready to be subcultured. Cells were passaged every three to four days. The old medium was removed and the cell monolayer was washed in phosphate-buffered saline (PBS) (Sigma-Aldrich).

Cells were subsequently dissociated with trypsin (TrypLE^{TM} Express, Invitrogen) and incubated for 3-5 minutes in the cell incubator. Flasks were tapped gently to aid in the detachment of any remaining cells and were visualised under an inverted microscope. Once the cells had detached and the media had turned cloudy, fresh 10%$^{v}/_{v}$ FBS/DMEM:F-12 was added to neutralise the trypsin, as trypsin is inactivated by serum. The cells were then centrifuged at 800rpm for 3 minutes and the supernatant was discarded. The cell pellet was resuspended in approximately 10mL of fresh culture medium and 5mL was aliquoted into two large (75cm^3) culture flasks. Culture flasks were supplemented with 5mL of fresh culture medium, and were visualised under an inverted microscope to confirm that cells were present. The culture flasks were placed in the 37°C incubator, providing an atmosphere of 5% CO_2 and 90% humidity.

2.1.3 Cyropreservation

Once a cell line is capable of sufficient expansion, the cells can be preserved by freezing at -70°C. This allows stocks of cells to be maintained without experiencing aging as well as protecting against contamination and incubator malfunction (Freshney, 2006). Good survival of cells is favoured if there is a high density of cells at freezing (1 x 10^6 cells/mL – 1 x 10^7 cells/mL).

The old medium was removed and the cell monolayer was washed in PBS. The cells were subsequently trypsinised as above. The cell pellet was resuspended in 3mL of cyroprotective medium (Lonza) containing DMSO (Sigma-Aldrich) supplemented with 10%$^{v}/_{v}$ FBS/DMEM:F-12 (50:50). Cells were split into two 1.5mL cyropreservation tubes and stored at -70°C.

2.1.4 Harvesting cells

The old medium was removed and the cell monolayer was washed in PBS. As mentioned previously, the cells were trypsinised and the supernatant was discarded and residual supernatant was removed using a syringe or Gilson P100. The prescribed protocol for RNA extraction was then followed.

2.1.5 Cell viability assay

Cells were quantified using the Bio-Rad TC10TM automated cell counter. This is a benchtop instrument that is able to count mammalian cells through the use of autofocus technology and digital image analysis algorithms. To perform cell viability assays, one part TC10 trypan blue was

mixed with one part cell suspension on Parafilm® and 10µL was added to one of the two chambers of the TC10 counting slide. The slide was then inserted into the slide slot of the cell counter which automatically detects the slide as well as the presence of trypan blue and thereby initiates the count. The cell counter is able to determine the number of viable cells on each slide.

2.2 Drug Treatments

All information on the drugs utilised in this study is listed in Appendix 4.

2.2.1 Valproic acid

The cancer cell lines DLD-1, SW480 and MCF-7 were serum starved overnight to synchronise all cells to the G0/G1 stage, and subsequently treated with two concentrations of VPA (1.5mM and 5mM) (Sigma-Aldrich) for 24 hours. VPA was prepared at a concentration of 50mg/mL using distilled water as a solvent, which was then added to 10%$^{v}/_{v}$ FBS/DMEM:F12 to make up 1.5mM and 5mM solutions respectively. No carrier controls were required. Untreated controls contained only 10%$^{v}/_{v}$ FBS/DMEM:F12 without VPA. Cells were treated at approximately 75%-80% confluency and were pelleted and frozen as well as seeded to coverslips after 24 hours.

2.2.2 Zebularine

Each of the cancer cell lines DLD-1, SW480 and MCF-7 were serum starved overnight to synchronise all cells to the G0/G1 stage, and subsequently treated with two concentrations of ZEB (0.1mM and 0.3mM) (Sigma-Aldrich) respectively, for 24 hours. ZEB was prepared at a concentration of 5mg/mL using DMSO as a solvent, which was then added to 10%$^{v}/_{v}$ FBS/DMEM:F12 to make up a 0.1mM and 0.3mM solutions respectively. Carrier controls contained 10%$^{v}/_{v}$ FBS/DMEM:F12 with DMSO replacing ZEB. Untreated controls contained only 10%$^{v}/_{v}$ FBS/DMEM:F12 without ZEB. Cells were treated at approximately 75%-80% confluency and were pelleted and frozen as well as seeded to coverslips after 24 hours.

2.2.3 Combination treatments

Colon cancer cell lines SW480 and DLD-1 were serum starved and treated with a combination of VPA and ZEB, denoted by SYN 1 (VPA 1.5mM and ZEB 0.1mM) and SYN 2 (VPA 5mM and ZEB 0.3mM) for 24 hours. VPA was prepared at a concentration of 50mg/mL using distilled water as a solvent, while ZEB was prepared at a concentration of 5mg/mL using DMSO as a solvent. Both these drugs were then added to 10%$^{v}/_{v}$ FBS/DMEM:F12 to make up the two combination treatments, SYN1 and SYN2, respectively. Carrier controls contained 10%$^{v}/_{v}$ FBS/DMEM:F12 with DMSO replacing ZEB only. No treatment controls contained only 10%$^{v}/_{v}$ FBS/DMEM:F12 without VPA or ZEB. Cells were treated at approximately 75%-80% confluency and were pelleted and frozen as well as seeded to coverslips after 24 hours.

2.3 Total RNA Isolation

RNA extractions were performed using the RNeasy Plus Mini kit (Qiagen) for cDNA synthesis and primer optimisation, as well as the Nucleospin® RNA II kit (Separations - Macherey Nagel) for final experiments.

2.3.1 RNeasy plus mini kit

This kit is designed to purify RNA and has an additional step which eliminates whole genomic DNA contamination, which is essential for relative quantification of gene expression.

RNA was isolated following the prescribed protocol from Qiagen. A 5mL solution of RLT buffer was prepared and supplemented with reducing agent β-mercaptoethanol (β-ME) (Sigma-Aldrich) at 10µL/mL. RLT buffer allows for the disruption of plasma membranes of cells and organelles to release all RNA contained in the sample. Incomplete disruption may result in inefficient lysis and reduced RNA yields. 600µL of β-ME/RLT buffer was added to the pellet and this was resuspended under a fume hood. The lysed cells were then frozen at -70°C. RNA is stable for 7 months after the addition of β-ME/RLT buffer. When ready to proceed these lysates were thawed out at room temperature (25°C) before the next step.

A 600µL volume (maximum volume 700µL) of cell lysate was pipetted directly into a QIAshredder spin column placed in a 2mL collection tube and centrifuged at 14 000rpm for 2 minutes. The homogenised lysate was then transferred to a gDNA Eliminator spin column placed in a 2mL collection tube and subsequently centrifuged at 10 900rpm for 30 seconds. The column was discarded and the flow-through was collected. One volume of refrigerated 70%$^{v}/_{v}$ ethanol (600µL) was added to the flow-through and mixed well by pipetting.

A maximum of 700µL of the sample was transferred each time to an RNeasy spin column placed in a 2mL collection tube until the entire 1200µL volume was transferred (to maximise RNA yields). Samples were centrifuged at 10 900rpm for 15 seconds after which the flow-through was discarded and the column was retained.

700µL of buffer RW1 was added to the RNeasy column and samples were centrifuged at 10 900rpm for 15 seconds to wash the spin column membrane. The flow-through was discarded and the column was retained.

500µL of buffer RPE was added to the RNeasy column and samples were centrifuged at 10 900rpm for 15 seconds to wash the spin column membrane. The flow-through was discarded and the column was retained.

500µL of buffer RPE was added to the RNeasy column and samples were centrifuged at 10 900rpm for 2 minutes to wash the spin column membrane. The flow-through was discarded and the column was retained. The longer centrifiguation step allows the spin column membrane to dry ensuring that no ethanol is carried over during RNA elution as downstream reactions may be hindered by the presence of residual ethanol.

The RNeasy spin column was then carefully removed from the collection tube to prevent contact with the flow-through, thus preventing the carry-over of ethanol. The RNeasy spin column was placed into a new 2mL collection tube and centrifuged at 14 000rpm for 1 minute. The RNeasy spin column was subsequently placed into a new 1.5mL collection tube, and 30µL of RNase-free water was added directly to the spin column membrane. The sample was incubated at room temperature (25°C) for 5 minutes and was then centrifuged thereafter at 10900rpm for 1 minute to elute the RNA. The RNA was subsequently quantified.

2.3.2 Nucleospin® RNA II kit

The Nucleospin® RNA II kit allows for the purification of RNA and isolates RNA of high integrity, reducing the risk of degradation and DNA contamination as a result of the on-column digestion with rDNase.

RNA was isolated following the protocol provided by Macherey-Nagel. Up to 5 x 10^6 cells could be pelleted and lysed by 350µL of buffer RA1 supplemented with 3.5µL of reducing agent β-ME. A total volume of 353.5µL of β-ME/RA1 was added to the cell pellet and vortexed vigorously. Cells were frozen at -70°C as RNA is stable for 7 months after the addition of β-ME/RA1 buffer. When ready to proceed, these lysates were thawed out at room temperature (25°C) before the next step.

The entire quantity of lysate was filtered through a Nucleospin® filter placed in a collection tube to reduce viscosity, and the mixture was centrifuged at 11000rpm for 1 minute. The Nucleospin® filter was discarded and 350µL ethanol (70%$^{v}/_{v}$) was added to the homogenised lysate to adjust RNA binding condtions. This was mixed by pipetting up and down about five times or by vortexing for about 5-10 seconds. The addition of ethanol leads to a stringy appearance of the solution, which needs to be disaggregated by mixing.

The total volume of ethanol was passed through a Nucleospin® RNA II column placed in a collection tube. Once the lysate was thoroughly mixed, it was loaded to the column and centrifuged for 30 seconds at 11000rpm to allow the binding of RNA to the column.

The column was placed in a new collection tube to which 350µL of membrane desalting buffer (MDB) was added and this was centrifuged at 11000rpm for 1 minute to allow the membrane to dry. Salt removal allows for more efficient DNA digestion.

The rDNase provided in a vial was reconstituted with 540µL RNase-free water. A DNase reaction mixture was prepared in a sterile 1.5mL tube where 10µL of reconstituted rDNase was added to 90µL of reaction buffer for rDNase and was mixed by flicking the tube. Subsequently, 95µL of this DNase reaction mixture was added directly to the centre of the silica membrane of the column. This was incubated for 15 minutes at room temperature (25°C).

The silica membrane was subsequently washed and dried through three washes. The initial step involved the addition of 200µL buffer RA2 to the Nucleospin® RNA II column in order to inactivate the rDNase. This was centrifuged at 11000rpm for 30 seconds. The column was then placed in a new collection tube, to which 600µL of buffer RA3 was added to the column to wash away any residual buffer added to the column in the previous wash, and this was centrifuged at 11000rpm for 30 seconds. The column was once again placed in a new collection tube to which 250µL of buffer RA3 was added to wash away all residual buffer that may still be present on the column; and to dry the membrane completely, this was centrifuged at 11000rpm for 2 minutes. The Nucleospin® RNA II column was then placed in a nuclease-free collection tube.

The last step involved the addition of 40µL RNase-free water to the column and this was incubated at room temperature (25°C) for 5 minutes to allow absorption into the membrane. The sample was then centrifuged at 11000rpm for 1 minute. Elution in a smaller volume of water allows a higher yield of RNA, thus 40µL was used instead of the recommended 60µL. The RNA was subsequently quantified.

2.3.3 RNA quantification

The quality of RNA was then assessed using a Nanodrop ND-1000 spectrophotometer which measures the optical density of the sample RNA. RNA of good quality displays an OD 260/280 ratio of 1.8 to 2.1 (a ratio below this indicates protein contamination and a ratio above this suggests the RNA has degraded) and an OD 260/230 ratio of 1.8 or greater (a ratio below this signifies salt contamination). The ND-1000 also assesses the concentration of RNA within a sample where an optimal concentration of 1000ng/µL or greater is generally used for relative quantification.

2.4 Total DNA Isolation

DNA extractions were performed using the QIAamp DNA Micro kit (Qiagen) for subsequent methylated and hydroxymethylated DNA quantification, as described in Chapter 4.

2.4.1 QIAamp DNA micro kit

This kit is designed to allow optimal purification of genomic and mitochondrial DNA from small sample volumes and prevents cross contamination between samples.

DNA was isolated following the protocol from Qiagen. 180µL buffer ATL was added to the pelleted sample and was transferred into a 1.5mL tube and left to stand until it reached room temperature (25°C), after which 20µL proteinase K was added and mixed by pulse-vortexing for 15 seconds. The sample was placed in a heated orbital incubator and kept overnight at 56°C until the sample was completely lysed.

Following lysis, 200mL buffer AL was added to allow optimal binding of DNA to the membrane and mixed by pulse-vortexing for 15 seconds. The lysate was transferred into a QIAshredder spin column and was centrifuged for 2 minutes at full speed (14000rpm). Subsequently, 200µL ethanol (96%-100%) was added to the lysate and pulse-vortexed for 15 seconds and was incubated for 5 minute at room temperature (25°C). The tube was briefly centrifuged to remove liquid from the lid. The lysate was transferred to a QIAamp MinElute column and centrifuged for 1 minute at 8000rpm.

The column was placed in a clean 2mL collection tube and the collection tube containing flow-through was discarded, after which 500µL buffer AW1 was added to the QIAamp MinElute column and centrifuged for 1 minute at 8000rpm. The column was placed in a clean 2mL collection tube and the collection tube containing flow-through was discarded. Subsequently, 500µL buffer AW2 was added to the QIAamp MinElute column and centrifuged for 1 minute at 8000rpm. The column was placed in a clean 2mL collection tube and the collection tube containing flow-through was discarded. Both buffers AW1 and AW2 wash away any contaminants that may be bound to the membrane.

The column was centrifuged at full speed (14000rpm) for 3 minutes to dry the membrane. The MinElute column was placed in a clean 1.5mL microcentrifuge tube and the collection tube containing flow-through was discarded. Subsequently, 30µL distilled water was carefully added to the centre of the membrane and incubated at room temperature (25°C) for 1 minute, and was centrifuged for 1 minute at full speed (14000rpm) to elute the DNA. The DNA was then quantified.

2.5 Methylated DNA Quantification

The MethylFlash™ Methylated DNA Quantification Kit (Epigentek) was used in conjunction with the MethylFlash™ Hydroxymethylated DNA Quantification Kit (Epigentek) to accurately and rapidly detect global DNA methylation status as well as DNA hydroxymethylation status (as described in Chapter 4) using an immunospecific detection method on a 96-stripwell microplate. This was achieved by measuring levels of 5-methylcytosine (5-mC) as well as 5-hydroxymethylcytosine (5-hmC). These kits ensure no cross-reactivity to hydroxymethylcytosine and unmethylated cytosine.

2.5.1 MethylFlash™ methylated DNA quantification kit (colorimetric)

In this assay, strip wells have a high DNA affinity to allow the binding of DNA, and the methylated portion of DNA is identified through the use of capture and detection antibodies and is then

quantified through a colorimetric analysis by reading the absorbance of a spectrophotometer, where the amount of methylated DNA is directly proportional to the OD intensity measured. An optimal amount of DNA that may be used is 100ng per reaction. To prepare a standard curve, buffer ME4 was diluted as seen in Table 2.1.

Table 2.1 Standard curve preparation using five different concentrations of ME4 buffer after diluted to 10ng/µL

Tube	ME4 (10ng/µl)	1x TE	Final ME4 Concentration
1	1.0µL	19.0µL	0.5ng/µL
2	1.0µL	9.0µL	1.0ng/µL
3	1.0µL	4.0µL	2.0ng/µL
4	2.5µL	2.5µL	5.0ng/µL
5	4.0µL	0.0µL	10.0ng/µL

All samples were performed in duplicate and DNA was bound to the strip wells. 80µL of binding solution ME2 and 1µL of buffer ME3 was added to each strip well respectively. 1µL of diluted ME4 was subsequently added according to Table 2.1, after which 1µL-8µL of sample DNA was added at 100ng, and the solution was mixed by gently tilting the plate several times or lightly shaking it to ensure the solution coated the bottom of the well evenly. The strip was then covered using Parafilm® and incubated at 37°C for 90 minutes. The ME2 binding solution was then removed from each well, which was washed three times with 150µL of diluted ME1 1X wash buffer.

To capture methylated DNA, buffer ME5 was diluted at a ratio of 1:1000 with diluted ME1, and 50µl was added to each well and incubated at room temperature (25°C) for 60 minutes. Diluted ME5 was removed from each well which was washed three times with 150µL of diluted ME1. Buffer ME6 was diluted at a ratio of 1:2000 with diluted ME1, and 50µl was added to each well and incubated at room temperature (25°C) for 30 minutes. Diluted ME6 was removed from each well which was washed four times with 150µL of diluted ME1. Buffer ME7 was diluted at a ratio of 1:5000 with diluted ME1, and 50µL was added to each well and incubated at room temperature (25°C) for 30 minutes. Diluted ME7 was removed from each well which was washed five times with 150µL of diluted ME1.

For signal detection, 100µL of buffer ME8 was added to each well and incubated at room temperature (25°C) for 1 to 10 minutes in the absence of light. Colour changes were monitored in both sample and control wells. The ME8 solution turned blue in the presence of ample methylated DNA, and once the positive control turned medium blue, 50µL of buffer ME9 was added to each well to stop the enzyme reaction. This generated a yellow colour change and the absorbance was subsequently read on a plate reader (ELX 800 Universal Plate Reader) at wavelength of 450nm, within 15 minutes of the reaction. Colour development for methylated DNA quantification can be seen in Figure 2.1

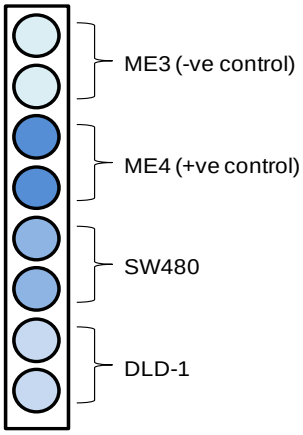


Figure 2.1 Schematic illustration of results demonstraing colour development associated with methylation (5-mC) patterns. SW480 cells displayed a brighter colour change than DLD-1 cells, indicating a greater probability of gene methylation.

2.5.2 MethylFlash™ hydroxymethylated DNA quantification kit (colorimetric)

The protocol for this assay was highly similar to the Methylated DNA Quantification kit. An optimal amount of DNA that may be used is 200ng per reaction. To prepare a standard curve, buffer HC5 was diluted as seen in Table 2.2.

Table 2.2 Standard curve preparation using five different concentrations of HC5 buffer after diluted to 10 ng/µL

Tube	HC5 (10ng/µL)	1x TE	Final HC5 Concentration
1	1.0µL	19.0µL	0.5ng/µL
2	1.0µL	9.0µL	1.0ng/µL
3	1.0µL	4.0µL	2.0ng/µL
4	2.5µL	2.5µL	5.0ng/µL
5	4.0µL	0.0µL	10.0ng/µL

All samples were prepared in duplicate and DNA was bound to the strip wells. Initially, 80µL of binding solution HC2 was added to each well, followed by 1µL of buffer HC3 and 1µL HC4 respectively. Subsequently, 1µL of diluted HC5 was added according to Table 2.2. 1µL-8µL of sample DNA was added at 200ng, and the solution was mixed by gently tilting the plate several times or lightly shaking it to ensure the solution coated the bottom of the well evenly. The strip was then covered using Parafilm® and incubated at 37°C for 90 minutes. The HC2 binding solution was then removed from each well, which was washed three times with 150µL of diluted ME1 1X wash buffer.

In order to capture hydroxymethylated DNA, buffer HC6 was diluted at a ratio of 1:1000 with diluted HC1, and 50µL was added to each well and incubated at room temperature (25°C) for 60 minutes. Diluted HC6 was removed from each well which was washed three times with 150µL of diluted HC1. Buffer HC7 was diluted at a ratio of 1:1000 with diluted HC1, and 50µL was added to each

well and incubated at room temperature (25°C) for 30 minutes. Diluted HC7 was removed from each well which was washed four times with 150µL of diluted HC1. Buffer HC8 was diluted at a ratio of 1:5000 with diluted HC1, and 50µL was added to each well and incubated at room temperature (25°C) for 30 minutes. Diluted ME7 was removed from each well which was washed five times with 150µL of diluted HC1.

For signal detection, 100µL of buffer HC9 was added to each well and incubated at room temperature (25°C) for 1 to 10 minutes in the absence of light. Colour changes were monitored in both the sample well and the control wells. The HC9 solution turned blue in the presence of sufficient hydroxymethylated DNA, and once the positive control turned medium blue, 50µL of buffer HC10 was added to each well to stop the enzyme reaction. This generated a yellow colour change and the absorbance was subsequently read on a plate reader at 450nm within 15 minutes of the reaction. Colour development for hyrdoxymethylated DNA quantification can be seen in Figure 2.2

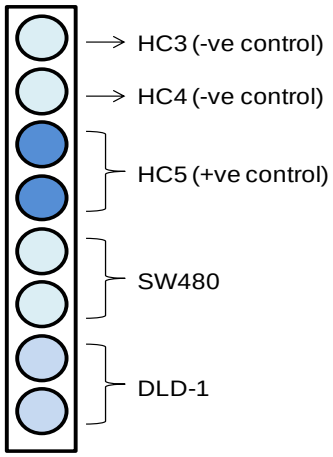


Figure 2.2 Schematic illustration of results showing colour development associated patterns with hydroxymethylation (5-hmC) patterns. DLD-1 cells displayed a brighter colour change than SW480 cells, indicating a higher likelihood of gene hydroxymethylation.

2.6 Primer Design

PCR primers are oligonucleotide sequences which hybridise to opposite strands and flank the gene region of interest within target DNA. When designing primers for PCR, it is crucial to ensure that they do not contain complementary bases within themselves or with other primers. One should evade 3' end complementarity to prevent the formation of primer-dimers or primer-oligomers. Primers are recommended to begin with ATG and end with either G or C bases as these are triple bonded.

The essential gene sequences were derived from http://www.ensemble.org and the exonic gene sequences were isolated from the complete sequence and confirmed using the BLAST program at http://www.ncbi.nlm.nih.gov and BLAT (http://genome.UCSC.edu/). These programs examine the homology of the primer sequence and match it to the correct chromosome and gene. Once it was confirmed that the primers only bind to the target gene they were mapped to the exonic gene

sequences and their quality as a pair were analysed using PRIMER DESIGNER for Windows Version 2.0 Serial # 53110. This program checks for the presence of hairpins, dimers and also assesses whether the melting temperatures (T_m) match. The concentration of primers was calculated by applying Equation 2.1.

$$(xOD/mL)(33\mu g/OD) = y\mu g/mL$$
$$\frac{y\mu g/mL}{M.w.(da)} = znmole/\mu L$$

[Equation 2.1]

To calculate molecular weight (M.w.) Equation 2.3 was employed.

$$M.w. = [(A\times 312.2)+(G\times 328.2)+(C\times 288.2)+(T\times 303.2)]-61$$

[Equation 2.2]

The T_m of each primer was calculated by applying Equation 2.3.

$$T_m = 4(G+C)+2(A+T)$$

[Equation 2.3]

Table 2.3 Primer sequences, melting temperatures, amplicon sizes and gene accession numbers for the various genes used in this study

Gene	Fwd Primer (5' – 3')	Rvs Primer (5' – 3')	T_m (Fwd & Rvs) and Amplicon Size	REF	Gene Accession Number
β-actin (ACTB)	GCACACTTAGCC TTCTTTGCACTT TCT	AGGCGTACAGG GATAGCACAGC CTGGATAG	64°C 172bp	Acc and Okuliez, 1995	OTTHUMG00 000023268
KLF4	ACCAGGCACTAC CGTAAACACA	GGTCCGACCTG GAAAATGCT	60°C 79bp	_____	ENSG000001 36826
β-catenin (CTNNB1)	GCTGGGACCTT GCATAACCTT	ATTTTCACCAGG GCAGGAATG	60°C 86bp	_____	ENSG000001 68036

2.7 Reverse Transcription

The Applied Biosystems TaqMan® Reverse Transcription Reagents kit was used to perform all reverse transcription reactions. The kit contained the reaction mix demonstrated in Table 2.4.

Table 2.4 Reverse transcription reagents and volumes

Reagent	1x	-RT
10x RT buffer	1µL	1µL
$MgCl_2$	2.2µL	2.2µL
dNTPs	2µL	2µL
Random Hexamer	0.5µL	0.5µL
RNase Inhibitor	0.2µL	0.2µL
Multiscribe Reverse Transcriptase	0.25µL	———
H_2O	3.85µL	4.1µL
RNA		
TOTAL VOLUME	10µL	10µL

Reverse transcription:

1. 25°C for 10 minutes
2. 48°C for 30 minutes
3. 95°C for 5 minutes

4°C hold infinity

2.8 PCR Optimisation

For this study two types of PCR were performed, namely conventional PCR and real-time PCR.

2.8.1 Conventional PCR

Conventional PCR was performed to simply optimise primers and ensure they were effective. For this the Applied Biosystems PCR Core Reagent kit was utilised containing the reaction mix in Table 2.5 and a gradient PCR was carried out.

Table 2.5 PCR core kit master mix

Reagent	1x
10x buffer A	1µL
$MgCl_2$ (1.5mM)	1µL
dNTPs (10mM)	0.2µL
FWD primer (2 µM)	1µL
RVS primer (2 µM)	1µL
Taq polymerase (COnc)	0.07µL
H_2O	5.73µL
cDNA	
TOTAL VOLUME	10µL

Commercially produced Sabax (Adcock Ingram) was used in 2mL vials. The template cDNA reverse transcribed from an RNA template was of high quality and yield ranged from 200ng/µL to 400ng/µL. The PCR products were visualised and analysed using a 1.5%$^{w}/_{v}$ agarose gel stained with ethidium bromide (see recipe in Appendix 3). Gradient PCR followed the following series of cycles:

1. 94°C for 10 minutes
2. 94°C for 1 minute
3. Specified gradient for 45 seconds
   (time can be reduced to 15 seconds to allow for more specific primer binding)
   Eg. Lower temperature of 55°C
   Upper temperature of 65°C
4. 72°C for 1 minute
5. 4°C hold forever

Repeat for 34 cycles

2.8.2 Real-time – PCR

Primers for Real-time (RT)-PCR were optimised and final experiments were performed on the Applied Biosystems Informatics (ABI) 7500 real-time PCR machine. The reference gene of interest used in all experiments was β-actin. SYBR® Green I dye (Applied Biosystems) was used to detect PCR product. Amplification and dissociation curves (essentially replaces the end point gel, where distinct melting curves characterise each PCR product) were performed for each sample. An absolute quantification was carried out for primer optimisation while the final experiment was performed using a relative quantification (plate) to assess the change in expression between the treatment group and the untreated control for each sample.

Table 2.6 SYBR Green master mix

Reagent	1x
2 x PCR master mix	5µL
FWD primer (2µM)	1µL
RVS primer (2µM)	1µL
cDNA	3µL
TOTAL VOLUME	10µL

The amplification curve followed the cycle:

Hot start at 94°C for 10 minutes

1. 94°C for 1minute
2. 55°C for 45 seconds
3. Appropriate primer melting temperature for 1 minute

Repeat for 35 cycles

The dissociation curve followed the cycle:

1. 95°C for 15 seconds
2. 60°C for 1 minute
3. 95°C for 15 seconds

} Repeat for 1 cycle

2.9 Microscopy

2.9.1 Seeding cells onto coverslips

Prior to the experiment, glass coverslips were soaked in 70%$^{v}/_{v}$ ethanol for a maximum of 30 minutes. Cells were cultured, harvested and pelleted as described previously. To resuspend the pellet, 6mL of 10%$^{v}/_{v}$ FBS/DMEM:F12 was added, of which 1mL of the resuspended pellet was diluted with approximately 8mL of 10%$^{v}/_{v}$ FBS/DMEM:F12. Each coverslip was held in a flame using forceps, heat sterilising and placed within the centre of a sterile petri dish. The suspended cells were then carefully transferred directly onto each coverslip to prevent spilling into the petri dish. The petri dishes were stored in a 37°C incubator, providing an atmosphere of 5% CO_2 and 90% humidity, for the cells to attach to the coverslips. After approximately five hours, 10%$^{v}/_{v}$ FBS/DMEM:F12 was added to the petri dishes to ensure the submersion of each coverslip. Fresh cell solution was prepared with the excess cells, which were transferred into two new culture flasks and incubated at 37°C in an atmosphere of 5% CO_2 and 90% humidity.

2.9.2 Fixing cells to the coverslips

After approximately 24 hours, a 3%$^{v}/_{v}$ formaldehyde/PBS solution was prepared from a 30%$^{v}/_{v}$ solution of formaldehyde (Univar) under a fume hood. The culture medium was removed and the cells rinsed three times with PBS. The PBS was discarded into a waste container under the fume hood and the 3%$^{v}/_{v}$ fixative solution was added to the coverslips at 1mL-1.5mL and kept at room temperature (25°C) for 15 minutes. The fixative was then poured off and the coverslips were washed three to four times with PBS. PBS was then added to the petri dishes containing the fixed cells, after which the dishes were sealed with Parafilm® and were stored in the 4°C fridge until the next step.

2.9.3 Immunofluorescence

2.9.3.1 *Incubation of fixed cells with primary antibody.*

A 0.5%$^{w}/_{v}$ bovine serum albumin (BSA) solution was prepared in 100mL of PBS. 125µL of triton X (Sigma-Aldrich) was added to 50mL of 0.5%$^{v}/_{v}$ BSA/PBS to make up a 0.25%$^{v}/_{v}$ solution of triton X. PBS was discarded from the petri dishes containing coverslips with fixed cells, and the 0.25%$^{v}/_{v}$ triton X/BSA solution was added to the petri dishes for 10 minutes. Triton X is a detergent that permeabilises the cell membrane and allows the primary antibody to enter the cell; thus one must be cautious when working with this solution to prevent contact with skin. The triton X was then

carefully discarded and 0.5%$^{v}/_{v}$ BSA/PBS was added to each petri dish. The coverslips were then drained of excess liquid and were subsequently transferred onto a dry labelled slide, with the cell side uppermost. A 1:100 dilution of primary antibody was prepared with 0.5%$^{v}/_{v}$ BSA/PBS and 100µL of each primary antibody solution was added to the coverslips. KLF4 rabbit polyclonal IgG and purified mouse anti β-catenin primary antibodies were used (information on antibodies in Appendix 3). Slides containing coverslips were incubated overnight at 4°C in a moist container lined with wet filter paper.

2.9.3.2 *Incubation of cells with secondary antibody*

After 24 hours, three 50mL beakers were filled with approximately 30mL of 0.5%$^{v}/_{v}$ BSA/PBS. Using fine forceps, each coverslip was removed from each slide and drained onto tissue paper to remove excess liquid. The coverslips were then sequentially dipped approximately ten times into each beaker containing 0.5%$^{v}/_{v}$ BSA/PBS to remove any residual primary antibody. The coverslips were then transferred back onto the slides, with the cell side facing upwards.

Alexa Fluor® 568 conjugated donkey anti-rabbit (KLF4) and Alexa Fluor® 568 conjugated donkey anti-mouse secondary antibodies (see Appendix 3) were prepared in a 1:200 dilution with 0.5%$^{v}/_{v}$ BSA/PBS, after which 100µL of secondary antibody was added to each coverslip. Slides containing coverslips were stored in a container lined with wet filter paper for 1 hour at room temperature (25°C) in a dark cupboard. Each coverslip was then removed from each slide and drained onto tissue paper to remove excess liquid and rinsed as described.

2.9.3.3 *Fluorescent staining of the actin cytoskeleton and nucleus*

The coverslips were then transferred back onto the slides, cell side up after drying and 100µL of Phalloidin was added to each coverslip. A 1:20 dilution of Alexa Fluor® 488 Phalloidin conjugate (Lonza) was prepared with 0.5%$^{v}/_{v}$ BSA/PBS. Phalloidin is a green-fluorescent dye which binds specifically at the interface between F-actin subunits securing adjacent subunits together. Slides containing coverslips were incubated in a moist container for 30-45 minutes at room temperature (25°C) in a dark cupboard, as Phalloidin is light sensitive. Each coverslip was then removed from each slide and drained onto tissue paper. The coverslips were then dipped approximately ten times into each beaker containing 0.5%$^{v}/_{v}$ BSA/PBS to remove any residual Phalloidin.

The coverslips were then transferred back onto the slides cell side up and 100µL of DAPI (Boehringer Mannheim) was added to each coverslip. A 1:10 000 dilution of DAPI was prepared with PBS. DAPI or 4',6-diamidino-2-phenylindole is a blue-fluorescent nuclear stain which preferentially stains double-stranded DNA and nuclei with little or no labelling of the cytoplasm. Slides containing coverslips were stored in a container lined with wet filter paper for 30-45 minutes at room temperature (25°C) in a dark cupboard as DAPI is light sensitive. Each coverslip was then removed from each slide and drained onto tissue paper to dry. The coverslips were then dipped

approximately ten times into each beaker containing 0.5%$^{v}/_{v}$ BSA/PBS to remove any residual DAPI. Coverslips were then mounted onto the slides cell side down using Gel Mount^{TM} aqueous mounting medium (Sigma-Aldrich). Coverslips were left to set and stored at 4°C until they were ready to be viewed under the Olympus IX71 and Zeiss laser scanning microscope, using a 63X objective (see software information in Appendix 3).

CHAPTER 3
HISTONE MODIFICATIONS

3.1 Introduction

Tumourigenesis is a consequence of genetic mutations leading to a loss-of-function or gain-of-function in cancer genes such as tumour suppressor or proto-oncogenes. In addition to this, there has been evidence that epigenetics plays a role in tumour development and in this chapter, one specific aspect of epigenetics will be discussed. Waddington originally defined epigenetics as "the casual interactions between genes and their products, which bring the phenotype into being", implicating the effects of chromatin modifications on gene expression (Waddington, 1942). Post-translational alterations in chromatin structure, in particular histone hyperacetylation and deacetylation, are crucial in the regulation of gene expression, however they may also lead to the inception of neoplasia (Archer and Hodin, 1999). These modifications may also include the methylation, phosphorylation, acetylation and ubiquitination of histone N-termini (Jenuwein, 2001; Wade *et al.*, 1997; Shilatifard, 2006). Hyperacetylation of histones is associated with the active transcription of genes leading to their expression, while hypoacetylation or histone deacetylation may result in the silencing of genes (Kochbin *et al*., 2001; Gray and Ekstrom, 2001; Umov and Wolffe, 2000; Marks *et al.*, 2000).

3.1.1 An overview of histone modifications

3.1.1.1 *The structure and organisation of chromatin*

Chromatin is organised in two types of structures which is determined according to the posttranslational modification. Loosely packed chromatin known as euchromatin is associated with actively transcribed genes, while compact chromatin contains silenced genes, as transcription factors are blocked from attaching and is known as heterochromatin (Jenuwein and Allis, 2001; Zheng and Hayes, 2003; Elgin, 1996). Heterochromatin is characterised by its low density of genes and abundance of repetitive sequences (Thiagalingam *et al.*, 2003). Chromatin is composed of building blocks known as nucleosomes, which are octamers of four core histone proteins, namely a tetramer of H3 and H4, as well as dimers of H2A and H2B, where each octamer is surrounded by a 146bp stretch of DNA as seen in Figure 3.1 (Strahl and Allis, 2000; Luger and Richmond, 1998). Histones generally comprise of two domains, a globular domain and an N-terminal tail that projects from the nucleosome that is post-translationally altered (Jenuwein and Allis, 2001).

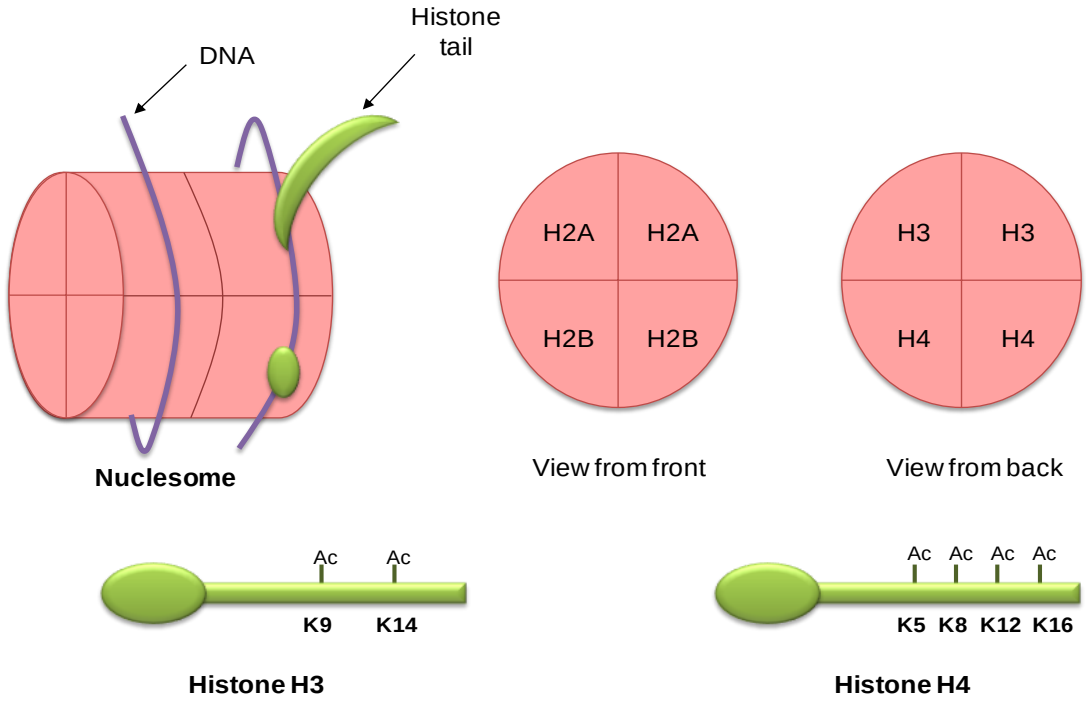


Figure 3.1 Schematic view of a nucleosome. Histones are indicated in pink, green represents the histone tail and purple shows DNA wound around the nucleosome. The histone tail of the nucleosome is acetylated, thus the chromatin structure is loosened which is characteristic of euchromatin. Histones H3 and H4 and their acetylated lysine residues are displayed (revised from De Ruiter *et al.*, 2003).

3.1.1.2 *Histone acetylation and deacetylation*

The most important chromatin modifications involved in the regulation of gene transcription, cell cycle progression as well as DNA replication, are acetylation and deacetylation of histone proteins (Wolffe and Guschin, 2000; Marzio *et al.*, 2000; Iizuka and Stillman, 1999). Histone acetylation involves the transfer of acetyl groups to the ε-amino group of histone lysine residues that are highly conserved and positively charged. This is catalysed by HATs, while HDACs restore the positive charge of histones by removing acetyl groups from lysine side chains in a reaction known as deacetylation (Shankar and Srivastavar, 2008; De Ruiter *et al*., 2003). Histone H3 may be acetylated at the two lysine positions, K9 and K14, whereas H4 acetylation takes place at positions K5, K8, K12, and K16 as displayed in Figure 3.1 (Bjerling *et al.*, 2002). Histone hyperacetylation is associated with enhanced gene transcription while deacetylation results in chromatin condensation and thus the silencing of target genes, such as tumour suppressors which may lead to tumourigenesis (Johnstone and Licht, 2003; Strahl and Allis, 2000).

3.1.1.3 *Characterisation of histone deacetylases*

There are eighteen HDACs in total that are divided into several different classes, distinguishable by their structural properties as well as their homology to yeast proteins. HDACs 1, 2, 3 and 8 are Class I HDACs and are localised in the nucleus of all human tissues. Class II HDACs are divided into Class IIa (HDAC 4, 7 and 9) and Class IIb (HDAC 6 and 10) and are localised in both the nucleus and the cytoplasm; and HDAC 11 is classified as a Class IV HDAC. Class III HDACs are also known as sirtuins (SIRT1-7) (Pollock and Richon, 2009). Class I, II and III HDACs display homology to yeast proteins Rpd3, Hda1 and Sir2 respectively (Pollock and Richon, 2009). Class I,

II and IV HDACs are dependent on co-factors binding to their active site, in this case this is Zn^{+2}, and are suppressed by Zn^{+2}-binding inhibitors such as Trichostatin A (TSA) and Vorinostat (SAHA), while Class III HDACs require the binding of NAD^{+} as a co-factor (Blander and Guarente, 2004). Figure 3.2 displays several isoforms of the different HDAC proteins.

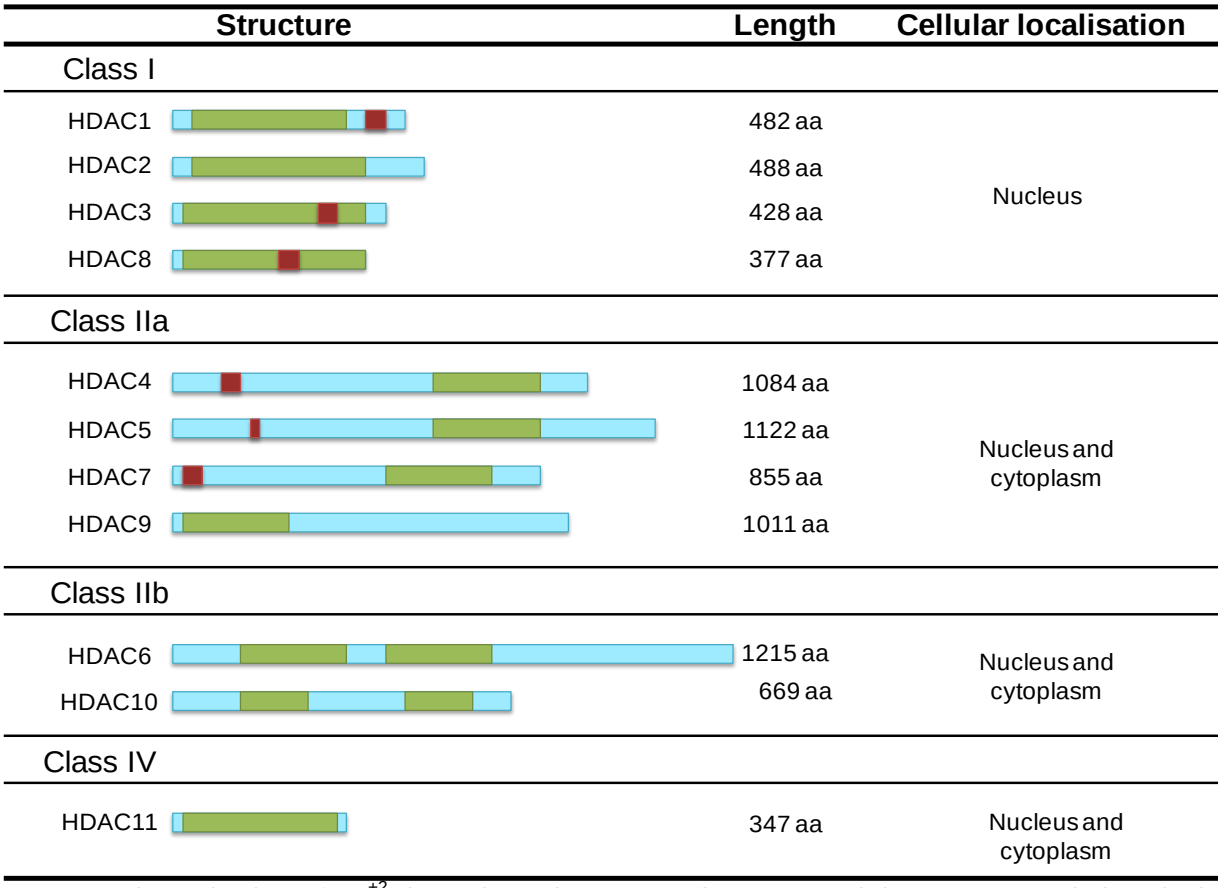


Figure 3.2 Schematic view of Zn^{+2} dependent Class I, II and IV HDACs (Class III HDACs being sirtuins), illustrating their varying lengths and localisation. The green areas represent the catalytic domains containing Zn^{+2} and the red regions are nuclear localisation sequences (NLS) (Kim and Bae, 2011; De Ruiter *et al.*, 2003).

3.1.1.4 *Histone deacetylases in cancer*

Histone modifications such as acetylation are often found to repress cancer, and tumourigenesis is characterised by a loss of histone acetylation, a frequent case in most cancers is the loss of K16 acetylation (Fraga *et al.*, 2005). There is some evidence that altered HDAC expression may lead to cancer, where several studies show that an increase in HDAC 1, HDAC 3 and HDAC 6 activity may lead to the induction of colon and breast cancer (Wilson *et al.*, 2006; Zhang *et al.*, 2005). An overexpression of HDACs in tumour suppressor genes at the promoter may block these regions from the binding of transcription factors leading to the onset and progression of cancer as seen in Figure 3.3 (Gui *et al.*, 2004). It was also found that a mutation in HDAC 2 leading to its loss of expression resulted in hereditary non-polyposis colorectal carcinoma (Ropero *et al.*, 2006). There has also been evidence that SIRT1 of the Class III HDACs has been down-regulated in colon cancers thereby displaying loss of acetylation of K9 of H3 and K16 of H4 which are substrates of SIRT1 (Ozdag *et al.*, 2006; Fraga *et al.*, 2005).

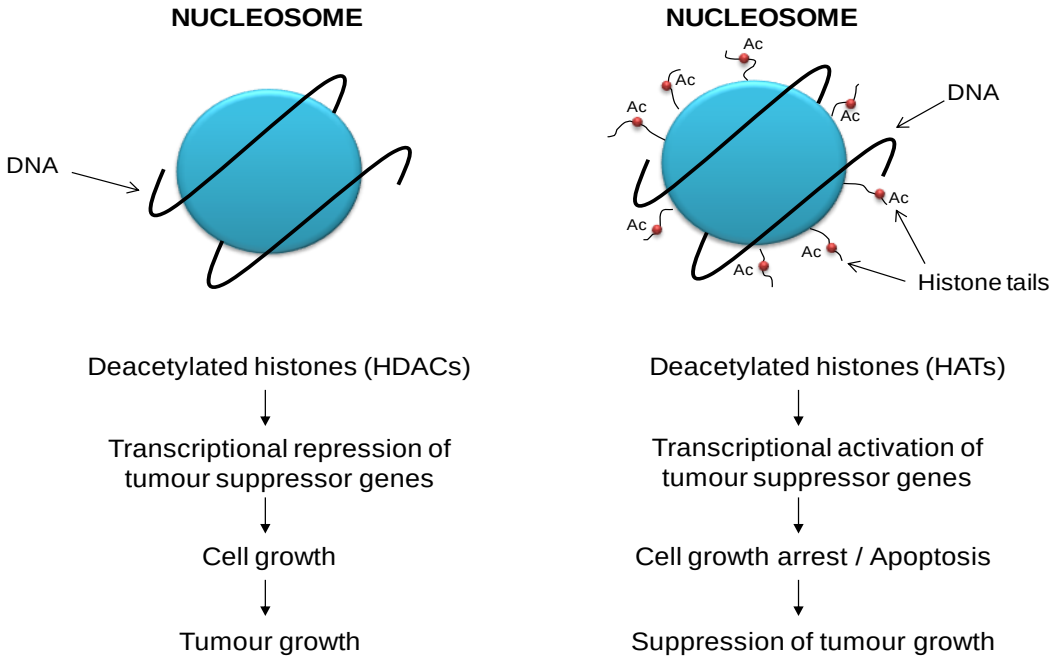


Figure 3.3 Mechanism of action of HDACs and HATs. A higher expression of HDACs may lead to the onset and progression of tumour growth. However, a lower concentration of acetyl groups on histone proteins may lead to the inhibition of tumour growth and thus apoptosis and cell cycle arrest (adapted from Marks *et al.,* 2000).

3.1.2 Epigenetic therapy by histone deacetylase inhibitors

In cancer, low levels of acetylation are associated with neoplasia, in particular tumour growth and metastasis, where reduced levels of H4 acetylation was found to be an important feature of gastric cancer (Song *et al.*, 2005; Toh *et al.*, 2004). This is a result of histone deacetylation via the action of HDACs, which seems to be linked to tumourigenesis (Yasui *et al.*, 2003). Epigenetic treatment by means of histone deacetylase inhibitors (HDACi) may induce cell differentiation, cell cycle arrest as well as apoptosis by inhibiting metastasis of cancer cells, and functions by inhibiting HDACs thus increasing the number of acetylated proteins, especially histones. This in turn up-regulates epigenetically silenced tumour suppressor genes thus exerting anti-proliferative effects on cells (Joseph *et al.*, 2004). HDAC inhibitors also function through the inhibition of angiogenesis by suppressing pro-angiogenic genes and inducing the transcription of anti-angiogenic genes (Kim *et al.*, 2001).

3.1.2.1 *Classification of HDAC inhibitors*

There are five distinct classes of HDAC inhibitors that are structurally classified, namely hydroxamic acids, short-chain fatty acids, cyclic tetrapeptides, cyclic peptides and benzamides (Marks *et al.*, 2001). Examples of hydroxamic acid based inhibitors are TSA, the first natural hydroxamic inhibitor of HDACs, and Vorinostat (SAHA), the first HDAC inhibitor approved for clinical use by the Food and Drug Administration (Yoshida *et al.*, 1990; Duvic *et al.*, 2007). Both are highly potent and known to inhibit Class I and II HDACs (Marks and Breslow, 2007). Short-chain fatty acids are the butyrates, such as sodium butyrate, however are an unfavourable choice due to their low potency and their lack of specificity (Newmark, *et al.*, 1994; Carducci *et al.*, 1997). Another class of compounds, the cyclic tetrapeptides contain a 2-amino-8-oxo-9,10-epoxy-

decanoyl (AOE) moiety, while cyclic peptides do not. Trapoxin is a cyclic tetrapeptide that binds to HDACs via the epoxide group and so inhibiting HDAC activity; while Apicidin, a cyclic peptide, induces cell cycle arrest by up-regulating p21/$^{WAF1/CIP1}$ and leads to an abundance of hyperacetylated histone H4. Both inhibitors are a product of fungal metabolism (Yoshida and Horinouchi, 1999; Kim *et al.*, 2000; Han *et al.*, 2000). Yet another modulating agent is MS-27-275, a benzamide that leads to an accumulation of hyperacetylation of histones H3 and H4 (Lee, 2001).

3.1.3 Valproic acid as a histone deacetylase inhibitor

VPA (N-dipropylacetic acid) also known as valproate was initially synthesised in 1882 by Burton and was found to display antiepileptic properties by Eymard in 1963 (Burton, 1882; Meunier *et al.*, 1963). Since then it has been used to treat a number of disorders such as bipolar syndrome and migraines (Rosenberg, 2007). As illustrated in Figure 3.4, VPA is an eight branched short-chain fatty acid that is highly stable in organic solvents at room temperature (25°C) and is easily transported to its target cells (Balbi *et al.*, 1991). It quickly distributes itself throughout the organism *in vivo* and binds to over 90% of plasma proteins (Johannessen and Johannessen, 2003). VPA has been found to exhibit strong antitumour effects by inhibiting GSK-3β activity by phosphorylating Ser9 thereby suppressing β-catenin and activating the Wnt pathway (Gould *et al.*, 2004; Gould and Manij, 2002; Bug *et al.*, 2005; Doble and Woodgett, 2003).

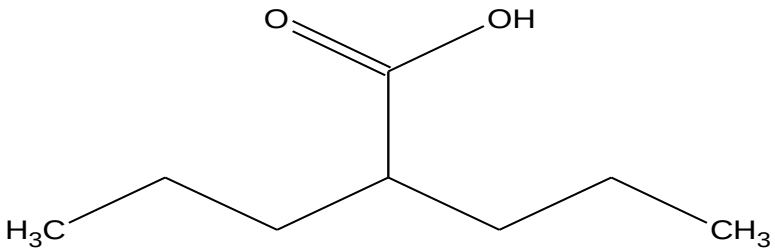


Figure 3.4 Chemical structure of VPA (2-propylpentanoic acid), an eight branched short-chain fatty acid (Hrebackova *et al.*, 2010).

VPA also promotes anti-tumourigenesis through the inhibition of HDACs Classes I and II, specifically HDACs 1, 2, 3, 4 and 8 (Phiel *et al.*, 2001). It binds to the catalytic domain of HDACs leading to the hyperacetylation of histone proteins H3 and H4 (Gottlicher *et al.*, 2001; Carew *et al.*, 2008). VPA was discovered to inhibit HDAC1 dose-dependently *in vitro*, where it inhibits all Class I HDACs (1-3) at a lower dose, while inhibiting Class IIa HDACs (4, 5 and 7) at higher doses and has no effect on Class IIb (6 and 10) HDACs whatsoever (Gurvich *et al.*, 2004). It therefore suppresses tumour growth by inducing cell differentiation and cell cycle arrest, as well as inhibiting angiogenesis (Gurvich *et al.*, 2004). This evidence suggests that VPA is a valuable epigenetic therapy in the prevention of cancer.

3.1.4 Experimental approach

The purpose of this chapter was to evaluate the expression levels of KLF4 and CTNNB1 following the epigenetic modulation of chromatin. Here, the early and late stage colorectal, as well as the

breast adenocarcinoma cell lines were treated with two doses of VPA for approximately 24 hours, and a relative quantification of KLF4 and CTNNB1 expression was performed applying the $2^{-\Delta\Delta Ct}$ method to analyse relative gene expression. Subsequently, KLF4 and β-catenin protein expression patterns were investigated through the utilisation of immunofluorescence techniques, where the results were later viewed under a confocal microscope.

3.2 Results

3.2.1 Relative quantification of gene expression

The 3 cell lines (SW480, DLD-1 and MCF7) were cultured as previously described, and from which RNA was isolated and reverse transcribed into cDNA to prepare for the relative quantification of gene expression through RT-PCR (Chapter 2.1, 2.2, 2.3, 2.6, 2.7, 2.8). For all treatments, C_t values were reviewed and a paired Students t-test was performed to compare sample means before and after treatment. The $2^{-\Delta\Delta Ct}$ method, as described in Appendix 5, was used to analyse relative gene expression in this study (Livak and Schmittgen, 2001).

3.2.1.1 *The effects of Valproic acid treatment on early stage colorectal adenocarcinoma cells (SW480)*

Colorectal cancer cells of an early stage were cultured as in Chapter 2.1, and treated with VPA as described in Chapter 2.2.1. A cell viability assay was performed (Chapter 2.1.5) to quantify SW480 cells before and after a low and high dose treatment with VPA. The viability of 'no treatment' control cells lay in the 95%-99% bracket, with a significant decrease observed when cells were treated with 1.5mM VPA (~94% live cells) and an even further reduction in numbers after treatment with a higher dose of VPA (~90% live cells) as seen in Figure 3.5 (SD= 0.02). As VPA was solubilised in water, there were no effects due to drug carriers, providing evidence that cell death could purely be a result of the drug treatment.

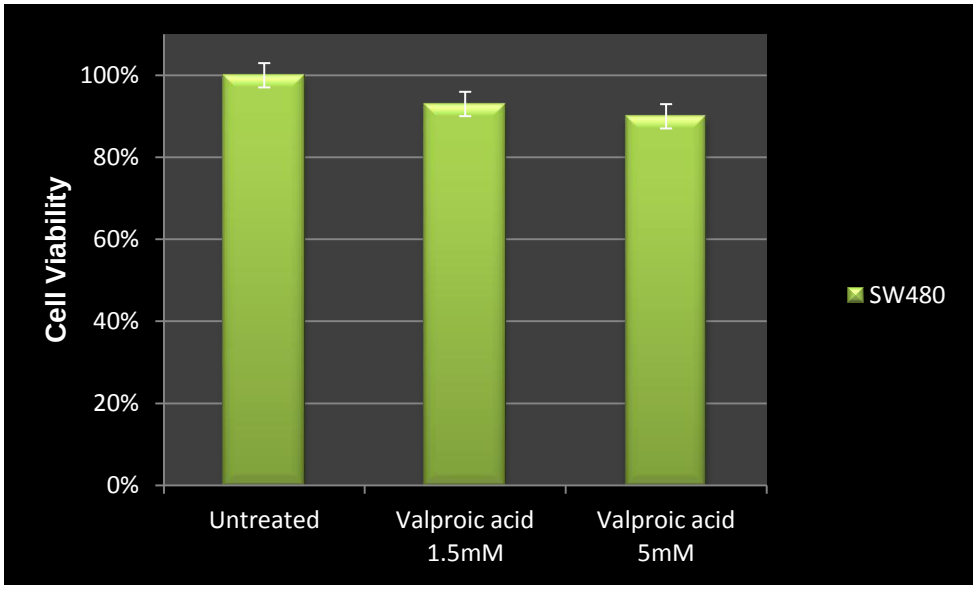


Figure 3.5 SW480 cell susceptibility to HDACi. Cells were treated with a low (1.5mM) and high dose (5mM) of VPA for 24 hours. Cell mortality possibly increased with an increase in VPA concentration (SD= 0.02).

Cells were prepared for confocal imaging as described in Chapter 2.9. Protein localisation and SW480 cell morphology before treatment is illustrated in Appendix 6 (Figure A6.1). Untreated SW480 cells retained an overall elongated and irregular shape, with prominent F-actin fibres. The nuclei appear to be large relative to the size of the cells and the cytoplasm appears to be scarce. KLF4 protein is clearly localised in the nucleus, supporting its role as a transcription factor. There is also a greater intensity of protein surrounding the nucleus and a low concentration within the cytoplasm. β-catenin is highly intense at the nuclear periphery, however its distribution throughout the nucleus and the cytoplasm is minimal. In comparison, there is a higher concentration of β-catenin than KLF4 within the cytoplasm of SW480 cells.

SW480 cells were treated with two concentrations of VPA, and its effect on KLF4 expression can be seen in Figure 3.6. When compared to the untreated samples, the mean increase in C_t value (M= 16.08, SD= 0.34, N= 3) was found to be significantly greater than zero where t(2)= 80.90, two-tailed p= 0.0001, providing evidence that treatment with 1.5mM VPA was effective in down-regulating KLF4 gene expression. The same overall result was seen with 5mM VPA, where t(2)= 4.23 and p= 0.0400 (M= 1.21, SD= 0.49, N= 3). Applying the $2^{-\Delta\Delta Ct}$ method revealed that treatment with 5mM VPA showed a less than one-fold difference in KLF4 up-regulation when compared to the lower dose treatment. Thus it is evident that treatment with both concentrations of VPA reduced KLF4 expression relative to the untreated samples, while the higher dose was effective in KLF4 up-regulation relative to the lower dose treatment.

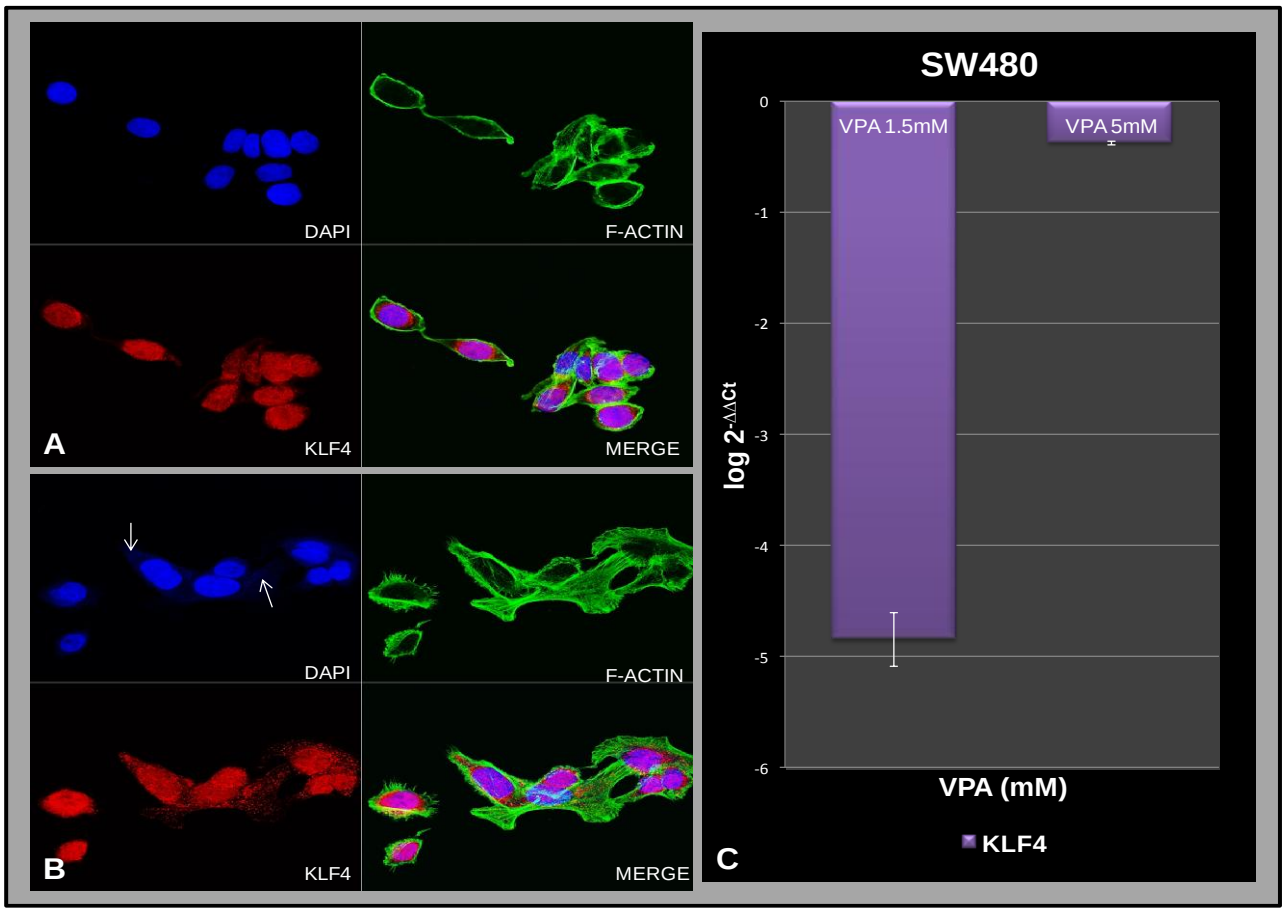


Figure 3.6 The effect of VPA on KLF4 expression in SW480 cells. [A] Confocal microscopy images after treatment with 1.5mM VPA (63x). [B] Confocal microscopy images after treatment with 5mM VPA (63x). Nuclei= blue, actin filaments= green, KLF4= red, co-localisation= pink. Nuclear content of potentially apoptised cells are clearly evident in the cytoplasm of cells treated with a high dose of VPA (arrowed). [C] Gene expression analysis of 1.5mM VPA (p= 0.0001, SD= 0.34) vs 5mM VPA (p= 0.0400, SD= 0.49) using the $2^{-\Delta\Delta Ct}$ method, relative to untreated controls.

The microscopy images shown in Figure 3.6 are similar to those seen in the untreated controls, however slight differences are evident. Both concentrations show distinct morphological changes from an irregular to a more oval cellular shape with a lower cytoplasmic to nuclear ratio, although this is more apparent in the lower dose cells. This could well be a result being the onset of programmed cell death. KLF4 localisation was most intense in the nucleus as seen previously, however treatment with 5mM VPA exhibited a greater localisation of protein in the cytoplasm than seen in the untreated controls. Also, nuclear content is evidently distributed throughout the cytoplasm of cells treated with a higher dose of VPA, as indicated by arrows (Figure 3.6B), confirming apoptosis.

SW480 cells were then treated with two concentrations of VPA to observe its effect on CTNNB1, which is illustrated in Figure 3.7. The mean increase in C_t value (M= 1.19, SD= 0.26, N= 3) from the untreated control was also found to be significantly greater than zero where t(2)= 7.97, two-tailed p= 0.0100, providing evidence that treatment with 1.5mM VPA effectively down-regulated CTNNB1 gene expression. A similar result was seen with 5mM VPA, where t(2)= 47.15 and p= 0.0004 (M= 17.40, SD= 0.63, N= 3). It was found here that treatment with a high dose of VPA was

more effective than a low dose in the down-regulation of CTNNB1, with a fourteen-fold reduction in its response. This result is antagonistic to that seen with KLF4.

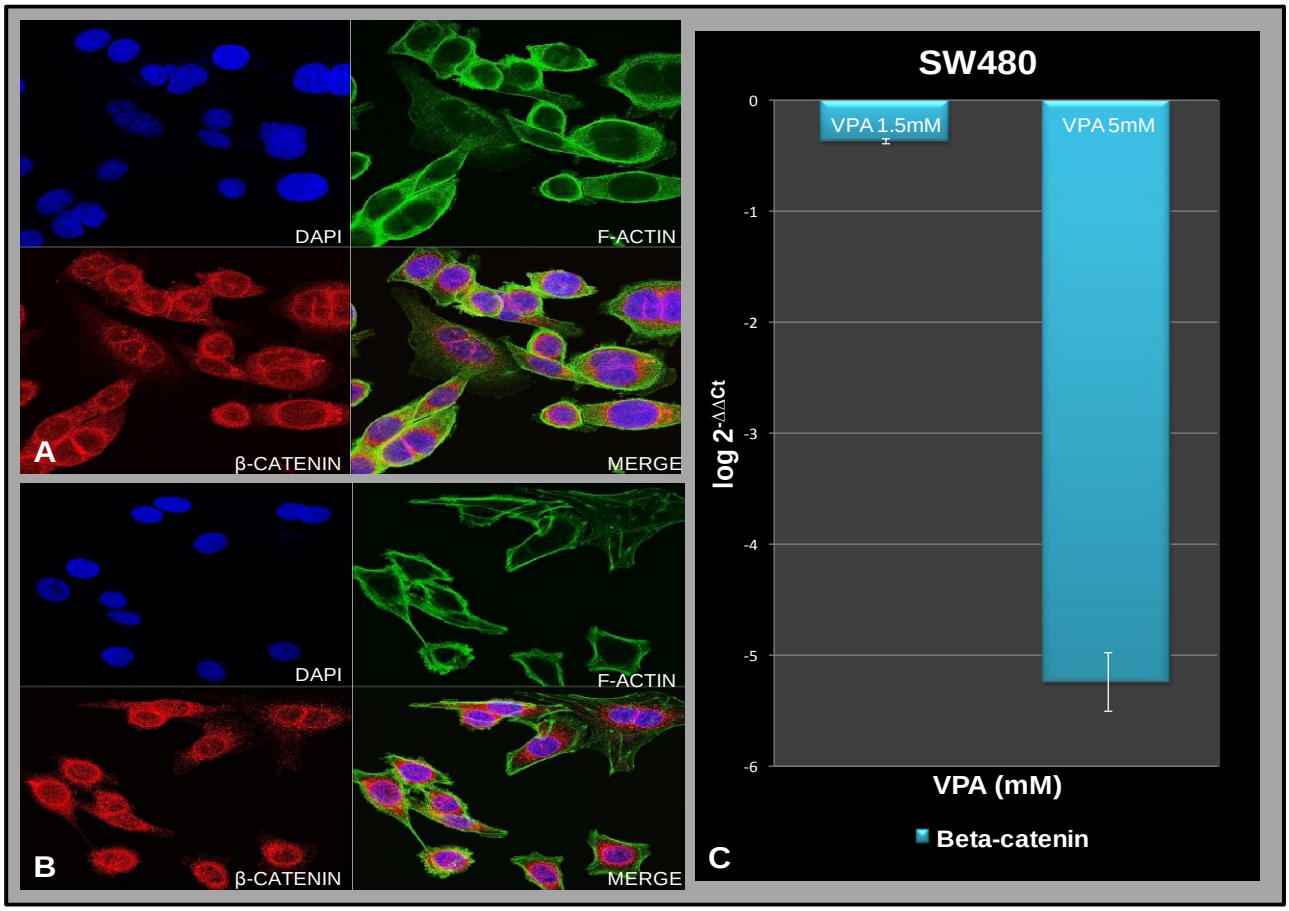


Figure 3.7 The effect of VPA on CTNNB1 expression in SW480 cells. [A] Confocal microscopy images after treatment with 1.5mM VPA (63x). [B] Confocal microscopy images after treatment with 5mM VPA (63x). Nuclei= blue, actin filaments= green, β-catenin= red, co-localisation= pink. High protein intensity is seen at the nuclear periphery of both treatments (arrowed). [C] Gene expression analysis of 1.5mM VPA (p= 0.0100, SD= 0.26) vs 5mM VPA (p= 0.0004, SD= 0.63) using the $2^{-\Delta\Delta Ct}$ method, relative to untreated controls.

Morphological changes in SW480 cells are comparable to those highlighting KLF4 expression with regards to cell shape, where it was observed to be less irregular and more oval, a possible result of the onset of apoptosis. A reduction in cell volume can also be seen, however the nuclear membrane is intact and the cytoplasm is free of nuclear content, as compared to Figure 3.6B. β-catenin localisation is once again evident in low concentrations throughout the cell with an intense signal evident at the outer periphery of the nuclear membrane, as indicated by arrows (Figures 3.7A and B). If apoptosis is a result of an increased VPA concentration, then the down-regulation of CTNNB1 seen in the gene expression data is validated. An opposing observation is the indication of mitotic behaviour, where both VPA concentrations seem to result in the nuclear division and subsequent cell division illustrated in Figures 3.7A and B.

3.2.1.2 *The effects of Valproic acid on late stage colorectal adenocarcinoma cells (DLD-1)*

Colorectal cancer cells of a late stage adenocarcinoma (Stage C) were cultured as in Chapter 2.1, and treated with VPA as described in Chapter 2.2.1. A cell viability assay was performed (Chapter 2.1.5) to quantify DLD-1 cells before and after a low and high dose treatment with VPA,

respectively. The viability of 'no treatment' control cells lay in the 95%-99% bracket, with a significant decrease after cells were treated with 1.5mM VPA (~93% live cells) and an even further reduction in cell count after treatment with a higher dose of VPA (~87% live cells) as seen in Figure 3.9 (SD= 0.04). Cell mortality proved to be greater in DLD-1 cells when compared to SW480 cells after drug administration. As VPA was solubilised in water, there were no effects due to drug carriers, providing evidence that cell death could purely be a result of the HDACi drug treatment.

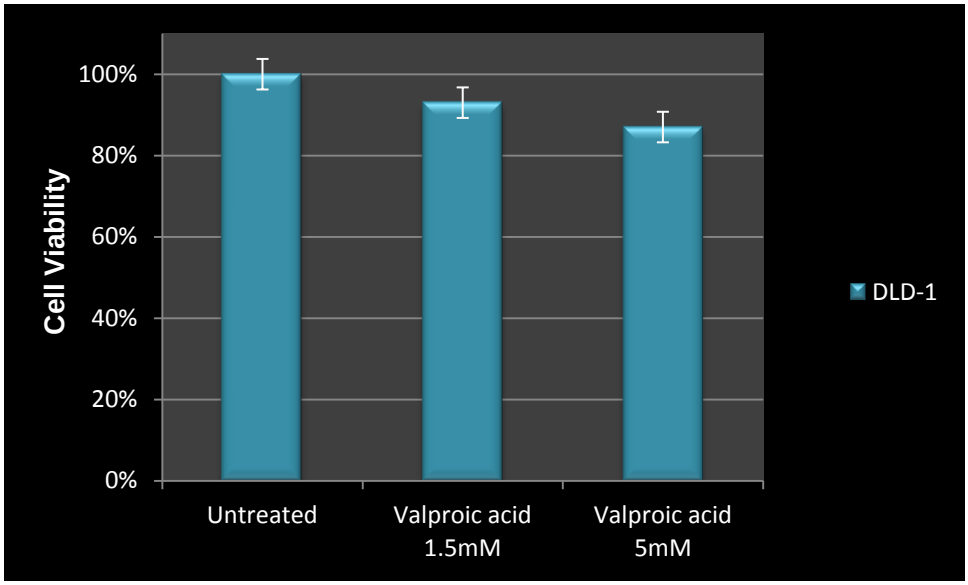


Figure 3.8 DLD-1 cell susceptibility to HDACi. Cells were treated with VPA (1.5mM and 5mM) for 24 hours. Cell mortality possibly increased with an increase in VPA concentration (SD= 0.04).

Cells were prepared for confocal imaging as described in Chapter 2.9. Protein localisation and DLA-1 cell morphology before treatment is illustrated in Appendix 6 (Figure A6.2). Untreated DLD-1 cells displayed an unusual and irregular shape, with prominent F-actin fibres and a relatively large nuclear to cytoplasmic ratio. KLF4 protein is clearly localised in the nucleus of DLD-1 cells as also seen in SW480 cells, reflecting its role as a transcription factor. Figure A6.2A shows a high concentration of KLF4 within the cytoplasm, with discreet aggregations to the nuclear periphery, indicating the localisation of KLF4 protein within Golgi bodies or ER. β-catenin is distributed throughout the nucleus and the cytoplasm at minimal intensity with a seemingly high concentration of protein localised at the cell and nuclear membrane. Once again, there is a higher concentration of β-catenin than KLF4 within the cytoplasm.

DLD-1 cells were treated with two concentrations of VPA, and its effect on KLF4 is illustrated in Figure 3.9. The mean increase in C_t value when evaluated against the untreated controls (M= 10.11, SD= 0.13, N= 3) was significantly greater than zero where t(2)= 127.02, two-tailed p= 0.00006, providing evidence that treatment with 1.5mM VPA was effective in down-regulating KLF4 gene expression. A similar result was seen with 5mM VPA, where t(2)= 13.64 and p= 0.00500 (M= 0.59, SD= 0.07, N= 3). Treatment with 5mM VPA displayed a less than one-fold increase in KLF4 expression relative to the 1.5mM treatment.

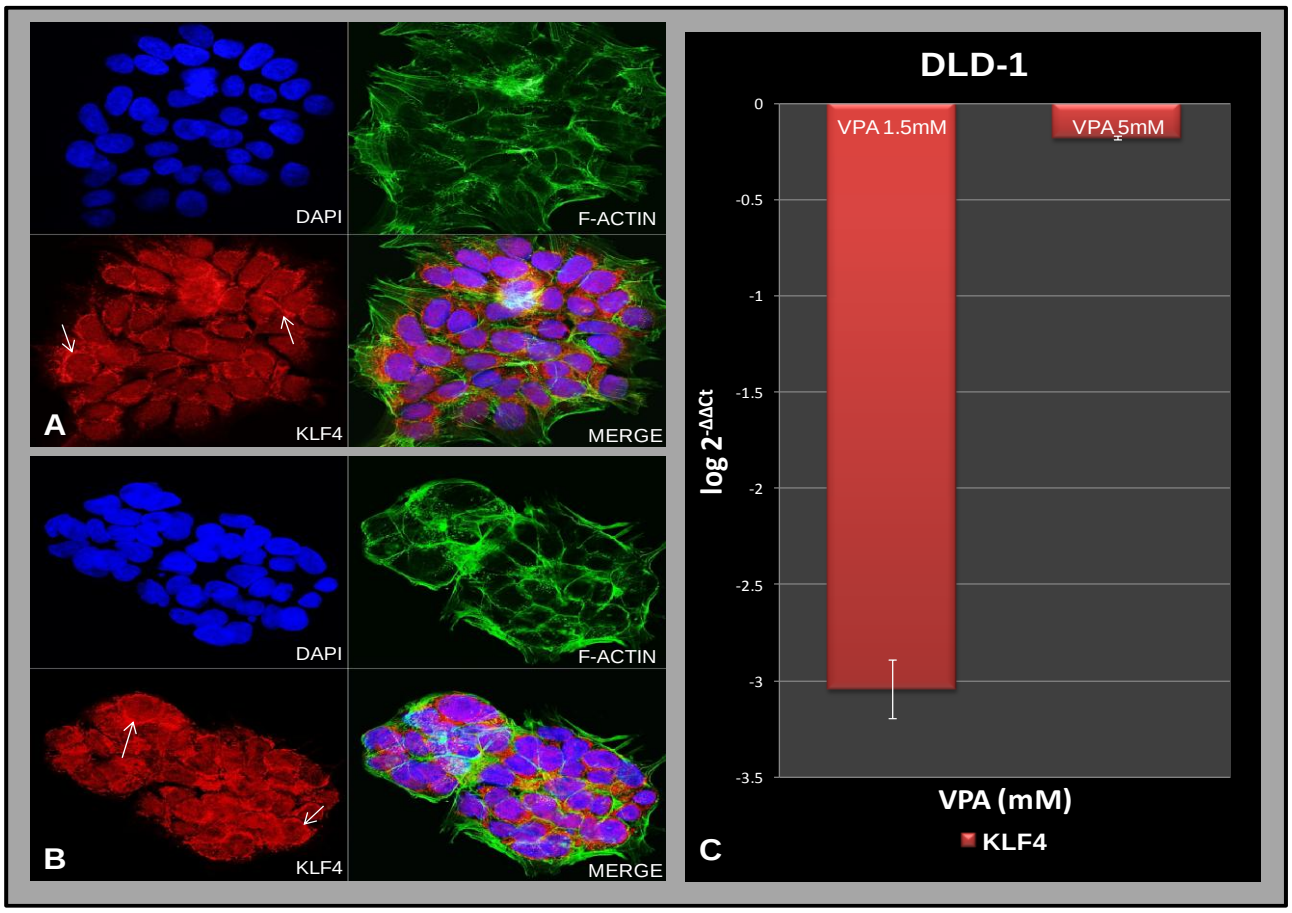


Figure 3.9 The effect of VPA on KLF4 expression in DLD-1 cells. [A] Confocal microscopy images after treatment with 1.5mM VPA (63x). [B] Confocal microscopy images after treatment with 5mM VPA (63x). Nuclei= blue, actin filaments= green, KLF4= red, co-localisation= pink. A high protein localisation was seen in nuclei and Golgi bodies or ER (arrowed) [C] Gene expression analysis of 1.5mM VPA (p= 0.00006, SD= 0.13) vs 5mM VPA (p= 0.00500, SD= 0.07) using the $2^{-\Delta\Delta Ct}$ method, relative to untreated controls.

Microscopy images show minor morphological changes when compared to the untreated controls, where the overall shape is slightly altered to a more oval structure as the concentration of VPA treatment is increased. KLF4 expression is again highly localised in the nucleus, with a predominant localisation around the nuclear periphery, with low to no localisation in the remaining cytoplasm. Another observation is the possible confinement of KLF4 in Golgi bodies throughout the cell, which can be seen by the continuous network they create around the nucleus, as indicated by arrows (Figures 3.9A and B) (Alberts *et al.*, 2002). This observation of increased KLF4 levels supports the relative gene expression data showing an up-regulation in KLF4 expression relative to low dose treatment.

DLD-1 cells were also treated with two concentrations of VPA, and its effect on CTNNB1 is illustrated in Figure 3.10. The mean increase in C_t value (M= 3.62, SD= 0.29, N= 3) was found to be significantly greater than zero where t(2)= 21.16, two-tailed p= 0.00200, providing evidence that treatment with 1.5mM VPA was effective in down-regulating CTNNB1 gene expression. A similar result was seen with 5mM VPA, where t(2)= 127.14 and p= 0.00006 (M= 10.20, SD= 0.14, N= 3). Treatment with both concentrations of VPA produced similar results in their effect on DLD-1 cells, with a high dose VPA displaying only a two-fold difference when compared to the low dose treatment. However, much like all previous results seen here in the colorectal cancer cell lines, the

5mM concentration of HDACi displayed a greater down-regulation of CTNNB1 than the loser dose treatment.

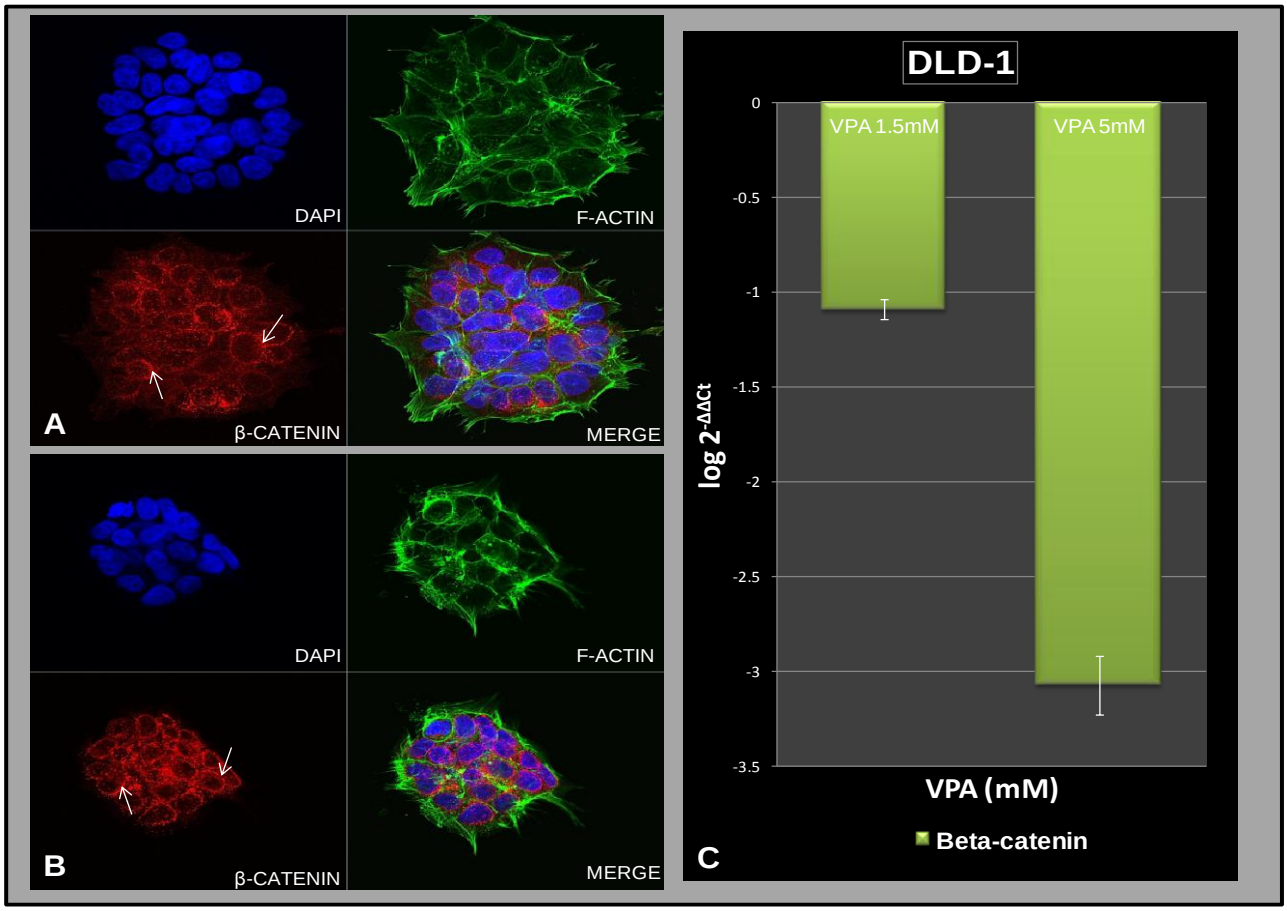


Figure 3.10 The effect of VPA on CTNNB1 expression in DLD-1 cells. [A] Confocal microscopy images after treatment with 1.5mM VPA (63x). [B] Confocal microscopy images after treatment with 5mM VPA (63x). Nuclei= blue, actin filaments= green, β-catenin= red, co-localisation= pink. β-catenin localisation seen at nuclear periphery (arrowed). [C] Gene expression analysis of 1.5mM VPA (p= 0.00200, SD= 0.29) vs 5mM VPA (p= 0.00006, SD= 0.14) using the $2^{-\Delta\Delta Ct}$ method, relative to untreated controls.

Figures 3.10A and B demonstrate a reduction in cell volume relative to the untreated control as the cytoplasm is reduced in size and in volume, as well as its inconsistent shape where some cells retain their irregular shape. The nucleus is also observed to be enlarged relative to the controls (See Figure A6.2B). β-catenin is concentrated at the nuclear periphery (see arrowed Figures 3.10A and B) at a higher intensity after treatment with 5mM VPA than that seen with 1.5mM VPA, while distributed throughout the cytoplasm and certain areas of the nucleus at lower intensities. Cells appear to be more compact when treated with a high dose of VPA than a low dose, although there are not many apparent changes between the two treatments.

3.2.1.3 *The effects of Valproic acid on breast adenocarcinoma cells (MCF-7)*

Breast cancer cells used as a positive control for KLF4 expression, were cultured as in Chapter 2.1, and treated with VPA as described in Chapter 2.2.1. A cell viability assay was performed (Chapter 2.1.5) to quantify MCF-7 cells before and after a low and high dose treatment with VPA. The viability of 'no treatment' control cells lay in the 95%-99% bracket, with a significant decrease observed when cells were treated with 1.5mM VPA (~94% live cells) and an even further reduction

in numbers after treatment with a higher dose of VPA (~77% live cells) as seen in Figure 3.11 (SD= 0.12). Cell mortality proved to be greater in breast cancer cells when compared to colorectal cancer cells after drug administration, thus MCF-7 cells showed a higher susceptibility to the drug. VPA was solubilised in water and not DMSO, providing evidence that cell death could essentially be an effect of the drug treatment.

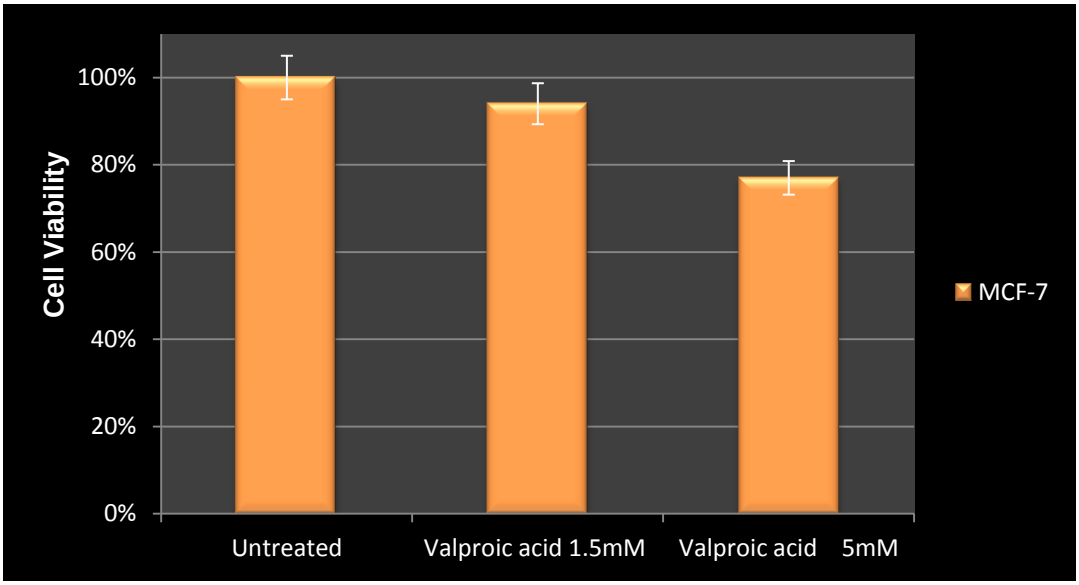


Figure 3.11 MCF-7 cell susceptibility to HDACi. Cells were treated with concentrations of 1.5mM and 5mM VPA for 24 hours, respectively. Cell mortality possibly increased with an increase in VPA concentration (SD= 0.12).

Cells were prepared for confocal imaging as described in Chapter 2.9. Protein localisation (KLF4 and β-catenin) and MCF-7 cell morphology before treatment is illustrated in Appendix 6 (Figure A6.3). Untreated MCF-7 cells also exhibited an irregular structure with prominent F-actin fibres, as well as enlarged nuclei size and lack of cytoplasm. KLF4 protein is clearly localised in the nucleus of MCF-7 cells as seen in both colorectal cancer cell lines, verifying its role as a transcription factor in breast cancer. The staining intensity for KLF4 is greater at the nuclear periphery (Figure A6.3A) with a low concentration seen within the cytoplasm, when compared to that observed in the nucleus. However, it is clear that KLF4 is found at a higher intensity in the cytoplasm relative to the colorectal cancer cell lines. β-catenin is distributed throughout the nucleus and the cytoplasm at minimal intensity with a seemingly high concentration of protein localised at the cell membrane (arrowed in Figure A6.3B).

MCF-7 cells were treated with two concentrations of VPA, and its effect on KLF4 is demonstrated in Figure 3.12. The mean decrease in C_t value compared to the untreated controls (M= 0.35, SD= 0.36, N= 3) was found to be greater than zero where t(2)= 1.67, two-tailed p= 0.23, providing evidence that treatment with 1.5mM VPA was effective in up-regulating KLF4 gene expression (n.s.). A similar result was seen with 5mM VPA, where t(2)= 8.11 and p= 0.01 (M= 1.87, SD= 0.39, N= 3). Treatment with 5mM VPA showed a five-fold difference in up-regulation when compared to the 1.5mM treatment. This result opposes that seen with the colorectal cancer cells, although the

commonality arises where the higher dose VPA treatment showed a stronger signal when compared to the lower dose VPA treatment in all three cell lines.

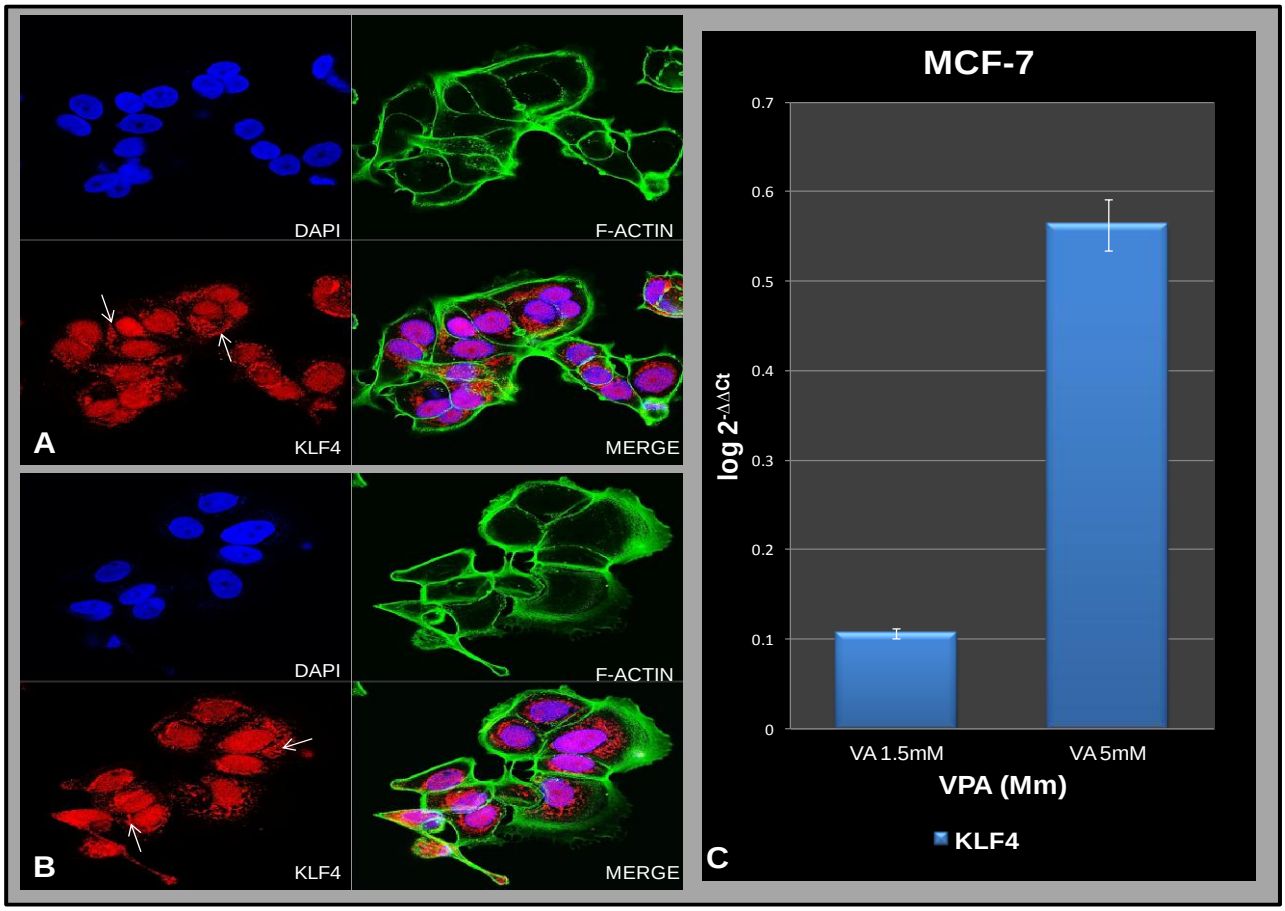


Figure 3.12 The effect of VPA on KLF4 expression in MCF-7 cells. [A] Confocal microscopy images after treatment with 1.5mM VPA. [B] Confocal microscopy images after treatment with 5mM VPA. Nuclei =blue, actin filaments =green, KLF4= red, protein co-localisation= pink. High intensity of KLF4 enclosed in nuclei and Golgi bodies (arrowed). [C] Gene expression analysis of 1.5mM VPA (p= 0.23, SD= 0.36, n.s.) vs 5mM VPA (p= 0.01, SD= 0.39) using the $2^{-\Delta\Delta Ct}$ method, relative to untreated controls.

Microscopy images show a defined oval shape of cells when compared to the untreated cells, as well as a low cytoplasm to nuclear ratio. Both treatments show few differences, and KLF4 is found at high intensities in the nucleus and surrounding the nuclear membrane. There is little to no protein in the cytoplasmic cavity. KLF4 is also seen in structures adhering to the nucleus that could potentially be Golgi bodies or ER, as indicated by arrows (see Figures 3.12A and B). The occurrence of Golgi bodies supports the gene expression data, showing an up-regulation in KLF4, relating to the increased production and storage of KLF4 protein.

MCF-7 cells were treated with two concentrations of VPA, and its effect on CTNNB1 is seen in Figure 3.13. The mean increase in C_t value (M= 1.07, SD= 0.27, N= 3) was significantly greater than zero where t(2)= 6.68, two-tailed p= 0.02, providing evidence that treatment with 1.5mM VPA was effective in down-regulating CTNNB1 gene expression. Alternatively treatment with 5mM VPA where t(2)= 3.16 and p= 0.02 showed an overall mean decrease (M= 1.11, SD= 0.61, N= 3), indicating that a higher dose of VPA was effective in up-regulating CTNNB1 expression. This is a unique finding, where the 1.5mM VPA produced a reduced CTNNB1 signal, while 5mM VPA

increased this signal two-fold, thus both concentrations had opposing effects on CTNNB1 expression.

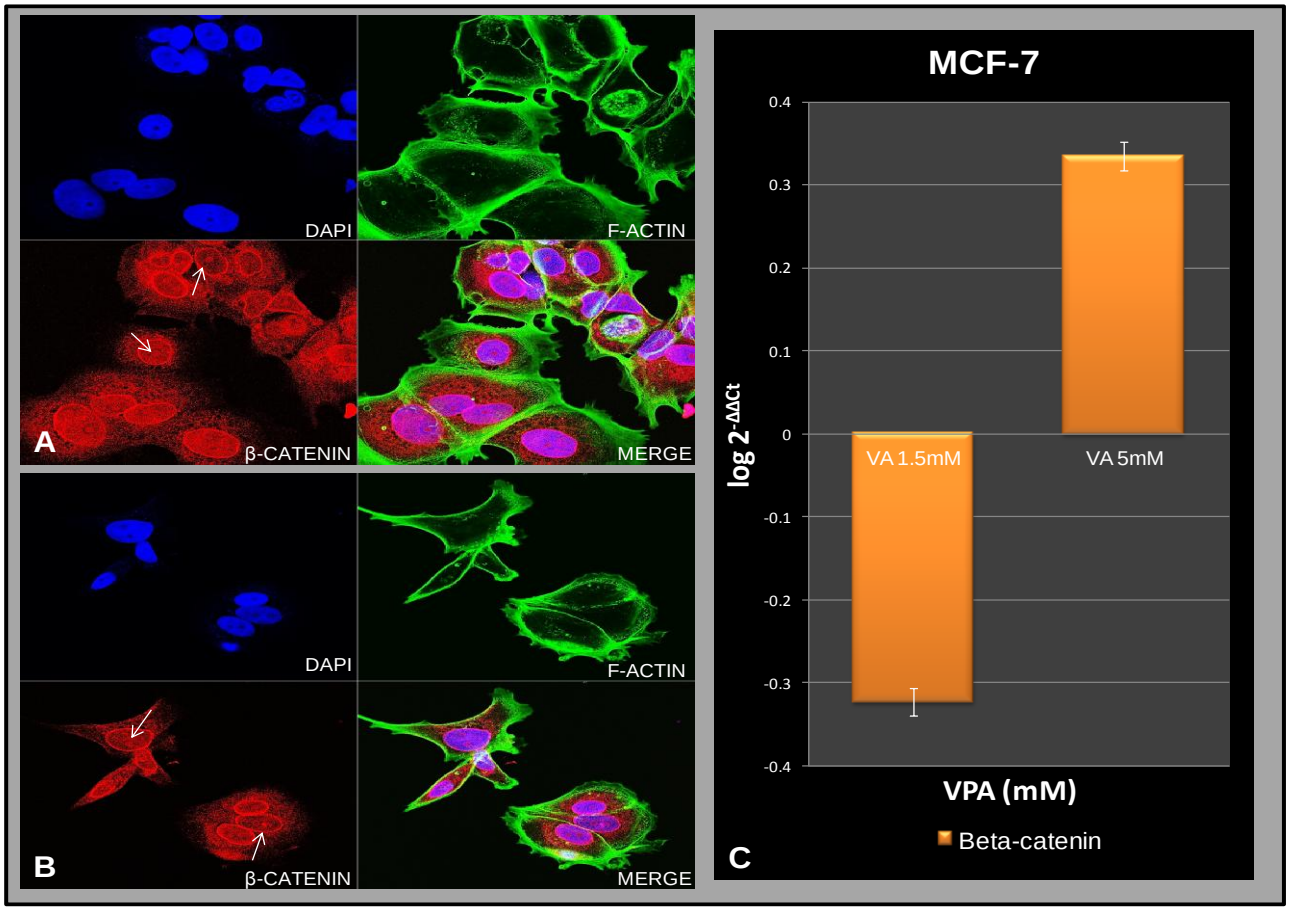


Figure 3.13 The effect of VPA on CTNNB1 expression in MCF-7 cells. [A] Confocal microscopy images after treatment with 1.5mM VPA. [B] Confocal microscopy images after treatment with 5mM VPA. Nuclei= blue, actin filaments= green, β-catenin= red, co-localisation= pink. High intensity of β-catenin is evident in nucleosomes within nuclei (arrowed). [C] Gene expression analysis of 1.5mM VPA (p= 0.02, SD= 0.27) vs 5mM VPA (p= 0.02, SD= 0.61) using the $2^{-\Delta\Delta Ct}$ method, relative to untreated controls.

Figures 3.13A and B demonstrate that the shape of cells range from oval to irregular, with a high volume of cytoplasm observed when compared to the colorectal cell images (see Figures 3.6 to 3.10). Nuclei are oval to round in shape and eccentrically localised, and there appears to be a high intensity of β-catenin in nucleosomes (arrowed Figures 3.13A and B) representing transcriptional "hotspots". These images are very different to those observed in the colorectal cell lines. Here, protein is found at high intensities at the nuclear periphery as well as in the nucleus and throughout the cytoplasm. Unlike the colorectal cells (see Figures 3.7 and 3.10) there is no evidence here of a specific localisation of β-catenin adjacent to the nucleus in Golgi complexes.

3.3 Discussion

Post-translational alterations in chromatin structure, particularly histone modifications, are crucial in gene regulation; however under adverse epigenetic conditions, they may lead to tumourigenic activity due to inactivation of tumour suppressor genes (Archer and Hodin, 1999). This chapter discusses the significance of these alterations on the expression of two vital genes implicated in

both colorectal and breast cancer cell lines. Here, this is considered in relation to colorectal and breast cancer derived cell lines, and in the particular effects of inhibitors on gene regulation. Typically, low levels of histone acetylation are associated with tumour development, and this is attributable to HDAC activity leading to their deacetylation (Yasui *et al.*, 2003). VPA was chosen as an HDACi in this study, due to its anti-tumour activity, as well as its high stability at room temperature (25°C) and favourable solubility properties (Gould *et al.*, 2004; Duenas-Gonzales *et al*., 2008).

3.3.1 The effect of Valproic acid on cell viability

Cell viability assays for all cell lines (colon and breast) demonstrated a general pattern of increased cell death that was directly proportional to the concentration of VPA; therefore as the dose increased so did cell death. For all treatments performed, water was used as a solvent, thus minimising any toxicity that may ordinarily be caused by the solubilising agent. The breast cancer cell line showed the greatest susceptibility to HDAC inhibition, demonstrating the highest cytotoxicity of all three cancer cell lines. The change of cell shape from an irregular to oval structure may also signify the apoptotic behaviour. It may be assumed that cell death was solely an outcome of treatment with VPA, and may lead to a reduction in cell proliferation preventing tumourigenesis, however the induction of cell death would need to be validated through the use of apoptotic markers such as Bcl-2 and Bax. Thus VPA dose-dependently reduced the viability of adenocarcinoma cell lines.

3.3.2 Valproic acid on gene expression in colorectal cancer cells

HDAC inhibition in early stage (Dukes' type B colorectal adenocarcinoma) colon cancer cells displayed dose-dependent gene regulation of KLF4 and CTNNB1, and all treatments were administered for 24 hours only. An evaluation of the relative gene quantification results indicated that KLF4 and CTNNB1 displayed an inverse relationship in their expression. Both low and high dose VPA treatments down-regulated KLF4 expression, however the expression of KLF4 was higher after high dose treatments relative to the low dose treatments, and KLF4 expression was still lower than the untreated controls. The reverse was seen for CTNNB1, where a low dose treatment down-regulated expression but a high dose treatment had a greater effect on transcript down-regulation. The same was observed in late stage cancer cells, however the fold increase and decrease monitored in both KLF4 and CTNNB1 respectively after high dose treatment was greater in SW480 cells. Image capturing provided evidence that DLD-1 cells clearly displayed the appearance of KLF4 protein in Golgi bodies adjacent to the nuclear periphery, representing their storage after production in the ER. However, this would need to be confirmed through the identification of Golgi-specific and ER-specific markers, such as RCAS1 (anti-Golgi) and Calnexin (anti-ER) antibodies respectively. RCAS1 is a type II transmembrane protein that is involved in Golgi functioning, while Calnexin is a chaperone protein localised in the ER membrane

(Engelsberg *et al.*, 2003; Bergeron *et al.*, 1994). The inhibition of the trans-Golgi Network (TGN) must also be taken into consideration, which may result in a blockade of KLF4 release.

A high intensity of protein is especially observed after high dose treatment, and when KLF4 expression is evidently up-regulated relative to the low dose treatment, suggesting an increase in protein production as a result of HDAC inhibition. KLF4 protein in both early and late stage cancer was localised in the nucleus and β-catenin was detected around the nuclear periphery. This is evidence substantiating the role of KLF4 as a transcription factor in the nucleus. β-catenin however translocates to the nuclear periphery where it associates with transcription factors, such as KLF4 and Wnt proteins (Zhang *et al.*, 2006). Confocal imaging here certainly illustrates that both these proteins concentrate within the nucleus and at the nuclear periphery where they may interact either directly with each other or indirectly through other transcription factors.

Data derived from the gene expression profiles in the present study, revealed that although the differential expression of KLF4 and CTNNB1 in colon cancer displayed aberrant transcript levels in both the early and late stage colorectal cancer cell lines, the pattern of gene regulation in both stages were very much alike. As described by Evans and colleagues, it is possible here that KLF4 maintains an inverse relationship with β-catenin, and that KLF4 is involved in the direct or indirect inhibition of β-catenin (see Evans *et al.*, 2010). Moreover, it has been previously reported by Xu *et al*. (2008) that loss of KLF4 expression is related to the progression of colon cancer; thus the up-regulation of KLF4 through HDACi activity strongly reduces the malignant phenotype of colon cancer cells. Furthermore, as indicated in the current study, the inverse expression of both these genes in colon cancer cells directly supports the cell viability data, that this transcriptional pattern may lead to apoptotic events. This notion is validated by other studies wherein the inhibition of β-catenin in colon cancer may contribute to apoptosis (Kim *et al.*, 2005; Han *et al.*, 2008). As β-catenin is an active member of the Wnt pathway, its down-regulation could result from the inhibition of the Wnt pathway, thereby leading to an increased risk of cell death (Watson, 2004; Yeh *et al*., 2011).

3.3.3 The effects of Valproic acid on gene expression in breast cancer cells

The effect of VPA on breast cancer cells supported the theory that KLF4 and CTNNB1 regulate one another, and also that the expression of CTNNB1 may be dependent on that of KLF4. However, gene expression profiles conflicted with the pattern attained in colon cancer gene regulation. KLF4 in contrast, was consequentially up-regulated following HDAC inhibitor treatment, and the higher dose treatments showed a greater up-regulation of gene expression. CTNNB1, notably displayed unusual results, wherein the lower dose VPA treatment down-regulated gene expression, after which it increased with the high dose treatment.

HDAC inhibition in breast cancer cells portrayed similar patterns of protein localisation as observed in late stage colon cancer cells, where KLF4 was contained at high levels in the nucleus and nuclear periphery, within Golgi bodies and ER. β-catenin however was found at greater intensity throughout the cytoplasm when compared to the early and late stage colon cancer cells. The high intensity of β-catenin localisation within nucleosomes demonstrated its high transcriptional activity. This would however need to be confirmed through the use of anti-nucleosome antibodies. Here, its nuclear localisation supports the gene expression data that demonstrates that CTNNB1 was up-regulated as a result of VPA treatment. This increased expression may affect its involvement in the Wnt pathway, where the β-catenin protein may form complexes with nuclear proteins such as TCF/LEF that are involved in breast cancer development.

The data produced could signify that a lower dose VPA treatment has a greater anti-tumourigenic effect on breast cancer cells than the high dose treatment, opposing results obtained from both colon cancer cell lines. The results display that a higher dose VPA treatment may lead to an increase in expression of both KLF4 and CTNNB1 possibly contributing to apoptosis, thus supporting the cell viability assay results produced. A related study performed on a range of cancer lines, using a non-steroidal anti-inflammatory drug (NSAID) known as Sulindac, generated similar results; Sulindac suppressed β-catenin in MCF-7 cells thereby inhibiting apoptosis, thus validating that its overexpression would result in cell death (Han *et al.*, 2008). Hence it would seem that overexpression of β-catenin may only be a product of an overactive Wnt pathway (He *et al*., 2004). KLF4 in breast cancer cells is regulated in a manner unlike that which is evident in colon cancer, where it serves as an oncogene. Thus, an increase in KLF4 expression in MCF-7 cells is related to a more malignant phenotype (Foster *et al.*, 2000; Yu *et al.*, 2011). Currently, with regards to this report, a low dose treatment caused a slight increase in expression compared to the untreated control, while a higher dose HDACi treatment could either be related to tumourigenic activity, or apoptosis when its relationship with β-catenin is taken into consideration.

3.3.4 Histone deacetylase inhibition by Valproic acid

A total of eighteen HDACs, divided into four classes, have been isolated. There is evidence that an increase in HDACs 1 and 3 (Class I) and HDAC 6 (Class IIb) activity may induce tumourigenesis in both colon and breast cancer. VPA has been found to dose-dependently inhibit HDAC1 *in vitro*, specifically blocking activity of nuclear Class I HDACs (1-3) at low doses, while inhibiting Class IIb HDACs (4, 5 and 6) at higher doses, but however has no effect HDACs 6 and 10 (Gurvich *et al.*, 2004). It does so by acting on the catalytic domain or N-terminal tails of histones H3 and H4, stimulating their hyperacetylation (Gottlicher *et al.*, 2001; Carew *et al.*, 2008). In addition to this, VPA has been found to induce the proteosomal degradation of HDAC2, a Class I HDAC (Kramer *et al.*, 2003). VPA was subsequently discovered to modify the expression of genes involved in the maintenance of chromatin structure, such as SMC proteins, DNA methyltransferases, and heterochromatin proteins in breast cancer (Marchion *et al.*, 2005).

Class I HDACs (HDACs 1, 2, 3 and 8), with the exception of HDAC 3, are localised in the nucleus (Yang *et al.*, 2002; Taplick *et al.*, 2001). As noted in the present study, the greatest intensity of KLF4 protein was found in the nucleus of all cell lines, there is a distinct possibility that HDACs 1, 2 and 8 are involved in the deacetylation of KLF4 associated histones. Therefore high dose VPA could cause histone hyperacetylation of the KLF4 gene, thereby inducing KLF4 expression. A related study performed in colon cancer cells using another short-fatty acid inhibitor, sodium butyrate, displayed similar results. Here, KLF4 was stimulated at a dose- and time-dependent manner, where the promoter region of the gene contains a butyrate-response element at a Sp1 binding domain with which butyrate interacts (Chen *et al.*, 2004). In the same report TSA, a hydroxamic acid based inhibitor that mimics the activity of VPA, was discovered to specifically inhibit HDAC1 (Chen *et al.*, 2004). VPA alters the Wnt pathway by affecting certain members involved in its regulation. This HDACi has been found to activate GSK-3 in colon cancer following its phosphorylation, leading to a series of the downstream effects such as the degradation of β-catenin resulting in its down-regulation (Vene and Tosetti, 2010).

VPA suppresses tumour growth by inducing cell differentiation as well as inhibiting angiogenesis (Gurvich *et al.*, 2004). It does so within the first 16 hours of treatment by stimulating G0/G1 cell cycle arrest and sometimes G2/M arrest when cells are exposed to high dose treatments; this occurs through the HDAC-mediated induction of tumour suppressor p21 and inhibition of cyclin A (Heerdt *et al.*, 1997; Xu *et al.*, 2005; Archer *et al.*, 1998; Li *et al.*, 2005; Chen *et al.*, 2004). VPA also plays a role in the instrinsic or extrinsic induction of apoptosis in breast cancer, while it is involved only in the instrinsic pathway in colon cancer cells (Insinga *et al.*, 2005). It is thought to transcriptionally alter the expression of members of the Bcl-2 family of proteins, by either the induction of the pro-apoptotic Bak protein or the inhibition of anti-apoptotic protein $BclX_L$ (Hague *et al.*, 1997). Another important tumour suppressor gene involved in apoptosis is p53, which was found to be hyperacetylated through VPA activity, but via non-histone proteins (Phiel *et al.*, 2001).

CHAPTER 4

DNA METHYLATION

4.1 Introduction

Since its discovery in 1983 by two renowned researchers from the John Hopkins University, the study of epigenetics has flourished, especially the field of DNA methylation and its involvement in tumourigenesis (Feinberg and Vogelstein, 1983). DNA methylation is a biochemical reaction in eukaryotes that involves the transfer of a methyl group to the fifth carbon of a cytosine ring (Singal and Ginder, 1999). It is known to be exceptionally important in the regulation of gene expression where a high frequency of methylation in the promoter region leads to a decrease in expression of the associated gene or to gene silencing resulting in cancer if said gene is a tumour suppressor; however it may affect the gene irregularly if methylation takes place within the transcribed region (Tate and Bird, 1993). DNA methylation is also involved in the regulation of transcription by preventing adhesion of transcription factors to regions of the DNA due to blocked sites (Bhaumik *et al.*, 2007). Although two major types of methylation involved in oncogenesis have been widely investigated, namely genome-wide hypomethylation and site-specific hypermethylation at promoters, this study focuses on the latter being the main culprit involved in cancer-related gene silencing (Esteller, 2008).

4.1.1 An overview on DNA methylation

4.1.1.1 *DNA methyltranferases (DNMTs)*

Enzymes involved in the transfer of methyl groups to the cytosine ring are known as DNA methyltransferases, and there are three known active DNMTs all highly expressed in cancer tissue, namely DNMT1, which was the first discovered, also known as maintenance DNMTs, as well as DNMT3a and DNMT3b, these being commonly known as *de novo* DNMTs (Bestor, 2000; Bestor *et al.*, 1988; Kanai and Hirohashi, 2007; Lei *et al*., 1996). DNMT3a and DNMT3b are involved in developing a pattern of methylation during embryogenesis and tend to display a greater affinity to unmethylated DNA, while DNMT1 is involved in maintaining this pattern of methylation throughout the development of the organism after DNA replication and has been shown to exhibit a preference for partially methylated DNA (McCabe *et al.*, 2009).

As depicted in Figure 4.1, DNMT1 is composed of a C-terminal portion or catalytic domain that shows great homology to prokaryotic restriction methyltransferases, and is also seen to make up the majority of the structure for DNMT2 (Bestor *et al.*, 1988). The catalytic domain is comprised of conserved motifs found in all DNMTs (Robertson, 2001). The N-terminal is the regulatory domain and is homologous throughout eukaryotes containing only specialised functions, such as the domain targeting replication foci which are subnuclear sites displaying continuous DNA replication, hence the term “maintenance” enzyme (Bestor and Verdine, 1994; Leonhardt *et al.*, 2000). Another portion contained in the N-terminal of DNMT1, DNMT3a and DNMT3b is the cysteine-rich domain

that binds zinc atoms, although its function remains to be unknown (Goll and Bestor, 2005). The N-terminal portion is seen to be lacking from DNMT2, this enzyme is characterised by its weak nature and possesses tRNA methyltransferase activity (Goll *et al.*, 2006; Hermann *et al.*, 2003).

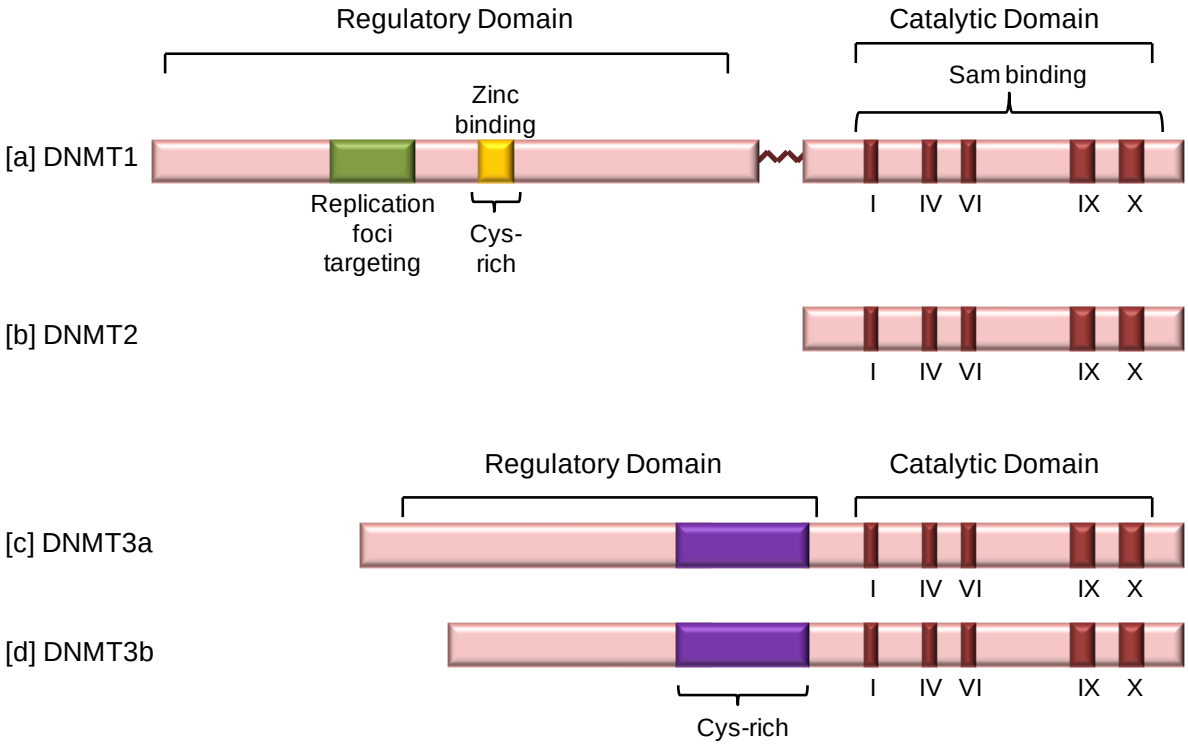


Figure 4.1 Structural analysis of three DNA methyltransferase (DNMT) families. All DMNTs include the catalytic domain in the C-terminal region that is comprised of conserved methyltransferase motifs I, IV, VI, IX and X. [a] DNMT1 contains a large regulatory section within its N-terminal region, exhibiting domains vital for maintaining methylation after DNA replication. [b] DNMT2 lacks this regulatory domain. [c and d] Both DNMT3a and DNMT3b contain regulatory domains that are divergent, however, their catalytic domains are homologous to each other and the rest of the DNMTs (Robertson, 2001; Bestor, 2000).

4.1.1.2 *CpG island methylation*

DNMTs are key enzymes involved in catalysing the major epigenetic modification, cytosine methylation (Worm and Guldberg, 2002). As seen in Figure 4.2, they function by adding a methyl group to the fifth carbon of the cytosine ring forming 5-methylcytosine, wherein S-adenosylmethionine (SAM) is used as a substrate in this reaction (Singal and Ginder, 1999; Worm and Guldberg, 2002). In mammals, this modification takes place mainly in the event of the occurrence of the sequence 5'- CG -3', that are commonly known as CpG dinucleotides or islands, where the "p" denotes a phosphate bond between the deoxycytidine and deoxyguanosine (Bird, 1986). The human genome contains approximately 29000 CpG islands, where most are generally unmethylated in normal tissues (Bird, 1986; Venter *et al.*, 2001, Lander *et al.*, 2001).

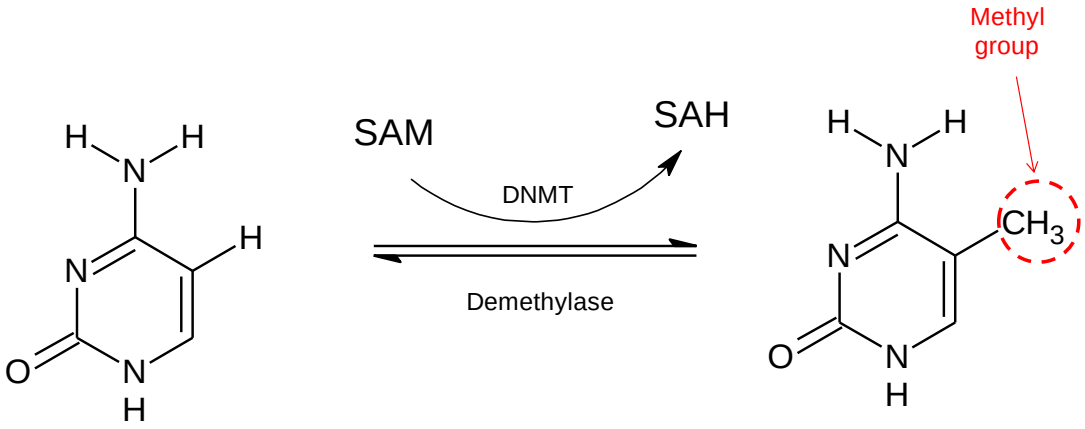


Figure 4.2 Schematic view of DNMT adding a methyl group to the fifth carbon of cytosine forming 5-methylcytosine. S-adenosylmethionine (SAM) is used as a substrate in the reaction and S-adenosylhomocysteine (SAH) is a by-product (Singal and Ginder, 1999; Worm and Guldberg, 2002).

CpG islands are localised within the 5' end of all housekeeping genes and most genes of somatic cells where they are found to be associated with exons and introns, as well as the 3' end of genes of some somatic cells, where they are associated with exons only (Gardiner-Garden and Frommer, 1987). As illustrated in Figure 4.3, methylation in non-cancerous cells is crucial for normal cellular development where global methylation of CpG dinucleotides is evident, however islands found in the 5' end of genes are unmethylated. The reverse is true in tumourigenic cells, where CpG islands residing in the 5' regions of the gene such as the promoters are hypermethylated and those within the remainder of the gene are unmethylated or less methylated (Gal-Yam *et al.*, 2008). The methylation frequency is inversely proportional to the transcriptional activation of the gene in question, thus a high level of methylation is related to gene silencing and *vice versa* (Worm and Guldberg, 2002).

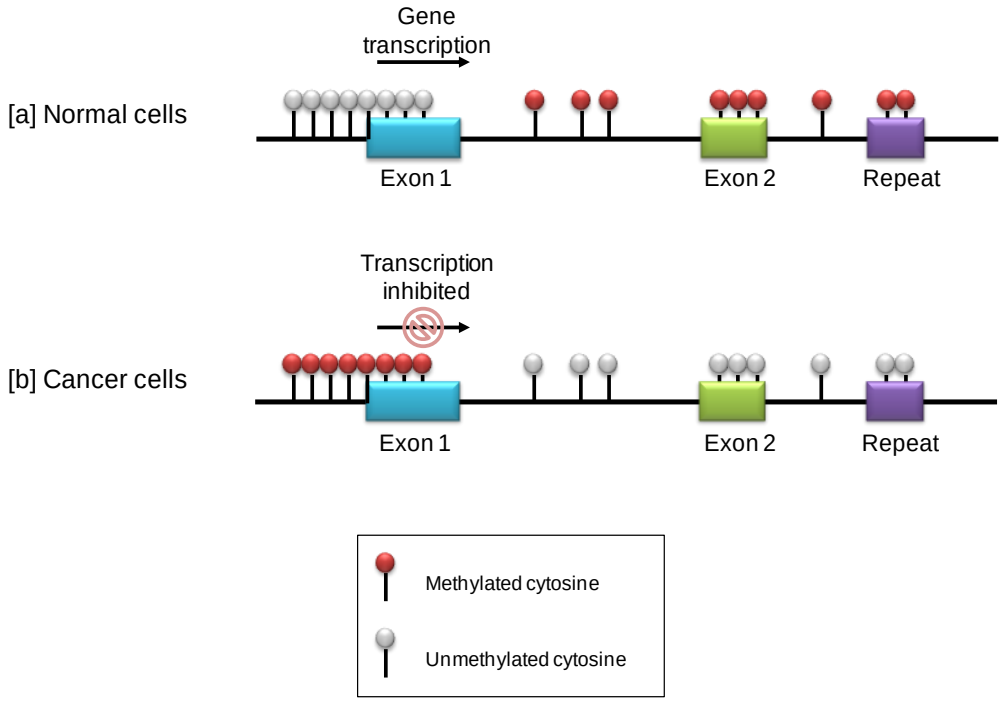


Figure 4.3 Schematic illustration of DNA methylation in normal and tumourigenic cells. [a] In normal cells, CpG islands in the 5' region are unmethylated while the opposite is seen in [b] cancer cells, where most CpG islands in the 5' region are hypermethylated (Gal-Yam *et al.*, 2008).

According to Garden-Gardiner and Frommer, in order to characterise a CpG island, one needs to follow three simple criteria, namely that CpG islands must be at least 200bp long, they must contain a GC content of 50%, and the observed CpG over the expected CpG (O/E) ratio must be greater than 0.60 (60%), where the O/E is a measure of the number of CpG islands in a particular region (Gardiner-Garden and Frommer, 1987). Takai and Jones (2002) found that DNA stretches exceeding 500bp, exhibiting a GC content of more than 55% and an O/E ratio of 0.65 (65%) or more, are possibly CpG islands associated with the 5' ends of genes, this definition excludes all Alu repeat sequences that are also GC rich (Takai and Jones, 2002). The O/E ratio is calculated as in Equation 4.1, where N represents the number of nucleotides in the sequence in question.

$$\frac{Observed}{Expected}CpG = \frac{Number of CpG}{Number of C \times Number of G} \times N \qquad \text{[Equation 4.1]}$$

4.1.1.3 *DNA methylation and gene silencing*

As mentioned earlier, the nature of the relationship between methylation and transcriptional activation is inversely proportional, leading to the belief that DNA methylation operates as a negative regulator or an inhibitor of gene transcription (Singal and Ginder, 1999). DNA methylation is accountable for the repression of transcription for several reasons, one being the blockage of binding sites by methylation, preventing the association of transcription factors with promoter regions (Tate and Bird, 1993). Other instigators are protein repressors of transcription, namely MeCP-1 (methyl cytosine binding protein 1) and MeCP-2 (methyl cytosine binding protein 2), both of which bind to CpG dinucleotides and inhibit transcription (Rountree and Selker, 1997). MeCP-1 binds to sites containing several methylated CpG islands and prevents the association of

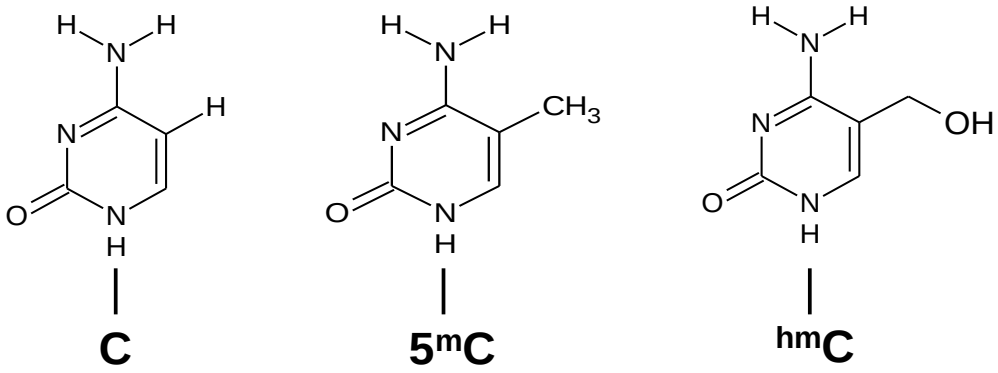
transcription factors and polymerases (Meehan *et al.,* 1989). MeCP-2 is however found in greater numbers in mammals than MeCP-1 and binds to a single CpG island with an additional methyl group (Meehan *et al.*, 1992). MeCP-2 was found to play a role in histone deacetylation as well as DNA methylation, and represses transcription similarly to MeCP-1 through the inhibition of transcription factors and polymerases (Nan *et al.*, 1998; Jones *et al*., 1998). This raises possibilities for other mechanisms of repression via MeCP-2 activity, such as through the modification of chromatin structure (Keshet *et al.*, 1986). Thus a factor to consider with regards to DNA methylation is whether it actually occurs as a result of gene activity; it may even occur before or in some cases as an effect of gene transcription (Singal and Ginder, 1999).

4.1.1.4 *Gene silencing and cancer*

As discussed previously, cancer cells are known to exhibit genome-wide hypomethylation as well as hypermethylation of promoter regions (Esteller, 2009). The hypermethylation of tumour suppressor genes may lead to their inactivation in cancer, and the first ever such gene to be discovered with a hypermethylated 5' end was the retinoblastoma (Rb1) gene (Greger *et al.*, 1994). With regards to the present study that will look at the methylation status of KLF4 and CTNNB1, as well as the effects of DNA methyltransferase inhibitors on the expression of KLF4, previous work performed on several colon cancer cell lines showed that KLF4 is a possible tumour suppressor gene and displays high levels of hypermethylation in its 5' untranslated region (Zhao *et al.*, 2004).

4.1.1.5 *Hydroxymethylated DNA*

A newly discovered nucleotide that is a result of an oxidation reaction, was initially found in bacteriophages in 1952 and has recently been identified in mouse brain and embryonic stem cells (Kriaucionis and Heintz, 2009; Wyatt and Cohen, 1952; Tahiliani *et al*., 2009). The nucleotide known as 5-hydroxymethylcytosine (5-hmC), is created through a reaction catalysed by Tet enzymes and involves the conversion of 5-methylcytosine through the gain of an oxygen atom (Tahiliani *et al*., 2009). Its oxidated chemical structure can be seen in Figure 4.4. This modified base comprises approximately 40% of methylated bases within CpG islands of Purkinje neurons of the cerebellar cortex (Kriaucionis and Heintz, 2009). It was also discovered that the change from 5-mC to 5-hmC reduced binding affinity of MBD proteins to methylated DNA, therefore while it is possible that it may play a role in the regulation of methylation and gene expression, similar to its modified counterpart 5-mC, its function is still undefined (Valinluck *et al*., 2004).



Unmethylated DNA Methylated DNA Hydroxymethylated DNA

Figure 4.4 Differences in chemical structure of methylated DNA. The oxidised version of 5-methylcytosine (5-mC) can be seen as 5-hydroxymethylcytosine (5-hmC) (revised from Valinlick *et al.*, 2004).

4.1.2 Epigenetic therapy mediated by DNA methyltransferase inhibitors

As these epigenetic changes, unlike genetic mutations, must be maintained through the activity of DNMTs, their reversible nature makes them appealing targets for therapeutic agents (Egger *et al.*, 2004). DNA methyltransferase inhibitors, also referred to as demethylating agents or hypomethylating agents, have been found to reverse the methylation status of DNA, thereby reinstating gene activity of silenced tumour suppressor genes and reducing cell proliferation, thus reducing tumour growth (Suzuki *et al.*, 2002; Baylin, 2004). The most widely studied DNMT inhibitors are commonly known as nucleoside analogues, with the ribose nucleoside 5-aza-CR being highly recognised in this category and functions as a mechanism-dependent suicide inhibitor (Santi *et al.*, 1984). During replication, it transforms itself to deoxynucleoside triphosphate and incorporates within the DNA structure instead of cytosine, where it binds to DNMTs preventing it from completing the methylation process (Michalowsky and Jones, 1987; Santi *et al.*, 1984). However, due to its ribose nature it must undergo several biochemical alterations before its complete incorporation into DNA, thus more readily incorporated analogues have been developed. In particular, 5-aza-CdR is a more effective deoxyribose analogue as it does not require any prior modifications for incorporation into DNA (Jones, 1985; Stresemann *et al.*, 2006).

Both these inhibitors have proven to be highly effective in numerous investigations in clinical trials and have acquired FDA approval for the treatment of myelodysplastic syndrome and acute myeloid leukaemia, with 5-aza-CR making headlines as the first epigenetic drug developed (Silverman *et al.*, 2002; Mund *et al.*, 2006). These compounds however are distinguished for their high levels of toxicity and low stability in solvents (Jutterman *et al.*, 1994). These adverse factors can be overcome by the use of a nucleoside inhibitor known to exhibit little toxicity and displaying a high stability, as well as affecting tumour cells directly (Zhou *et al.*, 2002; Cheng *et al.*, 2003; Cheng *et al.*, 2004).

4.1.3 Zebularine as a demethylating agent

As mentioned, agents such as 5-aza-CR and 5-aza-CdR are extremely effective in the eradication of tumour cells through the demethylation of DNA and thereby subsequent reactivation of tumour suppressor genes, however they exhibit poor stability and extreme toxicity in cells. Peter Jones of the Comprehensive Cancer Centre in Los Angeles discovered Zebularine, a useful inhibitor of DNA methylation, a decade ago. ZEB is a cytidine analogue that presented an original design primarily intended for the inhibition of cytidine deaminase (Cheng *et al.*, 2004). Other than exhibiting properties such as its long half life in aqueous solution, ZEB was found to be the first active demethylating agent when administered orally in mice (Cheng *et al.*, 2003). It was shown to inhibit cancer cell growth at a more advanced rate when compared to other drugs as well as reduce DNMT1 numbers and was advantageously highly selective towards cancer cells, while being less receptive to normal cells. All these factors as well as its ability to maintain demethylation through constant administration deems this drug a favourable demethylating agent (Cheng *et al.*, 2004).

ZEB is a 2-(I*H*)-pyrimidinone ribonucleoside where the pyrimidine ring lacks an amino group at the fifth carbon, as demonstrated in Figure 4.5 (Cheng *et al*., 2003; Cheng *et al.*, 2004). It displays a very similar mode of action to the other cytidine analogues, 5-aza-CR and 5-aza-CdR. During DNA synthesis, they are taken up and incorporated into the DNA after phosphorylation. During methylation, DNMT1 binds covalently to the sixth carbon of cytosine as well as the pyrimidinone ring of ZEB. Normally the transfer of the methyl group from SAM to cytosine frees DNMT1 from cytosine, however when the 2-(I*H*)-pyrimidinone ring replaces cytosine the transfer is blocked and the methyltransferase is trapped, leading to a reduction in methylation as the replication fork proceeds without the DNMT (Wu and Santi, 1985).

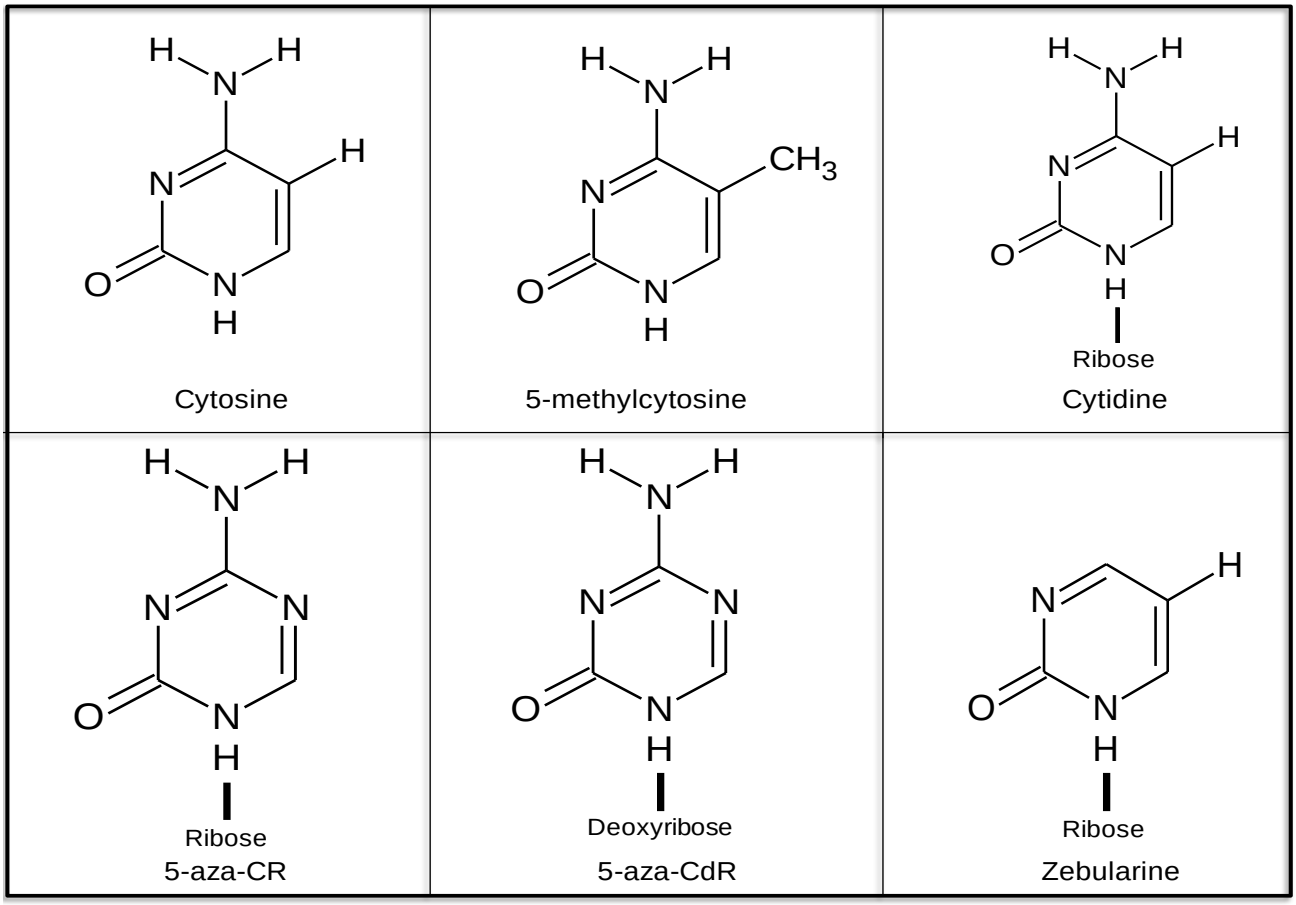


Figure 4.5 Structural differences between cytosine and 5-methylcytosine, and cytidine and its analogues. 5-aza-CR and 5-aza-CdR both contain a nitrogen at their fifth position, while ZEB contains a 2-(1*H*)-pyrimidinone ring. All three ring structures associate covalently with DNMTs once they are incorporated into DNA to trap them (Santini, Kantarjian and Issa, 2001; Zhou *et al.*, 2002; Cheng *et al.*, 2003).

4.1.4 Experimental approach

As a first approach here, a number of methylation specific bioinformatic tools were used to interrogate and analyse the gene sequences for KLF4 and CTNNB1, to evaluate the degree of methylation. For purposes of clarity, a background to each of the computational approaches is presented below to facilitate an understanding of the results obtained. Further, in order to gain some consensus with such methylation patterns, it is advisable to use a series of different predictive tools to obtain an overall view of the methylation status of the genes studied. In the next phase of this chapter, the global methylation status, and 5-hydroxymethylation levels are assessed in the colorectal adenocarcinoma lines studied here through the application of an ELISA based assay. Following this, the early and late stage colorectal, as well as the breast adenocarcinoma cell lines were treated with two doses of ZEB for approximately 24 hours, and a relative quantification of KLF4 and CTNNB1 expression was performed applying the $2^{-\Delta\Delta Ct}$ method to analyse relative gene expression. Lastly, KLF4 and β-catenin protein expression patterns were investigated through the utilisation of immunofluorescence techniques, where the results were later viewed under a confocal microscope.

4.2 Results

4.2.1 Bioinformatics

The identification of methylated sites within specific regions of DNA may be achieved by carrying out painstakingly long experiments, however their identification through the application of computational techniques is a growing field making the process more appealing (Bhasin *et al*., 2005). There are various tools available online for the detection and analysis of DNA methylation in regions of the DNA sequence, the most common being those involved in identifying sequences rich in CpG dinucleotides. Three programs were used to determine the methylation status of the KLF4 and CTNNB1, namely 'CpG Island Searcher' developed by Takai and Jones from the University of Southern California (Takai and Jones, 2002), 'MethyCancer' by He and colleagues at the Graduate University of the Chinese Academy of Sciences (He *et al.*, 2007), and 'Methylator' by Basin and Reche from Harvard University (Bhasin *et al.*, 2005).

4.2.1.1 *CpG Island Searcher*

The 'CpG Island Searcher' (http://cpgislands.usc.edu/) predicts the positions of dinucleotide clusters using an algorithm developed in previous work and is created to exclude other GC-rich sequences such as Alu repeats (Takai and Jones, 2003). This program is performed by PERL COMPILER (ActiveState, Vancouver, http://www.activestate.com/) using PERL SCRIPT created by D. Takai (Takai and Jones, 2002). The CpG island extraction algorithm, as described in Figure 4.6, applies a "sliding and jumping" window of 200bp that is placed at the start of a contig where the percentage (%) GC and Obs_{CpG}/Exp_{CpG} is calculated according to three major CpG criteria met by Gardiner-Garden and Frommer, namely (a) the length of CpG islands must be greater than 200bp, (b) the GC content must be greater than 50% and (c) the expected over observed ratio must be greater than 0.60 (Gardiner-Garden and Frommer, 1987). The window is then shifted 1bp until it meets the appropriate CpG criteria, after which the window is repeatedly shifted a further 200bp until the window fails to meet the criteria. The window is shifted back to the 5' end until it reaches the criteria again, thereby defining a start and end point. The total %GC and Obs_{CpG}/Exp_{CpG} is then calculated, and if a large CpG island is created that does not meet the criteria then 1bp of each side is removed until it does. If two CpG islands are separated by 100bp or less, then they are attached to form one large CpG island and %GC and Obs_{CpG}/Exp_{CpG} are recalculated (Takai and Jones, 2002). Takai and Jones then improved on this and redefined the criteria to exclude Alu repeat elements as the following, (a) the length of CpG islands must be at least 500bp, (b) the GC content must be greater than 55% and (c) expected over observed ratio must be greater than 0.65 (Takai and Jones, 2002).

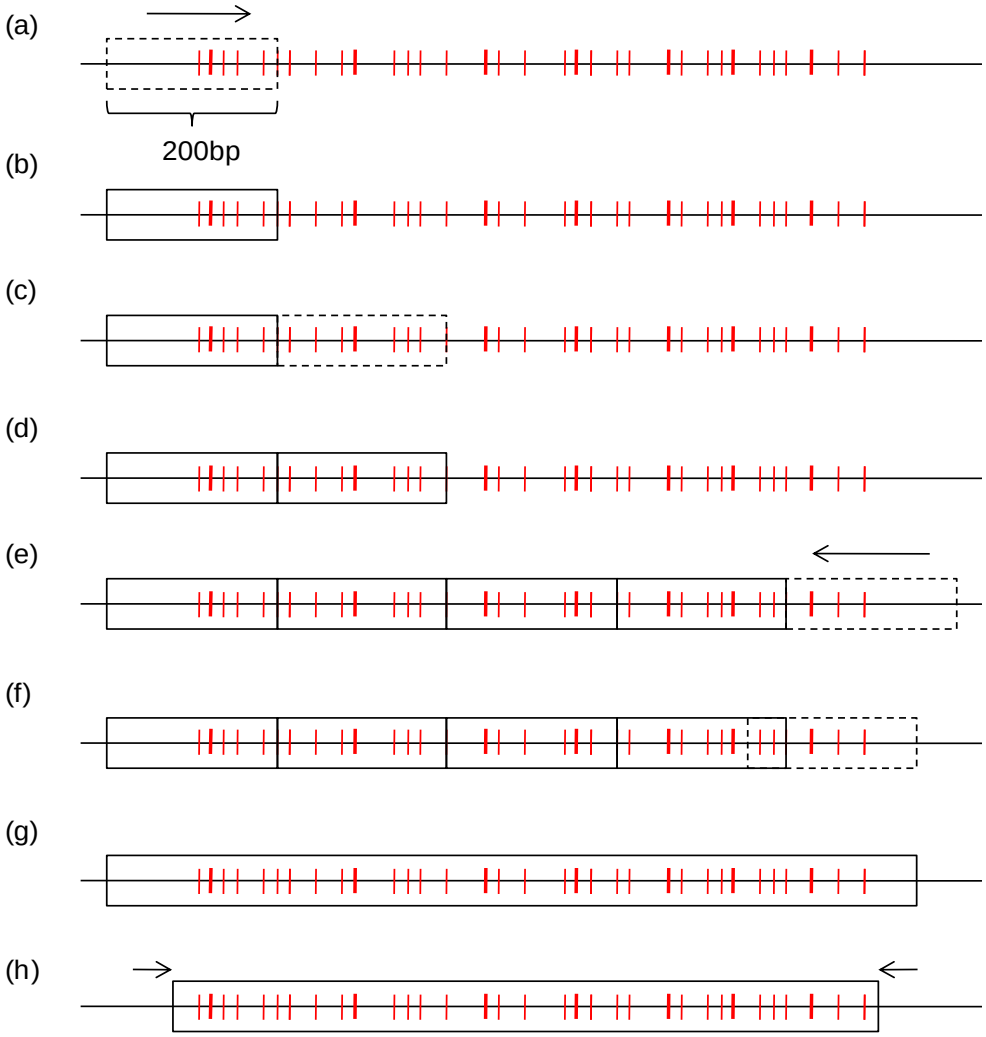


Figure 4.6 The CpG island extraction algorithm. (a) A 200bp window is positioned at the start of the contig and shifted until the region within the window meets the CpG island criteria. (b, c, d, e) The window is repeatedly shifted 200bp until it neglects to meet the criteria. (e and f) The last window is then shifted 1bp in the opposite direction until the criteria are met. (g and h) 1bp is removed from both sides of this long CpG island until the criteria are met (Modified from Takai and Jones, 2002).

Table 4.1 CpG Island Searcher results

	Input Sequence length (bp)	Start	End	%GC	Observed Cpg/Expected CpG	CGI length
KLF4	3662	1	2418	67.2	0.845	2418
CTNNB1	6609	520	1204	55	0.895	685

Table 4.1 illustrates results from the "CpG Island Searcher". Within the entire *KLF4* gene of 3662bp, a CpG island (CGI) was located between Exon 1 and Exon 2418 with a CGI length of 2418bp, occupying 66% of the total genome length. Total GC content was found to be 67.2% and the observed over expected CpG ratio (O/E ratio) was 0.845 (85%). The *CTNNB1* gene of 6609bp however displayed a CGI of 685bp located between Exon 520 and Exon 1204 that constitutes 10% of the genome, which is evidently smaller when compared to *KLF4*. The total GC content here was 55%, hence the lower frequency of CpG islands within the gene, and the O/E ratio was 0.895 (90%).

The results for both genes analysed clearly meet Takai and Jones criteria (Takai and Jones, 2002) therefore it follows that there is a greater chance that these CGIs are associated with the 5' regions of *KLF4* and *CTNNB1*, and exclude Alu-repetitive elements. Another observation is that the localisation of both CGIs within the first 2kb of the gene is additional evidence that they could be associated with the 5' region and thus might be contained within the promoter. It has been proposed that CpG islands residing in the 5' regions of genes are generally hypermethylated and linked to tumourigenicity (Gal-Yam *et al.*, 2008). The O/E ratios for both genes were considerably greater than 0.60, thus the observed frequency of CpG islands in both genes were comparatively larger than the expected frequency. It is clear however that the CGI found in *KLF4* was almost 2kb larger than that found in *CTNNB1*. However, despite the larger CGI and higher frequency of CG dinucleotides found in *KLF4*, the O/E ratio of *CTNNB1* was closer to 1.0 and slightly greater than that of *KLF4*, demonstrating a high methylation frequency in a smaller fragment of DNA.

4.2.1.2 *MethyCancer*

A growing set of about 20000 CpG island (CGI) clones were created through the sequencing of a CGI library to analyse CGIs within the human genome, as well as to evaluate methylation of DNA within promoter regions and others (Cross *et al*., 1994; He *et al.*, 2007). These were integrated with approximately 17132 CGI clones extracted from the UHN Human CpG Island Microarray Database, thus "MethyCancer" archives up to 34738 CGI clones (Heisler *et al*., 2005). The CpGi130 tool together with data from USCS (http://methycancer.psych.ac.cn/CpG130.do) was used for CGI prediction based on the following default conditions, (a) the length of the input sequence must be greater than 500bp, (b) the GC content must be greater than 55%, and (c) the ratio of the observed over expected ratio of CpG islands must not be less than 0.65 (Takai and Jones, 2002; Kuhn *et al*., 2007; He *et al*., 2007). Table 4.2 displays results of CpGi130 program in the search for CpG islands.

Table 4.2 CpGi130 results

	Input Sequence length (bp)	Start	End	%GC	Observed Cpg/Expected CpG	CGI length
KLF4	3662	1	2406	67.2	0.847	2406
CTNNB1	6609	518	1206	55	0.895	689

Table 4.2 displays results from the CpGi130 program that are almost identical to the results produced by the "CpG Island Searcher". A CGI of length 2406bp was located between Exon 1 and 2406 of *KLF4* composing 66% of the total genome. Total GC content and observed over expected CpG ratio (O/E ratio) were 67.2% and 0.847 (85%) respectively. The *CTNNB1* gene however contained a CGI of 689bp located between Exon 518 and Exon 1206 that constitutes 10% of the genome, which is once again evidently smaller when compared to *KLF4*. Total GC content was 55%, hence the lower frequency of CpG islands, and O/E ratio was 0.895 (90%).

The O/E ratios for both genes were yet again considerably greater than 0.60, thus the observed frequencies of CpG islands in both genes were comparatively larger than the expected frequency. It is once again clear that the CGI found in *KLF4* was almost 2kb larger than that found in *CTNNB1* and despite the larger CGI and higher frequency of CG dinucleotides found in *KLF4*, the O/E ratio of *CTNNB1* was closer to 1.0 and slightly greater than that of *KLF4*, demonstrating a high methylation frequency in a smaller fragment of DNA. The CGIs within both genes met Takai and Jones criteria (Takai and Jones, 2002) and were localised within the first 2kb, validating the theory that they could be associated with the 5' region and might be contained within the promoter and may exclude Alu-repetitive elements.

ChroView was then used to analyse each chromosome to generate a summary of %GC and MethyCancer clusters, providing methylation data.

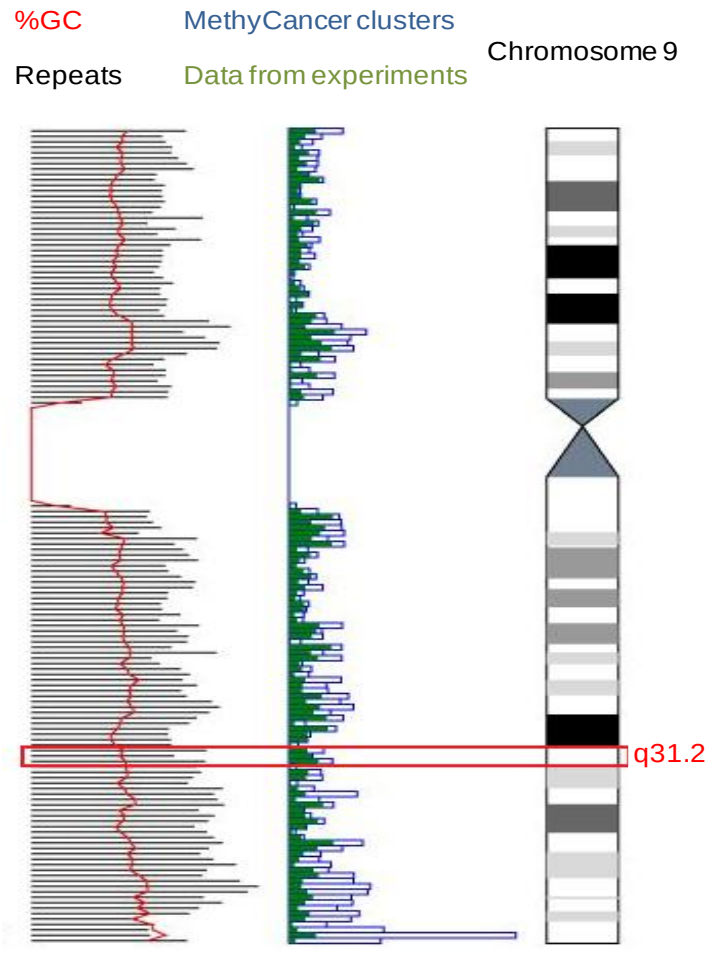


Figure 4.7 ChroView on human chromosome 9 focusing on position 9q31.2 illustrating the location of gene *KLF4.*

Figure 4.7 illustrates the results from the ChroView program for chromosome 9, and the position of *KLF4* is highlighted on the q-arm. GC content at this position is approximately 50% and the number of repeats is slightly above average. However, the MethyCancer clusters associated with this region is observed to be below average, with experimental data being exceptionally low. It is likely that the incidence of MethyCancer clusters is low due to the lack of experimental data relating to

this area. It has been discovered that the light chromosomal bands, much like the region containing *KLF4*, are generally early-replicating, euchromatic and GC-rich, and thus abundant in genes (Speicher and Nigel, 2005). From this analysis, it is possible that *KLF4* is only slightly methylated and minimally expressed in human cells.

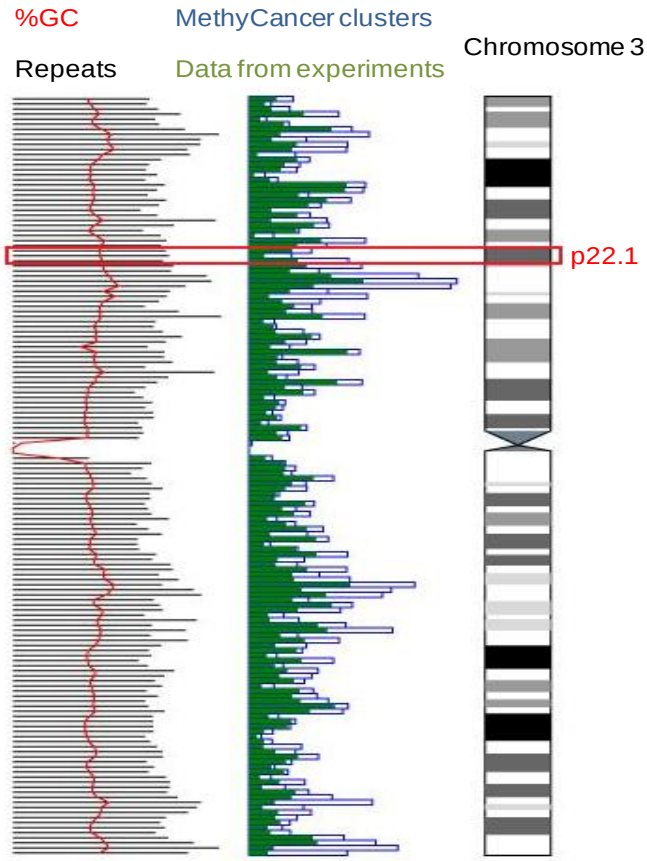


Figure 4.8 ChroView on human chromosome 3 focusing on position 3p22.1 illustrating the location of gene *CTNNB1*.

Figure 4.8 illustrates the results from the ChroView program for chromosome 3, and the position of *CTNNB1* is highlighted on the p-arm. GC content at this position is approximately 50% and the number of repeats is about average. The MethyCancer clusters as well as the experimental data associated with this region are observed to range between low to average. The chromosomal banding here appears to be darker than the area containing *KLF4*, and these areas are generally composed of genes that are later-replicating, heterochromatic and AT-rich (gene poor) (Speicher and Nigel, 2005). It is therefore likely that there is a higher frequency of methylation within this region than within *KLF4* as a result of greater levels of heterochromatism, and it is possible that this is due to the lack of experimental data associated with *KLF4*.

4.2.1.3 *Methylator*

The first ever algorithm for pattern recognition was developed over 70 years ago by R. A. Fischer (Fischer, 1936) and since then this algorithm has been manipulated for its application in several different fields including recognition of handwriting and objects as well as face detection, among others. Present day algorithms include the support vector machine (SVM) which has been used in

computational biology to recognise patterns in proteins as well as DNA (Noble *et al.*, 2004). A SVM is capable of processing different sequence lengths including biological data that is generally high-dimensional and noisy (Noble *et al.*, 2004). In order to classify a SVM, one has to understand four concepts, (i) the separating hyperplane that separates the classes, (ii) the maximum-margin hyperplane that has the greatest margin between two classes, (iii) the soft margin to separate classes when data is noisy and outliers are present, and (iv) the kernel function that adds an extra dimension to the data when two classes are non-separable (Noble, 2006).

An SVM was used to predict methylation sites using a program known as "Methylator" (http://bio.dfci.harvard.edu/Methylator/). The nucleotide sequence, limited to 10000 per query, was entered in a plain format. The SVM was employed using a non-commercially available package SVM_light (http://www.joachims.org) which is capable of defining a kernel as well as placing limits on the defined kernel. Training sets for the SVM are composed of vector inputs (*N* fragments) $\{x_1, x_2, x_3, ... x_i, ..., x_N\}$ and labels for each $\{y_1, y_2, y_3, ..., y_i, ..., y_N\}$. These labels denote the methylation status of each fragment (y_i {+1;-1}). Each nucleotide is represented using five binary sparse coding, for instance adenine is symbolised by 10000, cytosine by 01000 until all nucleotides have been represented, and this is characterised by the x_i. Equation 4.2 is used by the SVM to assign an *x* value to each fragment during training, where *k* is the kernel function, *b* the bias value and *i* provides the maximum margin hyperplane. A score ranging from -1.5 to 1.5 will be generated by the SVM and if the calculated score is greater than the threshold, then the cytosine residue is deduced to be methylated (Bhasin *et al*., 2005).

$$f(x) = sign\left(\sum_{i=1}^{N} Y_i \alpha_i, k(x_i, x) + b\right) \qquad \text{[Equation 4.2]}$$

The specificity of the results are directly proportional to the threshold value. At a low threshold value, results may reflect false positives, therefore an optimum threshold of -0.455 is used by default as the specificity and sensitivity are the same as seen in Figure 4.9.

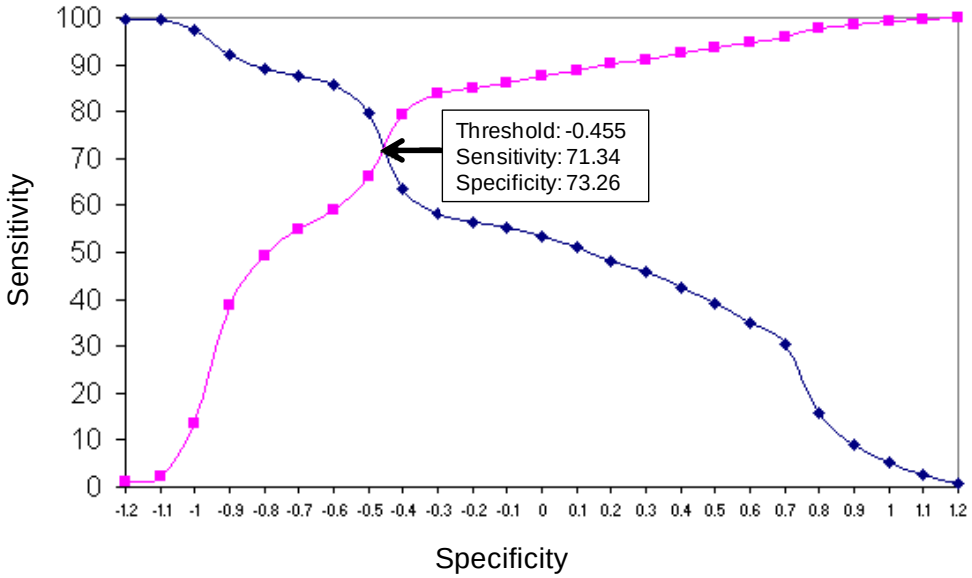


Figure 4.9 Graph displaying the threshold value and specificity of results are directly proportional to each other. The threshold value varies between -0.5 and 0.5, where an optimum value of -0.455 is preferred as this is where the specificity and sensitivity is the same (Methylator, 2011).

Output results for *KLF4* and *CTNNB1* show methylation predictions of CpG islands and can be seen in Appendix 7 and Appendix 8. There is a total of 254 methylated cytosines in the *KLF4* gene, most of which are confined to the first 2kb of the gene. Similarly, the *CTNNB1* gene comprises of 115 methylated cytosines, the majority of which are localised in the first 1kb of the gene. Once again, *KLF4* displays a higher frequency of CpG islands and possible methylation, validating results from the "CpG Island Searcher" and "CpGi130".

4.2.2 Global methylated DNA quantification

4.2.2.1 *Quantification of methylated DNA in the SW480 and DLD-1 cell lines*

The content of 5-mC otherwise known as methylated DNA was quantified using the MethylFlash™ Methylated DNA Quantification Kit (Epigentek) following the manufacturer's protocol (See Chapter 2.5.1). In this ELISA based assay, DNA is immobilized to wells coated with a DNA affinity substrate. The methylated fraction of DNA is recognized with a 5-methylcytosine antibody which contains a substrate that is hydrolysed to produce a colour reaction. The absorbance of this reaction is measured at 450nm. Similarly, 5-hydroxymethlated DNA derived from SW480 cells and DLD1 cells was quantified using the MethylFlash™ Hydroxymethylated DNA Quantification Kit (Epigentek) following the manufacturer's protocol (See Chapter 2.5.2), where the 5-hmC portion of DNA was recognised with an antibody to 5-hydroxymethylcytosine.

The colour changes associated with 5-mC can be observed in Chapter 2.5.1 (See Figure 2.1), where the darker the blue generated, the greater the level of methylation. The most methylated samples were the positive controls and least were the negative controls, ME4 and ME3 respectively. SW480 and DLD-1 were both paler than the positive control but darker than the negative control illustrating the possibility of methylation, however DNA from SW480 cells displayed a much deeper blue than DLD-1 derived DNA, proving that the methylation frequency

was higher than that found in DLD-1. As described in Table 2.1 (Chapter 2.5.1), a standard curve seen in Appendix 9 (Figure A9.1) was generated from a dilution series of ME4 buffer.

Table 4.3 Global DNA methylation status of two colorectal cancer cell lines

	SW480 (Stage A)	DLD-1 (Stage C)
Average sample OD	0.471	0.281
5-mC (ng)	0.355	0.145
5-mC (%)	0.36	0.15

Utilising the MethylFlash™ Methylation assay, the content of 5-mC was determined in SW480 and DLD-1 cell lines. As seen in Table 4.3, there were significant variations observed between these two cell lines, as 5-mC was more abundant in SW480 cells (0.36%) than in DLD-1 cells (0.15%). An overall mean difference of 0.168 was determined between the early and late stage cell lines (M= 0.168, SD= 0.060, N= 2), where t(1)= 3.680, two-tailed p= 0.030.

The colour changes associated with 5-hmC is demonstrated in Chapter 2.5.2 (See Figure 2.2), where the darker the blue generated, the greater the level of hydroxymethylation. The most methylated samples were the positive controls and least were the negative controls, HC5, HC3 and HC4 respectively. SW480 and DLD-1 were both much paler than the positive control, with DLD-1 displaying a slightly brighter blue than SW480, and SW480 and negative controls HC3 and HC4 were very similar in colour. Thus both samples displayed a much lower hydroxymethylation frequency when compared to their methylation frequency, although unlike its 5-mC levels, DLD-1 exhibited a higher 5-hmC frequency than SW480. As described in Table 2.2 (Chapter 2.5.2), a standard curve seen in Appendix 10 (Figure 10.1), was generated from a dilution series of HC5 buffer.

Table 4.4 Global DNA hydroxymethylation status of two colorectal cancer cell lines

	SW480 (Stage A)	DLD-1 (Stage C)
Average sample OD	0.128	0.15
5-hmC (ng)	0.0092	0.017
5-hmC (%)	0.0046	0.0085

The MethylFlash™ Hydroxymethylation assay was used to assess the 5-hmC content in SW480 and DLD-1 cell lines. As seen in Table 4.4, there was a negligibly low percentage of 5-hmC in DLD-1 cells and an even smaller percentage in SW480, both less than 0.01%. Both early and late stage cell lines displayed a significant mean difference of 0.022 (M= 0.022, SD= 0.001, N= 2), where t(1)= 22, two-tailed p= 0.020.

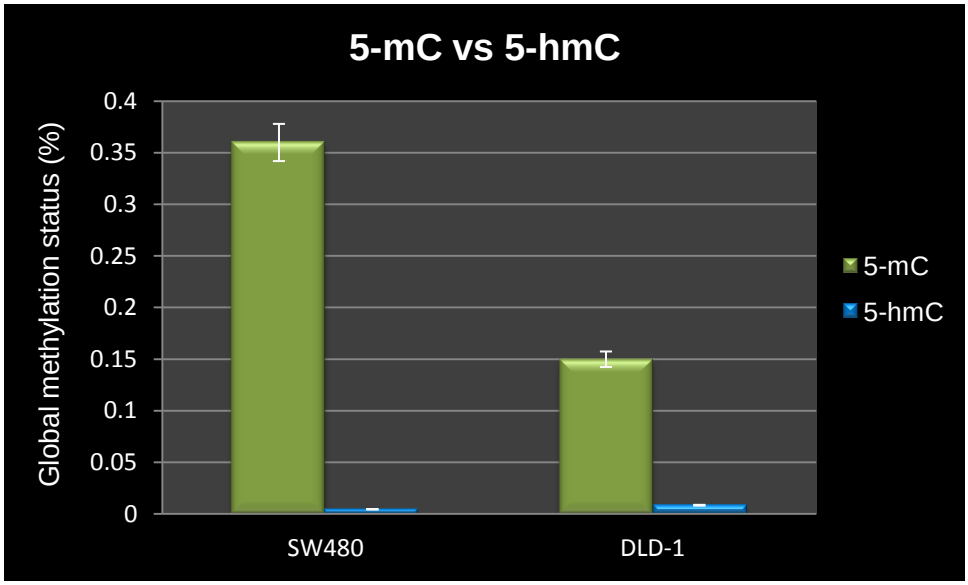


Figure 4.10 Graph exhibiting the difference between global 5-mC and 5-hmC in SW480 (N= 2, SD= 0.07, p= 0.04) and DLD-1 (N= 2, SD= 0.01, p= 0.03) cell lines.

It is clear from both the colour development assay and the colourimetric results, that the global methylation status in SW480 cells (t(1)= 5.88, two-tailed p= 0.04), is approximately two-fold greater than that of DLD-1 cells (t(1)= 16.38, two-tailed p= 0.03), however by comparison the hydroxymethylation status of both colorectal cancer cell lines is negligible, although the late stage cancer cells displayed higher levels of hydroxymethylated DNA than the early stage cancer cells. Thus, the early stage colon cancer cells exhibited a higher frequency of globally methylated DNA than the late stage colon cancer cells, and both early and late stage colon cancer cell lines contained a greater overall frequency of methylated DNA than hydroxymethylated DNA.

4.2.3 Relative quantification of gene expression

For all treatments, C_t values were reviewed and a paired Students t-test was performed to compare sample means before and after treatment. The $2^{-\Delta\Delta Ct}$ method was used to analyse relative gene expression in this study (Livak and Schmittgen, 2001). The C_t of the target gene was first normalised to that of the reference gene (in this case β–actin) for both test and calibrator samples following Equations A5.1 and A5.2 explained in Appendix 5. The C_t of the test sample was then normalised to the C_t of the calibrator as seen Equation A5.3. As a result, the ratio of the target gene in the test sample to the calibrator sample was obtained and normalised to the reference gene. The expression ratio may be calculated following Equation A5.4 in Appendix 5. All treated sample results are relative to the untreated samples.

4.2.3.1 *The effects of Zebularine on early stage colorectal adenocarcinoma cells (SW480)*

Colorectal cancer cells of an early stage were cultured as described in Chapter 2.1, and treated with ZEB as explained in Chapter 2.2.1. A cell viability assay was performed (seen in Chapter 2.1.5) to quantify SW480 cells before and after treatments with 1.5mM and 5mM concentrations of demethylating agent. The viability of 'no treatment' control cells rested in the 95-99% bracket. Results here proved to be very similar to that observed with the HDACi treatments, where a

significant decrease was observed after low dose treatment (94% live cells) and a higher dose treatment confirmed a greater drug susceptibility leading to a higher cell death (90% live cells), as illustrated in Figure 4.11 (SD= 0.02).

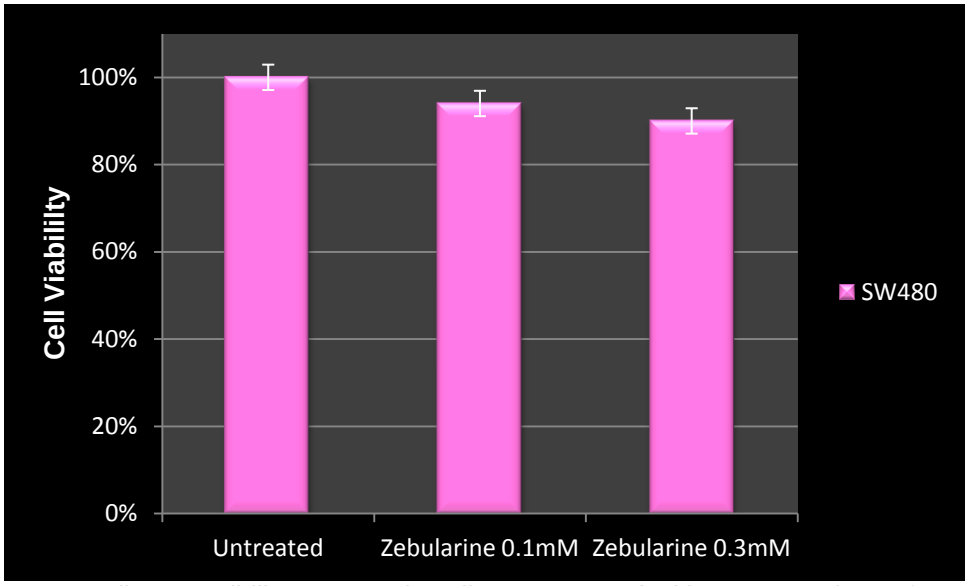


Figure 4.11 SW480 cell susceptibility to HDACi. Cells were treated with concentrations of 1.5mM and 5mM ZEB for 24 hours. Cell mortality possibly increased with an increase in ZEB concentration (SD= 0.02).

SW480 cells were treated with two concentrations of ZEB (0.1mM and 0.3mM respectively), and its effect in KLF4 is presented in Figure 4.12. When compared to the untreated samples, the mean increase in C_t value (M= 10.43, SD= 0.28, N= 3) was seen to be significantly greater than zero where t(2)= 63.75, two-tailed p= 0.0002, providing evidence that treatment with 0.1mM ZEB was effective in down-regulating KLF4 gene expression. The same overall result was seen with 0.3mM ZEB, where t(2)= 42.69 and p= 0.0005 (M= 1.95, SD= 0.07, N= 3). Applying the $2^{-\Delta\Delta Ct}$ method revealed that treatment with 0.3mM ZEB demonstrated a less than one-fold up-regulation in KLF4 expression when compared to the low dose treatment. It is therefore statistically significant that treatment with both concentrations of VPA reduced KLF4 expression relative to the untreated samples, while the higher dose treatment was effective in up-regulating KLF4 relative to the lower dose.

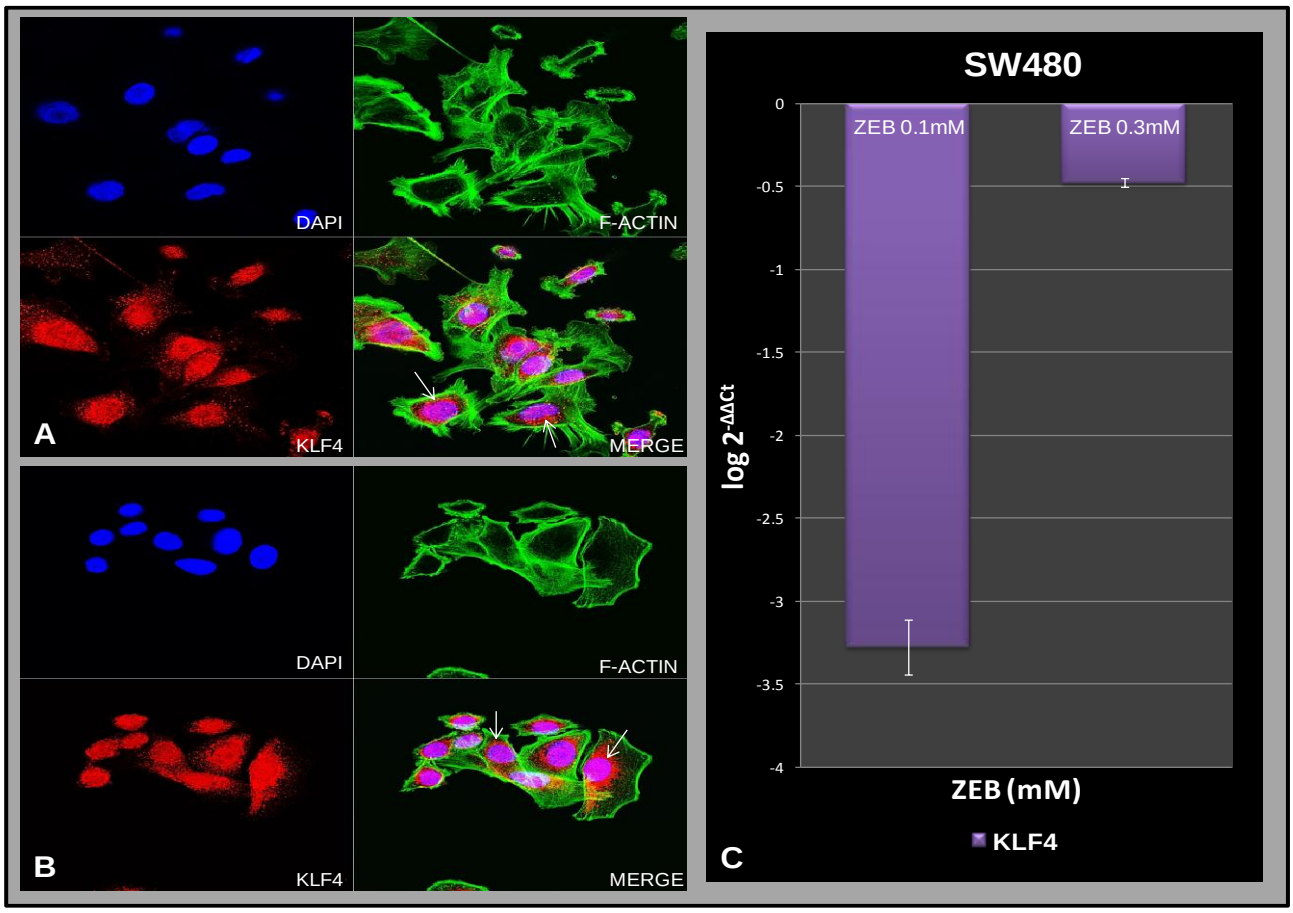


Figure 4.12 The effect of ZEB on KLF4 expression in SW480 cells. [A] Confocal microscopy images after treatment with 0.1mM ZEB (63x). [B] Confocal microscopy images after treatment with 0.3mM ZEB (63x). Nuclei= blue, actin filaments= green, KLF4= red, co-localisation= pink. Arrows indicate KLF4 localisation at nuclear periphery. [C] Gene expression of KLF4 after treatment with 0.1mM ZEB (p= 0.0002, SD= 0.28) vs 0.3mM ZEB (p= 0.0005, SD= 0.07) relative to untreated controls.

Although the microscopy images captured here were almost identical to the untreated controls seen in Figure A6.1 (refer to Appendix 6), there are however minor modifications evident. The overall irregular shape is preserved with both treatments, with a low cytoplasmic to nuclear ratio possibly associated with apoptosis. Here, though KLF4 localisation was mostly concentrated in the nucleus as observed in the untreated controls (see Figure A6.1), the intensity of the KLF4 localisation was much greater after treatment with both low and high doses of ZEB. KLF4 was also seen to be scattered throughout the cytoplasm and clustered at the nuclear periphery, as indicated by arrows (Figures 4.12A and B).

SW480 cells were also treated with two concentrations of ZEB to assess the effects on and to quantify the expression of CTNNB1. The mean increase in C_t value (M= 5.63, SD= 0.37, N= 3) from the untreated control was also found to be significantly greater than zero where t(2)= 25.78, two-tailed p= 0.0010, substantiating that treatment with 0.1mM ZEB was effective in down-regulating CTNNB1 gene expression. The same overall result was observed with 0.3mM ZEB, where t(2)= 35.78 and p= 0.0008 (M= 8.76, SD= 0.42, N= 3). Of particular note here, was that treatment with a higher dose of demethylating agent resulted in a two-fold down-regulation in CTNNB1 expression as compared with the lower dose treatment. This result is very similar to that observed with the HDACi treatments.

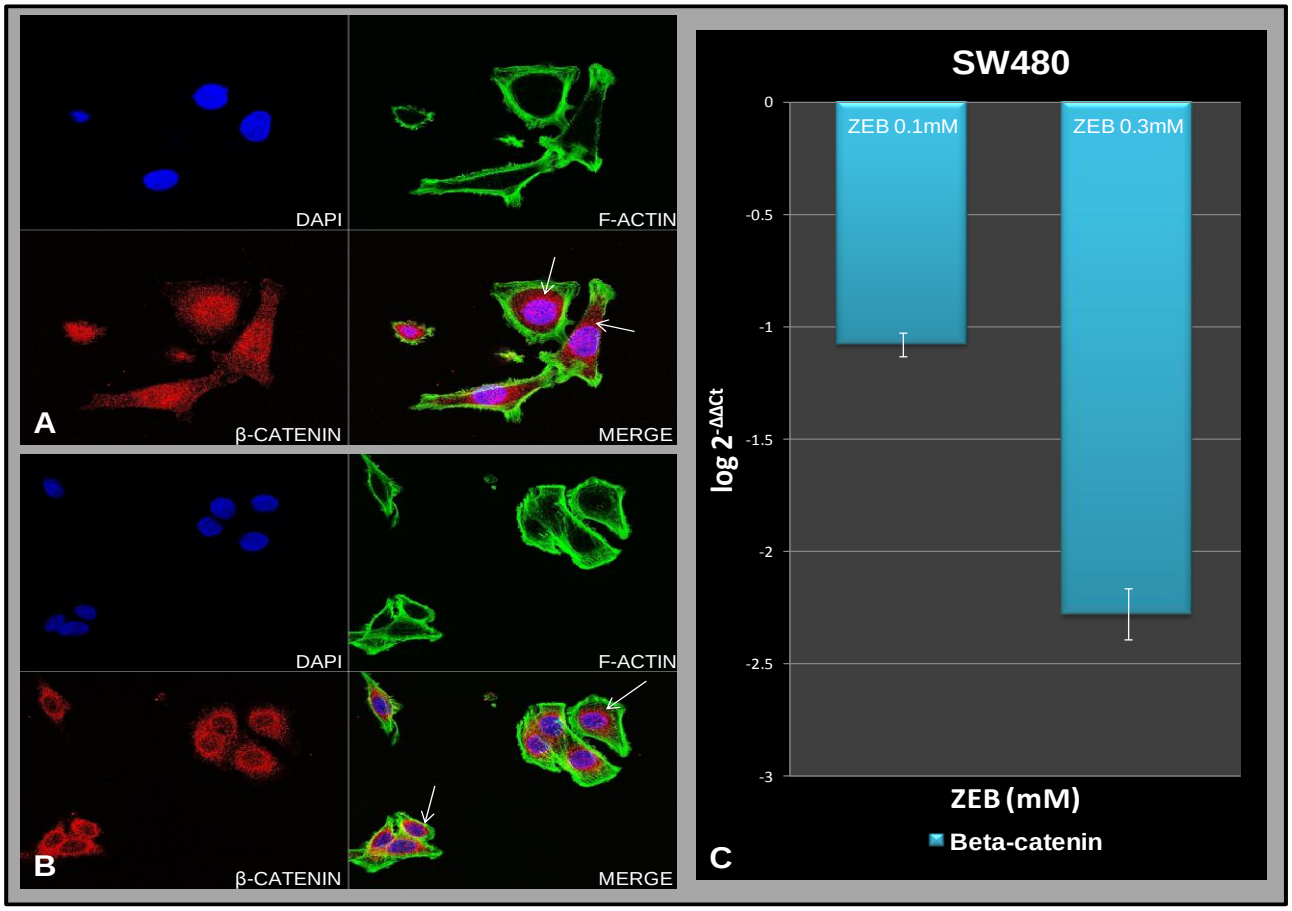


Figure 4.13 The effect of ZEB on CTNNB1 expression in SW480 cells. [A] Confocal microscopy images after treatment with 0.1mM ZEB (63x). [B] Confocal microscopy images after treatment with 0.3mM ZEB (63x). Nuclei= blue, actin filaments= green, β-catenin= red, nuclear associated protein β-catenin= pink. High β-catenin intensity seen at nuclear periphery (arrowed). [C] Gene expression of CTNNB1 after treatment with 0.1mM ZEB (p= 0.0010, SD= 0.37) vs 0.3mM ZEB (p= 0.0008, SD= 0.42) relative to untreated controls.

Morphological changes are very similar to those depicted in Figure 4.12, where a low nuclear to cytoplasm ratio was observed. β-catenin localisation is highly comparable to the untreated controls in Appendix 6 (refer to Figure A6.2), where protein is evidently distributed throughout the cytoplasm, with a higher intensity at the cell membrane and nuclear periphery (arrowed Figures 4.13A and B).

4.2.3.2 *The effects of Zebularine on late stage colorectal adenocarcinoma cells (DLD-1)*

Colorectal cancer cells of a late stage were cultured as described in Chapter 2.1, and treated with ZEB as seen in Chapter 2.2.2. A cell viability assay was performed (refer to Chapter 2.1.5) to quantify DLD-1 cells before and after treatment with the demethylating agent. The viability of 'no treatment' DLD-1 control cells remained in the 95%-99% bracket, with a significant decrease after cells were treated with 0.1mM VPA (~93% live cells) and an even further reduction in cell count after treatment with a higher dose of VPA (~89% live cells) as seen in Figure 4.14 (SD= 0.02). DLD-1 cells notably displayed a greater propensity to cell mortality than the SW480 cells after drug administration, indicating that DLD-1 cells were possibly more susceptible to drug treatments.

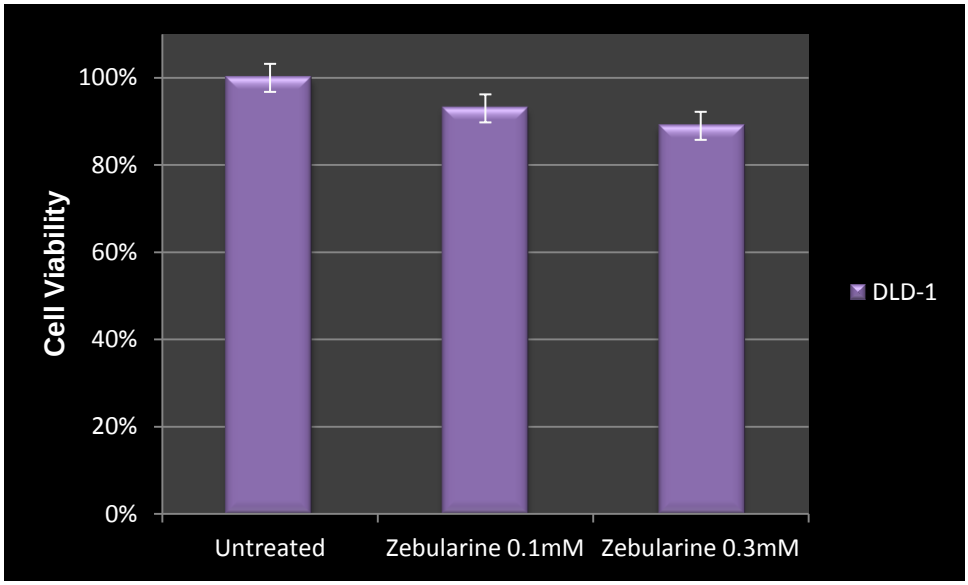


Figure 4.14 DLD-1 cell susceptibility to HDACi. Cells were treated with concentrations of 1.5mM and 5mM ZEB, respectively, for 24 hours. Cell mortality possibly increased with an increase in ZEB concentration (SD= 0.02).

DLD-1 cells were treated with two concentrations of ZEB, and its effect on KLF4 is illustrated in Figure 4.15. The mean increase in C_t value (M= 1.10, SD= 0.08, N= 3) when evaluated against the untreated controls was significantly greater than zero, where t(2)= 23.96, two-tailed p= 0.001, providing evidence that treatment with 0.1mM ZEB was effective in down-regulating KLF4 gene expression. Alternatively treatment with 0.3mM ZEB, where t(2)= 10.68 and p= 0.008 demonstrated an overall mean decrease in the C_t value (M= 0.28, SD= 0.04, N= 3) showed that a higher dose of ZEB was effective in up-regulating KLF4 gene expression. Treatment with a higher dose of ZEB exhibited approximately a six-fold increase in KLF4 expression when compared to the low dose treatment.

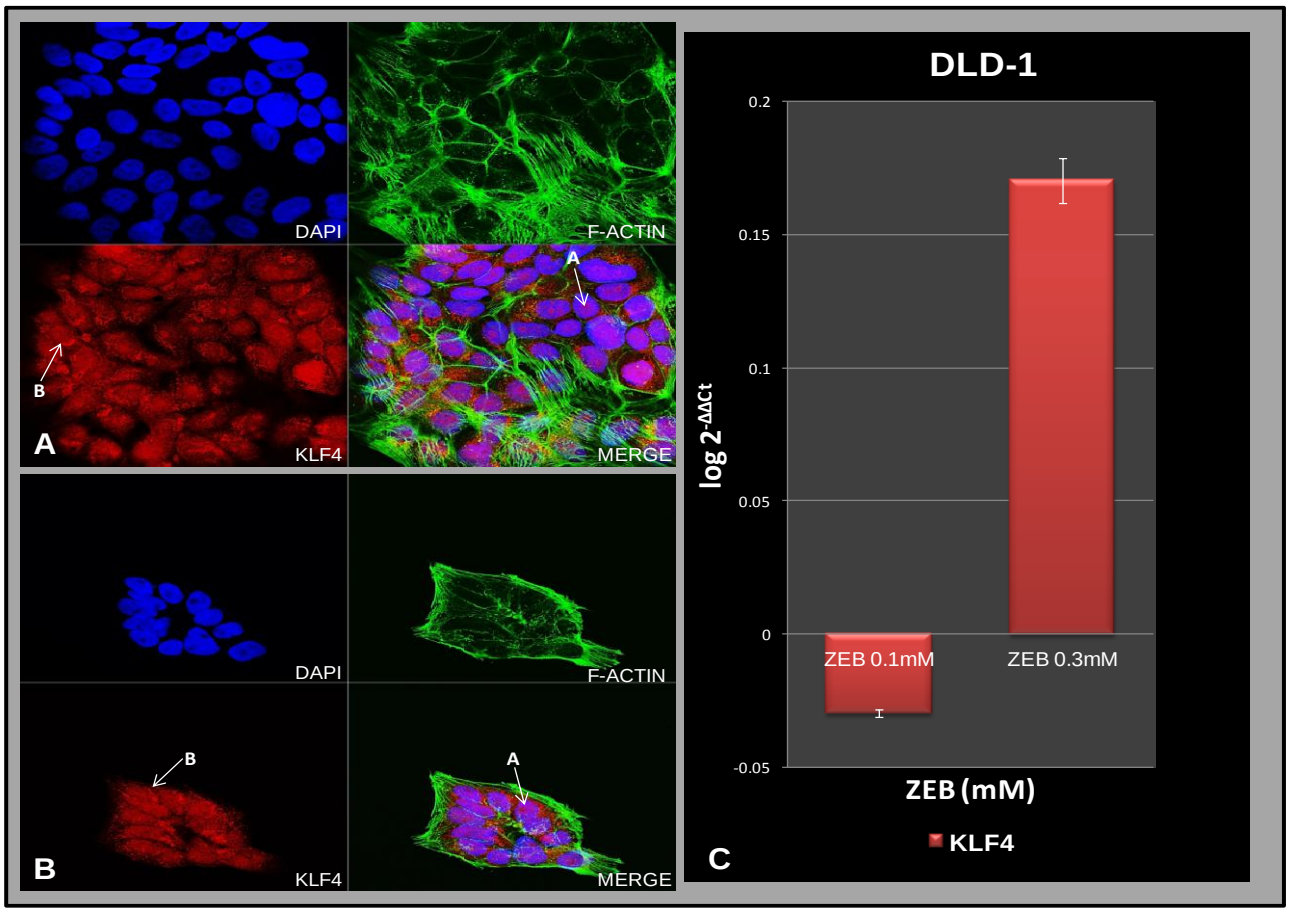


Figure 4.15 The effect of ZEB on KLF4 expression in DLD-1 cells. [A] Confocal microscopy images after treatment with 0.1mM ZEB (63x). [B] Confocal microscopy images after treatment with 0.3mM ZEB (63x). Nuclei= blue, actin filaments= green, KLF4= red, nuclear localised KLF4= bright pink. High KLF4 intensity within nucleosomes (arrow A) and Golgi bodies (arrow B) [C] Gene expression of KLF4 after treatment with 0.1mM ZEB (p= 0.001, SD= 0.08) vs 0.3mM ZEB (p= 0.008, SD= 0.04) relative to untreated controls.

Confocal imaging demonstrated minor morphological changes with regards to the cell shape, where treatment with both doses of ZEB effected little or no morphological changes, when compared to the untreated controls in Appendix 6 (Figure A6.3). The cytoplasmic to nuclear ratio is once again low, suggesting apoptotic activity. KLF4 protein is clearly localised in nucleosomes, as indicated in Figures 4.15A and B by arrow A, thereby signifying transcription sites for KLF4 production. Protein is also intensely localised in the nucleus and periphery, and it evidently observed in Golgi bodies as seen by the C-shaped structures adhering to the nucleus (arrow B in Figures 4.15A and B). These observations support the gene expression data showing an up-regulation in KLF4 expression relative to low dose treatment.

DLD-1 cells were also treated with two concentrations of ZEB to quantify the effects of this demethylating agent on the expression of CTNNB1. The mean decrease in C_t value (M= 3.64, SD= 0.07, N= 3) was found to be significantly greater than zero where t(2)= 86.60, two-tailed p= 0.0001, providing evidence that treatment with 0.1mM ZEB was effective in up-regulating CTNNB1 gene expression. Alternatively, a higher dose treatment with ZEB displayed an overall mean increase in the C_t value, where t(2)= 12.59 and p= 0.0060 (M= 4.88, SD= 0.67, N= 3), demonstrating that 0.3mM ZEB effectively down-regulated CTNNB1 expression almost two hundred-fold, relative to the low dose treatment. The results obtained here contradict those seen previously (see Figure

4.12) and are completely antagonistic to the gene expression data obtained with KLF4 (see Figure 4.15C).

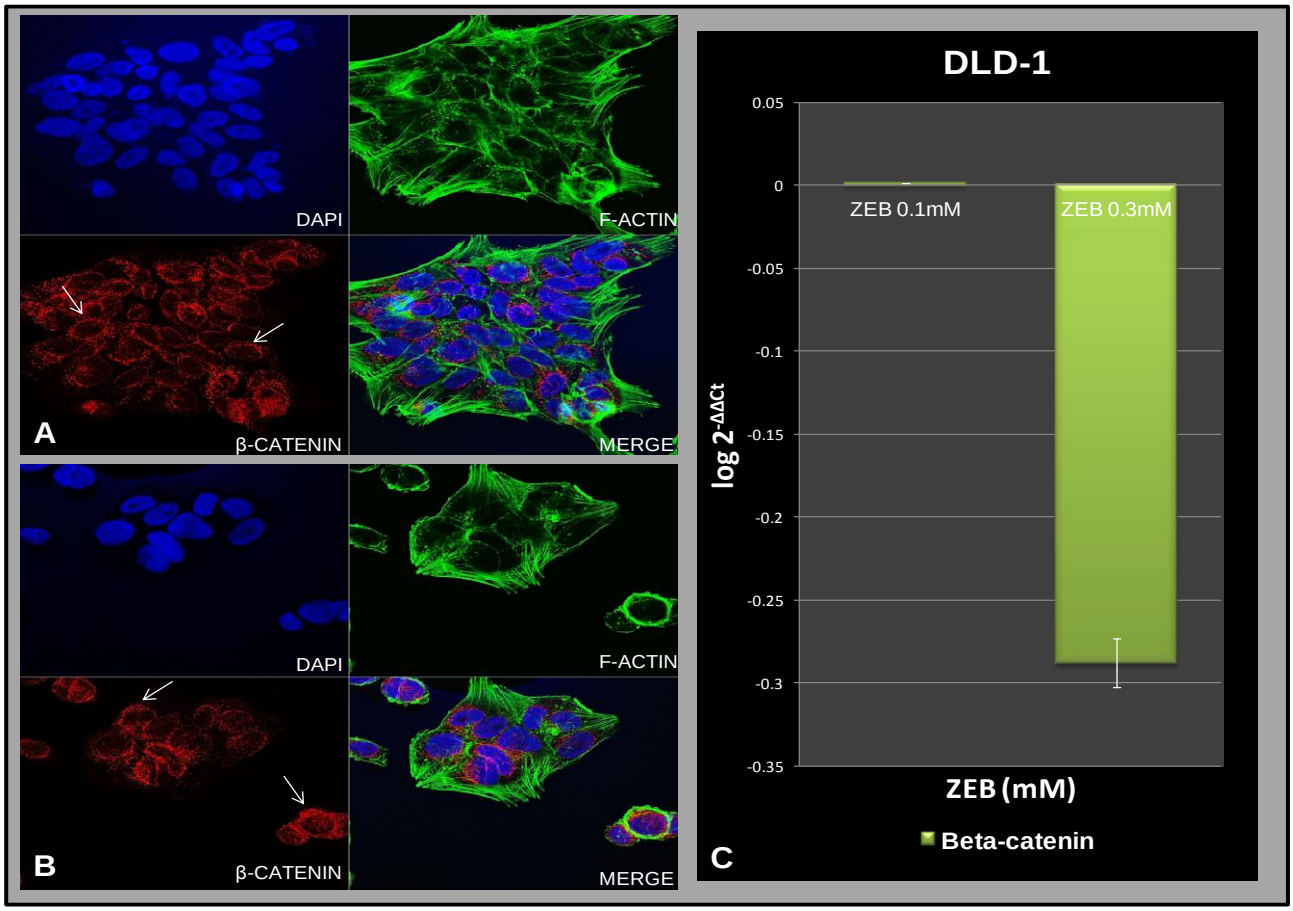


Figure 4.16 The effect of ZEB on CTNNB1 expression in DLD-1 cells. [A] Confocal microscopy images after treatment with 0.1mM ZEB (63x). [B] Confocal microscopy images after treatment with 0.3mM ZEB (63x). Nuclei= blue, actin filaments= green, β-catenin= red. β-catenin is intensely localised at the nuclear periphery. Note: there is no β-catenin protein observed in the nucleus [C] Gene expression of CTNNB1 after treatment with 0.1mM ZEB (p= 0.0001, SD= 0.07) vs 0.3mM ZEB (p= 0.0060, SD= 0.67) relative to untreated controls.

Figures 4.16A and B display an overall irregular cellular shape, however the cell volume seems less than that observed in the untreated controls (Figure A6.3). β-catenin is highly concentrated at the nuclear periphery (arrowed Figures 4.16A and B) and is scarcely distributed throughout the cytoplasm. There is no evidence of β-catenin within the nuclei. Cells appear more compact and oval in shape after high dose treatment (Figure 4.16B) with ZEB than compared to the low dose treatment (Figure 4.16A).

4.2.3.3 *The effects of Zebularine on MCF7 breast adenocarcinoma cells*

Breast cancer cells were cultured as described in Chapter 2.1, and treated with ZEB (see Chapter 2.2.2). A cell viability assay was performed (Chapter 2.1.5) to quantify MCF-7 cells before and after a low and high dose treatment with ZEB. The viability of 'no treatment' control cells lay in the 95%-99% range, with a significant decrease observed when cells were treated with 0.1mM ZEB (~97% live cells) and an even further reduction in numbers after treatment with a higher dose of ZEB (~79% live cells) as illustrated in Figure 4.17 (SD= 0.13). Cell mortality proved to be greater in

breast cancer cells when compared to colorectal cancer cells after drug administration, thus MCF-7 cells proved to show a greater susceptibility to this drug.

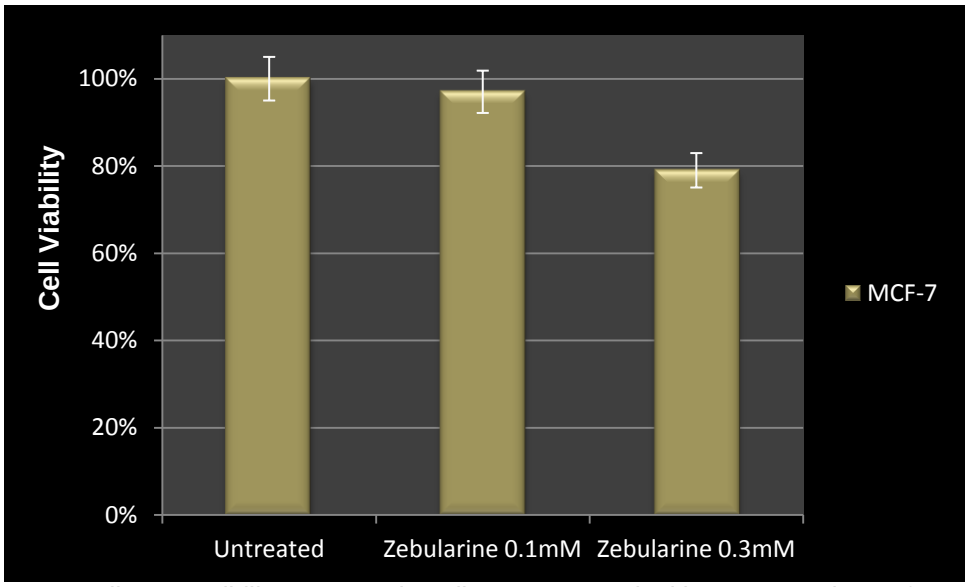


Figure 4.17 DLD-1 cell susceptibility to HDACi. Cells were treated with concentrations of 1.5mM and 5mM ZEB, respectively, for 24 hours. Cell mortality possibly increased with an increase in ZEB concentration (SD= 0.13).

MCF-7 cells were treated with two doses of ZEB, and its effect on KLF4 expression was observed (Figure 4.18). The mean decrease in C_t value (M= 3.38, SD= 0.12, N= 3) was found to be greater than zero where t(2)= 48.96, two-tailed p= 0.0004, providing evidence that treatment with 0.1mM ZEB was effective in up-regulating KLF4 gene expression. Treatment with 0.3mM ZEB where t(2)= 16.11 and p= 0.0030 (M= 4.90, SD= 0.52, N= 3) also showed an overall mean decrease, illustrating that a higher dose of ZEB was two-fold more effective in up-regulating KLF4 gene expression, than a low dose treatment in breast cancer cells.

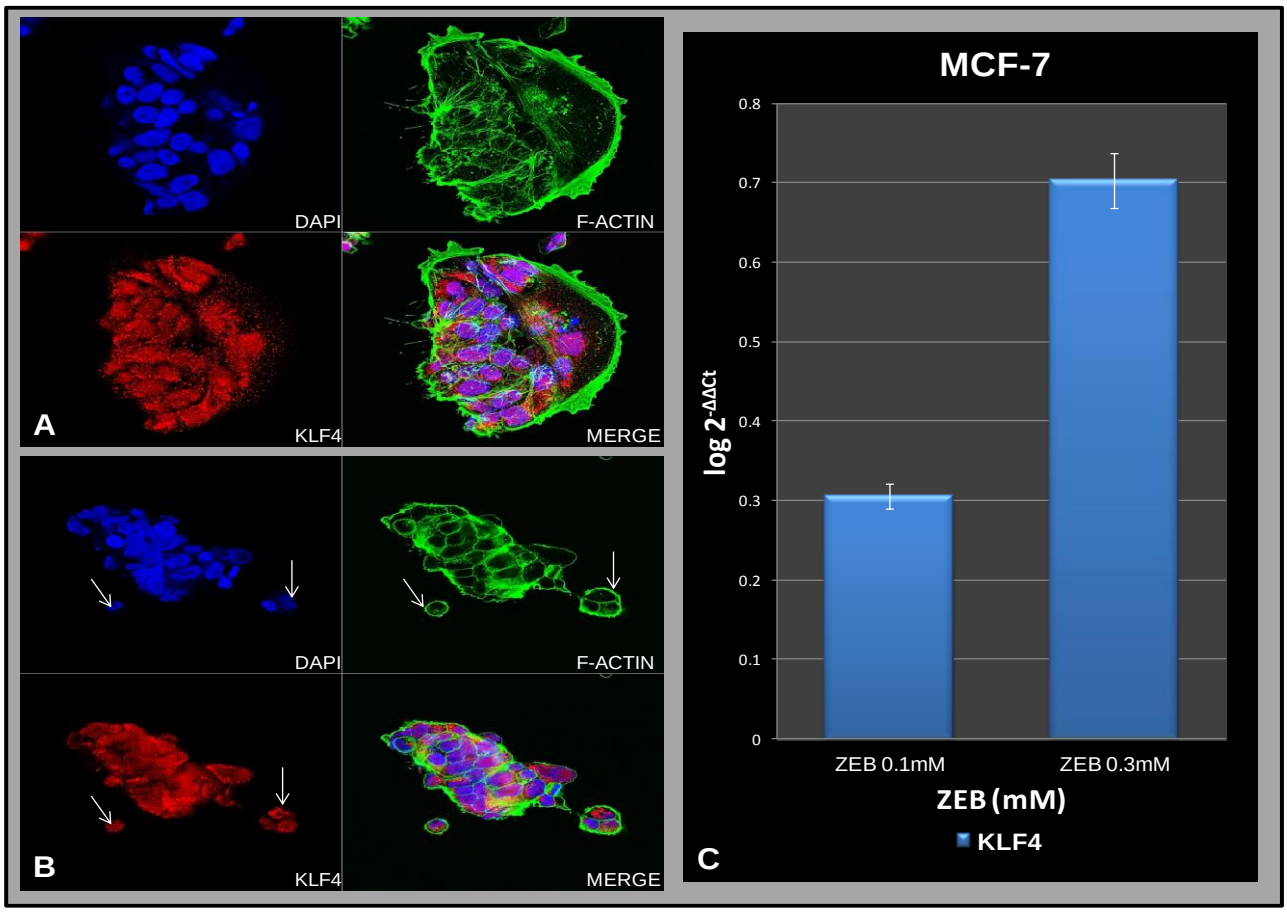


Figure 4.18 The effect of ZEB on KLF4 expression in MCF-7 cells. [A] Confocal microscopy images after treatment with 0.1mM ZEB (63x). [B] Confocal microscopy images after treatment with 0.3mM ZEB (63x). Nuclei= blue, actin filaments= green, KLF4= red, co-localisation= pink. Membrane blebbing was observed in late stage breast cancer cells (arrowed). [C] Gene expression of KLF4 after treatment with 0.1mM ZEB (p= 0.0004, SD= 0.12) vs 0.3mM ZEB (p= 0.0030, SD= 0.52) relative to untreated controls.

Confocal imaging displayed a change in cell shape from irregular to oval with a low cell volume. This was most evident in the high dose ZEB treatment, where the cytoplasmic to nuclear ratio was minimal and membrane blebbing was observed (see arrowed Figure 4.18B), suggesting apoptosis. Protein localisation remained at the nuclear periphery, with low concentrations scattered throughout the cytoplasm. Nuclei appear to be enlarged, which may potentially be a result of an alteration in chromatin status after ZEB treatment, thereby leading to DNA demethylation and an increase in KLF4 transcription levels.

MCF-7 cells were also treated with two doses of ZEB to examine its effect on CTNNB1 expression. The mean increase in C_t value (M= 0.57, SD= 0.83, N= 3) was found to be significantly greater than zero where t(2)= 1.20, two-tailed p= 0.17, providing evidence that treatment with 0.1mM ZEB up-regulated CTNNB1 gene expression (n.s.). Alternatively, treatment with 0.3mM ZEB demonstrated a mean decrease, where t(2)= 4.91 and p= 0.03 (M= 1.16, SD= 0.40, N= 3). Thus, as understood in Chapter 3.3.1.3 with the HDACi treatments, the higher dose ZEB resulted in a three-fold increase in CTNNB1 expression when compared to the low dose treatment.

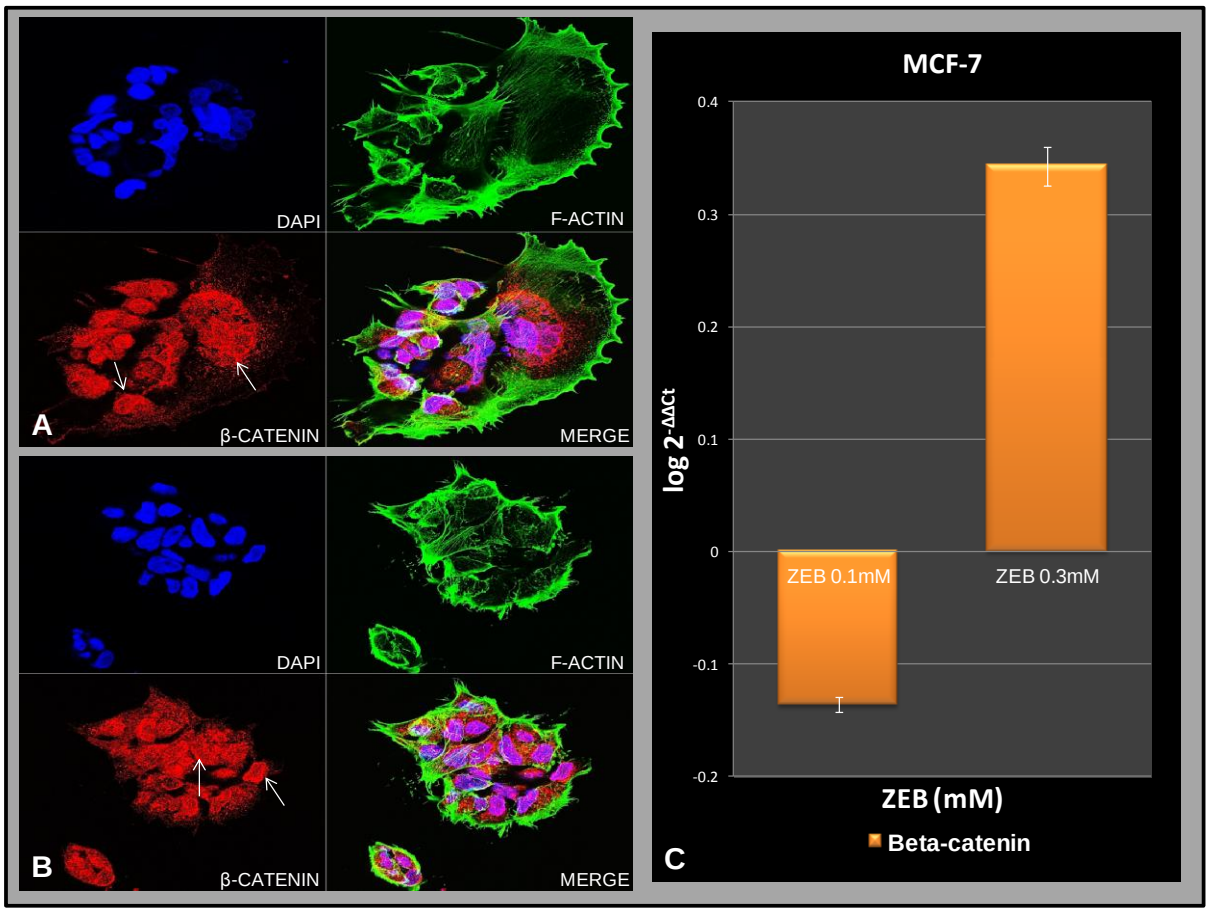


Figure 4.19 The effect of ZEB on CTNNB1 expression in MCF-7 cells. [A] Confocal microscopy images after treatment with 0.1mM ZEB (63x). [B] Confocal microscopy images after treatment with 0.3mM ZEB (63x). Nuclei= blue, actin filaments= green, β-catenin= red, co-localisation= pink. High peri-nuclear intensity of β-catenin is indicated by arrows. [C] Gene expression of CTNNB1 after treatment with 0.1mM ZEB (p= 0.17, SD= 0.83, n.s.) vs 0.3mM ZEB (p= 0.03, SD= 0.40) relative to untreated controls.

Figures 4.19A and B illustrate that the shape of cells range from oval to irregular, and the volume of cytoplasm is relatively low. Here, β-catenin protein displays a high intensity of peri-nuclear (arrowed Figures 4.19A and B) and cytoplasmic localisation, as well as traces of nuclear localisation. The peripheral pattern of localisation may relate to the relaxation of chromatin post treatment, allowing for peripheral transcription.

4.3 Discussion

Although DNA hypermethylation is a recurrent anomaly in several malignancies, it is possible to reverse the effects of methylation on gene segments creating a multitude of possibilities in the field of gene therapy (Das and Singal, 2004). This chapter discusses the significance of DNA hypermethylation on the expression of two key genes in colorectal and breast cancer cell lines, and the effects of inhibitors on gene regulation. DNA hypermethylation is associated with neoplasia, while the opposite, hypomethylation, is found in benign tissue (Esteller, 2008). The methylation patterns in KLF4 and CTNNB1 genes were analysed through the execution of computational techniques, and related to the methylation status of early and late stage cancer cells. ZEB was selected here as the demethylating agent of choice as a result of its low toxicity and high stability in solution (Cheng *et al*., 2004). ZEB drug concentrations of approximately 0.2mM to 0.4mM proved to inhibit DNMT activity optimally, while all concentrations less than that displayed minimal DNMT

inhibition, as seen in previous studies, thus most favourable concentrations of 0.1mM and 0.3mM were selected (Billam *et al.*, 2009; Cheng *et al.*, 2003).

4.3.1 Analysis and quantification of methylation patterns

Methylation through the action of DNA methyltransferases (DNMTs) commonly takes place at CpG dinucleotides, via the addition of a methyl group to the fifth carbon of the cytosine ring (refer to Figure 4.2) (Singal and Ginder, 1999; Bird, 1986). The 'CpG Island Searcher' and 'CpGi130' programs were utilised to predict the positions of CGIs in *KLF4* and *CTNNB1* using two slightly different approaches. The 'CpG Island Searcher' applied the "sliding and jumping" window technique explained in Figure 4.6, relating to the initial criteria met by Gardiner-Garden and Frommer (Gardiner-Garden and Frommer, 1987). The 'CpGi130' tool from MethyCancer identified CGIs based on the revised criteria met by Takai and Jones from sequence clones derived from the Sanger Institute (Takai and Jones, 2002).

Both of these bioinformatic tools generated consistent results for *KLF4* and *CTNNB1*, and excluded the potential occurrence of Alu-repeat sequences. The O/E ratios for both genes were always considerably greater than 0.60. Although the CGI discovered in *KLF4* was clearly approximately 2kb larger than that observed in *CTNNB1*, the O/E ratio of *CTNNB1* was closer to 1.0 and slightly greater than that of *KLF4*, demonstrating a high methylation frequency in a smaller fragment of DNA. Both genes contained CGIs that abided by the Takai and Jones criteria (Takai and Jones, 2002) and were localised within the first 2kb of the gene, confirming the hypothesis that they could most certainly be associated with the 5' region and might well be contained within the promoter and could thereby pose a valid target of hypermethylation. It must be said however, that there is a greater chance that this is more likely to be true of *KLF4.*

The ChroView results from MethyCancer demonstrated that the *CTNNB1* gene was more heterochromatic than *KLF4* and therefore contained a greater frequency of silenced genes, although this may be a result of a lack of experimental data in *KLF4* research. On the other hand, ChroView did provide evidence that *KLF4* was rich in GC content, which proved to be consistent with the CpG island predictor programs relating to the high frequency of CpG islands. The Methylator program utilised a support vector machine (SVM) to predict CGI localisation through pattern recognition systems, revealing that *KLF4* contained a higher frequency of methylated cytosines that was confined within the 5' portion of the gene, validating results from both the "CpG Island Searcher" and "CpGi130". It is therefore evident that *KLF4* contains a larger CpG island in the 5' region than *CTNNB1* that may be prone to methylation.

Recent studies have expanded on the analysis of methylation in mammalian cells, and the discovery of 5-hydroxymethylation has initiated new interest in this field. An assay was performed to measure the amount of whole DNA hydroxymethylation as opposed to DNA methylation in early

and late stage colorectal cancer cell lines. As a result, it was found that the global methylation status of SW480 cells was two-fold greater than that observed in DLD-1 cells, thus the earlier stage cells displayed a higher frequency of methylation when compared to the advanced stage cells. The hydroxymethylation status of both early and late cells were negligible, even though the late stage cells displayed a slightly greater level of hydroxymethylation, validating the theory that 5-hmC is found at low levels in colorectal cancer and higher levels in other non-cancerous tissues such as the brain, liver, kidney as well as the colon (Li and Liu, 2011).

The reduced frequency of 5-hmC in colon cancer cells as opposed to normal intestinal tissue may be a result of several contributing factors, although the major instigator is still unknown. A reduction in Tet enzyme production or a mutation in the gene encoding the enzyme may bring about these changes (Delhommeau *et al*., 2009; Ko *et al*., 2010). A decrease in 5-hmC may also be a result of increased levels of 5-hydroxymethylcytosine DNA-glycosylase that acts on DNA by removing the 5-hmC unit (Cannon *et al.*, 1988). The authenticity of these results was determined through ruling out the existence of 5-hmC, thus the status of methylation in the colorectal cells exploited was purely of a 5-mC nature.

4.3.2 The effect of Zebularine on cell viability

Cell viability assays for all cell lines demonstrated a general pattern of increased cell death that was proportional to the concentration of ZEB; therefore as the dose increased so did the cell death. The breast cancer cell line showed the greatest susceptibility to demethylation with the highest cytotoxicity of all three cancer cell lines. The change of cell shape from an irregular to oval structure in certain cases may also signify the apoptotic behaviour. Thus ZEB dose-dependently reduced the viability of both colon and breast adenocarcinoma cell lines.

It is possible that cell death was a sole consequence of ZEB treatment, even though DMSO was used as a solvent for all treatments administered. DMSO has been reported to induce apoptosis in cancer cells, as well as to stimulate cell differentiation and alter cell morphology (Kim *et al*., 1980; Tsao *et al*., 1982; Grunt *et al*., 1991; Ossowski and Belin, 1985). While this solvent does not modify genetic material, it does however remove free radicals produced by damaged tissues that generally damage DNA and cell membranes, aiding in the transformation of their respiratory system from aerobic to anaerobic. This process in turn preserves the normal state of cells for an adequate period of time to allow them to undergo apoptosis (Warburg, 2012).

4.3.3 The effects of Zebularine on gene expression in colorectal cancer cells

Demethylation in early stage colon cancer cells displayed very similar results to that observed in cells treated with the HDAC inhibitor. Cells displayed dose-dependent gene regulation of KLF4 and CTNNB1 after 24 hour treatments. An analysis of the relative quantification results proved that KLF4 and CTNNB1 displayed an inverse relationship, much like that seen in Chapter 3. Low dose

ZEB treatments down-regulated KLF4 expression in SW480 cells, however treatments with a higher concentration demonstrated patterns of up-regulation, even though KLF4 expression was somewhat still less than the untreated controls. The reverse was seen for CTNNB1 in SW480 cells where a low dose treatment down-regulated expression but a high dose treatment had a greater effect on transcript down-regulation. The late stage colon cancer cells however displayed extreme results, where the low dose treatments were consistent with that seen in the early stage cells for KLF4, yet the higher dose treatments up-regulated KLF4 gene expression six-fold relative to the low dose treatment. In contrast, CTNNB1 was up-regulated as a result of low dose ZEB treatments, and down-regulated almost two hundred-fold following a high dose treatment. Thus, ZEB had a greater effect on regulating the expression of KLF4 and CTNNB1 in late stage colon cancer cells.

Confocal microscopy clearly demonstrated the appearance of KLF4 protein in Golgi bodies as well as ER in DLD-1 cells, representing their storage after production. However, this would need to be confirmed through the identification of Golgi-specific and ER-specific markers, such as RCAS1 (anti-Golgi) and Calnexin (anti-ER) antibodies respectively. RCAS1 is a type II transmembrane protein that is involved in Golgi functioning, while Calnexin is a chaperone protein localised in the ER membrane (Engelsberg *et al.*, 2003; Bergeron *et al.*, 1994). A higher intensity of protein is observed after high dose treatment where KLF4 expression was increased relative to the low dose treatment, suggesting an increase in transcription and translation as a potential result of DNA demethylation. KLF4 protein in both early and late stage cancer was localised in the nucleus while β-catenin was detected around the nuclear periphery. However a greater concentration of β-catenin was observed in the nucleus of SW480 cells after low dose treatment than that seen with high dose treatment, exhibiting consistency in results as seen in the gene expression data, as the expression of β-catenin decreased with a higher dose treatment. This is evidence substantiating the role of KLF4 as a transcription factor.

β-catenin translocates to the nuclear periphery where it associates with transcription factors, such as KLF4 and Wnt proteins (Zhang *et al.*, 2006). Confocal imaging illustrates that both these proteins colocalise within the nucleus and at the nuclear periphery where they interact either directly with each other or indirectly through other transcription factors. The high intensity of β-catenin localisation in early stage cancer cells, suggests a greater nuclear interaction of β-catenin with KLF4. ZEB treatments resulted in nuclei enlargement, which may potentially be the result of a shift in chromatin status, thereby leading to DNA demethylation and thus an increase in KLF4 transcription levels. This was validated by the increase in KLF4 protein within nucleosomes after ZEB treatment in DLD-1 cells, however this would need to be confirmed through the use of anti-nucleosome antibodies.

It was also highly evident that SW480 cells retained their overall irregular morphology after ZEB treatments, however DLD-1 and MCF7 cells displayed an overall change to a more rounded structure, reducing the adhesive abilities of cells and resulting in cellular detachment, indicating potential apoptotic events (Bonnotte *et al.*, 1998; Agarwal *et al.*, 2002; Ramasamy *et al.*, 2012). In addition to this, ZEB treatment led to alterations of the cytoskeletal structure as observed in MCF7 cells, where membrane blebbing was observed. As this is dependent on caspase-3 levels in the cells, there is a possibility that the typically caspase-3 deficient MCF-7 cells underwent a reconstitution of caspase-3 after ZEB treatment, thereby increasing the chances of apoptosis (Mills *et al.*, 1999; Devarajan *et al.*, 2002; Andrade *et al.*, 2010). This however would need to be confirmed through the use of caspase-3 antibodies, or other pro-apoptotic markers, namely Bax or Bcl-2 (Oltvai *et al.*, 1993).

Data from the gene expression profiles revealed that the differential expression of KLF4 and CTNNB1 in colon cancer displayed aberrant transcript levels in early and late stage cell lines, however gene expression in both stages were highly similar with slight differences. It is evident that KLF4 maintains an inverse relationship with β-catenin, and that KLF4 is involved in the direct or indirect inhibition of β-catenin (Evans *et al.*, 2010). It was recently discovered that the loss of KLF4 expression is related to the tumourigenic activity in colon cancer, thus the up-regulation of KLF4 through DNA demethylation reverses the malignancy of colon cancer cells by inducing differentiation (Xu *et al*., 2008). The inverse expression of both these genes in colon cancer cells supports the cell viability assay data obtained here, that this transcriptional pattern of genes may lead to apoptotic events. Several other studies validate this statement, providing evidence that the inhibition of β-catenin in colon cancer may contribute to apoptosis (Kim *et al.*, 2005; Han *et al.*, 2008). As β-catenin is an active member of the Wnt pathway, the down-regulation of β-catenin could result from the inhibition of the Wnt pathway, leading to an increased tendency of cell death (Watson, 2004; Yeh *et al*., 2011).

KLF4 expression within the normal gastrointestinal epithelium is known to be elevated, therefore making it possible that its expression may be higher in early stage colon cancers than late stage colon cancers, in its progression to a more malignant phenotype (Flandez *et al.*, 2008). Hypothetically, early stage cancer cells would exhibit the lowest incidence of methylation, deeming ZEB less effective when compared to its activity in advanced stage cancer cells. ZEB reduced KLF4 expression in early stage cells after low dose treatments, after which high dose treatments increased expression levels relative to this; however the expression of KLF4 remained lower than that of the ‘no treatment’ control. It is most likely that the KLF4 gene in late stage cancers presents a greater frequency of hypermethylation than early stage cancers, and is thereby either expressed at lower levels or is completely silenced. Treatments with high dose ZEB largely elevated expression levels of KLF4, validating this theory.

4.3.4 The effect of Zebularine on gene expression in breast cancer cells

The effect of DNA demethylation on KLF4 and CTNNB1 expression in breast cancer cells was consistent with the results observed involving HDAC inhibition. It has been determined that these genes work in accordance with one another in both breast and colon cancer cell lines (Zhang et al., 2006), however gene expression profiles obtained in this study presented data that disputed colon cancer regulation. KLF4 was up-regulated following DNA methyltransferase inhibition by ZEB, which proved to be more effective with the higher dose treatments. The extent of the up-regulation observed here was nevertheless greater than that observed with the HDACi treatments. The transcription of CTNNB1 once again displayed unusual results, where the lower dose ZEB treatment down-regulated gene expression after which it was increased with a high dose treatment, relative to the untreated controls.

Localisation of KLF4 and β-catenin protein in breast cancer cells was consistent with results seen in the previous chapter. KLF4 demonstrated nuclear localisation as well as a high concentration at the nuclear periphery and within Golgi bodies. β-catenin was found at high intensities throughout the cytoplasm in its translocation to the nucleus, and was scattered at low frequencies within the nucleus. Its nuclear localisation validates data generated from the gene expression profiles that CTNNB1 was up-regulated following ZEB treatment. Thus its expression through DNA demethylation supports its role in the Wnt signalling pathway, where β-catenin protein may form complexes with nuclear proteins like TCF/LEF that are involved in breast cancer development.

ZEB treatment has illustrated that a lower dose has a greater anti-tumourigenic effect on breast cancer cells than the high dose treatment, contradicting results obtained from the colon cancer cell lines. The higher dose treatment results in the overexpression of both KLF4 and CTNNB1, more than likely contributing to apoptosis and thereby confirming the cell viability assay results. This was observed by membrane blebbing seen in cells treated with a high dose ZEB, however this would need to be confirmed through the application of blebbing markers, such as antibodies to DAPK and DRP-1 proteins (Inbal *et al.*, 2002). As explained previously, a related study performed on a several cancer cell lines treated with Sulindac, a non-steroidal anti-inflammatory drug (NSAID), generated similar results, where this NSAID suppressed β-catenin in MCF-7 cells thereby inhibiting apoptosis, thus validating that its overexpression would result in cell death (Han *et al.*, 2008). As a result, overexpression of β-catenin can only be a product of an overactive Wnt pathway (He *et al*., 2004). KLF4 is uniquely regulated in breast cancer cells, where it plays a role as an oncogene. Thus, an increase in KLF4 expression in MCF-7 cells is related to a more malignant phenotype (Foster *et al.*, 2000; Yu *et al.*, 2011). A low dose treatment thereby displayed a slight increase in KLF4 gene expression relative to untreated control, while a higher dose HDACi treatment could either be associated with tumourigenic activity, or apoptosis, when its relationship with β-catenin is taken into consideration.

4.3.5 DNA methyltransferase inhibition by Zebularine

DNA methylation is an essential mechanism involved in the regulation of gene expression through the hypermethylation or hypomethylation of DNA segments (Tate and Bird, 1993). Gene silencing is associated with hypermethylation of promoter regions, and acts by preventing the adhesion of transcription factors to DNA segments due to blocked sites, thereby leading to oncogenic activity (Bhaumik *et al.*, 2007). This was clearly the case with KLF4, as the analysis of the gene structure through bioinformatics provided substantial evidence that the large CGI produced here followed the criteria proposed by Takai and Jones and was located within the first 2kb of the gene segment, composing more than 60% of the entire KLF4 gene (Takai and Jones, 2002).

DNA methylation is a biochemical reaction in eukaryotes that involves the transfer of a methyl group to the fifth carbon of a cytosine ring, catalysed by DNA methyltransferases (Singal and Ginder, 1999). There are four known DNMTs, three of which are actively expressed in colon and breast cancer tissue, namely DNMT1, DNMT3a and DNMT3b (Bestor, 2000; Bestor *et al.*, 1988; Kanai and Hirohashi, 2007; Lei *et al*., 1996). DNMT3a and DNMT3b, commonly known as *de novo* DNMTs, are involved in developing a pattern of methylation during embryogenesis, while DNMT1 plays a role in maintaining this pattern of methylation throughout the development of the organism after DNA replication (McCabe *et al.*, 2009).

ZEB is a 2-(I*H*)-pyrimidinone ribonucleoside that is taken up during DNA synthesis and is incorporated into the DNA after post-transcriptional modifications (Cheng *et al*., 2003; Cheng *et al.*, 2004). It is primarily involved in the total inhibition of DNMT1 activity, and the fractional inhibition of the DNMT3a and DNMT3b population, all three of which are relevant in colon and breast cancer (Cheng *et al*., 2004). ZEB has no effect on DNMT2 as this weak enzyme lacks a regulatory domain and possesses only tRNA methyltransferase activity (Goll *et al.*, 2006; Hermann *et al.*, 2003). It is essentially active during methylation, where DNMT1 binds covalently to the sixth carbon of cytosine as well as the pyrimidinone ring of ZEB. Normally the transfer of the methyl group from SAM to cytosine frees DNMT1 from cytosine, however when the 2-(I*H*)-pyrimidinone ring replaces cytosine the transfer is blocked and the methyltransferase is trapped leading to a reduction in methylation, as the replication fork proceeds without the DNMT (Wu and Santi, 1985).

ZEB thereby acts on the promoter region of KLF4 in colon cancer by inhibiting DNMTs associated with this gene, namely DNMT1, and possibly DNMT3a and DNMT3b to a lower degree. Several other cancers have displayed similar epigenetic activities with KLF4. An investigation of KLF4 in gastric cancer produced results that confirmed the hypermethylation of the promoter leading to its depletion, although this is more commonly reported in colon cancers (Cho *et al*., 2007; Wei *et al.*, 2005; Wei *et al*., 2006). The KLF4 promoter in medulloblastoma cell lines were also discovered to contain a high frequency of CpG hypermethylation thereby suppressing the gene (Nakahara *et al.*, 2010). Another study examined the expression of KLF9 in endometrial carcinomas, where an up-

regulation of this Kruppel-like factor was accompanied by the down-regulation of DNMT1 as well as the increased expression of KLF4 (Simmons *et al*., 2011). ZEB affects the Wnt pathway by activating the expression of negative Wnt regulators that have been silenced in cancer cells through their promoter methylation, such as WNT7A in pancreatic cancer and WNT9A in colon cancer (Sato *et al*., 2003; Shu *et al.*, 2006). This subsequently down-regulates β-catenin, inhibits cell proliferation and activates apoptotic proteins (Baylin and Ohm, 2006).

ZEB has been discovered to preferentially inhibit the growth of colon cancer cells, by up-regulating p53-mediated $p21^{WAF1}$ mRNA levels leading to cell cycle arrest in the G1 phase (Cheng *et al*., 2004; Waga *et al.*, 1994). $p27^{KIP1}$, another CDK-inhibitor protein, was unaffected by demethylation (Cheng *et al.*, 2004). A further key observation made in the same study was the demethylation of p16 after drug treatment, this being a CDK-inhibitor containing a high frequency of 5' hypermethylation. ZEB was found to induce the expression of this gene leading to cell cycle arrest (Cheng *et al.*, 2004). Studies done on pancreatic cancer cell lines revealed that treatment with ZEB strongly up-regulated the pro-apoptotic protein Bax and reduced the expression of anti-apoptotic protein Bcl-2 leading to apoptosis (Neureiter *et al.*, 2007). The methylation status of *DAPK* and *Caspase 8* was also altered resulting in their activation leading to apoptotic events (Pompeia *et al.*, 2004; Kissil *et al.*, 1997).

ZEB in breast cancer induces the expression of p21 and reduces cyclin-D levels, consequently arresting the cell cycle in S-phase. At higher doses, ZEB was capable of increasing pro-apoptotic protein expression of Bax (Billam, Sobolewski and Davidson, 2009). ZEB is also known to target several aspects of epigenetic therapy other than increased cell cycle arrest and apoptosis in cancer cells. An example of such is the removal of methyl groups from the promoter region of *MLH1*, thereby reactivating the gene and increasing sensitivity to chemotherapy (Plumb *et al.*, 2000). *In vivo* studies proved that ZEB actively prevents intestinal tumours in mice through oral administration, but however had no effect when presented to monkeys (Holleran *et al.*, 2005; Yoo *et al*., 2008).

CHAPTER 5

COMBINATION THERAPY

5.1 Introduction

As discussed in the previous chapters, there is evidence that cancer is a result of various epigenetic modifications, and thus in the case of this study two highly stable therapeutic epigenetic modifying agents have been assessed. VPA has been found to induce differentiation and cell cycle arrest through the inhibition of HDACs, while ZEB is capable of reactivating silenced genes through the demethylation of tumour suppressors (Gottlicher *et al.*, 2001; Gurvich *et al.*, 2004; Cheng *et al.*, 2004). Individually these anticancer agents have shown great success in their *in vitro* and *in vivo* activities, and there is further evidence that these drugs may be used in combination to enhance their overall therapeutic effects on cancer cells.

5.1.1 Synergistic activity of HDAC inhibitors and demethylating agents

There is a mutual physical and functional relationship between chromatin structure and methylation of DNA sites, where inactive or heterochromatin contains hypermethylated DNA sites and active or euchromatin contains hypomethylated DNA (Razin and Cedar, 1977). It is apparent that the solitary treatment with either an HDAC inhibitor or demethylating agent may be efficient in the treatment of cancer cells. However, there may be cases where this has minimal effect on the reactivation of silenced genes, whereas a combined treatment may lead to a more successful anti-proliferative outcome (Cameron *et al.*, 1999).

Other than there being a physical link between these two epigenetic states, it has been discovered that the drugs involved in targeting HDACs and those affecting methylation status are also well associated. As illustrated in Figure 5.1, HDAC inhibitors play an additional role in DNA demethylation that is independent of replication, such as in the demethylation of brain or heart tissues that are no longer mitotic (Cervoni and Szyf, 2001). ZEB is a replication-dependent DNMT inhibitor that functions at the replication fork and would be non-functional in brain and heart tissue, while VPA is an HDAC inhibitor that induces ectopic demethylation that is independent of replication, and has been reported to demethylate the *reelin* gene in the mouse model, mainly in the brain (Detich *et al*., 2003; Milutonovic *et al.*, 2007; Tremolizzo *et al.*, 2002).

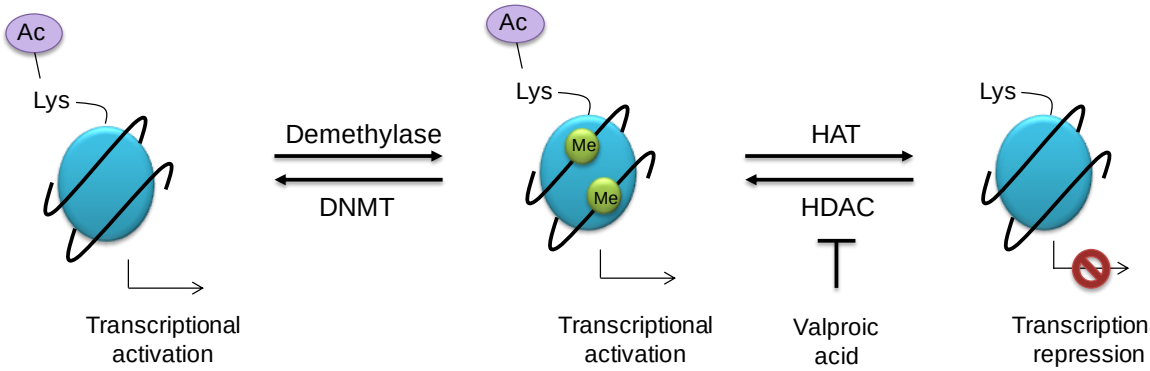


Figure 5.1 Schematic diagram illustrating the effects of HDAC inhibitors on DNA methylation. DNA is demethylated through the acetylation of target genes via HDAC inhibitors such as VPA (Szyf, 2009).

There are several synergistic mechanisms of action that are responsible for the anti-cancer effects brought about through the use of HDAC inhibitors and DNMT inhibitors. One is via the induction of apoptosis, for example studies showed the use of TSA in cells was highly cytotoxic and this was augmented when cells were first treated with 5-aza-CdR. These results were either accountable to the demethylation or acetylation of apoptotic genes leading to their activation (Weiser *et al.*, 2001). Another mechanism is through the induction of genes involved in cellular differentiation as well as cell cycle regulatory genes such as those transcribing cyclin dependent kinases (Guan *et al.*, 2000; Cameron *et al.*, 1999). HDAC inhibitors and DNMT inhibitors may work in synergy to enhance the reactivation of specific genes that have undergone epigenetic silencing (Kikuchi *et al.*, 2002; Yang *et al.*, 2001).

5.1.2 Combination therapy in clinical practice

The first study to demonstrate the combined effect of an HDAC inhibitor and DNMT inhibitor, in this case sodium butyrate and 5-aza-CR, was conducted by Jahanageer and colleagues and was found to up-regulate the β-adrenergic receptor in HeLa cells (Jahangeer *et al.*, 1982). This was followed by a multitude of investigations, using the same combination or a range of different inhibitors, an example being the effect of TSA and 5-aza-CdR on cell lines in the search to discover any new tumour suppressor genes (Cameron *et al.*, 1999; Suzuki *et al.*, 2002; Yamashita *et al.*, 2002). Numerous clinical trials are underway to test the efficacy of these combinations in human subjects, which are capable of targeting separate epigenetic modifications simultaneously. A study demonstrating the effect of VPA and 5-aza-CR in patients with advanced cancers was found to exhibit genome-wide demethylation as well as an overall increase in histone acetylation, and another investigating synergy between VPA and 5-aza-CdR in leukaemia patients showed similar results with *p15* reactivation (Braiteh *et al.*, 2008; Garcia-Manero *et al.*, 2006; Soriano *et al.*, 2007). Therefore it can be seen that the synergy between these two modifications are highly complex and require the activity of several other factors.

5.1.3 Experimental approach

The purpose of this chapter was to evaluate the expression levels of KLF4 and CTNNB1 following the epigenetic modulation of both chromatin and methylation patterns. Here, the early and late

stage colorectal cell lines were treated synergistically with two doses of VPA and ZEB for approximately 24 hours, and a relative quantification of KLF4 and CTNNB1 expression was performed applying the $2^{-\Delta\Delta Ct}$ method to analyse relative gene expression. Subsequently, KLF4 and β-catenin protein expression patterns were investigated through the utilisation of immunofluorescence techniques, where the results were later viewed under a confocal microscope.

5.2 Results

5.2.1 Relative quantification of gene expression

For all treatments, Ct values were reviewed and a paired Students t-test was performed to compare sample means before and after treatment. The $2^{-\Delta\Delta Ct}$ method was used to analyse relative gene expression in this study (Livak and Schmittgen, 2001). The C_t of the target gene was initially normalised to that of the reference gene (in this case β–actin) for both test and calibrator samples following Equations 3.1 and 3.2 (Chapter 3.3.1). The C_t of the test sample was then normalised to the C_t of the calibrator as seen in Equation 3.3. As a result, the ratio of the target gene in the test sample to the calibrator sample was found, which was normalised to the reference gene. The expression ratio can be calculated following Equation 3.4 (Chapter 3.3.1). All treated sample results are relative to the untreated samples.

5.2.1.1 *The effects of low and high dose synergistic treatments on early stage colorectal adenocarcinoma cells (SW480)*

Colorectal cancer cells of an early stage were cultured as in Chapter 2.1, and treated synergistically with low and high doses of VPA and ZEB as described in Chapter 2.2. A cell viability assay was performed (Chapter 2.1.5) to quantify SW480 cells before and after a low and high dose treatment with both synergistic treatments. The viability of ‘no treatment’ control cells lay in the 95%-99% bracket, with a negligible decrease observed when cells were treated with SYN1 (~98% live cells) and a further decline in numbers after treatment with a higher dose of treatment (SYN 2) (~96% live cells) as seen in Figure 5.2 (SD= 0.01). These results proved that early stage cancer cells exhibited minimal susceptibility to both these combination treatments.

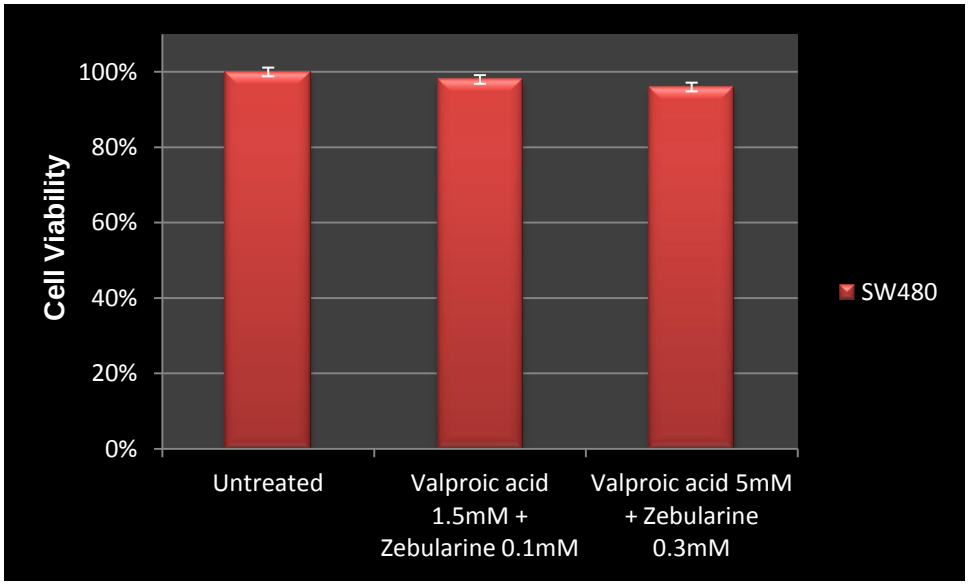


Figure 5.2 SW480 cell susceptibility to HDACi. Cells were treated with concentrations of 1.5mM VPA + 0.1mM ZEB (SYN 1) and 5mM VPA + 0.3mM ZEB (SYN 2) for 24 hours. Cell mortality possibly increased with an increase in VPA and ZEB concentration (SD= 0.01).

SW480 cells were treated with two combinations of HDACi and demethylating agent and its effect on KLF4 was examined, as seen in Figure 5.3. Relative to the untreated samples, the mean increase in C_t value (M= 0.91, SD= 0.03, N= 3) was found to be greater than zero where t(2)= 34.09, two-tailed p= 0.0009, providing evidence that treatment with 1.5mM VPA + 0.1mM ZEB was effective in down-regulating KLF4 gene expression. The same overall result was seen with 5mM VPA + 0.3mM ZEB, where t(2)= 2.27 and p= 0.1500 (M= 0.07, SD= 0.05, N= 3, n.s.). Applying the $2^{-\Delta\Delta Ct}$ method revealed that treatment with the SYN 2 combination displayed a less than one-fold up-regulation in KLF4 expression when compared to the low dose combination treatment. Thus it is statistically significant that treatment with both combinations reduced KLF4 expression, while the SYN 2 combination treatment was effective in up-regulating KLF4 expression relative to the SYN combination treatment.

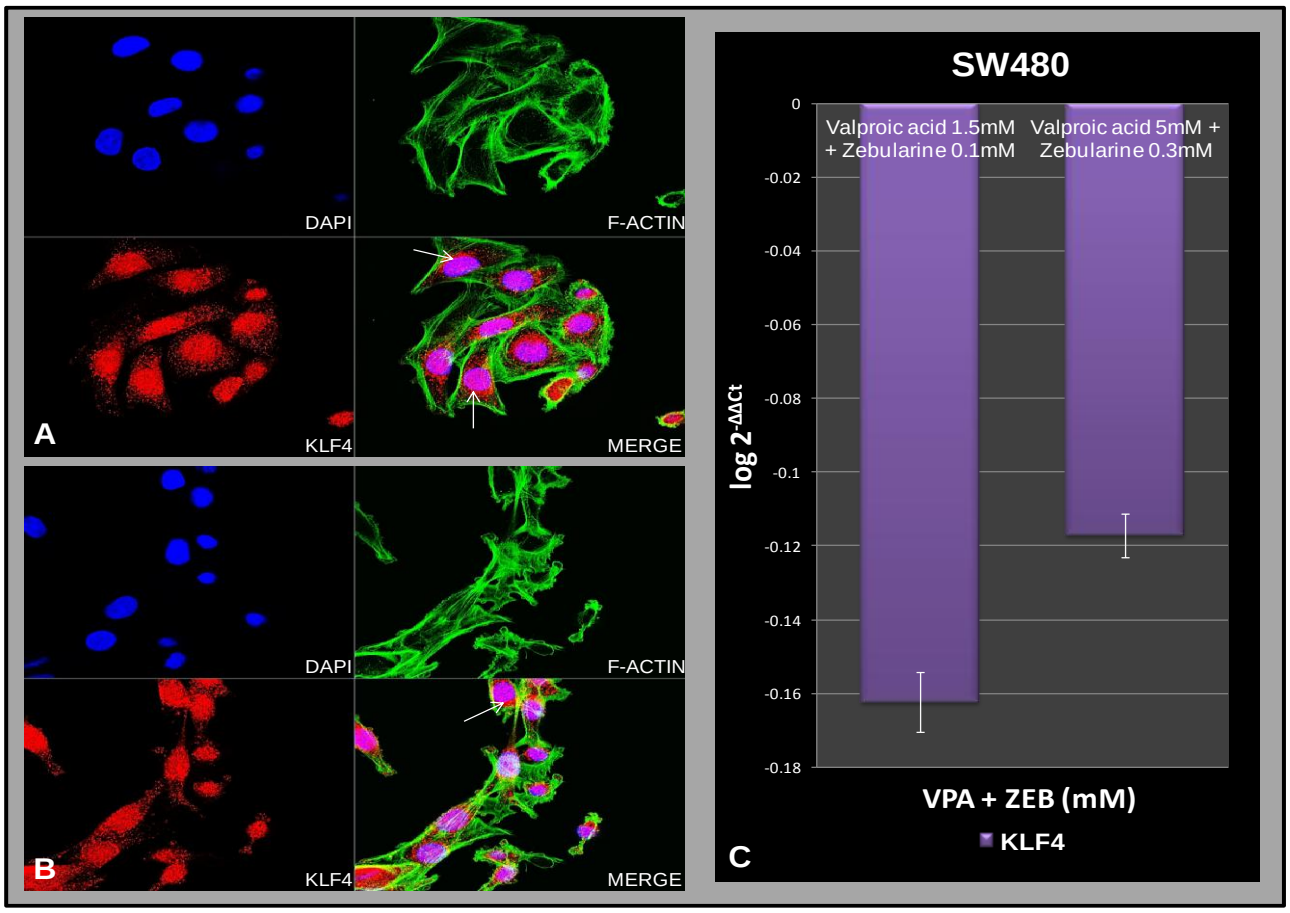


Figure 5.3 The synergistic effect of VPA and ZEB on KLF4 expression in SW480 cells. [A] Confocal microscopy images after treatment with 1.5mM VPA and 0.1mM ZEB (63x). [B] Confocal microscopy images after treatment with 5mM VPA and 0.3mM ZEB (63x). Nuclei= blue, actin filaments= green, KLF4= red, co-localisation in nuclei= pink. High intensity of KLF4 protein is observed within the nucleus and nuclear periphery (arrowed). [C] Gene expression of low dose VPA + ZEB (SYN 1) (p= 0.0009, SD= 0.03) vs. high dose VPA + ZEB (SYN 2) (p= 0.1500, SD= 0.05, n.s.) relative to untreated controls.

Confocal imaging shown in Figures 5.3A and B, illustrates that both combination treatments have minimal effect on the cell morphology, although the higher dose treatments display a low cytoplasm to nuclear ratio with a low cytoplasmic volume suggesting apoptosis. Both treatments show similar protein localisation to that observed in the untreated controls from Figure A6.1 (Appendix 6), with a high nuclear concentration of KLF4 as well as its accumulation at the nuclear periphery (arrowed in Figures 5.3A and B) and its uniform distribution throughout the cytoplasm.

SW480 cells were then treated with the SYN 1 and SYN 2 combinations to examine its effect on CTNNB1 as seen in Figure 5.4. The mean increase in C_t value (M= 2.44, SD= 0.26, N= 3) relative to the untreated samples was found to be significantly greater than zero where t(2)= 16.61, two-tailed p=0.0030, providing evidence that treatment with 1.5mM VPA + 0.1mM ZEB was effective in down-regulating KLF4 gene expression. The same overall result was seen with 5mM VPA + 0.3mM ZEB, where t(2)= 32.02 and p= 0.0009 (M= 4.42, SD= 0.24, N= 3). Of particular note, treatment with the SYN 2 combination of high dose treatments was almost two-fold more effective in down-regulating CTNNB1 expression, relative to the low dose combination treatment. These results are antagonistic to that observed in Figure 5.3 with KLF4.

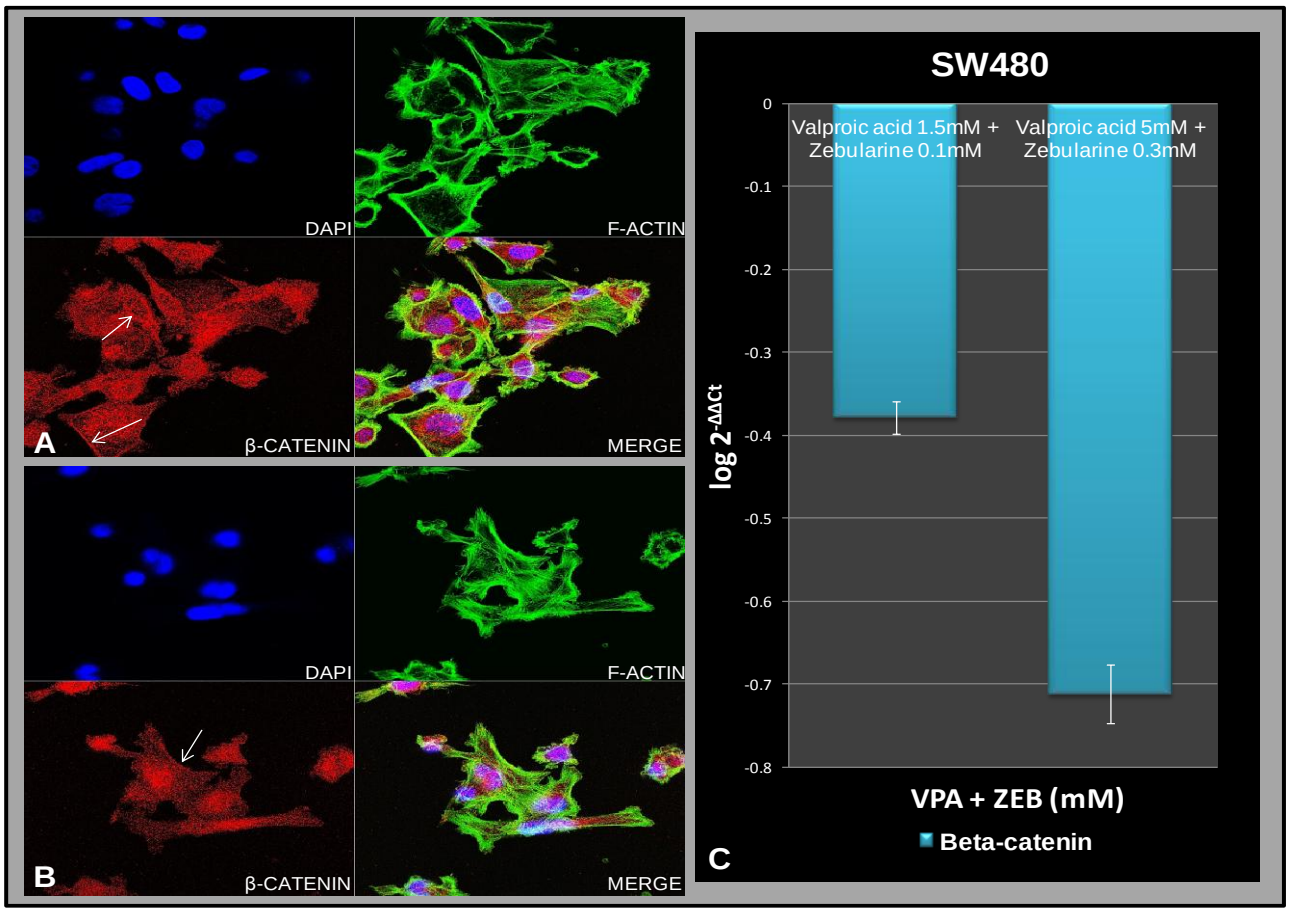


Figure 5.4 The synergistic effect of VPA and ZEB on CTNNB1 expression in SW480 cells. [A] Confocal microscopy images after treatment with 1.5mM VPA and 0.1mM ZEB (63x). [B] Confocal microscopy images after treatment with 5mM VPA and 0.3mM ZEB (63x). Nuclei= blue, actin filaments= green, β-catenin= red, protein co-localisation= pink. High β-catenin protein intensity at cell membrane periphery (arrowed). [C] Gene expression of low dose VPA + ZEB (p= 0.0030, SD= 0.26) vs. high dose VPA + ZEB (p= 0.0009, SD= 0.24) relative to untreated controls.

Morphological changes observed in Figures 5.4A and B are negligible, where the elongated and irregular shape of the cells is retained after treatment, although the cell volume has evidently decreased relative to the untreated controls (Figure A6.1). β-catenin is localised throughout the cell at great intensity, although its sub-nuclear containment as well as its concentration at the membrane periphery (arrowed Figures 5.4A and B) is higher than that observed previously (see Figure 4.13 in Chapter 4 and Figure 3.7 in Chapter 3).

5.2.1.2 *The effects of low and high dose synergistic treatments on late stage colorectal adenocarcinoma cells (DLD-1)*

Colorectal cancer cells representing a late stage colorectal adenocarcinoma (stage C) were cultured as in Chapter 2.1, and treated synergistically with low and high doses of VPA and ZEB as described in Chapter 2.2. A cell viability assay was performed (Chapter 2.1.5) to quantify DLD-1 cells before and after a low and high dose treatment with both synergistic treatments. The viability of 'no treatment' control cells lay in the 95%-99% bracket, with a substantial decrease in cell viability when cells were treated with SYN 1 (~93% live cells) and a further decline in numbers after treatment with a higher dose of combination treatment (SYN 2) (~89% live cells) as seen in Figure

5.5 (SD= 0.03). These results established that late stage cancer cells exhibited a greater susceptibility to both these combination treatments when compared to early stage cells.

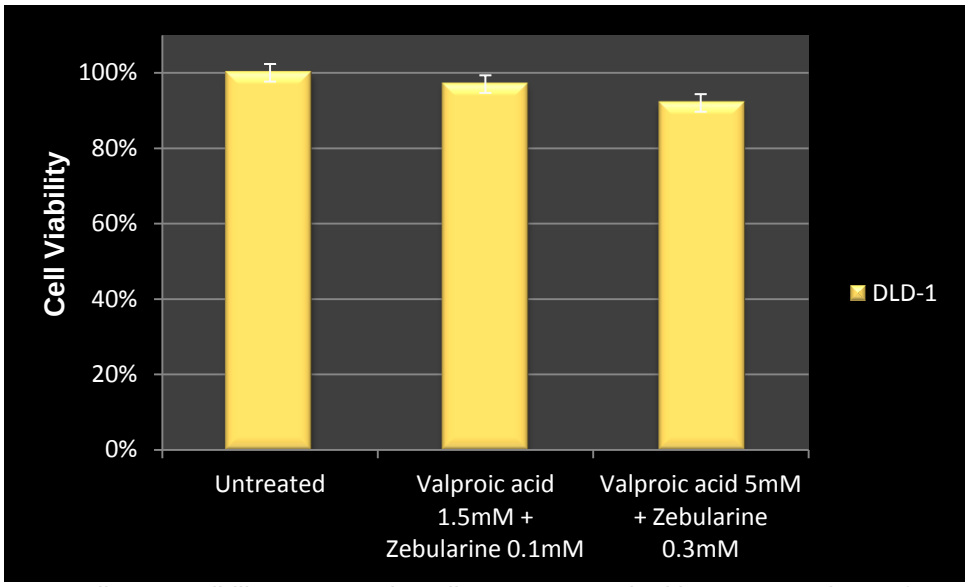


Figure 5.5 DLD-1 cell susceptibility to HDACi. Cells were treated with concentrations of 1.5mM and 5mM VPA, respectively, for 24 hours. Cell mortality possibly increased with an increase in VPA and ZEB concentration. Also treated with ZEB at concentrations of 0.1mM and 0.3mM (SD= 0.03).

DLD-1 cells were treated with two combinations of VPA and ZEB, and its effect on KLF4 was investigated. Relative to the untreated samples, the mean increase in C_t value (M= 3.77, SD= 0.18, N= 3) was found to be significantly greater than zero where t(2)= 37.08, two-tailed p= 0.00070, providing evidence that treatment with 1.5mM VPA + 0.1mM ZEB was effective in down-regulating KLF4 gene expression. Alternatively, a mean decrease in C_t value was observed with 5mM VPA + 0.3mM ZEB, where t(2)= 124.96 and p= 0.00006 (M= 1.19, SD= 0.02, N= 3). Treatment with SYN 2 displayed a massive twenty two-fold increase in KLF4 expression relative to the low dose treatment.

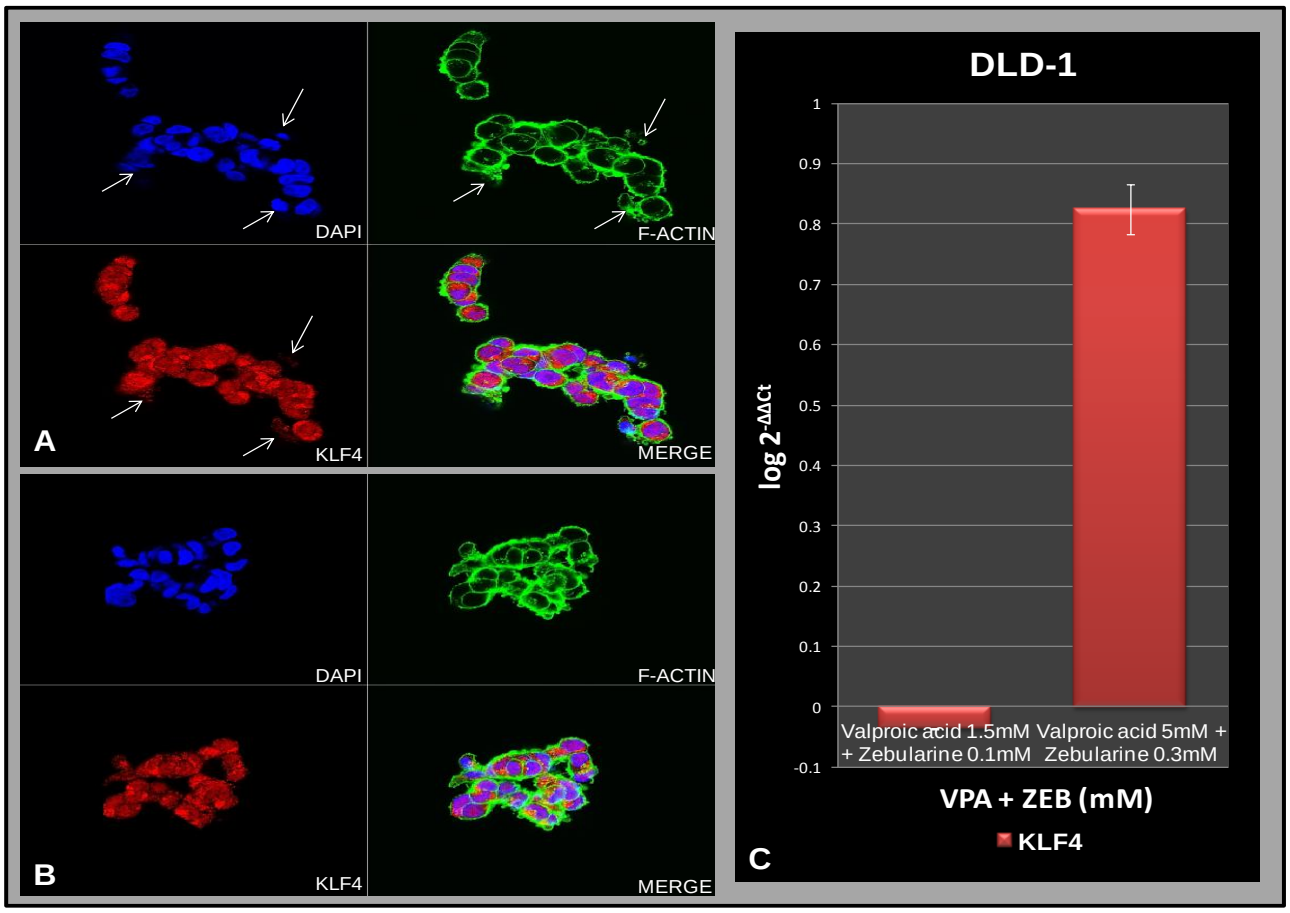


Figure 5.6 The synergistic effect of VPA and ZEB on KLF4 expression in DLD-1 cells. [A] Confocal microscopy images after treatment with 1.5mM VPA and 0.1mM ZEB (63x). [B] Confocal microscopy images after treatment with 5mM VPA and 0.3mM ZEB (63x). Nuclei= blue, actin filaments= green, KLF4= red, co-localisation in nuclei= pink. Arrows indicate possible membrane blebbing suggesting apoptosis. [C] Gene expression of low dose VPA + ZEB (p= 0.00070, SD= 0.18) vs. high dose VPA + ZEB (p= 0.00006, SD= 0.02) relative to untreated controls.

While confocal imaging displays similar results as seen previously (see Figure 5.3), the cell shape has however changed drastically following treatment with both the low and high combinations of HDACi and demethylating agent. Here the overall shape is oval to round, and the cell volume is severely reduced, suggesting apoptosis. Also there is the possibility of membrane blebbing indicated by arrows in Figure 5.6A. The KLF4 protein is once again contained within the nucleus as well as the nuclear periphery and Golgi bodies are apparent bordering the nucleus.

DLD-1 cells were treated with both combinations of HDACi and demethylating agent, and its effects on the expression of CTNNB1 were then analysed. The mean increase in C_t value (M= 1.24, SD= 0.10, N= 3) was found to be significantly greater than zero where t(2)= 21.05, two-tailed p= 0.002, providing evidence that treatment with 1.5mM VPA + 0.1mM ZEB was effective in down-regulating KLF4 gene expression. The same overall result was seen with 5mM VPA + 0.3mM ZEB, where t(2)= 20.92 and p= 0.002 (M= 1.29, SD= 0.11, N= 3). Treatment with the high dose combination showed an almost two-fold down-regulation in CTNNB1 expression when compared to the low dose combination treatment. Overall, results displayed in Figure 5.7 show that CTNNB1 expression is antagonistic to KLF4 expression.

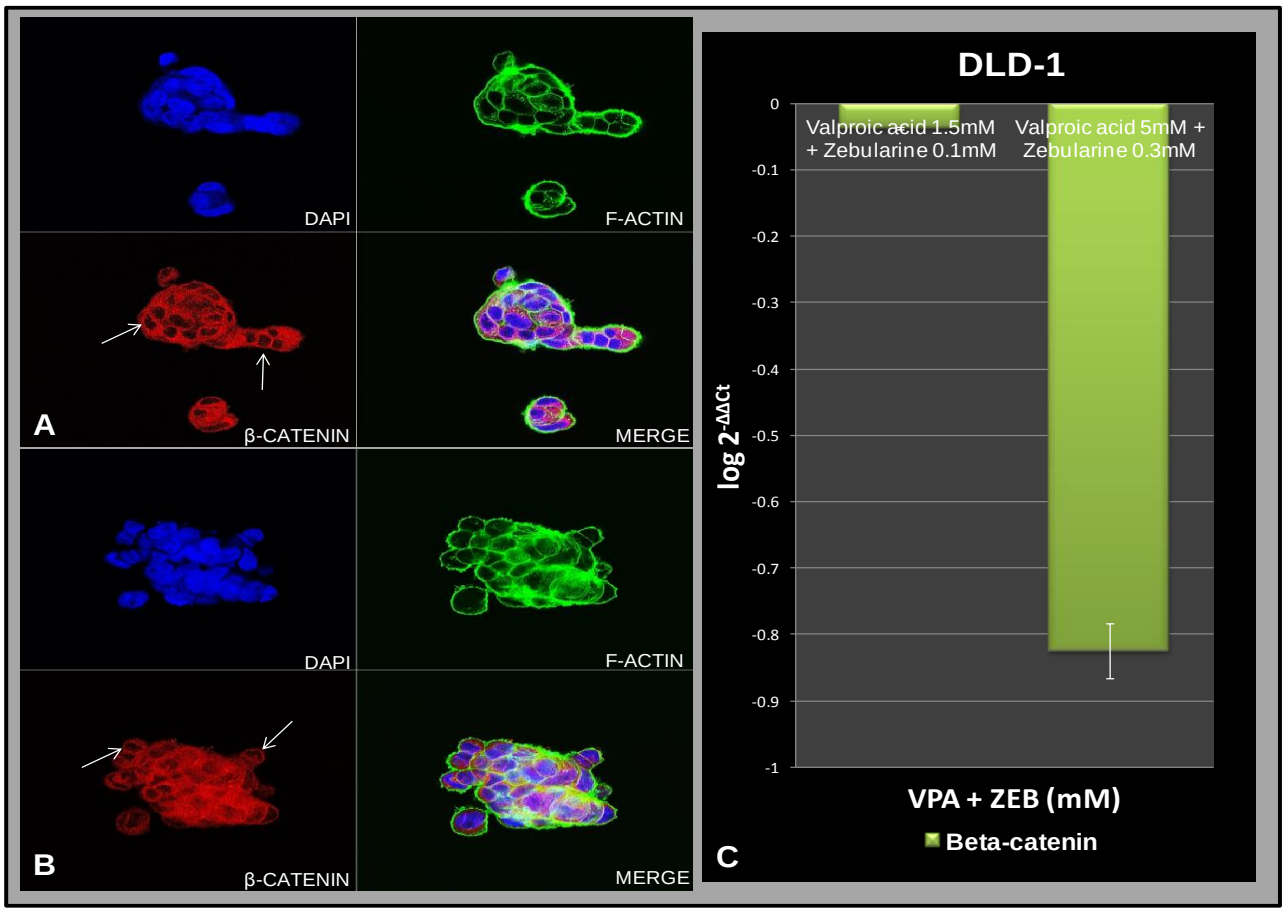


Figure 5.7 The synergistic effect of VPA and ZEB on CTNNB1 expression in DLD-1 cells. [A] Confocal microscopy images after treatment with 1.5mM VPA and 0.1mM ZEB (63x). [B] Confocal microscopy images after treatment with 5mM VPA and 0.3mM ZEB (63x). Nuclei= blue, actin filaments= green, β-catenin= red, protein co-localisation= pink. Peri-nuclear localisation of β-catenin indicated by arrows [C] Gene expression of low dose VPA + ZEB (p= 0.002, SD= 0.10) vs. high dose VPA + ZEB (p= 0.002, SD= 0.11) relative to untreated controls.

Figures 5.7A and B display similar results as those observed in Figure 5.5, where the cell structure is more oval or rounded in shape, and the cell volume has significantly reduced. Cells seem to have clustered and are overlapping, and this is a result of apoptosis. β-catenin is concentrated at the nuclear periphery at high intensity (arrowed in Figures 5.7A and B), and is scarcely distributed throughout the cell and nucleus.

5.3 Discussion

It has been established that alterations in chromatin structure as well as the methylation of discreet regions of DNA leads to the reversible silencing of gene elements. VPA induces differentiation and cell cycle arrest through the inhibition of HDACs, while ZEB is capable of reactivating silenced genes through the demethylation of tumour suppressor genes (Gottlicher *et al.*, 2001; Gurvich *et al.*, 2004; Cheng *et al.*, 2004). This chapter discusses the effect of synergistic inhibition of these epigenetic mechanisms on colon cancer cells through the use of high and low dose combination therapies of an HDAC and a demethylation agent.

5.3.1 The effect of combination therapies on cell viability

Cell viability assays for each of the colon cancer cell lines SW480 and DLD-1 demonstrated a general pattern of increased cell death that was proportional to the concentration of VPA and ZEB; therefore as the dose of synergistic treatment increased, so did cell death. The early stage colon cancer cell line exhibited the greatest susceptibility to treatment with the highest cytotoxicity of both cancer cell lines. The change of cell shape from an irregular to oval structure in late stage colon cancer cells may also validate this apoptotic behaviour. This however would have to be assessed using a marker of apoptosis, such as Bax or Bcl-2. The combination treatments thereby dose-dependently reduced the viability of colorectal adenocarcinoma cell lines.

It is possible here that cell death was a sole consequence of epigenetic treatment, even though DMSO was used for all treatments administered, as a solvent for the demethylation agent. DMSO was found to induce apoptosis in cancer cells in numerous investigations, as well as stimulate cell differentiation and alter cell morphology (Kim *et al*., 1980; Tsao *et al*., 1982; Grunt *et al*., 1991; Ossowski and Belin, 1985). Notably, while DMSO does not modify genetic material, it does however remove free radicals produced by damaged tissues that destroy DNA and cell membranes, aiding in the transformation of the cell respiratory system from aerobic to anaerobic, thereby preserving the normal state of cells for an adequate period of time to allow them to undergo apoptosis (Warburg, 2012).

5.3.2 Combination therapy on gene expression in colorectal cancer cells

Early stage colon cancer cells after treatment displayed very similar results to that observed in cells treated solely with either VPA or ZEB. Cells displayed dose-dependent gene regulation of KLF4 and CTNNB1 after 24 hour treatments. Relative quantification results were analysed and displayed similar data to those seen in previous chapters, thereby supporting the theory that there is a possibility of an inverse relationship between KLF4 and CTNNB1. Low dose combination treatments down-regulated KLF4 expression in SW480 cells, and higher dose treatments demonstrated patterns of up-regulation relative to this, even though KLF4 expression was lower than that observed in untreated controls. The reverse was seen for CTNNB1 in SW480 cells, where a low dose treatment down-regulated gene expression and a high dose treatment had a greater effect on transcript down-regulation. The late stage colon cancer cells however displayed extreme results, where the low dose treatments were consistent with that seen in the early stage cells for KLF4, yet the higher dose treatments demonstrated an immense twenty two-fold up-regulation, relative to the low dose treatment. CTNNB1 was evidently up-regulated as a result of low dose treatments, and down-regulated two-fold after treatment with a higher dose. Thus, the synergistic treatments had a greater effect on the expression of KLF4 and CTNNB1 in late stage colon cancer cells, as seen previously.

Fluorescence imaging clearly demonstrated the appearance of KLF4 protein in Golgi bodies in DLD-1 cells, possibly representing its storage site after synthesis. A high intensity of protein is especially observed after high dose combination treatment (SYN 2), where KLF4 expression is evidently up-regulated relative to the low dose (SYN 1) treatment, suggesting an increase in protein production as a result of DNA demethylation. KLF4 protein in both early and late stage cancer was localised in the nucleus, substantiating its role as a transcription factor. β-catenin was detected around the nuclear periphery, where it translocates to and associates with transcription factors, such as KLF4 and Wnt proteins. A greater concentration of β-catenin was then again observed in the nucleus of SW480 cells after low dose treatment than that seen with high dose treatment, exhibiting consistency in results, as seen in the gene expression data, where the expression of β-catenin decreased with a higher dose treatment. Confocal imaging illustrates that both these proteins concentrate at the nuclear periphery where they interact either directly with each other or indirectly through other transcription factors. Another observation made follows upon what is understood from with the cell viability assays carried out here; as the dose of treatment increases in late stage cancer cells, so does cell cytotoxicity. This is validated through the change in overall cell shape from irregular to round, while the cell volume is drastically reduced and cells seem to cluster, suggesting the onset of apoptosis. Membrane blebbing was also observed in late stage colon cancer cells, however this would need to be validated through the application of blebbing markers, such as antibodies to DAPK and DRP-1 proteins (Inbal *et al.*, 2002).

Data from the gene expression profiles revealed that the differential expression of KLF4 and CTNNB1 in colon cancer displayed aberrant transcription levels in early and late stage cell lines, however gene expression in both stages showed minimal change. It is evident that KLF4 maintains an inverse relationship with β-catenin, and that KLF4 is involved in the direct or indirect inhibition of β-catenin (Evans *et al.*, 2010). It was recently discovered that the loss of KLF4 expression is related to the tumourigenic activity in colon cancer, thus the up-regulation of KLF4 through DNA demethylation reverses the malignancy of colon cancer cells by inducing differentiation (Xu *et al*., 2008). The inverse expression of both these genes in colon cancer cells supports results produced by the cell viability assays that this switch may indeed lead to apoptotic events. Several studies validate this statement by providing evidence that the inhibition of β-catenin in colon cancer may contribute to apoptosis (Kim *et al.*, 2005; Han *et al.*, 2008). As β-catenin is an active member of the Wnt pathway, the down-regulation of β-catenin could result from the inhibition of the Wnt pathway, leading to an increased risk of cell death (Watson, 2004; Yeh *et al*., 2011).

5.3.3 Epigenetic modulation through combination therapies

Due to their involvement in the establishment of neoplasms and their potential reversibility, epigenetic therapies are fast becoming a more attractive field in the prospective treatment of cancers. We have seen the success of solitary treatments with VPA and ZEB on colon cancer

cells, therefore the efficacy of synergistic treatments on the expression of KLF4 and CTNNB1 will be considered below.

Even though DNA methylation and histone deacetylation is performed separately and through the catalytic activity of different enzymes, there is a strong physical and functional relationship between chromatin structure and methylation of DNA sites, where inactive or heterochromatin contains hypermethylated DNA sites and active or euchromatin contains hypomethylated DNA (Razin and Cedar, 1977). Despite an accumulation of evidence supporting this association between both epigenetic systems, there is no proof of which mechanism is more critical in the inception of gene silencing and which follows, although it is clear that there is a definite cross-talk between DNA methylation and histone modifications.

There are however several situations that may arise depending on the strength of either epigenetic modification (Vaissiere *et al*., 2008). On this basis, gene silencing could solely be a result of DNA methylation or histone deacetylation, or a combination of both. Another possible case is the loss of gene activity due to histone deacetylation being the initial source, followed by DNA hypermethylation through DNMTs within the same gene or region (Vaissiere *et al*., 2008). It has been established through numerous investigations that these two epigenetic mechanisms are capable of manipulating one another; one such example was explored with the treatment of *Neurospora* with TSA, where this HDACi enhanced the hypomethylation status of silenced genes resulting in their activation (Selker *et al.*, 2002; Cervoni and Szyf, 2001). Thus as HDAC activity was inhibited, DNA found adjacent to acetylated histones was consequentially demethylated (Cervoni and Szyf, 2001). Another study reported that 5-aza-CdR enhanced the acetylation of histones H3 and H4 that was initially induced by the HDACi depsipeptide (Weiser *et al.*, 2001; Zhu and Otterson, 2003).

The first experiments investigating the association between HDACs and methylated DNA were through the analysis of the MeCP-2 protein in the early development of *Xenopus* and mice species (Jones *et al.*, 1998; Nan *et al.*, 1998). There are two types of transcriptional inhibition in gene silencing, direct inhibition through the blocking of transcription factor binding sites and indirect inhibition involving MeCP-2 methyl-binding proteins (Bird, 2002). The latter is considered to recruit HDAC inhibitors to methylated DNA segments aiding in gene silencing (Jones *et al.*, 1998; Nan *et al.*, 1998). Combined treatments with HDAC inhibitors and demethylating agents have been proven to synergistically activate tumour suppressor genes that are epigenetically silenced at a higher rate than sole treatment with either inhibitor, exerting an anti-neoplastic effect on cancer cells. An example of such is the silencing of the COX-2 gene in gastric cancer due to promoter hypermethylation, which was re-expressed after combined treatment with TSA and 5-aza-CdR (Kikuchi *et al*., 2002). Another was the activation of the *ER-α* gene in breast cancer cells, that was

re-expressed up to four hundred-fold after treatment with the same drug combination, relative to separate treatments with either inhibitor (Yang *et al*, 2001).

In the present study, the KLF4 gene was greatly up-regulated after high dose combination treatment with VPA and ZEB in late stage colon cancer cells, although it was clear in the previous chapters that the latter had a greater effect on this up-regulation. Thus the major contributor to this change in KLF4 expression was evidently the demethylating portion of the combination treatment. Both ZEB and VPA affect the Wnt pathway by modifying key members involved in its regulation, such as the activation of GSK-3 as well as the negative Wnt regulator, WNT9A (Vene and Tosetti, 2010; Shu *et al.*, 2006). This may lead to a series of the downstream effects, ultimately down-regulating β-catenin thereby inhibiting cell proliferation and activating apoptotic events (Baylin and Ohm, 2006).

Several studies have produced data supporting the statement that combination treatments with HDAC inhibitors and demethylating agents enhance apoptosis in cancer cells (Zhu *et al*., 2001). It was reported that the sequential treatment of thoracic cancer cells with 5-aza-CdR and depsipeptide respectively resulted in the induction of apoptosis at a more enhanced rate than with single treatments (Weiser *et al.*, 2001). Thus combination treatments may induce apoptotic activity by demethylating or hyperacetylating genes that are involved in the induction of apoptosis, or these mechanisms may work in unison to enhance this gene expression (Zhu and Otterson, 2003). It was discovered that synergism of HDAC inhibitors and DNMT inhibitors lead to an overexpression of $p19^{INK4D}$ (CDKN2D), which regulates cell growth and controls G1 progression (Zhu *et al.*, 2001; Okuda *et al.*, 1996). Treatments were also found to induce silenced genes involved in cellular differentiation, such as Drg-1 in colon cancer cells, as well as Pax 5 involved in B cell development in the immunotherapy of cancer (Guan *et al.*, 2000; Danbara *et al.*, 2002). In summary, VPA and ZEB in combination immensely up-regulated gene expression relative to sole treatments with either epigenetic modulator, as the most evident up-regulation of KLF4 was observed with the high dose synergistic treatment of the late stage cancer cells.

CHAPTER 6

GENERAL DISCUSSION

Both VPA and ZEB displayed dose-dependent regulation on gene expression in early and late stage cancer cells, as well as breast cancer cells. Supporting evidence by Evans et al. (2010) may confirm that an antagonistic relationship exists between KLF4 and β-catenin in colon cancer cells, although this was not apparent in breast cancer cells. KLF4 has been found to display tumour suppressor properties in colon cancer and has oncogenic attributes in breast cancer. However, after VPA and ZEB administration, there was a clear up-regulation of KLF4 in breast cancer cells. Therefore the data obtained signifies that the lower dose treatments had a greater potential tumourigenic effect on the cells. The higher dose treatments displayed an increase in apoptotic events, as observed in the cell viability assays. The greatest up-regulation in KLF4 and CTNNB1 expression was seen with the higher VPA doses, when compared to that observed with ZEB. The higher dose treatments were also related to a more malignant phenotype seen by the nuclear localisation of KLF4, according to Pandya *et al.* (2004), as illustrated in the confocal microscopy images.

All VPA treatments in colon cancer cells displayed an initial down-regulation in KLF4 expression and an up-regulation with high dose treatment, providing evidence that all treatments were dose-dependent. This was seen after ZEB treatment of early stage cancer cells, however late stage cancer cells exhibited a far greater up-regulation of KLF4 relative to the untreated control and the low dose treatment. This could be a result of hypomethylation of the KLF4 gene promoter region after treatment. Thus there is a better chance that the KLF4 gene is more greatly affected by methylation than by histone deacetylation. A higher dose of VPA may have had a greater effect on the up-regulation of KLF4. The most evident up-regulation of KLF4 was observed with the high dose synergistic treatment of the late stage cancer cells, thus both treatments immensely up-regulated gene expression relative to sole treatments with either epigenetic modulator.

Due to the fact that KLF4 expression within the normal gastrointestinal epithelium is up-regulated, it is therefore possible that its expression may be higher in early stage colon cancers than late stage colon cancers, in its progression to a more malignant phenotype (Flandez *et al.*, 2008). In theory, early stage cancer cells would exhibit the lowest incidence of methylation and HDAC activity, thus VPA and ZEB would not affect the expression levels at the degree at which these treatments affect advanced stage cancer cells. Treatment with both VPA and ZEB initially reduced KLF4 expression in early stage cells after low dose treatments, after which high dose treatments increased expression levels relative to this; however the expression of KLF4 remained lower than that of the untreated control. It is most likely that the KLF4 gene in late stage cancers presents a greater frequency of hypermethylation and histone deacetylase activity than early stage cancers, and is thereby either expressed at lower levels or is completely silenced. Treatments with high

dose ZEB, and with VPA and ZEB in combination, largely elevated expression levels of KLF4, thus validating this hypothesis.

CTNNB1 was greatly down-regulated after high dose treatment with VPA in late stage cells, displaying a completely antagonistic effect when compared to KLF4. A pattern of down-regulation was observed with CTNNB1 after all treatments, with high dose treatments displaying a greater overall reduction in expression levels relative to low dose treatments. Thus all treatments played a role in the down-regulation and potential suppression of the Wnt pathway, exerting an anti-tumourigenic effect on the cells.

KLF4 protein localisation was found to be entirely nuclear, like most transcription factors, and has been discovered to contain two strong and independent nuclear localisation signals (NLS) (Figure 1.5), one within the three zinc fingers and one adjacent to the first zinc finger (Shields and Yang, 1997). KLF4 binds to the consensus sequence 5'-$^{G}/_{A}{}^{G}/_{A}GG^{C}/_{T}G^{C}/_{T}$-3' existing on several genes and other transcription factors (Shields and Yang, 1998). β-catenin however was predominantly localised at the nuclear periphery, and has no distinguishable NLS (Fagotto *et al*., 1998; Henderson and Fagotto, 2002).

6.1 KLF4/β-catenin cross-talk and its involvement in the Wnt pathway

Levels of KLF4 in intestinal neoplasia display an inverse relationship to the size of the tumour, thus it is strongly down-regulated in colon cancer cells (Dang *et al.*, 2000). KLF4 has been discovered at high levels in differentiated intestinal epithelial tissue, where it directly associates with β-catenin at the nuclear periphery, inhibiting this oncogenic gene product (Zhang *et al.*, 2006). Focusing on the biology of colonic epithelium (elaborated in Chapter 1.3), it has been established that there are three lineages that the stem cells produced in the colon crypts may follow, namely enterocytes, goblet cells and enteroendocrine cells (Chandler and Lagasse, 2010). As illustrated in Figure 6.1, the expression of KLF4 decreases while CTNNB1 expression increases as the pluripotency of the epithelial cells increases within the colonic crypts, exhibiting an antagonistic relationship between the products of these two genes (Zhang *et al.*, 2006). Thus the association between KLF4 and β-catenin are vital in the regulation and homeostasis of colonic epithelium.

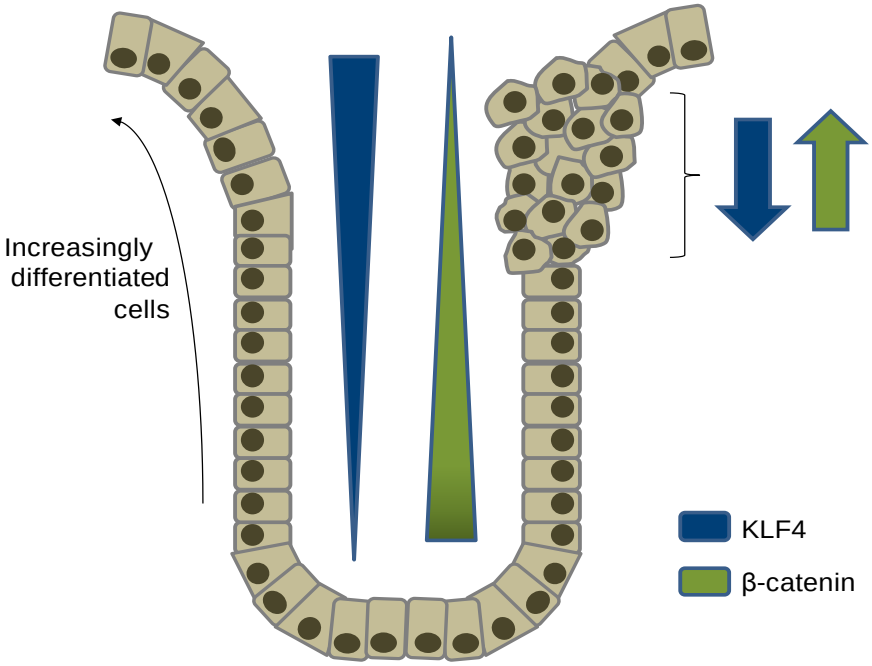


Figure 6.1 Linking the biology of colonic epithelium with the expression of KLF4 and CTNNB1. As KLF4 levels increase, β-catenin levels decrease along with the pluripotency of the cells (modified from Evans *et al.*, 2010; McConnell and Yang, 2010).

The mechanism of KLF4 action has been reviewed previously, in its inhibtion of β-catenin and subsequent suppression of the Wnt pathway (Zhang *et al.*, 2006; Evans *et al.*, 2010). KLF4 binds to the C-terminus of β-catenin and interacts with its transactivating domain, and does not associate with the twelve ARM repeats (Evans *et al.*, 2010). The essential region of KLF4 that is thought to be involved in the association with β-catenin were amino acids 350-401 as well as the zinc finger binding domains, as illustrated in Figure 6.2 (Evans *et al.*, 2010). It was also determined that the C-terminal region of endogenous KLF4 interacts directly with the HMG (high-mobility group) of TCF4, which is a conserved DNA-binding motif (Figure 6.3) (Evans *et al.*, 2010; Grosshcedl *et al.*, 1994). β-catenin contains a binding domain for the N-terminus of TCF4 at ARM repeat 3-10, while both β-catenin and TCF4 bind to KLF4 independently of each other (Evans *et al*., 2010).

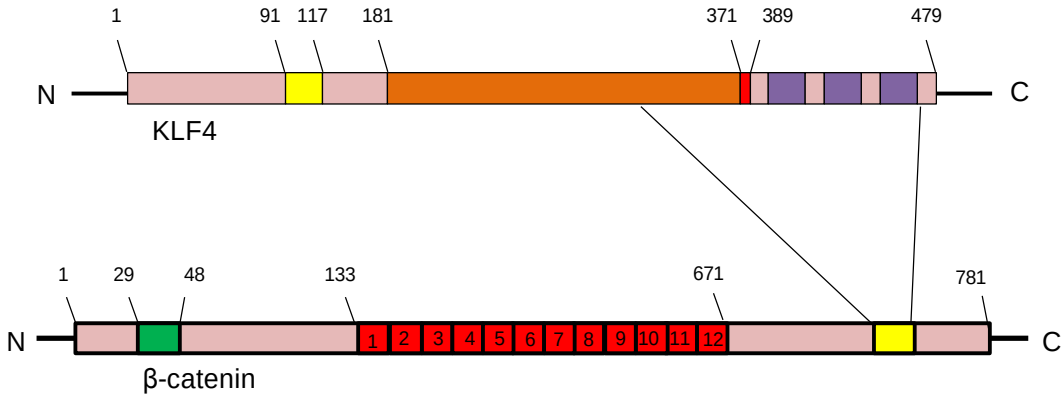


Figure 6.2 Schematic diagram illustrating the association of KLF4 protein with β-catenin. Amino acids 350-401 of KLF4 bind to the transactivation domain of β-catenin within the C-terminal. The ARM repeat region of β-catenin is not necessary in this relationship (Evans *et al.*, 2010).

β-catenin has been identified as a possible contributor to the progression of tumourigenesis, with approximately 15% of colon cancer tumours being a result of β-catenin mutations, and the rest are

attributable to APC mutations (Maiti *et al.*, 2000; Fearon, 2011). The nuclear interaction between β-catenin and KLF4 are crucial in the inhibition of the Wnt pathway, and KLF4 blocks TCF4 from binding to its consensus sequence, as illustrated in Figure 6.3, thereby contributing to the anti-tumourigenic activities of the cell (Evans *et al.*, 2010). It was also established that KLF4 may compete with p300/CBP, another Wnt regulator, for binding to the C-terminus of β-catenin, thus inhibiting its recruitment (Evans *et al.*, 2010). p300 and CBP are acetyltransferases known to activate Wnt target genes such as the surviving gene via the acetylation of β-catenin, thereby contributing to tumourigenicity (Ma *et al.*, 2005; Hecht *et al.*, 2000).

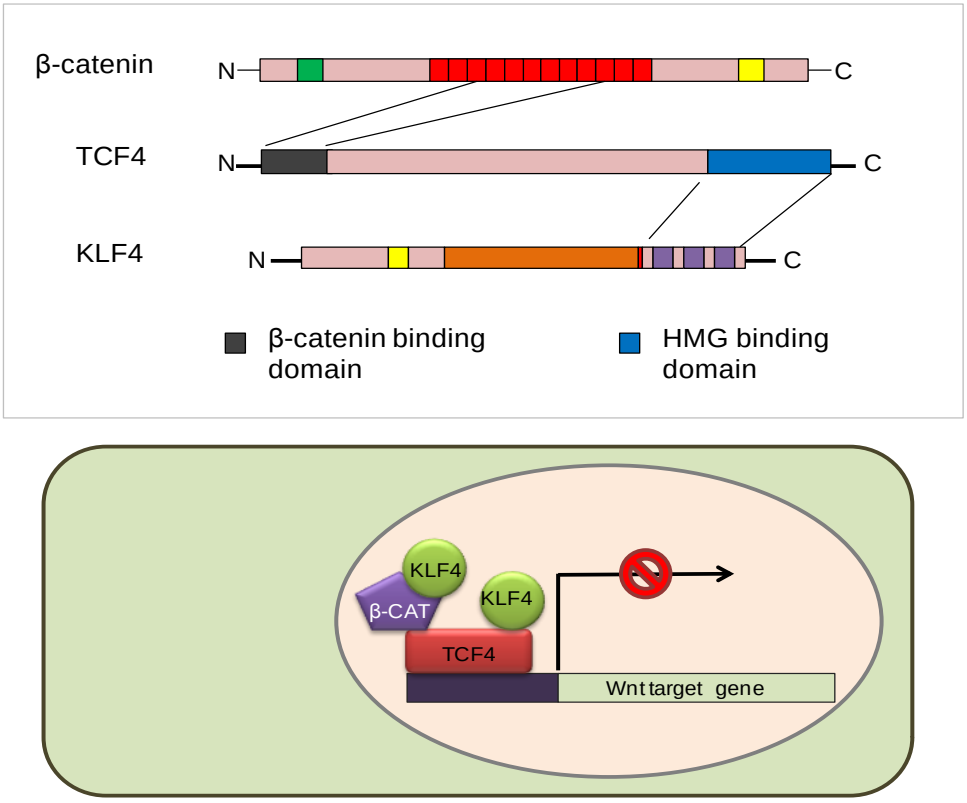


Figure 6.3 Schematic diagram demonstrating the nuclear association of KLF4 and β-catenin with TCF4. The ARM repeat region of β-catenin interacts directly with the N-terminus of TCF4, while the C-terminus of KLF4 associates with the HMG domain of TCF4. β-catenin and TCF4 however bind KLF4 independently of one another. KLF4 inhibits the binding of TCF4 to its consensus sequence on Wnt target genes, thereby repressing the Wnt signalling pathway (Zhang *et al.*, 2006; Evans *et al.*, 2010; Cho and Dressler, 1998).

6.2 The effect of KLF4 on the regulation of cell proliferation in colon cancer cells

KLF4 has been deemed a regulator of cell proliferation through several investigations. The epigenetic modification of KLF4 in colon cancer cells has resulted in its activation, more so after ZEB treatment. The up-regulation of KLF4 plays a major role in growth arrest through the inhibition of DNA synthesis, thereby exerting an anti-proliferative role in colon cancer cells (Shields *et al.*, 1996). The induction of KLF4 through epigenetic modulation elevates the expression levels of CDKN1A, involved in the induction of differentiation and cell cycle arrest, thereby encoding CDK inhibitors $p21^{WAF1/CIP1}$ and $p57^{Kip2}$ (Zhang *et al.*, 2000; Chen *et al.*, 2003). Several investigations demonstrated that KLF4 activation subsequently inhibits the formation of cyclin/CDK complexes through the repression of cyclin D1, cyclin D2, cyclin E and cyclin B1, thereby arresting the cell

cycle (Figure 6.4) (Shie *et al.*, 2000; Klaewsongkram *et al.*, 2007; Yoon *et al.*, 2005; Yoon and Yang, 2004).

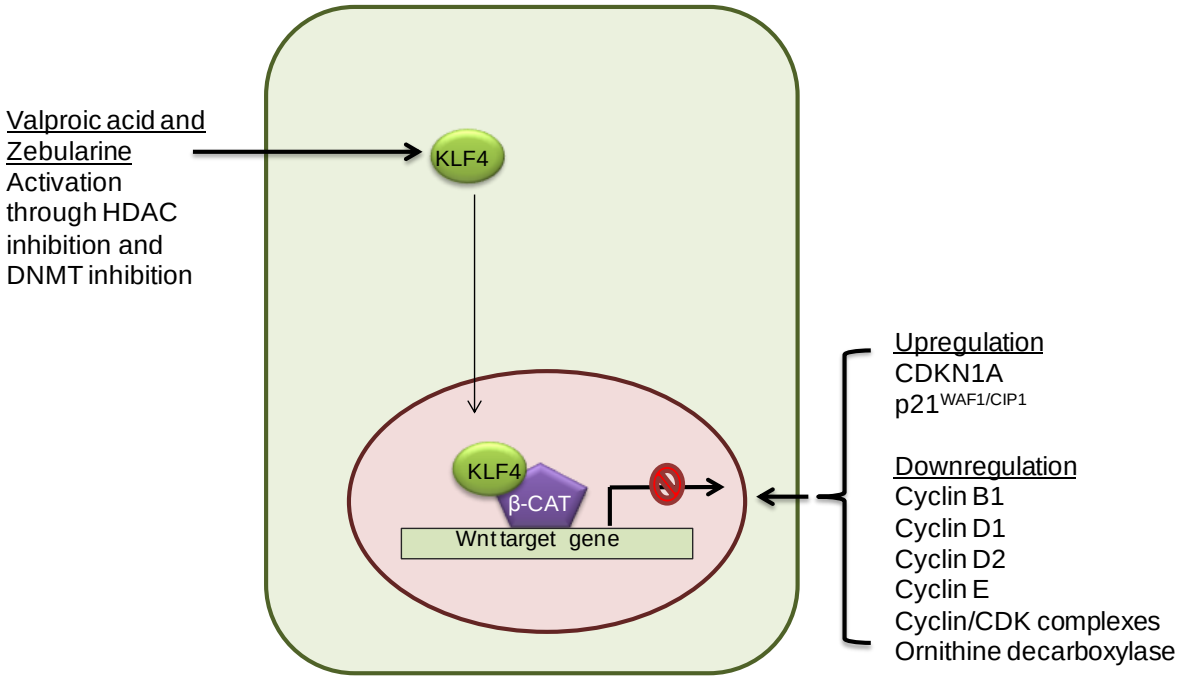


Figure 6.4 KLF4 in cell cycle regulation and tumour suppression. The activation of KLF4 leads to the up-regulation of CDKN1A which subsequently elevates p21 levels in the cell. This results in the inhibition of cyclin B1, D1, D2 and E, arresting the cell cycle in G1/S-phase thereby reducing cell proliferation and tumour formation (Zhang *et al.*, 2000; Shie *et al.*, 2000; Klaewsongkram *et al.*, 2007; Yoon *et al.*, 2005; Yoon and Yang, 2004; Cheng and Yang, 2003; Chen *et al.*, 2001).

KLF4 is involved in two major checkpoints of the cell cycle, namely the G1/S-phase and the G2/M-phase. The inducible expression of KLF4 plays a role in cell cycle arrest at the G1/S-phase through p21 activation (Yoon and Yang, 2004; Yoon *et al*., 2003; Chen *et al.*, 2001). In addition arresting the cell cycle G1/S-phase, high levels of KLF4 have been discovered to inhibit the expression of an enzyme called ornithine decarboxylase that is involved in polyamine synthesis (Chen, *et al.*, 2002). Polyamines are compounds that bind to DNA segments, and their repression may lead to the retardation of cell growth (Rato *et al.*, 2011; Wang *et al.*, 2003). KLF4 however binds to and inhibits p53, thereby blocking apoptosis driven by DNA damage (Rowland *et al.*, 2005). There is a possibility however that treatment with VPA alone, or in synergy with ZEB, may hyperacetylate the *p53* gene thereby increasing its expression levels (Phiel *et al.*, 2001). ZEB may also alter the methylation status of *DAPK* and *Caspase 8* leading to apoptotic events (Pompeia *et al.*, 2004; Kissil *et al.*, 1997). A study performed on rats demonstrated that the inhibition of β-catenin and TCF4 in cancer cells resulted in the activation of apoptotic genes leading to cell death (Chen *et al.*, 2001a).

6.3 KLF4 expression in breast cancer cells

Contradicting the results observed in colon cancer cells, KLF4 was detected at high levels in breast adenocarcinoma cells and has been defined as an oncogene, thereby contributing to the tumourigenicity of breast tumours (Foster *et al.*, 2000). According to Pandya *et al.* (2004), it has

also been established that high concentrations of KLF4 protein in the nucleus is linked to the clinical outcome of a more tumourigenic phenotype through the effect of KLF4-induced neoplasia, as was observed in the MCF-7 cells of the present study. The mechanism of action of KLF4 is through its repression of p53, which is aberrantly overexpressed in breast cancer cells (Rowland *et al*., 2005). KLF4 associates with Mucin-1 (MUC1) and binds to the PE21 element at the promoter region of *p53* (Figure 6.5), reducing levels of p53, thereby inhibiting apoptosis of malignant cells (Wei *et al*., 2007; Roland *et al.,* 2005). Thus, the lower expression of KLF4 observed in MCF-7 cells after low dose treatment with VPA as well as ZEB restores p53 levels, resulting in programmed cell death. VPA may engage in the HDAC inhibition of p53, elevating its expression level. MUC1 transcription factor has also been discovered to bind securely to β-catenin, stabilising this protein and leading to the downstream activation of Wnt responsive genes (Yamamoto *et al.*, 1997; Li *et al.*, 1998; Huang *et al.*, 2003).

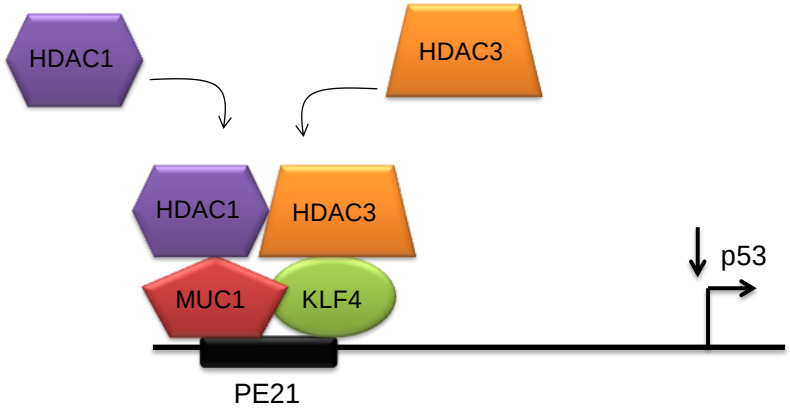


Figure 6.5 KLF4 is involved in the regulation of p53 through its association with MUC1. The KLF4/MUC1 complex binds to the PE21 element of the p53 promoter and is involved in the recruitment of HDACs 1 and 3, thereby enhancing the deacetylation of p53 and inhibiting its expression (Adapted from Wei *et al.*, 2007)

A link between KLF4 and the estrogen receptor-α (ERα) has been reported, where KLF4 binds to ERα, which prevents ERα from binding to the promoter regions of its target genes, so inhibiting its activity and reducing ERα-induced proliferation; this however occurs only in the presence of estrogen (Akaogi *et al.*, 2009). Notch1 has also been monitored in breast cancer cells, and was found to be activated by KLF4, thereby activating the Notch pathway contributing to the formation of neoplasia (Lui *et al.*, 2009). It was discovered that estrogen inhibits Notch signalling in an ERα dependent manner (Rizzo *et al.*, 2008). Moreover, treatment with low dose VPA and ZEB down-regulated KLF4, thus reducing levels of Notch1 leading to the repression of the Notch signalling pathway, and contributing to an anti-neoplastic phenotype. Moreover, there is an association between the Wnt and Notch signalling pathways, where an up-regulation of Wnt1 stimulates the Wnt pathway and leads to the subsequent activation the Notch pathway, and this relationship produces a malignant phenotype in breast cancer cells (Ayyanan *et al.*, 2006).

6.4 Valproic acid and Zebularine in clinical trials

Several epigenetic modulators have been introduced to humans in Phase I and Phase II clinical trials in the therapy of cancer (Marks *et al*, 2001; Kramer *et al.*, 2001). A Phase I investigation of VPA involving twelve patients with cervical cancer was published, and displayed an overall of six patients containing hyperacteylated histones, whereas eleven patients exhibited great levels of H3 acetylation and seven patients showed hyperacetylation of H4 (Chavez-Blanco *et al.*, 2005). Another Phase I trial involving Vaproic acid revealed that twelve out of sixteen patients with advanced solid tumours demonstrated an increase in H3 and H4 acetylation, this however in a non dose-dependent manner; and a reduction in HDAC2 levels was also observed (Atamaca *et al.*, 2007). A Phase I/II study reported that advanced leukaemia patients treated with a combination of VPA and 5-aza-CdR displayed global H3 and H4 hyperacetylation as well as transient DNA hypomethylation (Garcia-Manero *et al.*, 2006). An additional Phase I/II clinical trial investigating the effect of 5-aza-CR, VPA and all-*trans* retinoic acid (ATRA) on myeloid leukaemia patients showed similar results (Soriano *et al.*, 2007). A Phase II trial exploiting VPA in combination with hydralazine exhibited the same results as the Phase I/II trials with the addition of gene activation in breast cancer tumours (Arce *et al.*, 2006). There have been no human trials performed with ZEB to date, however its long half-life in solution and low toxicity deems this DNMT inhibitor a favourable option in its potential clinical applications (Cheng *et al.*, 2003).

CHAPTER 7

CONCLUDING REMARKS AND FUTURE DEVELOPMENTS

7.1 Concluding remarks

KLF4 is a complex transcription factor that has been discovered to regulate tumourigenesis in colon cancer cells. Its role as a transcriptional activator and repressor, as well as its oncogenic and tumour suppressor abilities renders this zinc finger protein a unique and valuable component in cancer therapeutics. As the first study to observe the effects of VPA and ZEB on KLF4 expression, several key details were highlighted here. KLF4 was differentially expressed in early and late stage colon cancer cells as a tumour suppressor, as well as in breast cancer as an oncogene. All treatments displayed dose-dependent gene regulation, and KLF4 induction was greater in late stage colon cancer cells after treatment with ZEB as a demethylating agent, when compared to VPA treatment. KLF4 was also induced at great levels after synergistic treatment with VPA and ZEB in late stage colon cancer cells. KLF4 inhibition in breast cancer cells was highest after sole treatments with lower concentrations of ZEB and VPA respectively. The expression levels of KLF4 and β-catenin were antagonistic to one another, as the induction of KLF4 led to its association with β-catenin, and thereafter its subsequent inhibition of β-catenin. The down-regulation of β-catenin resulted in the reduction or inhibition of the Wnt pathway, thereby exerting anti-tumourigenic and anti-proliferative properties on the cells.

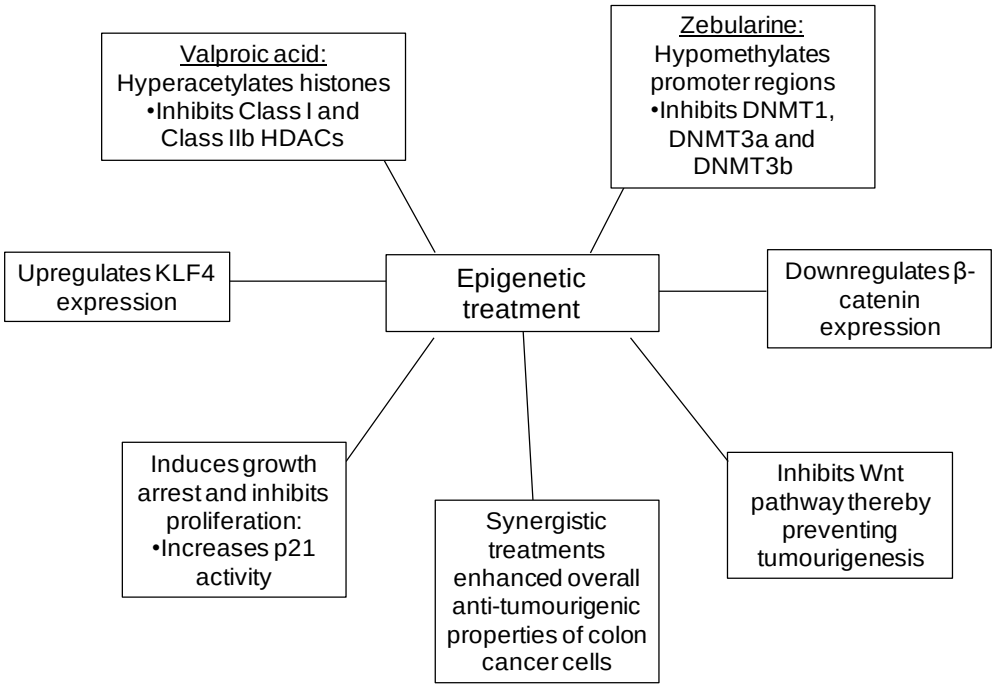


Figure 7.1 The anti-tumourigenic effects of epigenetic treatments with VPA and ZEB

7.2 Future developments

Assessing the effects of the epigenetic induction of KLF4 in cancer cells opens doors for prospective studies. To supplement this study, potential advancements may be to analyse the induction and expression of apoptotic proteins through Western blotting, this to rule out other factors contributing to cell death. Another crucial aspect is to determine whether all treatments are

time-dependent, or whether sequential treatment with the demethylation agent followed by the HDAC inhibitor affects KLF4 induction. In addition to this, a range of concentrations of VPA and ZEB could be exploited to evaluate the dose-dependency of each treatment. Increasing the dose of both these treatments in colon cancer cells may induce KLF4 expression. A comparison of KLF4 levels in colon cancer cells with a normal intestinal epithelium cell line is also appealing. Another target would be to examine the changes of KLF4 and β-catenin gene expression, as well as other genes involved in the Wnt signalling pathway through the application of pathway-focused PCR arrays (Arikawa *et al.*, 2011).

To determine patterns of DNA methylation within the KLF4 gene, bisulphite sequencing would be an additional option to explore (Fraga and Esteller, 2002). Also, other strategies of sequencing, besides bisulfite sequencing, may be investigated to assess the behaviour of the newly discovered form of methylation mentioned in this study, namely 5-hydroxymethylation (Huang *et al.*, 2010). miRNA's, in particular miRNA-145 has been discovered to regulate the expression of pluripotent markers including KLF4, thus a study on the effect of epigenetic modulation on miRNA-145 may be of great interest (Xu *et al.*, 2009). The treatment of cancer through immunotherapy is an expanding field, and studies have shown that ZEB induces the expression of immune-related genes as a result of hypermethylation (Liu *et al.*, 2007). A crucial aspect of the Wnt signalling pathway in colon cancer is the complexing of β-catenin with TCF4, therefore drugs that interrupt the association of these two proteins, as well as the expression levels of TCF4, would be valuable in the therapy of colon cancer (Graham *et al.*, 2001).

Acc, C. I., Okuliez, W. C. (1995) Differential gene regulation by estrogen and progesterone in the primate endometrium. *Molecular and Cellular Endocrinology.* **115**: 95-103

Ailles, L. E., Weissman, I. L. (2007). Cancer stem cells in solid tumors. *Current Opinion in Biotechnology*. **18**: 460-466

Akaogi, K., Nakajima, Y., Ito, I., *et al.* (2009) KLF4 suppresses estrogen-dependent breast cancer growth by inhibiting the transcriptional activity of ERα. *Oncogene*. **28**: 2894-2902

Alberts, B., Bray, D., Lewis, J. *et al.* (1994) Molecular Biology of the Cell. Garland Science New York, 3rd edition

Alberts, B., Johnson, A., Lewis, J., *et al.* (2002) Molecular Biology of the Cell. Garland Science New York, 4rd edition

An SVM Based Method for DNA Methylation Prediction (2010) Methylator. [http://bio.dfci.harvard.edu/Methylator/about.html]. Date accessed 23 October 2010

Andrade, R., Cristol, L., Prado, R., *et al.* (2010) Plasma membrane and nuclear envelope integrity during the blebbing stage of apoptosis: a time-lapse study. *Biology of the Cell*. **102 (1)**: 25-35

Arce, C., Perez-Plasencia, C., Gonzalez-Fierro, A., *et al*. (2006) A proof-of-principle study of epigenetic therapy added to neoadjuvant doxorubicin cyclophosphamide for locally advanced breast cancer. *PLoS ONE*. **1 (1)**: e98

Archer, S. Y., Hoden, R. A. (1999) Histone acetylation and cancer. *Current Opinion in Genetics and Development*. **9**: 171-174

Archer, S. Y., Meng, S., Shei, A., *et al.* (1998) $p21^{WAF-1}$ is required for butyrate-mediated growth inhibition of colon cancer cells. *Proceedings of the National Academy of Sciences USA*. **95**: 6791-6796

Argarwal, B., Halmos, B., Feoktistov, A. S., *et al.* (2002) Mechanism of lovastatin-induced apoptosis in intestinal epithelial cells*. Carcinogenesis*. **23 (3)**: 521-528

Arikawa, E., Quellhorst, G., Han, Y, *et al.* (2011) RT2 Profiler™ PCR Arrays: Pathway-Focused Gene Expression Profiling with qRT-PCR. *SA Biosciences: Technical Article*. 1-11

Atmaca, A., Al-Batran, S. E., Maurer, A., *et al.* (2007) Valproic acid (VPA) in patients with refractory advanced cancer: a dose escalating phase I clinical trial. *British Journal of Cancer*. **97**: 177-182

Attadia, V. (1993) Effects of 5-aza-2′-deoxycytidine on differentiation and oncogene expression in the human monoblastic leukemia cell line U-937. *Leukemia.* **7 (Suppl. 1)**: 9-16

August, D. A., Ottow, R. T., Sugarbaker, P. H. (1984) Clinical perspective of human colorectal cancer metastasis. *Cancer Metastasis Reviews*. **3**: 303-324

Ayyanan A, Civenni G, Ciarloni L, *et al*. (2006) Increased Wnt signaling triggers oncogenic conversion of human breast epithelial cells by a Notch-dependent mechanism. *Proceedings of the National Academy of Sciences USA*. **103**: 3799-3804

Balbi, A., Sottofattori, E., Mazzei, M., *et al.* (1991) Study of bioequivalence of magnesium and sodium valproates. *Journal of Pharmaceutical and Biomedical Analysis*. **9**: 317-321

Baylin, S. B. (2004) Reversal od gene silencing as a therapeutic target for cancer – roles for DNA methylation and its interdigitation with chromatin. *Novartis Foundation Symposium*. **259**: 226-233

Baylin, S. B., Ohm, J. E. (2006) Epigenetic gene silencing in cancer - a mechanism for early oncogenic pathway addiction? *Nature Reviews Cancer*. **6**: 107-116

Bender, C. M., Pao, M. M., Jones, P. A. (1998) Inhibition of DNA methylation by 5-aza-2′-deoxycytidine suppresses the growth of human tumor cell lines. *Cancer Research*. **58**: 95-101

Bergeron, J. J., Brenner, M. B., Thomas, D. Y., *et al.* (1994) Calnexin: a membrane-bound chaperone of the endoplasmic reticulum. *Trends in Biochemical Science*. **19 (3)**: 124-128

Bestor, T. H. (2000) The DNA methyltransferases of mammals. *Human Molecular Genetics*. **9**: 2395-2402

Bestor, T. H., Laudano, A., Mattaliano, R.*et al.* (1988). Cloning and sequencing of a cDNA encoding DNA methyltransferases of mouse cells. The carboxyl-terminal domain of the mammalian enzyme is related to bacterial restriction methyltransferases. *Journal of Molecular Biology.* **203**: 971-983

Bestor, T. H., Verdine, G. L. (1994) DNA methyltransferases. *Current Opinion in Cell Biology*. **6**: 3803-3809

Bhasin, M., Zhang, H., Reinherz, E. L. (2005) Prediction of methylated CpGs in DNA sequences using a support vector machine. *FEBS Letters.* **579 (20)**: 4302-4308

Bhaumik, S. R., Smith, E., Shilatifard, A. (2007) Covalent modifications of histones during development and disease pathogenesis. *Nature Structural and Molecular Biology.* **14**: 1008-1016

Billam, M., Sobolewski, M. D., Davidson, N. E. (2009) Effects of a novel DNA methyltransferase inhibitor Zebularine on human breast cancer cells. *Breast Cancer Research and Treatment*. **120 (3)**: 581-592

Bird, A. (2002) DNA methylation patterns and epigenetic memory. *Genes and Development*. **16 (1)**: 6-21

Bird, A. P. (1986) CpG-rich islands and the function of DNA methylation. *Nature*. **321**: 209-213

Bishop, J. M. (1991) Molecular themes in oncogenesis. *Cell.* **64**: 235-248

Bjerling, P., Silverstein, R. A., Thon, G., *et al.* (2002) Functional divergence between histone deacetylases in fission yeast by distinct cellular localization and in vivo specificity. *Molecular and Cellular Biology*. **22**: 2170-2181

Blander, G., Guarente, L. (2004) The Sir2 family of protein deacetylases. *Annual Review of Biochemistry*. **73**: 417-435

Boman, B. M., Huang, E. (2008) Human colon cancer stem cells: a new paradigm in gastrointestinal oncology. *Journal of Clinical Oncology*. **26**: 2828-2838

Bonnette, B., Favre, N., Reveneau, S., *et al.* (1998) Cancer cell sensitization to Fas-mediated apoptosis by sodium butyrate. *Cell Death and Differentiation*. **5 (6)**: 480-487

Bouchard, J., Momparler, R. L. (1983) Incorporation of 5-aza-2′-deoxycytidine- 5′-triphosphate into DNA. Interactions with mammalian DNA polymerase alpha and DNA methylase. *Molecular Pharmacology*. **24**: 109-114

Braiteh, F., Soriano, A. O., Garcia-Manero, G., *et al.* (2008) Phase I study of epigenetic modulation with 5-azacytidine and valproic acid in patients with advanced cancers. *Clinical Cancer Research*. **14 (19)**: 6296-6301

Brembeck, F. H., Rosário, M., Birchmeier, W. (2006) Balancing cell adhesion and Wnt signalling, the key role of β-catenin. *Current opinion in Genetics and Development*. **16**: 51-59

Brittan, M., Wright, N. A. (2002) Gastrointestinal stem cells. *Journal of Pathology*. **197**: 492-509

Bug, G., Gul, H., Schwarz, K., *et al.* (2005) Valproic acid stimulates proliferation and self-renewal of hematopoietic stem cells. *Cancer Research*. **65**: 2537-2541

Burton, B. S. (1882) On the propyl derivatives and decomposition products of ethylacetoacetate. *American Chemical Journal*. **3**: 385-395

Cameron, E. E., Bachman, K. E., Myohanen, S., *et al.* (1999) Synergy of demethylation and histone deacetylase inhibition in the re-expression of genes silenced in cancer. *Nature Genetics.* **21 (1)**: 103-107

Cancer fact Sheet (2011) World Health Organisation. [http://www.who.int/mediacentre/factsheets/fs297/en/]. Date accessed 30 August 2011

Cannon, S. V., Cummings, A., Teebor, G. W. (1988) 5- Hydroxymethylcytosine DNA glycosylase activity in mammalian tissue. *Biochemical and Biophysical Research Communications*. **151 (3)**: 1173-1179

Carducci, M., Bowling, M. K., Eisenberger, M., *et al.* (1997) Phenylbutyrate (PB) for refractory solid tumors: phase I clinical and harmacologic evaluation of intravenous and oral PB. *Anticancer Research*. **17**: 3972-3973

Carew, J. S., Giles, F. J., Nawrocki, S. T. (2008) Histone deacetylase inhibitors: mechanisms of cell death and promise in combination cancer therapy. *Cancer Letters*. **269**: 7-17

Cervoni, N., Szyf, M. (2001) Demethylase activity is directed by histone acetylation. *Journal of Biological Chemistry.* **276**: 40778-40787

Chandler, J. M., Lagasse, E. (2010) Cancerous stem cells: deviant stem cells with cancer-causing misbehaviour. *Stem Cell Research & Therapy.* **1 (13):** 1-9

Chavez-Blanco, A., Segura-Pacheco, B., Pe´rez-Ca´rdenas, E., *et al.* (2005) Histone acetylation and histone deacetylase activity of magnesium valproate in tumor and peripheral blood of patients with cervical cancer. A phase I study. *Molecular Cancer*. **4 (1)**: 22

Chen, S., Guttridge, D. C., You, Z., *et al.* (2001a) WNT-1 Signaling Inhibits Apoptosis by Activating β-Catenin/T Cell Factor–Mediated Transcription. *Journal of Cellullar Biology.* **152 (1)**: 87-96

Chen, X., Johns, D. C., Geiman, D. E., *et al*. (2001) Kruppel-like factor 4 (gut-enriched Kruppel-like factor) inhibits cell proliferation by blocking G1/S progression of the cell cycle. *The Journal of Biological Chemistry*. **276**: 30423-30428

Chen, X., Whitney, E. M., Gao, S. Y., *et al*. (2003) Transcriptional profiling of Kruppel-like factor 4 reveals a function in cell cycle regulation and epithelial differentiation. *Journal of Molecular Biology*. **326**: 665-677

Chen, Y., Fang, J., Zhu, H., *et al.* (2004) Histone acetylation regulates $p21^{WAF1}$ expression in human colon cancer cell lines. *World Journal of Gastroenterology*. **10 (18)**: 2643-2646

Chen, Z. Y., Rex, S., Tseng, C. (2004) Kruppel-Like Factor 4 Is Transactivated by Butyrate in Colon Cancer Cells. *Journal of Nutrition*. **134**: 792-798

Chen, Z. Y., Shie, J. L., Tseng, C. C. (2002) Gut-enriched Kruppel-like factor represses ornithine decarboxylase gene expression and functions as checkpoint regulator in colonic cancer cells. *The Journal of Biological Chemistry*. **277**: 46831-46839

Cheng, J. C., Matsen, C. B., Gonzales, F. A., *et al.* (2003) Inhibition of DNA methylation and reactivation of silenced genes by Zebularine*. The Journal of the National Cancer Institute*. **95 (5)**: 399-409

Cheng, J. C., Weisenberger, D. J., Gonzales, F. A., *et al.* (2004) Continuous Zebularine Treatment Effectively Sustains Demethylation in Human Bladder Cancer Cells. *Molecular and Cellular Biology.* **24 (3)**: 1270-1278

Cheng, J. C., Yoo, C. B., Weisenberger, D. J., *et al.* (2004) Preferential response of cancer cells to zebularine. *Cancer Cell*. **6**: 151-158

Cho, E. A., Dressler, G. R. (1998) TCF-4 binds *β*-catenin and is expressed in distinct regions of the embryonic brain and limbs. *Mechanisms of Development*. **77 (1)**: 9-18

Cho, Y. G., Song, J. H., Kim, C. J., *et al.* (2007) Genetic and epigenetic analysis of the *KLF4* gene in gastric cancer. *Acta Pathologica, Microbiologica et Immunologica Scandinavica.* **115**: 802-808

Clevers, H. (2006). Wnt/beta-catenin signaling in development and disease. *Cell*. **127 (3)**: 469-480

Comings, D. E. (1973) A general theory of carcinogenesis. *Proceedings of the National Academy of Sciences.* **70 (12):** 3324-3328

Constantinides, P. G., Jones, P. A., Gevers, W. (1977) Functional striated muscle cells from non-myoblast precursors following 5-azacytidine treatment. *Nature*. **267**: 364-366

Cross, S. H., Charlton, J. A., Nan, X, *et al.* (1994) Purification of CpG islands using a methylated DNA binding column. *Nature Genetics*. **6**: 236-244

Danbara, M., Kameyama, K., Higashihara, M., *et al.* (2002) DNA methylation dominates transcriptional silencing of Pax5 in terminally differentiated B cell lines. *Molecular Immunology*. **38 (15)**: 1161-1166

Dang, D. T., Bachman, K. E., Mahatan, C. S., *et al.* (2000) Decreased expression of the gut-enriched Kruppel like factor gene in intestinal adenomas of multiple intestinal neoplasia mice and in colonic adenomas of familial adenomatous polyposis patients. *FEBS Letters*. **476 (3)**: 203-207

Dang, D. T., Pevsner, J., Yang, V. W. (2000) The biology of the mammalian Krüppel-like family of transcription factors. *The International Journal of Biochemistry and Cell Biology*. **32 (11-12)**: 1103-1121

Das, P. M., Singal, R. (2004) DNA Methylation and Cancer. *Journal of Clinical Oncology*. **22 (22)**: 4632-4642

De Ruiter, A. J. M., Van Gennip, A. H., Caron, H. N., *et al.* (2003) Histone deacetylases (HDACs): characterization of the classical HDAC family. *Biochemical Journal*. **370**: 737-749

Delhommeau, F., Dupont, S., Della Valle, V., *et al.* (2009) Mutation in TET2 in myeloid cancers. *The New England Journal of Medicine.* **360 (22)**: 2289-2301

Detich, N., Bovenzi, V., Szyf, M. (2003) Valproate induces replication-independent active DNA demethylation. *Journal of Biological Chemistry.* **278**: 27586-27592

Devrajan, E., Sahin, A. A., Chen, J. S., *et al.* (2002) Down-regulation of caspase 3 in breast cancer: a possible mechanism for chemoresistance. *Oncogene*. **21 (57)**: 8843-8851

Dick, J. E. (2003) Breast cancer stem cells revealed. *Proceedings of the National Academy of Sciences*. **100 (7)**: 3547-3549

DMSO and Cancer: Treating Cancer with DMSO (2012) LeQuadrillage Family Health & Wellness Center. [http://www.lequadrillage.com/dmso.html]. Date accessed 25 March 2012

Doble, B. W., Woodgett, J. R. (2003) GSK-3: tricks of the trade for a multi-tasking kinase. *Journal of Cell Science*. **116**: 1175-1186

Dravid, G., Ye, Z., Hammond, H. *et al*. (2005) Defining the role of Wnt/β-catenin signaling in the survival, proliferation, and self-renewal of human embryonic stem cells. *Stem Cells*. **23**: 1489-1501

Duenas-Gonzales, A., Candaleria, M., Perez-Plascencia, C., *et al.* (2008) Valproic acid as epigenetic cancer drug: preclinical, clinical and transcriptional effects on solid tumors. *Cancer Treatment Reviews*. **34**: 206-222

Duvic, M., Talpur, R., Ni, X., *et al.* (2007) Phase 2 trial of oral vorinostat (suberoylanilide hydroxamic acid, SAHA) for refractory cutaneous T-cell lymphoma (CTCL). *Blood*. **109**: 31-39

Egger, G., Liang, G., Aparicio, A., *et al.* (2004) Epigenetics in human disease and prospects for epigenetic therapy. *Nature.* **429**: 457-463

Elgin, S. C. R. (1996) Heterochromatin and gene regulation in Drosophila. *Current Opinion in Genetics and Development*. **6 (2)**: 193-202

Ellis, L., Atadja, P. W., Johnstone, R. W. (2009) Epigenetics in cancer: targeting chromatin modifications. *Molecular cancer therapy*. **8 (6)**: 1409-1420

Engelsberg, A., Hermosilla, R., Karsten, U., *et al.* (2003) The Golgi protein RCAS1 controls cell surface expression of tumor-associated O-linked glycan antigens. *The Journal of Biological Chemistry*. **278 (25)**: 22998-23007

Esteller, M. (2008) Epigenetics in cancer. *New England Journal of Medicine*. **358**: 1148-1159

Evans, M. J., Kaufman, M. H. (1981). Establishment in culture of pluripotential cells from mouse embryos. *Nature*. **292**: 154-156

Evans, P. M., Chen, X., Zhang, W., *et al.* (2010) KLF4 Interacts with β-Catenin/TCF4 and Blocks p300/CBP Recruitment by β-Catenin. *Molecular and Cellular Biology*. **30 (2)**: 372-381

Evans, P. M., Zhang, W., Chen, X., Yang, *et al.* (2007). Kruppel-like factor 4 is acetylated by p300 and regulates gene transcription via modulation of histone acetylation. *The Journal of Biological Chemistry*. **282**: 33994-34002

Fabrizi, E., Martino, S., Pelacchi, F. *et al.* (2010) Therapeutic implications of colon cancer stem cells. *World Journal of Gastroenterology.* **16 (31)**: 3871-3877

Fagotto, F., Gluck, U., Gumbiner, B. M. (1998) Nuclear localization signal-independent and importin/karyopherin-independent nuclear import of beta-catenin. *Current Biology*. **8 (4)**: 181-190

Fearon, E. R. (2011) Molecular genetics of colorectal cancer. *Annual Review of Pathology: Mechanisms of Disease*. **6**: 479-507

Feinberg, A. P., Tycko, B. (2004) The history of cancer epigenetics. *Nature Reviews Cancer.* **4**: 143-153

Feinberg, A. P., Vogelstein, B. (1983) Hypomethylation distinguishes genes of some human cancers from their normal counterparts. *Nature*. **301**: 89-92

Fisher, R. A. (1936). The use of multiple measurements in taxonomic problems. *Annals of Eugenics.* **7**: 111-132

Flandez, M., Guilmeau, S., Blache, P., *et al.* (2008) KLF4 regulation in intestinal epithelial cell maturation. *Experimental Cell Research*. **314**: 3712-3723

Folkman, J. (1990) What is the evidence that tumours are angiogenesis-dependent? *Journal of the National Cancer Institute.* **82:** 4-6

Foster, K. W., Frost, A. R., Mckie-Bell, P., *et al.* (2000) Increase of GKLF Messenger RNA and Protein Expression during Progression of Breast Cancer. *Cancer Research*. **60**: 6488-6495

Fraga, M. F., Ballestar, E., Villar-Garea, A., *et al.* (2005) Loss of acetylation at Lys16 and trimethylation at Lys20 of histone H4 is a common hallmark of human cancer. *Nature Genetics*. **37**: 391-400

Fraga, M. F., Esteller, M. (2002) DNA methylation: a profile of methods and applications. *BioTechniques.* **33 (3)**: 632, 634, 636-349

Gal-Yam, E. N., Saito, Y., Egger, G., *et al.* (2008) Cancer epigenetics: modifications, screening and therapy. *The Annual Review of Medicine*. **59**: 267-280

Garcia-Manero, G., Kantarijan, H. M., Sanchez-Gonzalez, B., *et al.* (2006) Phase 1/2 study of the combination of 5-aza-2'-deoxycytidine with valproic acid in patients with leukemia. *Blood*. **108 (10)**: 3271-3279

Gardiner-Garden, M., Frommer, M. (1987) CpG Isands in vertebrate genomes. *Journal of Molecular Biology*. **196**: 261-282

Gene: CTNNB1 (2011) Ensembl. [http://www.ensembl.org/Homo_sapiens/Gene/Summary?db=core;g=ENSG00000168036;r=3:41236328-41301587;t=ENST00000396185]. Date accessed 25 September 2011

Gene: KLF4 (2011) Ensembl. [http://www.ensembl.org/Homo_sapiens/Gene/Summary?db=core;g=ENSG00000136826;r=9:110247133-110252763;t=ENST00000374672]. Date accessed 6 September 2011

Ghaleb, A. M., Yang, V. W. (2008) The pathobiology of Krüppel-like factors in colorectal cancer. *Current Colorectal Cancer Reports.* **4 (2)**: 59-64

Globocan 2008: Fast Stats (2010) IARC 2010. [http://globocan.iarc.fr/factsheets/populations/factsheet.asp?uno=900]. Date accessed 30 August 2011

Goll, M. G., Bestor, T. H. (2005) Eukaryotic cytosine methyltransferases. *Annual Review of Biochemistry*. **74**: 481-514

Goll, M. G., Kirpekar, F., Maggert, K. A., *et al.* (2006) Methylation of tRNAAsp by the DNA methyltransferase homolog Dnmt2. *Science.* **311**: 395-398

Gottardi, C. J., Gumbiner, B. M. (2001) Adhesion signaling: How β-catenin interacts with its partners. *Current biology*. **11**: R792-R794

Gottlicher, M., Minucci, S., Zhu, P., *et al.* (2001) Valproic Acid defines a novel class of HDAC inhibitors inducing differentiation of transformed cells. *The EMBO Journal*. **20 (24)**: 6969-6978

Gould, T. D., Chen, G., Manji, H. K. (2004) In vivo evidence in the brain for lithium inhibition of glycogen synthase kinase-3. *Neuropsychopharmacology.* **29**: 32-38

Gould, T. D., Manji, H. K. (2002) The Wnt signaling pathway in bipolar disorder. *Neuroscientist.* **8**: 497-511

Graham, T. A., Ferkey, D. M., Mao, F., *et al.* (2001) Tcf4 can specifically recognize beta-catenin using alternative conformations. *Nature Structural Biology*. **8 (12)**:1048-1052

Gray, G. G., Ekstrom, T. J. (2001) The human histone deacetylase family. *Experimental Cell Research*. **262**: 75-83

Greger, V., Debus, N., Lohmann, D., *et al.* (1994) Frequency and parental origin of hypermethylated RB1 alleles in retinoblastoma. *Human Genetics*. **94 (5)**: 491-496

Grosshcedl, R., Giese, K., Pagel, J. (1994) HMG domain proteins: architectural elements in the assembly of nucleoprotein structures. *Trends in genetics*. **10 (3)**: 94-100

Grunstein, M. (1997). Histone acetylation in chromatin structure and transcription. *Nature*. **389**: 349-352

Grunt, T. W., Somay, C., Pavelka, M., *et al*. (1991) The effects of dimethyl sulfoxide and retinoic acid on the cell growth and the phenotype of ovarian cancer cells. *Journal of Cell Science*. **100**: 657-686

Guan, R. J., Ford, H. L., Fu, Y., *et al.* (2000) Drg-1 as a differentiation-related, putative metastatic suppressor gene in human colon cancer. *Cancer Research.* **60 (3)**: 749-755

Gui, C. Y., Ngo, L., Xu, W. S., Richon *et al.* (2004) Histone deacetylase (HDAC) inhibitor activation of p21WAF1 involves changes in promoter-associated proteins, including HDAC1. *Proceedings of the National Academy of Sciences USA*. **101**: 1241-1246

Gurvich, N., Tsygankova, O. M., Meinkoth, J. L., *et al.* (2004) Histone deacetylase is a target of valproic acid-mediated cellular differentiation. *Cancer Research*. **64**: 1079-1086

Hague, A., Diaz, G. D., Hicks, D. J., *et al.* (1997) Bcl-2 and bak may play a pivotal role in sodium butyrate-induced apoptosis in colonic epithelial cells; however overexpression of bcl-2 does not protect against bak-mediated apoptosis. *International Journal of Cancer*. **72**: 898-905

Han, A., Song, Z., Tong, C., *et al.* (2008) Sulindac suppresses β-catenin expression in human cancer cells. *European Journal of Pharmacology*. **583 (1)**: 26-31

Han, J. W., Ahn, S. H., Park, S. H., e*t al.* (2000) Apicidin, a histone deacetylase inhibitor, inhibits proliferation of tumour cells via induction of p21WAF1/CIP1 and gelsolin. *Cancer Research*. **60**: 6068-6074

Harris, T. J. C., Peifer, M. (2005) Decisions, decisions: β-catenin chooses between adhesion and transcription. *Trends in Cell Biology*. **15 (5)**: 234-237

He, B., You, L., Uematsu, K., *et al.* (2004) A Monoclonal Antibody against Wnt-1 Induces Apoptosis in Human Cancer Cells. *Neoplasia*. **6 (1)**: 7-14

He, X. (2003) A Wnt-Wnt situation. *Developmental Cell*. **4 (6)**: 791-797

He, X., Chang, S., Zhang, J., *et al*. (2007) MethyCancer: the database of human DNA methylation and cancer. *Nucleic Acids Research*. **36**: D836-D841

Hecht, A., Vleminckx, K., Stemmler, M. P., *et al.* (2000) The p300/CBP acetyltransferases function as transcriptional coactivators of β-catenin in vertebrates. *The EMBO Journal*. **19 (8)**: 1839-1850

Heerdt, B. G., Houston, M. A., Augenlicht, L. H. (1997) Short-chain fatty acid-initiated cell cycle arrest and apoptosis of colonic epithelial cells is linked to mitochondrial function. *Cell Growth and Differentiation*. **8**: 523-532

Heisler, L. E., Torti, D., Boutros, P. C., *et al*. (2005) CpG Island microarray probe sequences derived from a physical library are representative of CpG Islands annotated on the human genome. *Nucleic Acids Research*. **33**: 2952-2961

Henderson, B. R., Fagotto, F. (2002) The ins and outs of APC and β-catenin nuclear transport. *EMBO Reports*. **3 (9)**: 834-839

Hermann, A., Schmitt, S., Jeltsch, A. (2003) The human Dnmt2 has residual DNA-(cytosine-C5) methyltransferase activity. *The Journal of Biological Chemistry.* **278:** 31717-31721

Hirschmann-Jax, C., Foster, A. E., Wulf, G. G., Nuchtern J. G. *et al.* (2004) A distinct “side population” of cells with high drug efflux capacity in human tumor cells. *The National Academy of Sciences of the USA.* **101 (39)**: 14228-14233

Ho, M. W. (1979) Beyond neo-Darwinism – an epigenetic approach to evolution. *Journal of Theoretical Biology.* **78**: 573-591

Holleran, J. L., Parise, R. A., Joseph, E., *et al.* (2005) Plasma pharmacokinetics, oral bioavailability, and interspecies scaling of the DNA methyltransferase inhibitor, zebularine. *Clinical Cancer Research*. **11**: 3862-3868

Houghton, J. M, Morozov, A., Smirnova, I., *et al.* (2007) Stems cells and cancer. *Seminars in Cancer Biology*. **17**: 191-203

Hrebackova, J, Hrabeta,, J., Eckschlager, T. (2010) Valproic acid in the complex therapy of malignant tumours. *Current Drug Targets*. **11**: 361-379

Huang, L., Ren, J., Chen, D., *et al.* (2003) MUC1 cytoplasmic domain coactivates Wnt target gene transcription and confers transformation. *Cancer Biology and Therapy*. **2**: 702-706

Huang, Y., Pastor, W. A., Shen, Y., *et al.* (2010) The Behaviour of 5-Hydroxymethylcytosine in Bisulfite Sequencing. *PLoS One*. **5 (1)**: e888

Huber, A. H., Nelson, W. J., Weis, W. I. (1997) Three-dimensional structure of the armadillo repeat region of β-Catenin. *Cell*. **90**: 871-882

Iizuka, M., Stillman, B. (1999). Histone acetyltransferase HBO1 interacts with the ORC1 subunit of the human initiator protein. *Journal of Biological Chemistry.* **274**: 23027-23034

Inbal, B., Bialik, S., Sabanay, I., *et al*. (2002) DAP kinase and DRP-1 mediate membrane blebbing and the formation of autophagic vesicles during programmed cell death. *The Journal of Cell Biology*. **157 (3)**: 455-468

Insinga, A., Monestiroli, S., Ronzoni, S., *et al.* (2005) Inhibitors of histone deacetylases induce tumor-selective apoptosis through activation of the death receptor pathway. Nature Medicine. **11**: 71-76

Iyer, L., Ratain, M. J. (1998) Clinical pharmacology of camptothecins. *Cancer Chemotherapy and Pharmacology*. **42 (Suppl)**: S31-S43

Jahangeer, S., Elliott, R. M., Henneberry, R. C. (1982) β -Adrenergic receptor induction in HeLa cells: synergistic effect of 5-azacytidine and butyrate. *Biochemical and Biophysical Research Communication*. **108**: 1434-1440

Jemal, A., Siegel, R., Ward, E., *et al.* (2009) Cancer statisitics, 2009. *CA Cancer Journal for Clinicians.* **59:** 225-249

Jenuwein, T. (2001) Re-SET-ting heterochromatin by histone methyltransferases. *Trends in Cell Biology.* **11**: 266-73

Jenuwein, T., Allis, C. D. (2001) Translating the histone code. *Science*. **293**: 1074-1080

Johannessen, C. U., Johannessen, S. I. (2003) Valproate: past, present, and future. *CNS Drug Reviews*. **9 (2)**: 199-216

Johnstone, R. W. and Licht, J. D. (2003). Histone deacetylase inhibitors in cancer therapy: is transcription the primary target? *Cancer Cell*. **4**: 13-18

Jones, P. A. (1985) Altering gene expression with 5-azactytidine. *Cell*. **40**: 485-486

Jones, P. L., Veenstra, G. J., Wade, P. A., *et al.* (1998) Methylated DNA and MeCP2 recruit histone deacetylase to repress transcription*. Nature Genetics*. **19 (2)**: 187-191

Joseph, J., Mudduluru, G., Antony, S., Vashistha *et al.* (2004) Expression profiling of sodium butyrate (nab)-treated cells: Identification of regulation of genes related to cytokine signaling and cancer metastasis by nab. *Oncogene*. **23**: 6304-6315

Juttermann, R., Li, E., Jaenisch, R. (1994) Toxicity of 5-aza-2′-deoxycytidine to mammalian cells is mediated primarily by covalent trapping of DNA methyltransferase rather than DNA demethylation. *Proceedings of the National Academy of Sciences USA*. **91**: 11797-11801

Kanai, Y., Hirohashi, S. (2007) Alterations of DNA methylation associated with abnormalities of DNA methyltransferasesin human cancers during transition from a precancerous to a malignant state. *Carcinogenesis*. **28**: 2434-2442

Kaneda, A., Feinberg, A. P. (2005) Loss of imprinting of IGF2: a common epigenetic modifier of intestinal tumor risk. *Cancer Research.* **65**: 11236-11240

Kelmer, R. (1993) From cadherins to catenins: cytoplasmic protein interactions and regulation of cell adhesion. *Trends in Genetics*. **9 (9)**: 317-321

Keshet, I., Lieman-Hurwitz, J., Cedar, H. (1986) DNA methylation affects the formation of active chromatin. *Cell*. **44 (4)**: 535-543

Kikuchi, T., Itoh, F., Toyota, M., *et al.* (2002) Aberrant methylation and histone deacetylation of cyclooxygenase 2 in gastric cancer. *International Journal of Cancer.* **97 (3)**: 272-277

Kim, H., Bae, S. (2011) Histone deacetylase inhibitors: molecular mechanisms of action and clinical trials as anti-cancer drugs. *American Journal of Translational Research*. **3 (2)**: 166-179

Kim, M. S., Kwon, H. J., Lee, Y. M., *et al.* (2001) Histone deacetylases induce angiogenesis by negative regulation of tumor suppressor genes. *Nature Medicine*. **7**: 437-443

Kim, M. S., Son, M. W., Kim, W. B., e*t al.* (2000) Apicidin, an inhibitor of histone deacetylase, prevents H-ras-induced invasive phenotype. *Cancer Letters*. **157**: 23-30

Kim, T. H., Xiong, H., Zhang, Z., *et al.* (2005) β-Catenin activates the growth factor endothelin-1 in colon cancer cells. *Oncogene*. **24**: 597-604

Kim, Y. S., Tsao, D., Siddiqui, B., *et al.* (1980) Effects of sodium butyrate and dimethylsulfoxide on biochemical properties of human colon cancer cells. *Cancer*. **45**: 1185-1192

Kissil, J. L., Feinstein, E., Cohen, O., *et al*. (1997) DAP-kinase loss of expression in various carcinoma and B-cell lymphoma cell lines: possible implications for role as tumor suppressor gene. *Oncogene*. **15 (4)**: 403-407

Klaewsongkram, J., Yang, Y., Golech, S., *et al.* (2007). Kruppel-like factor 4 regulates B cell number and activation-induced B cell proliferation. *The Journal of Immunology*. **179**: 4679-4684

Klein, G. (1988) Oncogenes and tumor suppressor genes. *Acta Oncologica.* **27 (4)**: 427-437

Klonisch, T., Wiechec, E., Hombach-Klonisch, S. *et al*. (2008). Cancer stem cell markers in common cancers – therapeutic implications. *Trends in Molecular Medicine*. **14 (10)**: 450-460

Knudson, A. G. (1971) Mutation and cancer: statistical study of retinoblastoma. *Proceedings of the National Academy of Sciences.* **68 (4):** 820-823

Ko, M., Huang, Y., Jankowska, A. M., *et al.* (2010) Impaired hydroxylation of 5-methylcytosine in myeloid cancers with mutant TET2. *Nature.* **468 (7325)**: 839-843

Kochbin, S., Verdel, A., Lemercier, C., *et al.* (2001) Functional significance of histone deacetylase diversity. *Current Opinion in Genetics and Development*. **11**: 162-166

Kouzarides, T. (1999). Histone acetylases and deacetylases in cell proliferation. *Current Opinion in Genetics and Development*. **9**: 40-48

Kramer, O. H., Gottlicher, M., Heinzel, T. (2001) Histone deacetylase as a therapeutic target. *Trends in Endocrinology and Metabolism*. **12 (7)**: 294-300

Kramer, O. H., Zhu, P., Ostendorf, H. P., *et al.* (2003) The histone deacetylase inhibitor valproic acid selectively induces proteasomal degradation of HDAC2. *The EMBO Journal*. **22 (13)**: 3411-3420

Kraus, C., Liehr, T., Hulsken, J. *et al.* (1994) Localization of the human beta-catenin gene (CTNNB1) to 3p21: a region implicated in tumor development. *Genomics*. **23**: 272-274

Kriaucionis, S., Heintz, N. (2009) The nuclear DNA base 5- hydroxymethylcytosine is present in Purkinje neurons and the brain. *Science*. **324 (5929)**: 929-930

Kuhn, R. M., Karolchik, D., Zweig, A. S., *et al*. (2007) The UCSC genome browser database: update 2007. *Nucleic Acids Research*. **35**: D668-D673

Laity, J. H., Lee, B. M., Wright, P. E. (2001) Zinc finger proteins: new insights into structural and functional Diversity. *Current Opinion in Structural Biology*. **11**: 39-46

Lander, E. S., Linton, L. M., Birren, B., *et al.* (2001) Initial sequencing and analysis of the human genome. **409**: 860-921

Lapidot, T., Sirard, C., Vormoor, J., *et al*. (1994) A cell initiating human acute myeloid leukaemia after transplantation into SCID mice. *Nature*. **367:** 645-648

Lee, B. I., Park, S. H., Kim, J. W., e*t al.* (2001) MS-275, a histone deacetylase inhibitor, selectively induces transforming growth factor beta type II receptor expression in human breast cancer cells. *Cancer Research*. **61 (3)**: 931-934

Lei, H., Oh, S. P., Okano, M., *et al.* (1996) De novo DNA cytosine methyltransferase activities in mouse embryonic stem cells. *Development*. **122 (10)**: 3195-3205

Leonhardt, H., Rahn, H., Weinzierl, P., *et al.* (2000) Dynamics of DNA replication factories in living cells. *The Journal of Cell Biology*. **149 (2)**: 271-280

Li, W., Lui, M. (2011) Distribution of 5-hydroxymethylcytosine in different human tissues. *Journal of Nucleic Acids*. 2011 (Article ID 870726): 1-5

Li, X., Shu, Q., Su, J. M., *et al.* (2005) Valproic acid induces growth arrest, apoptosis, and senescence in medulloblastomas by increasing histone hyperacetylation and regulating expression of p21Cip1, CDK4, and CMYC. *Molecular Cancer Therapeutics*. **4**: 1912-1922

Li, Y., Bharti, A., Chen, D., *et al*. (1998) Interaction of glycogen synthase kinase 3h with the DF3/MUC1 carcinoma-associated antigen and β-catenin. *Molecular and Cellular Biology.* **18**: 7216-7224

Livak, K. J., Schmittgen, T. D. (2001) Analysis of relative gene expression data using Real-Time Quantitative PCR and the $2^{-\Delta\Delta Ct}$ method. *Methods.* **25**: 402-408

Longley, D. B., Harkin, D. P., Johnston, P. G. (2003) 5-Fluorouracil: mechanisms of action and clinical strategies. *Nature Reviews Cancer.* **3**: 330-338

Lowry, W. E., Richter, L., Yachechko, R., *et al.* (2008) Generation of human induced pluripotent stem cells from dermal fibroblasts. *Proceedings of the National Academy of Sciences.* **105 (8)**: 2883-2888

Luger, K., Richmond, T. J. (1998) The histone tails of the nucleosome. *Current Opinion in Genetics and Development*. **8**: 140-146

Lui, H., Xue, Z. T., Sjogren, H. O., *et al.* (2007) Low dose Zebularine treatment enhances immunogenicity of tumor cells. *Cancer Letters*. **257 (1)**: 107-115

Lui, Z., Teng, L., Bailey, S. K., *et al.* (2009) Epithelial transformation by KLF4 requires Notch1 but not canonical Notch1 signalling. *Cancer Biology and Therapy*. **8 (19)**: 1840-1851

Lustig, B., Behrens, J. (2003) The Wnt signalling pathway and its role in tumour development. Journal of Cancer Research and Clinical Oncology. **129 (4)**: 199-221

Ma, H., Nguyen, C., Lee, K., *et al*. (2005) Differential roles for the coactivators CBP and p300 on TCF/b-catenin-mediated survivin gene expression. *Oncogene*. **24**: 3619-3631

Maiti, S., Alam, R., Amis, C. I., *et al.* (2000) Frequent Association of *β-Catenin* and *WT1* Mutations in Wilms Tumors. *Cancer Research*. **60 (22)**: 6288-6292

Marchion, D. C., Bicaku, E., Daud, A. I., *et al.* (2005) Valproic acid alters chromatin structure by regulation of chromatin modulation proteins. *Cancer Research*. **65**: 3815-3822

Markowitz, S. A., Bertagnolli, M. M. (2009) Molecular basis of colorectal cancer. *New England Journal of Medicine*. **361:** 2449-2460

Marks, P. A., Breslow, R. (2007) Dimethyl sulfoxide to vorinostat: development of this histone deacetylase inhibitor as an anticancer drug. *Nature Biotechnology*. **25**: 84-90

Marks, P. A., Richon, V. M., Breslow, R., *et al.* (2001) Histone deacetylase inhibitors as new cancer drugs. *Current Opinion in Oncology*. **13**: 477-483

Marks, P. A., Richon, V. M., Rifkind, R. A. (2000) Histone deacetylase inhibitors: differentiation or apoptosis of transformed cells. *Journal of the National Cancer Institute*. **92 (15)**: 1210-1216

Marson, A., Foreman, R., Chevalier, B. *et al.* (2008) Wnt signaling promotes reprogramming of somatic cells to pluripotency. *Cell Stem Cell*. **3**: 132-135

Martin, G.R. (1981). Isolation of a pluripotent cell line from early mouse embryos cultured in medium conditioned by teratocarcinoma stem cells. *Proceedings of the National Academy of Sciences USA*. **78**: 7634-7638

Marzio, G., Wagener, C., Gutierrez, M. I., *et al.* (2000). E2F family members are differentially regulated by reversible acetylation. *Journal of Biological Chemistry.* **275**: 10887-10892

Matzke, M. A., Mette, M. F., Aufsatz, W., *et al.* (1999) Host defences to parasitic sequences and the evolution of epigenetic control mechanisms. *Genetica*. **107(1-3)**: 271-287

McCabe, M.T., Brandes, J. C., Vertino, P. M. (2009) Cancer DNA methylation: molecular mechanisms and clinical implications. *Clinical Cancer Research*. **15**: 3927-3937

McConnell, B. B., Yang, V. W. (2010) Mammalian Kruppel-like factors in health and disease. *Physiological Reviews.* **90 (4)**: 1337-1381

Meehan, R. R, Lewis, J. D., Cross, S., *et al.* (1992) Transcriptional repression by methylation of CpG. *Journal of Cell Science*. **16 (Suppl)**: 9-14

Meehan, R. R., Lewis, J. D., McKay, S., *et al.* (1989) Identification of a mammalian protein that binds specifically to DNA containing methylated CpGs. *Cell*. **58 (3)**: 499-507

Meunier, H., Carraz, G., Neunier, Y., *et al.* (1963) Pharmacodynamic properties of N-dipropylacetic acid. *Therapie*. **18**: 435-438

Meyerhardt, J. A., Mayer, R. J. (2005) Systemic therapy for colorectal cancer. *The New England Journal of Medicine*. **352**: 476-87

Michalowsky, L. A., Jones, P. A. (1987) Differential nuclear-protein binding to 5-azacytosine-containing DNA as a potential mechanism for 5-aza-2'-deoxycytidine resistance. *Molecular and Cellular Biology.* **7**: 3076-3083.

Mills, J. C., Stone, N. L., Pittman, R. N. (1999) The Role of the Cytoplasm in the Execution Phase. *The Journal of Cell Biology*. **146 (4)**: 703-708

Milutinovic, S., D'Alessio, A. C., Detich, N., *et al.* (2007) Valproate induces widespread epigenetic reprogramming which involves demethylation of specific genes. *Carcinogenesis*. **28**: 560-571

Momparler, R. L., Eliopolous, N., Ayoub, J. (2000) Evaluation of an inhibitor of DNA methylation, 5-aza-2′-deoxycytidine, for the treatment of lung cancer and the future role of gene therapy. *Advances in Experimental Medicine and Biology*. **456**: 433-446

Mund, C., Bruekner, B., Lyko, F. (2006) Reactivation of epigenetically silenced genes by DNA methyltransferase inhibitors. *Epigenetics*. **1 (1)**: 7-13

Nagai, R., Friedman, S. L., Kasuga, M. (2009) The Biology of Krüppel-like Factors. Springer Tokyo. 67-79

Nakahara, Y., Northcott, P. A., Li, M., *et al*. (2010) Genetic and epigenetic inactivation of Kruppel-like factor 4 in medulloblastoma. *Neoplasia*. **12 (1)**: 20-27

Nan, X. S., Ng, H. H., Johnson, C. A., *et al.* (1998) Transcriptional repression by the methyl-Cpg-binding protein MeCP2 involves a histone deacetylase complex. *Nature*. **393 (6683)**: 386-389

Neureiter, D., Zopf, S., Thorsten, L., *et al.* (2007) Apoptosis, proliferation and differentiation patterns are influenced by Zebularine and SAHA in pancreatic cancer models. *Scandinavian Journal of Gastroenterology*. **42**: 103-116

Newmark, H. L., Lupton, J. R., Young, C. W. (1994) Butyrate as a differentiating agent: pharmacokinetics, analogues and current status. *Cancer Letters*. **78**: 1-5

Noble, W. S. (2006) What is a support vector machine? *Nature Biotechnology*. **24 (12)**: 1565-1567

Noble, W. S., Scholkopf, B., Tsuda, K., *et al.* (2004) Chapter 3: Support Vector Machine Applications in Compuational Biology. Kernel methods in computational biology. Cambridge, MIT Press

Nollet, F., Berx, G., Molemans, F. *et al.* (1996) Genomic organization of human β-catenin gene (CTNNB1). *Genomics*. **32**: 413-424

Nowell, P. C. (1976) The clonal evolution of tumor cell populations. *Science*. **194 (4260)**: 23-28

Oltvai, Z. N., Milliman, C.L., Korsmeyer, S. J. (1993) Bcl-2 heterodimerizes in vivo with a conserved homolog, Bax, that accelerates programmed cell death. *Cell*. **74 (4)**: 609-619

Ortega, J., Vigil, C. E., Chodkiewicz, C. (2010) Current progress in targeted therapy for colorectal cancer. *Cancer Control*. **17 (1)**: 7-15

Ossowski, L., Belin, D. (1985) Effect of dimethyl sulfoxide on human carcinoma cells, inhibition of plasminogen activator synthesis, change in cell morphology, and alteration of response to cholera toxin. *Molecular and Cellular Biology*. **5 (12)**: 3552-3559

Ozdag, H., Teschendorff, A. E., Ahmed, A. A., *et al.* (2006) Differential expression of selected histone modifier genes in human solid cancers. *BMC Genomics.* **7**: 90

P35222: CTNB1_HUMAN (2011) UniProt/Swiss-Prot. [http://www.uniprot.org/uniprot/P35222]. Date accessed 25 September 2011

Pandya, A. Y., Talley, L. I., Frost, A. R., *et al*. (2004) Nuclear Localization of KLF4 Is Associated with an Aggressive Phenotype in Early-Stage Breast Cancer. *Clinical Cancer Research*. **10**: 2709-2719

Patel, B. B., Yu, Y., Du, J., *et al.* (2009) Age-related increase in colorectal cancer stem cells in macroscopically normal mucosa of patients with adenomas: a risk factor for colon cancer. *Biochemical and Biophysical Research Communications*. **378:** 344-347

Peidra, J., Martinez, D., Castano, J., *et al.* (2001) Regulation of β-catenin structure and activity by tyrosine phosphorylation. *The Journal of Biological Chemistry.* **276 (23)**: 20436-20443

Peifer, M., Berg, S., Reynolds, A. B. (1994) A repeating amino acid motif shared by proteins with diverse cellular roles. *Cell*. **76**: 789-791

Phiel, C. J., Zhang, F., Huang, E. Y., *et al.* (2001) Histone deacetylase is a direct target of valproic acid, a potent anticonvulsant, mood stabilizer, and teratogen. *The Journal of Biological Chemistry*. **276**: 36734-36741

Philipsen, S., Suske, G. (1999) A tale of three fingers: the family of mammalian Sp/XKLF transcription factors. *Nucleic Acids Research*. **27**: 2991-3000

Piedra, J., Miravet, S., Castano, J. *et al.* (2003) p120 Catenin-associated Fer and Fyn tyrosine kinases regulate beta-catenin Tyr-142 phosphorylation and beta-catenin-alpha-catenin Interaction. *Molecular and Cellular Biology*. **23 (7)**: 2287-2297

Pinto, D., Clevers, S. (2005) Wnt, stem cells and cancer in the intestine. *Biology of the Cell*. **97**: 185-196

Plumb, J. A., Strathdee, G., Sludden, J., *et al.* (2000) Reversal of drug resistance in human tumor xenografts by 2'-deoxy-5-azacytidine-induced demethylation of the hMLH1 gene promoter. *Cancer Research*. **60 (21)**: 6039-6044

Polakis, P. (1999) The oncogenic activation of β-catenin. *Current Opinion in Genetics and Development*. **9 (1)**: 15-21

Pollock, R. M., Richmon, V. M. (2009) Epigenetic approaches to cancer therapy. *Drug Discovery Today: Therapeutic Strategies*. **6 (2)**: 71-79

Pompeia, C., Hodge, D. R., Plass, C., *et al.* (2004) Microarray Analysis of Epigenetic Silencing of Gene Expression in the KAS-6/1 Multiple Myeloma Cell Line. *Cancer Research*. **64**: 3465-3473

Potten, C. S., Kellett, M., Roberts, S. A., *et al.* (1992) Measurement of in vivo proliferation in human colorectal mucosa using bromodeoxyuridine. *Gut.* **33**: 71-78

Ramasamy, S., Wahab, N. A., Abidin, N. Z., *et al.* (2012) Growth inhibition of human gynecologic and colon cancer cells by *Phyllanthus watsonii* through apoptosis induction. *PLoS One*. **7 (4)**: e34793

Ramaswamy, S., Ross, K. N., Lander, E. S. *et al.* (2003) A molecular signature of metastasis in primary solid tumors. *Nature Genetics.* **33**: 49-54

Rato, C., Amirova, S. R, Bates, D. G, *et al.* (2011) Translational recoding as a feedback controller: systems approaches reveal polyamine-specific effects on the antizyme ribosomal frameshift. *Nucleic Acid Research.* **39 (11)**: 4587-4597

Razin, A., Cedar, H. (1977) Distribution of 5-methylcytosine in chromatin. *Proceedings of the National Academy of Sciences USA*. **74**: 2725-2728

Reya, T., Clevers, H. (2005) Wnt signalling in stem cells and cancer. *Nature*. **434**: 843-850

Rich, J. N., Bao, S. (2007). Chemotherapy and cancer stem cells. *Cell Stem Cell*. **1**: 353-354

Riggleman, B., Weischaus, E., Schedl, P. (1989) Molecular analysis of the armadillo locus: uniformly distributed transcripts and a protein with novel internal repeats are associated with a Drosophila segment polarity gene. *Genes and Development*. **3 (1)**: 96-113

Rizzo, P., Miao, H., D'Souza, G., *et al.* (2008) Cross talk between Notch and the estrogen receptor in breast cancer suggests novel therapeutic approaches. *Cancer Research.* **68 (13)**: 5226-5235

Robertson, K. D. (2001) DNA methylation, methyltransferases and cancer. *Oncogene.* **20**: 3139-3155

Ropero, S., Fraga, M. F., Ballestar, E., *et al.* (2006) A truncating mutation of HDAC2 in human cancers confers resistance to histone deacetylase inhibition. *Nature Genetics*. **38**: 566-569

Rosenberg, G. (2007) The mechanisms of action of valproate in neuropsychiatric disorders: can we see the forest for the trees? *Cellular and Molecular Life Sciences*. **64**: 2090-2103

Rountree, M. R., Selker, E. U. (1997) DNA methylation inhibits elongation but not initiation of transcription in Neurospora crassa. *Genes and Development*. **11 (18)**: 2383-2395

Roura, S., Miravet, S., Piedra, J., *et al.* (1999) Regulation of E-cadherin/catenin association by tyrosine phosphorylation. *The Journal of Biological Chemistry*. **274 (51)**: 36734-36740

Rowland, B. D., Bernards, R., Peeper, D. S. (2005) The KLF4 tumour suppressor is a transcriptional repressor of p53 that acts as a context-dependent oncogene. *Nature Cell Biology*. **7**: 1074-1082

Sancho, E., Battle, E., Clevers, H. (2004) Signaling pathways in intestinal development and cancer. *Annual Review of Cell and Developmental Biology*. **20**: 695-723

Santi, D. V., Garrett, C. E., Barr, P. J. (1983) On the mechanism of inhibition of DNA-cytosine methyltransferases by cytosine analogs. *Cell.* **33**: 9-10

Santi, D. V., Norment, A., Garrett, C. E. (1984) Covalent bond formation between a DNA-cytosine methyltransferase and DNA containing 5- azacytosine. *Proceedings of the National Academy of Sciences USA.* **81**: 6993-6997

Santini, V., Kantarjian, H. M., Issa, J. (2001) Changes in DNA methylation in neolpasia: pathophysiology and therapeutic implications. *Annals of Internal Medicine*. **134**: 573-586

Sato, N., Fukushima, N., Maitra, A., *et al.* (2003) Discovery of novel targets for aberrant methylation in pancreatic carcinoma using high-throughput microarrays. *Cancer Research*. **63**: 3735-3742

Selker, E. U., Freitag, M., Kothe, G. O., *et al.* (2002) Induction and maintenance of nonsymmetrical DNA methylation in *Neurospora. Proceedings of the National Academy of Sciences USA.* **99 (Suppl 4)**: 16485-16490

Shankar, S., Srivastava, R. K. (2008) Histone deacetylase inhibitors: mechanisms and clinical significance in cancer: HDAC inhibitor-induced apoptosis. *Advances in Experimental Medicine and Biology*. **615**: 261-298

Sherr, C. J. (2004) Principles of tumor suppression. *Cell.* **116:** 235-246

Shie, J. L., Chen, Z. Y., Fu, M., *et al.* (2000) Gut-enriched Kruppel-like factor represses cyclin D1 promoter activity through Sp1 motif. *Nucleic Acids Research*. **28**: 2969-2976

Shields, J. M., Christy, R. J., Yang, V. W. (1996) Identification and characterization of a gene encoding a gutenriched Krüppel-like factor expressed during growth arrest. *The Journal of Biological Chemistry*. **271 (33)**: 20009-20017

Shields, J. M., Yang, V. W. (1997) Two potent nuclear localization signals in the gut-enriched Krüppel-like factor define a subfamily of closely related Krüppel proteins. *The Journal of Biological Chemistry.* **272 (29)**: 18504-18507

Shields, J. M., Yang, V. W. (1998) Identification of the DNA sequence that interacts with the gut-enriched Krüppel-like factor. *Nucleic Acids Research*. **26 (3)**: 796-802

Shilatifard, A. (2006) Chromatin modifications by methylation and ubiquitination: implications in the regulation of gene expression. *Annual Review of Biochemistry.* **75**: 243-69

Shu, J., Jelinek, J., Chang, H., *et al.* (2006) Silencing of bidirectional promoters by DNA methylation in tumorigenesis. *Cancer Research*. **66**: 5077-5084

Silverman, L. R, Demakos, E. P., Peterson, B. L., *et al.* (2002) Randomized controlled trial of azacitidine in patients with the myelodysplastic syndrome: a study of the cancer and leukemia group b. *Journal of Clinical Oncology*. **20**: 2429-2440

Singal, R., Ginder, G. D. (1999) DNA methylation. *Blood*. **93 (12)**: 4059-4070

Song, J., Noh, J. H., Lee, J. H., *et al.* (2005) Increased expression of histone deacetylase 2 is found in human gastric cancer. *Acta Pathologica, Microbiologica et Immunologica Scandinavica*. **113**: 264-268

Soriano, A. O., Yang, H., Faderl, S., *et al.* (2007) Safety and clinical activity of the combination of 5-azacytidine, valproic acid, and all-*trans* retinoic acid in acute myeloid leukemia and myelodysplastic syndrome. *Blood*. **110 (7)**: 2302-2308

Speicher, M. R., Carter, N. P. (2005) The new cytogenetics: blurring the boundaries with molecular biology. *Nature Reviews Genetics*. **6 (10)**: 782-792

Spivakov, M., Fisher, A. G. (2007) Epigenetic signatures of stem-cell identity. *Nature Reviews Genetics*. **8**: 263-271

Statistics: National Cancer Registry (2011) CANSA – The Cancer Association of South Africa. [http://www.cansa.org.za/cgi-in/giga.cgi?cat=821&limit=10&page=0&sort=D&cause_id=1056&cmd=cause_dir_news]. Date accessed 7 January 2011

Stewart, R., Stojkovic, M., Lako, M. (2006) Mechanisms of self-renewal in human embryonic stem cells. *European Journal of Cancer*. **42**: 1257-1272

Strahl, B. D. and Allis, C. D. (2000). The language of covalent histone modifications. *Nature*. **403**: 41-45

Stratton, M. R., Campbell, P. J., Futral, P. A. (2009) The cancer genome. *Nature Reviews*. **458 (9)**: 719-724

Stresemann, C., Brueckner, B., Musch, T., Stopper, *et al.* (2006) Functional diversity of DNA methyltransferase inhibitors in human cancer cell lines. *Cancer Research*. **66**: 2794-2800

Suzuki, H., Gabrielson, E., Chen, W., *et al.* (2002) A genomic screen for genes up-regulated by demethylation and histone deacteylation inhibition in colorectal cancer. *Nature Genetics*. **31**: 141-149

Szyf, M. (2009) Epigenetic, DNA methylation and chromatin modifying drugs. *The Annual Review of Pharmacology and Toxicology*. **49**: 243-263

Tahiliani, M., Koh, K. P., Shen Y., *et al.* (2009) Conversion of 5- methylcytosine to 5-hydroxymethylcytosine in mammalian DNA by MLL partner TET1. *Science*. **324 (5929)**: 930-935

Takahashi, K., Tanabe, K., Ohnuki, M., *et al.* (2007) Induction of pluripotent stem cells from adult human fibroblasts by defined factors. *Cell*. **131**: 1-12

Takahashi, K., Yamanaka, S. (2006) Induction of pluripotent stem cells from mouse embryonic and adult fibroblast cultures by defined factors. *Cell*. **126 (4)**: 663-676

Takai, D., Jones, P. A. (2002) Comprehensive analysis of CpG islands in human chromosomes 21 and 22. *Proceedings of the National Academy of Sciences*. **99 (6)**: 3740-3745

Takai, D., Jones, P. A. (2003) The CpG island searcher: a new WWW resource. *In Silico Biology*. **3**: 235-240

Taplick, J., Kurtev, V., Kroboth, K., *et al*. (2001) Homo-oligomerisation and nuclear localisation of mouse histone deacetylase 1. *Journal of Molecular Biology.* **308**: 27-38

Tate, P. H., Bird, A. P. (1993) Effects of DNA methylation on DNA-binding proteins and gene expression. *Current Opinion in Genetics and Development*. **3 (2)**: 226-231

Thiagalingam, S., Cheng, K., Lee, H. J., *et al.* (2003) Histone deactylases: Unique players in shaping the epigenetic histone code. *Annals of the New York Academy of Sciences*. **983**: 84-100

Toh, Y., Ohga, T., Endo, K., *et al.* (2004) Expression of the metastasis-associated mta1 protein and its relationship to deacetylation of the histone H4 in esophageal squamous cell carcinomas. *International Journal of Cancer*. **110**: 362-367

Torado, M., Francipane, M.G., Medema, J. P., *et al.* (2010) Colon cancer stem cells: promise of targeted therapy. *Gastroenterology*. **138**: 2151-2162

Tremolizzo, L., Carboni, G., Ruzicka, W. B., *et al.* (2002) An epigenetic mouse model for molecular and behavioral neuropathologies related to schizophrenia vulnerability. *Proceedings of the National Academy of Sciences USA*. **99**: 17095-17100

Tsao, D., Morita, A., Bella, A., *et al.* (1982) Differential effects of sodium butyrate, dimethyl sulfoxide, and retinoic acid on membrane-associated antigen, enzymes, and glycoproteins of human rectal adenocarcinoma cells. *Cancer Research*. **42**: 1052-1058

Urnov, F. D., Wolffe, A. (2000) Chromatin organisation and human disease. *Emerging Therapeutic Targets*. **4**: 665-685

Vaissiere, T., Sawan, C., Herceg, Z. (2008) Epigenetic interplay between histone modifications and DNA methylation in gene silencing. *Mutation Research*. **659**: 40-48

Valinluck, V., Tsai, H. H., Rogstad, D. K., *et al.* (2004) Oxidative damage to methyl-CpG sequences inhibits the binding of the methyl-CpG binding domain (MBD) of methyl-CpG binding protein 2 (MeCP2). *Nucleic Acids Research*. **32 (14)**: 4100-4108

Vene, R., Tosetti, F. (2010) The role of glycogen synthase kinase-3 in the decision between cell survival and cell death. *Emerging Signaling Pathways in Tumor Biology*. 95-116

Venter, J. C., Adams, M. D., Myers, E. W., *et al.* (2001) The sequence of the human genome. *Science*. **291**: 1304-1351

Vermeulen, L., Sprick, M. R., Kemper, K., *et al*. (2008) Cancer stem cells – old concepts, new insights*. Cell Death and Differentiation*. **15:** 947-958

Vunjak-Novakovic, G., Freshney, R. I. (2006) Culture of Cells for Tissue Engineering. New Jersey: Jon Wiley & Sons, Inc.

Waddington, C. H. (1942) The epigenotype. *Endeavour.* **1**: 18-20

Wade, P. A., Pruss, D., Wolffe, A. P. (1997) Histone acetylation: chromatin in action. *Trends in Biochemical Science.* **22**: 128-32

Waga, S., Hannon, G.J., Beach, D., *et al.* (1994) The p21 inhibitor of cyclin-dependent kinases controls DNA replication by interaction with PCNA. *Nature*. **369**: 574-578

Wang, C., Delcros, J. G., Cannon, L., *et al.* (2003) Defining the molecular requirements for the selective delivery of polyamine conjugates into cells containing active polyamine transporters. *Journal of Medical Chemistry.* **46 (24)**: 5129-5138

Watson, A. J. M. (2004) Apoptosis and Colorectal Cancer. *Gut*. **53**: 1701-1709

Wei, D., Gong, W., Kanai, M., *et al.* (2005) Drastric down-regulation of Kruppel-like factor 4 expression is critical in human gastric cancer development and progression. *Cancer Research*. **65**: 2746-2754

Wei, D., Kanai, M., Huang, S., *et al.* (2006) Emerging role of KLF4 in human gastrointestinal cancer. C*arcinogenesis.* **27 (1)**: 23-31

Wei, X., Xu, H., Kufe, D. (2007) Human Mucin 1 oncoprotein represses transcription of the p53 tumor suppressor gene. *Cancer Research*. **67**: 1853-1858

Weiser, T. S., Guo, Z. S., Ohnmacht, G. A., *et al.* (2001) Sequential 5-Aza-2'-deoxycytidine-Depsipeptide FR901228 Treatment Induces Apoptosis Preferentially in Cancer Cells and Facilitates Their Recognition by Cytolytic T Lymphocytes Specific for NY-ESO-1. *Journal of Immunotherapy*. **24 (2)**: 151-161

Wilson, A. J., Byun, D. S., Popova, N., *et al.* (2006) Histone deacetylase 3 (HDAC3) and other class I HDACs regulate colon cell maturation and p21 expression and are deregulated in human colon cancer. *The Journal of Biological Chemistry*. **281**: 13548-13558

Wolffe, A. P., Guschin, D. (2000). Chromatin structural features and targets that regulate transcription. *Journal of Structural Biology.* **129**: 102-122

Worm, J., Gulberg, P. (2002) DNA methylation: an epigenetic pathway to cancer and a promising target for anticancer therapy. *Journal of Oral Pathology and Medicine*. **31 (8)**: 443-449

Wu, J. C., Santi, D. V. (1985) On the mechanism and inhibition of DNA cytosine methyltransferases. *Progress in Clinical and Biological Research.* **198**: 119-129

Wyatt, G. R., Cohen, S. S. (1952) A new pyrimidine base from bacteriophage nucleic acids. *Nature*. **170 (4338)**: 1072-1073

Xu, J., Lu, B., Xu, F., *et al*. (2008) Dynamic down-regulation of Kruppel-like factor 4 in colorectal adenoma-carcinoma sequence. *Journal of Cancer Research and Clinical Oncology*. **134**: 891-898

Xu, N., Papagiannakopoulos, T., Pan, G., *et al.* (2009) MicroRNA-145 Regulates OCT4, SOX2, and KLF4 and Represses Pluripotency in Human Embryonic Stem Cells. *Cell*. **137**: 647-658

Xu, W. S., Perez, G., Ngo, L., *et al.* (2005) Induction of polyploidy by histone deacetylase inhibitor: a pathway for antitumor effects. *Cancer Research*. **65**: 7832-7839

Yamamoto, M., Bharti, A., Li, Y., *et al*. (1997) Interaction of the DF3/MUC1 breast carcinoma-associated antigen and β-catenin in cell adhesion. *The Journal of Biological Chemistry*. **272**: 12492-12494

Yamanaka, S. (2007) Strategies and new developments in the generation of patient-specific pluripotent stem cells. *Cell Stem Cell*. **1**: 39-49

Yamashita, K. Upadhyay, S., Osada, M., *et al.* (2002) Pharmacologic unmasking of epigenetically silenced tumor suppressor genes in esophageal squamous cell carcinoma. *Cancer Cell.* **2**: 485-495

Yang, G., Lu, X., Fu, H. *et al.* (2009) Chemotherapy not only enriches but also induces cancer stem cells. *Bioscience Hypotheses*. **2**: 393-395

Yang, V. W. (1998) Eukaryotic transcription factors: identification, characterization and functions. *Journal of Nutrition*. **128**: 2045-2051

Yang, W. M., Tsai, S. C., Wen, Y. D., *et al*. (2002) Functional domains of histone deacetylase-3. *The Journal of Biological Chemistry*. **277**: 9447-9454

Yang, X., Phillips, D. L., Ferguson, A. T., *et al.* (2001) Synergistic activation of functional estrogen receptor (ER)-alpha by DNA methyltransferase and histone deacetylase inhibition in human ER-alpha-negative breast cancer cells. *Cancer Research.* **61 (19)**: 7025-7029

Yap, T. A., Garrett, M. D., Walton, M. I., *et al.* (2008) Targeting the PI3K–AKT–mTOR pathway: progress, pitfalls, and promises. *Current Opinion in Pharmacology*. **8**: 393-412

Yasui, W., Oue, N., Ono, S., *et al.* (2003) Histone acetylation and gastrointestinal carcinogenesis. *Annals of the New York Academy of Science*. **983**: 220-231

Yeh, C., Yao, C., Yan, J., *et al.* (2011) Apoptotic Cell Death and Inhibition of Wnt/β-Catenin Signaling Pathway in Human Colon Cancer Cells by an Active Fraction (HS7) from Taiwanofungus camphorates. *Evidence-based Complementary and Alternative Medicine*. Volume 2011, Article ID 750230: 1-13

Yet, S. F., McA'Nulty, M. M., Folta, S. C., *et al*. (1998) Human EZF, a Kruppel-like zinc finger protein, is expressed in vascular endothelial cells and contains transcriptional activation and repression domains. *The Journal of Biological Chemistry*. **273**: 1026-1031

Yoo, C. B., Chuang, J., C., Byun, H., *et al*. (2008) Long-term Epigenetic Therapy with Oral Zebularine Has Minimal Side Effects and Prevents Intestinal Tumors in Mice. *Cancer Prevention Research.* **1**: 233-240

Yoon, H. S., Chen, X., Yang, V. W. (2003) Kruppel-like factor 4 mediates p53-dependent G1/S cell cycle arrest in response to DNA damage. *The Journal of Biological Chemistry.* **278**: 2101-2105

Yoon, H. S., Ghaleb, A. M., Nandan, M. O., *et al.* (2005) Kruppel-like factor 4 prevents centrosome amplification following gamma-irradiation-induced DNA damage. *Oncogene*. **24**: 4017-4025

Yoon, H. S., Yang, V. W. (2004) Requirement of Kruppel-like factor 4 in preventing entry into mitosis following DNA damage. *The Journal of Biological Chemistry*. **279**: 5035-5041

Yoshida, M., Horinouchi, S. (1999) Trichostatin and leptomycin. Inhibition of histone deacetylation and signal-dependent nuclear export. *Annals of the New York Academy of Science*. **886**: 23-36

Yoshida, M., Kijima, M., Akita, M., *et al.* (1990) Potent and specific inhibition of mammalian histone deacetylase both in vivo and in vitro by trichostatin A. *The Journal of Biological Chemistry*. **265**: 17174-17179

Yu, F., Li, J., Chen, H., *et al.* (2011) Kruppel-like factor 4 (KLF4) is required for maintenance of breast cancer stem cells and for cell migration and invasion. *Oncogene*. **30**: 2161-2172

Yu, J., Vodyanik, M. A., Smuga-Otto, K., *et al.* (2007) Induced pluripotent stem cell lines derived from human somatic cells. *Science*. **318**: 1917-1920

Zhang, H., Wang, Z. Z. (2008) Mechanisms that mediate stem cell self-renewal and differentiation. *Journal of Cellular Biochemistry*. **103**: 709-718

Zhang, W., Chen, X., Kato, Y., *et al.* (2006) Novel cross talk of Kruppel-like factor 4 and β-catenin regulates normal intestinal homeostasis and tumor repression. *Molecular and Cellular Biology*. **26 (6)**: 2055-2064

Zhang, W., Geiman, D. E., Shields, J. M., *et al*. (2000) The gut enriched Kruppel-like factor (Kruppel-like factor 4) mediates the transactivating effect of p53 on the p21WAF1/Cip1 promoter. *The Journal of Biological Chemistry.* **275**: 18391-18398

Zhang, W., Lui, H. T. (2002) MAPK signal pathways in the regulation of cell proliferation in mammalian cells. *Cell Research*. **12 (1)**: 9-18

Zhang, Z. G., Harstrick, A., Rustum, Y. M. (1992) Modulation of fluoropyrimidines: role of dose and schedule of leucovorin administration. *Seminars in Oncology*. **19 (Suppl) 3**: 10-5

Zhang, Z. G., Yamashita, H., Toyama, T., *et al.* (2005) Quantitation of HDAC1 mRNA expression in invasive carcinoma of the breast. *Breast Cancer Research and Treatment*. **94:** 11-16

Zhao, W., Hisamuddin, I. M., Nandan, M. O., *et al.* (2004) Identification of Kruppel-like factor 4 as a potential tumour suppressor gene on colorectal cancer. *Oncogene*. **24**: 395-402

Zheng, C., Hayes, J. J. (2003) Structures and interactions of the core histone tail domains. *Biopolymers*. **68 (4)**: 539-546

Zhou, L., Cheng, X., Connolly, B. A., *et al.* (2002). Zebularine: a novel DNA methylation inhibitor that forms a covalent complex with DNA methyltransferases. *Journal of Molecular Biology*. **321**: 591-599

Zhu, W. G., Dai, Z., Ding, H., *et al.* (2001) Increased expression of unmethylated CDKN2D by 5-aza-2'-deoxycytidine in human lung cancer cells. *Oncogene*. **20 (53)**: 7787-7796

Zhu, W. G., Lakshmanan, R. R., Beal, M. D., *et al.* (2001) DNA methyltransferase inhibition enhances apoptosis induced by histone deacetylase inhibitors. *Cancer Research*. **61 (4)**: 1327-1333

Zhu, W. G., Otterson, G. A. (2003) The interaction of histone deacetylase inhibitors and DNA methyltransferase inhibitors in the treatment of human cancer cells. *Current Medical Chemistry - Anti-Cancer Agents.* **3 (3)**: 187-199

A1 Exonic sequence with mapped primers for *KLF4*

ACTCCTCTGGCCTTCTCTTGAGGCTCCCAGTTCACGCTGCACAGTGCTGGGCACTGCCTCCT
CTCCACACCCCTAGCGCCCCCCACCCCTCAGCAGAAGGGCCCGCGAGGAACCGTGCGAGGT
CAGGCCGAGCGCCGGCACCGCCACCGGCACTGGCGCTGAGCGACGAGAGCGGACTCCTGC
GAGCGCAGAGAGGGAGGGGGAGATGGAGGGCTGGATGAGTCACGCGGATAATCGCGCTCT
TCTCCAGCGCGCAGACAGCGCGGCAAGCGCGTATGCTAGCAGGGGTGCGGACGCGTGACC
GTGCCGCCCGCTGACCCCACCAGTCTTCGCGGGCTTCGAACCCAGGGAGCCGACAATGGCG
GGCAGTTTCCCGACCAGAGAGAACGAACGTGTCTGCGGGCGCGCGGGGAGCAGAGGCGGT
GGCGGGCGGCGGCGGCACCGGGAGCCGCCGAGTGACCCTCCCCCGCCCCTCTGGCCCCC
CACCCTCCCACCCGCCCGTGGCCCGCGCCCATGGCCGCGCGCGCTCCACACAACTCACCG
GAGTCCGCGCCTTGCGCCGCCGACCAGTTCGCAGCTCCGCGCCACGGCAGCCAGTCTCACC
TGGCGGCACCGCCCGCCCACCGCCCCGGCCACAGCCCCTGCGCCCACGGCAGCACTCGAG
GCGACCGCGACAGTGGTGGGGGACGCTGCTGAGTGGAAGAGAGCGCAGCCCGGCCACCGG
ACCTACTTACTCGCCTTGCTGATTGTCTATTTTTGCGTTTACAACTTTTCTAAGAACTTTTGTAT
ACAAAGGAACTTTTTAAAAAAGACGCTTCCAAGTTATATTTAATCCAAAGAAGAAGGATCTCGG
CCAATTTGGGGTTTTGGGTTTTGGCTTCGTTTCTTCTCTTCGTTGACTTTGGGGTTCAGGTGC
CCCAGCTGCTTCGGGCTGCCGAGGACCTTCTGGGCCCCCACATTAATGAGGAGGACCGGTG
GGACGCGCCGGAACGACGGCCGAAAGCCGCCCCTGACTCTCCTGTCTCCGCTCCCTGCCTT
GCTCGCAGGCAGCCACCTGGCGAGTCTGACATGGCTGTCAGCGACGCGCTGCTCCCATCTT
TCTCCACGTTCGCGTCTGGCCCGGCGGGAAGGGAGAAGACACTGCGTCAAGCAGGTGCCCC
GAATAACTTCTTCGACCCGGGAGTGGGCCGAGATTGCAGCGCTGGCGCCCTGGGTTCCCGG
GTGCTTCCTGCCTGACCAGTCCCCATGTCTGGGCGGTGCAGTCGCGCGTGGCCCGCCAGCA
CGTCAGTATGTCGGGTGGCAACAGGGGACCACCACTGACAGGTCTCTCCCGCCCTGTCCCC
GCAGCGCTGGCGGGAGGAGCTCTCCCACATGAAGCGACTTCCCCCAGTGCTTCCCGGCCGC
CCCTATGACCTGGCGGCGGCGACCGTGGCCACAGACCTGGAGAGCGGCGGAGCCGGTGCG
GCTTGCGGCGGTAGCAACCTGGCGCCCCTACCTCGGAGAGAGACCGAGGAGTTCAACGATC
TCCTGGACCTGGACTTTATTCTCTCCAATTCGCTGACCCATCCTCCGGAGTCAGTGGCCGCCA
CCGTGTCCTCGTCAGCGTCAGCCTCCTCTTCGTCGTCGCCGTCGAGCAGCGGCCCTGCCAG
CGCGCCCTCCACCTGCAGCTTCACCTATCCGATCCGGGCCGGGAACGACCCGGGCGTGGCG
CCGGGCGGCACGGGCGGAGGCCTCCTCTATGGCAGGGAGTCCGCTCCCCCTCCGACGGCT
CCCTTCAACCTGGCGGACATCAACGACGTGAGCCCCTCGGGCGGCTTCGTGGCCGAGCTCC
TGCGGCCAGAATTGGACCCGGTGTACATTCCGCCGCAGCAGCCGCAGCCGCCAGGTGGCG
GGCTGATGGGCAAGTTCGTGCTGAAGGCGTCGCTGAGCGCCCCTGGCAGCGAGTACGGCAG
CCCGTCGGTCATCAGCGTCAGCAAAGGCAGCCCTGACGGCAGCCACCCGGTGGTGGTGGC
GCCCTACAACGGCGGGCCGCCGCGCACGTGCCCCAAGATCAAGCAGGAGGCGGTCTCTTCG
TGCACCCACTTGGGCGCTGGACCCCCTCTCAGCAATGGCCACCGGCCGGCTGCACACGACT
TCCCCCTGGGGCGGCAGCTCCCCAGCAGGACTACCCCGACCCTGGGTCTTGAGGAAGTGCT
GAGCAGCAGGGACTGTCACCCTGCCCTGCCGCTTCCTCCCGGCTTCCATCCCCACCCGGGG

CCCAATTACCCATCCTTCCTGCCCGATCAGATGCAGCCGCAAGTCCCGCCGCTCCATTACCA
AGGTCAGTCCCGGGGATTTGTAGCTCGGGCTGGGGAGCCCTGTGTGTGCTGGCCCCACTTC
GGGACACACGGGATGATGCTCACCCCACCTTCTTCACCCCTAGAGCTCATGCCACCCGGTTC
CTGCATGCCAGAGGAGCCCAAGCCAAAGAGGGGAAGACGATCGTGGCCCCGGAAAAGGACC
GCCACCCACACTTGTGATTACGCGGGCTGCGGCAAAACCTACACAAAGAGTTCCCATCTCAA
GGCACACCTGCGAACCCACACAGGTGAGAAACCTTACCACTGTGACTGGGACGGCTGTGGAT
GGAAATTCGCCCGCTCAGATGAACTG**ACCAGGCACTACCGTAAACACA**CGGGGCACCGCCC
GTTCCAGTGCCAAAAATGCGACCG**AGCATTTTCCAGGTCGGACC**ACCTCGCCTTACACATGA
AGAGGCATTTTTAAATCCCAGACAGTGGATATGACCCACACTGCCAGAAGAGAATTCAGTATT
TTTTACTTTTCACACTGTCTTCCCGATGAGGGAAGGAGCCCAGCCAGAAAGCACTACAATCAT
GGTCAAGTTCCCAACTGAGTCATCTTGTGAGTGGATAATCAGGAAAAATGAGGAATCCAAAAG
ACAAAAATCAAAGAACAGATGGGGTCTGTGACTGGATCTTCTATCATTCCAATTCTAAATCCGA
CTTGAATATTCCTGGACTTACAAAATGCCAAGGGGGTGACTGGAAGTTGTGGATATCAGGGTA
TAAATTATATCCGTGAGTTGGGGGAGGGAAGACCAGAATTCCCTTGAATTGTGTATTGATGCA
ATATAAGCATAAAAGATCACCTTGTATTCTCTTTACCTTCTAAAAGCCATTATTATGATGTTAGA
AGAAGAGGAAGAAATTCAGGTACAGAAAACATGTTTAAATAGCCTAAATGATGGTGCTTGGTG
AGTCTTGGTTCTAAAGGTACCAAACAAGGAAGCCAAAGTTTTCAAACTGCTGCATACTTTGACA
AGGAAAATCTATATTTGTCTTCCGATCAACATTTATGACCTAAGTCAGGTAATATACCTGGTTTA
CTTCTTTAGCATTTTTATGCAGACAGTCTGTTATGCACTGTGGTTTCAGATGTGCAATAATTTGT
ACAATGGTTTATTCCCAAGTATGCCTTAAGCAGAACAAATGTGTTTTTCTATATAGTTCCTTGC
CTTAATAAATATGTAATATAAATTTAAGCAAACGTCTATTTTGTATATTTGTAAACTACAAAGTAA
AATGAACATTTTGTGGAGTTTGTATTTTGCATACTCAAGGTGAGAATTAAGTTTTAAATAAACCT
ATAATATTTTATCTGAA

Forward primer **ACCAGGCACTACCGTAAACACA**
Reverse primer **GGTCCGACCTGGAAAATGCT**

Protein sequence for KLF4

MRQPPGESDMAVSDALLPSFSTFASGPAGREKTLRQAGAPNNRWREELSHMKRLPPVLPGRPY
DLAAATVATDLESGGAGAACGGSNLAPLPRRETEEFNDLLDLDFILSNSLTHPPESVAATVSSSAS
ASSSSSPSSSGPASAPSTCSFTYPIRAGNDPGVAPGGTGGGLLYGRESAPPPTAPFNLADINDVS
PSGGFVAELLRPELDPVYIPPQQPQPPGGGLMGKFVLKASLSAPGSEYGSPSVISVSKGSPDGSH
PVVVAPYNGGPPRTCPKIKQEAVSSCTHLGAGPPLSNGHRPAAHDFPLGRQLPSRTTPTLGLEEV
LSSRDCHPALPLPPGFHPHPGPNYPSFLPDQMQPQVPPLHYQELMPPGSCMPEEPKPKRGRRS
WPRKRTATHTCDYAGCGKTYTKSSHLKAHLRTHTGEKPYHCDWDGCGWKFARSDELTRHYRKH
TGHRPFQCQKCDRAFSRSDHLALHMKRHF

A2 Exonic sequence with mapped primers for *CTNNB1*

AGCAAAGAATCACCCCACACAAAGATGGCGCGTGCAGAATTTGTGAAAGCGAAAAAGAAGAC
GAAGGAGAAGCAAAGAGGGACGGAATACTGCAGTGCTAGGGTGACATAATTTTTTGTTTAAGA
TCCAGTAAGACTCCCTGTTTTTAATACATATAAAGCAACAGACATGTATATGTCGATAAACTGA
GGGTTTGCGTCCCTATTGCCTGGTGCAAGCTACAGCAAAAAACCGGTGATATCACATCTACAA
ATCTCAATGGATTCAAAAACAATATGAAAATTTTTAGCTGACAAGAACATGTCTGCTGCCTGCA
GTCCCTGCAATAGCTCACCATGTTGCCTACTAACCAAAAGATCAAAAATTATCGATTTCATGGC
GCTGCGAGGTCTGGAAAGAAAAGCTACTTTAAAATTTGCATTGTTTAAGAAATGACTTAAAAGA
AAAGAATCATTTTTTTTTCTGAATACTTTGGAAGGTGAAAATGGCTTGTTTTAATCTTATCCATG
ATTTACTATAATTCTATTATTTTTAGCAGCTGGAGTCCAGAAATGATTTTTTCGATGAATTTAGG
ATTTTGCCGCAGTATACATCTGCAGTCCCAGAATCCTCCGAGGTACTCCTAAGGACTTGTTGA
ATTGCGGGCTTGGCGCCCGTTCTACGGAGAGTTCACAGCCTTCGTGAGTGGGGACAGAAGG
CGGCTCGGCCCGGTGATTCAGGTCGAAATTCAAGCTGAACAGCCTGCTGAGAGGCTGCGCC
GGTGGCGGCAGGATACAGCGGCTTCTGCGCGACTTATAAGAGCTCCTTGTGCGGCGCCATTT
TAAGCCTCTCGGTCTGTGGCAGCAGCGTTGGCCCGGCCCCGGGAGCGGAGAGCGAGGGGA
GGCGGAGACGGAGGAAGGTCTGAGGAGCAGCTTCAGTCCCCGCCGAGCCGCCACCGCAGG
TCGAGGACGGTCGGACTCCCGCGGCGGGAGGAGCCTGTTCCCCTGAGAGTTGGGGTTCGG
GCGCTGAGGCAGAGACGCCACCCTAAGTCCCATCAGTCCTGGGGATCGGACCAGTGGACTT
TCTCTTAAGATTTCCTCTTTCATTCTTAAGAATAGAAGTGTTATTATTTTTTTTAATGCCCTGGCT
ATGTGAGTTTGAATCGAAGCAACTTTAAACCTTAGAGCAACTAAACTCTAAGTGCAGCGGGTG
CGATGCGTCAGTAGGGTGAGCACATAAAAAATCCATGTCTTGCACCTGTATTTTAGCGTACTA
TGCAGAAAATTTTCCTGAAGTGATTGGTAAGTTTTGGCTAATTGGGAGCACTAGAATTGGGCC
CTTAATGGTTGGCAGGGTGTGGTGGAGGAGAGACAGCCCTTAGTCCAAAGGCTCAGGCCAG
AAAAAGAAAGAGGAAGGCTTTCCTTTTCCTTTCCGGAGCAGGGTTCTGCCCTAGGTCTTGCTT
GGCAGTCTATTTGATTTCTTTAGCAGTTAATGCTCAGTTTTTTGGCATATGTGGATCTGCCTCC
AGAGCAGGTACAAGGGTATTTGAAGTATACCATACAACTGTTTTGAAAATCCAGCGTGGACAA
TGGCTACTCAAGGCTACCTTTTGCTCCATTTTCTGCTCACTCCTCCTAATGGCTTGGTGAAATA
GCAAACAAGCCACCAGCAGGAATCTAGTCTGGATGACTGCTTCTGGAGCCTGGATGCAGTAC
CATTCTTCCACTGATTCATTCTAAAAATATTTCAATGGGTCATATCACAGATTCTTTTTTTTTAAA
TTAAAGTAACATTTCCAATCTACTAATGCTAATACTGTTTCGTATTTATAGCTGATTTGATGGAG
TTGGACATGGCCATGGAACCAGACAGAAAAGCGGCTGTTAGTCACTGGCAGCAACAGTCTTA
CCTGGACTCTGGAATCCATTCTGGTGCCACTACCACAGCTCCTTCTCTGAGTGGTAAAGGCAA
TCCTGAGGAAGAGGATGTGGATACCTCCCAAGTCCTGTATGAGTGGGAACAGGGATTTTCTC
AGTCCTTCACTCAAGAACAAGTAGCTGATATTGATGGACAGTATGCAATGACTCGAGCTCAGA
GGGTACGAGCTGCTATGTTCCCTGAGACATTAGATGAGGGCATGCAGATCCCATCTACACAG
TTTGATGCTGCTCATCCCACTAATGTCCAGCGTTTGGCTGAACCATCACAGATGCTGAAACAT
GCAGTTGTAAACTTGATTAACTATCAAGATGATGCAGAACTTGCCACACGTGCAATCCCTGAA
CTGACAAAACTGCTAAATGACGAGGACCAGGTGGTGGTTAATAAGGCTGCAGTTATGGTCCAT
CAGCTTTCTAAAAAGGAAGCTTCCAGACACGCTATCATGCGTTCTCCTCAGATGGTGTCTGCT

ATTGTACGTACCATGCAGAATACAAATGATGTAGAAACAGCTCGTTGTACC**GCTGGGACCTTG**
CATAACCTTTCCCATCATCGTGAGGGCTTACTGGCCATCTTTAAGTCTGGAGG**CATTCCTGCC**
CTGGTGAAAATGCTTGGTTCACCAGTGGATTCTGTGTTGTTTTATGCCATTACAACTCTCCAC
AACCTTTTATTACATCAAGAAGGAGCTAAAATGGCAGTGCGTTTAGCTGGTGGGCTGCAGAAA
ATGGTTGCCTTGCTCAACAAAACAAATGTTAAATTCTTGGCTATTACGACAGACTGCCTTCAAA
TTTTAGCTTATGGCAACCAAGAAAGCAAGCTCATCATACTGGCTAGTGGTGGACCCCAAGCTT
TAGTAAATATAATGAGGACCTATACTTACGAAAAACTACTGTGGACCACAAGCAGAGTGCTGA
AGGTGCTATCTGTCTGCTCTAGTAATAAGCCGGCTATTGTAGAAGCTGGTGGAATGCAAGCTT
TAGGACTTCACCTGACAGATCCAAGTCAACGTCTTGTTCAGAACTGTCTTTGGACTCTCAGGA
ATCTTTCAGATGCTGCAACTAAACAGGAAGGGATGGAAGGTCTCCTTGGGACTCTTGTTCAGC
TTCTGGGTTCAGATGATATAAATGTGGTCACCTGTGCAGCTGGAATTCTTTCTAACCTCACTTG
CAATAATTATAAGAACAAGATGATGGTCTGCCAAGTGGGTGGTATAGAGGCTCTTGTGCGTAC
TGTCCTTCGGGCTGGTGACAGGGAAGACATCACTGAGCCTGCCATCTGTGCTCTTCGTCATC
TGACCAGCCGACACCAAGAAGCAGAGATGGCCCAGAATGCAGTTCGCCTTCACTATGGACTA
CCAGTTGTGGTTAAGCTCTTACACCCACCATCCCACTGGCCTCTGATAAAGGCTACTGTTGGA
TTGATTCGAAATCTTGCCCTTTGTCCCGCAAATCATGCACCTTTGCGTGAGCAGGGTGCCATT
CCACGACTAGTTCAGTTGCTTGTTCGTGCACATCAGGATACCCAGCGCCGTACGTCCATGGG
TGGGACACAGCAGCAATTTGTGCTTCCTGAACTAATTGCAAGTTACGGGGAACTTCGGGTATA
TAATGTAAATAATTACAGTCTAATAATTGTTCCTCAAACTTTACAGAGGAGAATGCCCTGTTTGT
TAACCATGTTTCTTTTGGCAGGAGGGGGTCCGCATGGAAGAAATAGTTGAAGGTTGTACCGG
AGCCCTTCACATCCTAGCTCGGGATGTTCACAACCGAATTGTTATCAGAGGACTAAATACCAT
TCCATTGTTTGTGCAGCTGCTTTATTCTCCCATTGAAAACATCCAAAGAGTAGCTGCAGGGGT
CCTCTGTGAACTTGCTCAGGACAAGGAAGCTGCAGAAGCTATTGAAGCTGAGGGAGCCACAG
CTCCTCTGACAGAGTTACTTCACTCTAGGAATGAAGGTGTGGGTAAGTAAAAAGGAACCAAAG
CCTTTAGCAGATGTGTACATTGAAGTCTCAGTTTTTCCTCAAGGGCCTTTTTCTCCTTGTCTCT
TAGCGACATATGCAGCTGCTGTTTTGTTCCGAATGTCTGAGGACAAGCCACAAGATTACAAGA
AACGGCTTTCAGTTGAGCTGACCAGCTCTCTCTTCAGAACAGAGCCAATGGCTTGGAATGAG
GTAGGGAAATGTGAGCAGTTATTTATCTGGTAGTTTCCTAGAGCAGGTATGGCAGCTTGTTCT
TTCCTCTCAAAACACTTAGTACACATTCATTTGCATTGATGTTTCCCTGGCTTGAGTATTTCTTC
TTTATGCTGTCTAGCAACTGCTCTGAGGAAGAACTATAATACAAGCTTTAAAGAGTCTGTTCAG
AATCATTACAAATAAGTTGTGTTATTTAAAATTATAATTCATAAGGGAGAAAGATGAAAAATGTT
ACCAGATTAAAGAAGATTTTTCAAAAGGATGTAAGGAAAGAGGCAGTGTTAAACACTGTTAAG
AGGACAGTTTATCAGTATTTTTTACTAAACTTTAATAAAACTTTTCTATTTGAATTTCTGCTATGA
ATTTTTCTTCAGCATTTGTCCTCAGTACAGGTGGTTCCTTGAAACATTGTTTCTAATAAAACTAG
AACATCCTGATATTTTATCCATTCTATAGAGATCATTGATGGTACACAGACATACAGTGGATTA
TGTTTGTTGAGTGAATGGAAAGAGAGATTGTTAGGTTTACAACGATGCAGCTCTTGAGACCGG
AGTTTAAGATCAGCCTGGGCAACATAGTGAAACCCCATCTTTAGCTGGGCATGGAGATGGAT
GCCTATAGTCCTAGCTACTGGGGAGACGGGGGCAGGAGGATTGCTTGAACCCAGGAGTTAA
CAGACTGCACTCAGTGACAGAGCCAGACTCCAACACAAAAAAAAAAAAAAAAAAAACTGCT

GATCTTGGACTTGATATTGGTGCCCAGGGAGAACCCCTTGGATATCGCCAGGATGGATCCTA
GCTATCGTTCTTTTCACTCTGGTGGATATGGCCAGGATGCCTTGGGTATGGACCCCATGATGG
AACATGAGATGGGTGGCCACCACCCTGGTGCTGACTATCCAGTTGATGGGCTGCCAGATCTG
GGGCATGCCCAGGACCTCATGGATGGGCTGCCTCCAGGTGACAGCAATCAGCTGGCCTGGT
TTGATACTGACCTGTAAATCATCCTTTAGGTAAGAAGTTTTAAAAAGCCAGTTTGGGTAAAATA
CTTTTACTCTGCCTACAGAACTTCAGAAAGACTTGGTTGGTAGGGTGGGAGTGGTTTAGGCTA
TTTGTAAATCTGCCACAAAAACAGGTATATACTTTGAAAGGAGATGTCTTGGAACATTGGAATG
TTCTCAGATTTCTGGTTGTTATGTGATCATGTGTGGAAGTTATTAACTTTAATGTTTTTTGCCAC
AGCTTTTGCAACTTAATACTCAAATGAGTAACATTTGCTGTTTTAAACATTAATAGCAGCCTTTC
TCTCTTTATACAGCTGTATTGTCTGAACTTGCATTGTGATTGGCCTGTAGAGTTGCTGAGAGG
GCTCGAGGGGTGGGCTGGTATCTCAGAAAGTGCCTGACACACTAACCAAGCTGAGTTTCCTA
TGGGAACAATTGAAGTAAACTTTTTGTTCTGGTCCTTTTTGGTCGAGGAGTAACAATACAAATG
GATTTTGGGAGTGACTCAAGAAGTGAAGAATGCACAAGAATGGATCACAAGATGGAATTTATC
AAACCCTAGCCTTGCTTGTTAAATTTTTTTTTTTTTTTTTTTAAGAATATCTGTAATGGTACTGAC
TTTGCTTGCTTTGAAGTAGCTCTTTTTTTTTTTTTTTTTTTTTTTTGCAGTAACTGTTTTTTAAGT
CTCTCGTAGTGTTAAGTTATAGTGAATACTGCTACAGCAATTTCTAATTTTTAAGAATTGAGTAA
TGGTGTAGAACACTAATTCATAATCACTCTAATTAATTGTAATCTGAATAAAGTGTAACAATTGT
GTAGCCTTTTTGTATAAAATAGACAAATAGAAAATGGTCCAATTAGTTTCCTTTTTAATATGCTT
AAAATAAGCAGGTGGATCTATTTCATGTTTTTGATCAAAAACTATTTGGGATATGTATGGGTAG
GGTAAATCAGTAAGAGGTGTTATTTGGAACCTTGTTTTGGACAGTTTACCAGTTGCCTTTTATC
CCAAAGTTGTTGTAACCTGCTGTGATACGATGCTTCAAGAGAAAATGCGGTTATAAAAAATGG
TTCAGAATTAAACTTTTAATTCATTCGATTGGAAGTAGGAGTCAAAGTGACCCTTGTCTACTGT
GATGCTGAATTCATGACTAAGAGACTATTGGTGAACTTATCCTGGCTGTGATTACAGACGTCA
AGAGGGAGTATTCCAGCGACACTAAGAAAATAATGCAAGAGAACGCCAGCGAAGAGTGCCCA
GGCAACACTGACAGACTAGAAAAAAAATATCAGGAGATGAAGCTGACACAGTGAGAGCAGCC
CAGGTGCTTCTTGGTGCTTGTTATTACAGACACACACTTCACACAGGGGAGGATTATTTTAATT
CTGTGGCCTTCAGATCTCATAAATACAAGTAAAAACAAGCAGGTAACTATGATAACTTTACTTC
AGAGAGTTTAAATTTCAAAAATAAACCTATCCATCC

Forward primer **GCTGGGACCTTGCATAACCTT**

Reverse primer **ATTTTCACCAGGGCAGGAATG**

Protein sequence for CTNNB1

MATQADLMELDMAMEPDRKAAVSHWQQQSYLDSGIHSGATTTAPSLSGKGNPEEEDVDTSQVL
YEWEQGFSQSFTQEQVADIDGQYAMTRAQRVRAAMFPETLDEGMQIPSTQFDAAHPTNVQRLA
EPSQMLKHAVVNLINYQDDAELATRAIPELTKLLNDEDQVVVNKAAVMVHQLSKKEASRHAIMRSP
QMVSAIVRTMQNTNDVETARCTAGTLHNLSHHREGLLAIFKSGGIPALVKMLGSPVDSVLFYAITTL
HNLLLHQEGAKMAVRLAGGLQKMVALLNKTNVKFLAITTDCLQILAYGNQESKLIILASGGPQALVN
IMRTYTYEKLLWTTSRVLKVLSVCSSNKPAIVEAGGMQALGLHLTDPSQRLVQNCLWTLRNLSDA

ATKQEGMEGLLGTLVQLLGSDDINVVTCAAGILSNLTCNNYKNKMMVCQVGGIEALVRTVLRAGD
REDITEPAICALRHLTSRHQEAEMAQNAVRLHYGLPVVVKLLHPPSHWPLIKATVGLIRNLALCPAN
HAPLREQGAIPRLVQLVRAHQDTQRRTSMGGTQQQFVEGVRMEEIVEGCTGALHILARDVHNRIV
IRGLNTIPLFVQLLYSPIENIQRVAAGVLCELAQDKEAAEAIEAEGATAPLTELLHSRNEGVATYAAA
VLFRMSEDKPQDYKKRLSVELTSSLFRTEPMAWNETADLGLDIGAQGEPLGYRQDDPSYRSFHS
GGYGQDALGMDPMMEHEMGGHHPGADYPVDGLPDLGHAQDLMDGLPPGDSNQLAWFDTDL

A3 List of reagents and ingredients

10%$^{v}/_{v}$ FBS/DMEM:F12

5mL fetal bovine serum (Invitrogen)
45mL DMEM:F12 (Invitrogen)
100µL 10 000U penicillin/mL 10 000ug streptomycin/mL (Lonza BioWhittaker ®)

2.5%$^{v}/_{v}$ FBS/DMEM:F12

20mL fetal bovine serum (GIBCO Invitrogen)
30mL DMEM:F12 (Lonza BioWhittaker ®)
100µL 10 000U penicillin/mL 10 000ug streptomycin/mL (Lonza BioWhittaker ®)

50:50 Cyroprotective medium

5mL Cyroprotective medium (Lonza)
5mL DMEM:F12

10X TBE

108g Tris (Saarchem)
55g Boric acid (Sigma)
9.3g EDTA (Merck)
Prepared to 1L pH 8.3

1X TBE

100mL 10X TBE
900mL dH_2O
Prepared to 1L

1.5%$^{w}/_{v}$ Agarose gel

1.5g Agarose powder (Bio-Rad)
100mL 1X TBE
6.5µL Ethidium bromide (Promega)

200mL PBS
1X PBS tablet (Sigma-Aldrich)
200mL dH_2O

3%$^{v}/_{v}$ Formaldehyde

16.5mL PBS (Sigma-Aldrich)
1.5mL Formaldehyde (Univar)

0.5%$^{v}/_{v}$ BSA/PBS

0.5g bovine serum albumin (Sigma-Aldrich)
100mL PBS (Sigma-Aldrich)

0.25%$^{v}/_{v}$ BSA/PBS/Triton X

50mL 0.5%$^{v}/_{v}$ BSA/PBS (Sigma-Aldrich)
125µL Triton X (Lonza)

Primary antibody 1:100

1µL primary antibody (KLF4 and β-catenin)
99µL 0.5%$^{v}/_{v}$ BSA/PBS

GKLF (H-180)
Rabbit polyclonal IgG
200ug/mL
Santa Cruz
Cat. no. sc-20691

Purified mouse anti B-Catenin
MAb 50ug, 0.2mL, 250ug/mL
BD Transduction laboratories
Cat. no. 610153

Secondary antibody 1:200

1µL secondary antibody (Santa-Cruz)
199µL 0.5%$^{v}/_{v}$ BSA/PBS

Alexa Fluor® 568 conjugated donkey anti rabbit (KLF4)
0.5mL
Life Technologies
A10042

Alexa Fluor® 568 conjugated donkey anti mouse (B-catenin)
0.5mL
Life Technologies
A10037

Alexa Fluor® 488 Phalloidin 1:20

5µL Alexa Fluor® Phalloidin (Lonza)
95µL 0.5%$^{v}/_{v}$ BSA/PBS

DAPI 1:10 000

1µL DAPI (Boehringer Mannheim)
9 999µL/~10mL PBS

Microscope and software information

Olympus IX71- inverted microscope with epifluorescence
Software: analySIS FIVE, Olympus Soft Imaging Systems, Germany

Zeiss Laser Scanning Microscope, LSM 780, ZEN Software (2011)

A4 Drug information

Valproic acid (P4543: Sigma-aldrich)

Empirical formula: $C_8H_{15}NaO_2$
Molecular weight: 166.19
Solubility: H_2O – 50mg/mL

Zebularine (Z4775: Sigma-aldrich)

Empirical formula: $C_9H_{12}N_2O_5$
Molecular weight: 228.20
Solubility: DMSO – 16mg/mL

A5 The $2^{-\Delta\Delta Ct}$ method

The $2^{-\Delta\Delta Ct}$ method was used to analyse relative gene expression in this study (Livak and Schmittgen, 2001). The C_t of the target gene was first normalised to that of the reference gene (in this case β–actin) for both test and calibrator samples following Equations 3.1 and 3.2:

$$\Delta C_{t(test)} = C_{t(test,target)} - C_{(ref,test)} \quad \text{[Equation A5.1]}$$

$$\Delta C_{t(calibrator)} = C_{t(test,calibrator)} - C_{(ref,calibrator)} \quad \text{[Equation A5.2]}$$

The C_T of the test sample was then normalised to the C_T of the calibrator as seen below:

$$\Delta\Delta C_{t(calibrator)} = \Delta C_{t(test)} - \Delta C_{(calibrator)} \quad \text{[Equation A5.3]}$$

As a result, the ratio of the target gene in the test sample to the calibrator sample is found, which is normalised to the reference gene. All treated sample results are relative to the untreated samples. The expression ratio can be calculated as in Equation 3.4:

$$2^{-\Delta\Delta C_t} = Normalised\ \exp ression\ ratio \quad \text{[Equation A5.4]}$$

A6 Microscopy control images

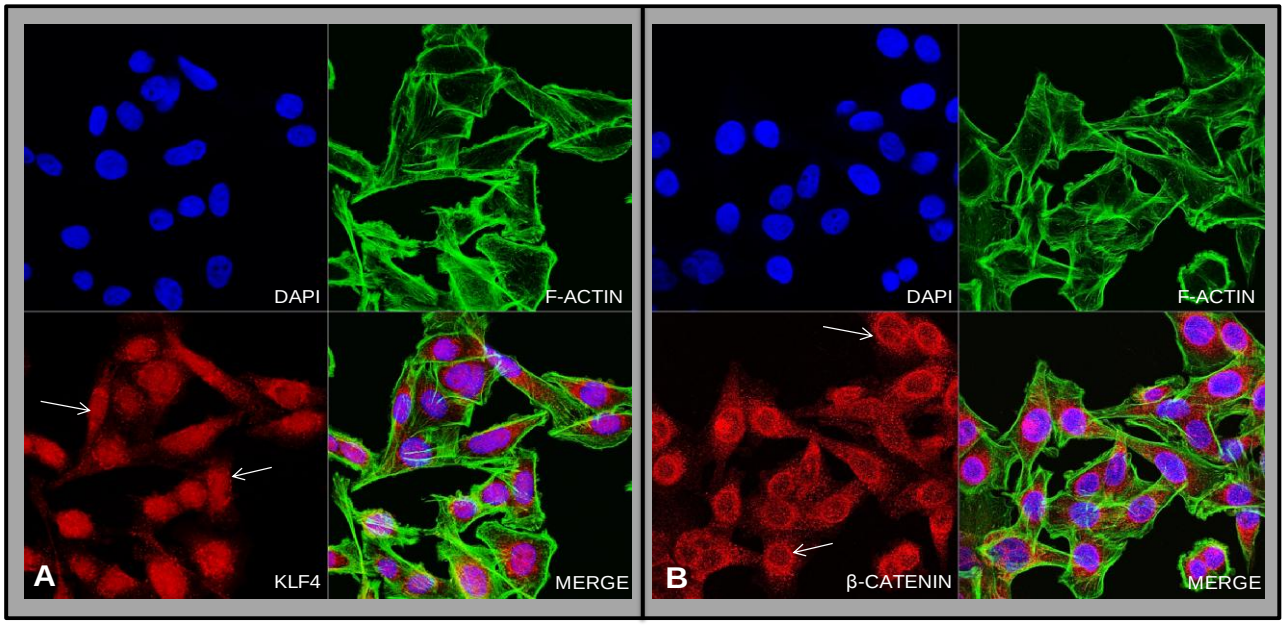


Figure A6.1 Microscopy images of untreated SW480 cells representing protein localisation for [A] KLF4 (63x) and [B] β-catenin (63x). Nuclei= blue, actin filaments= green, protein= red, protein co-localisation= pink. [A] KLF4 protein is highly condensed within nuclei, as indicated by arrows. [B] β-catenin is localised at the nuclear periphery, as revealed by the arrows.

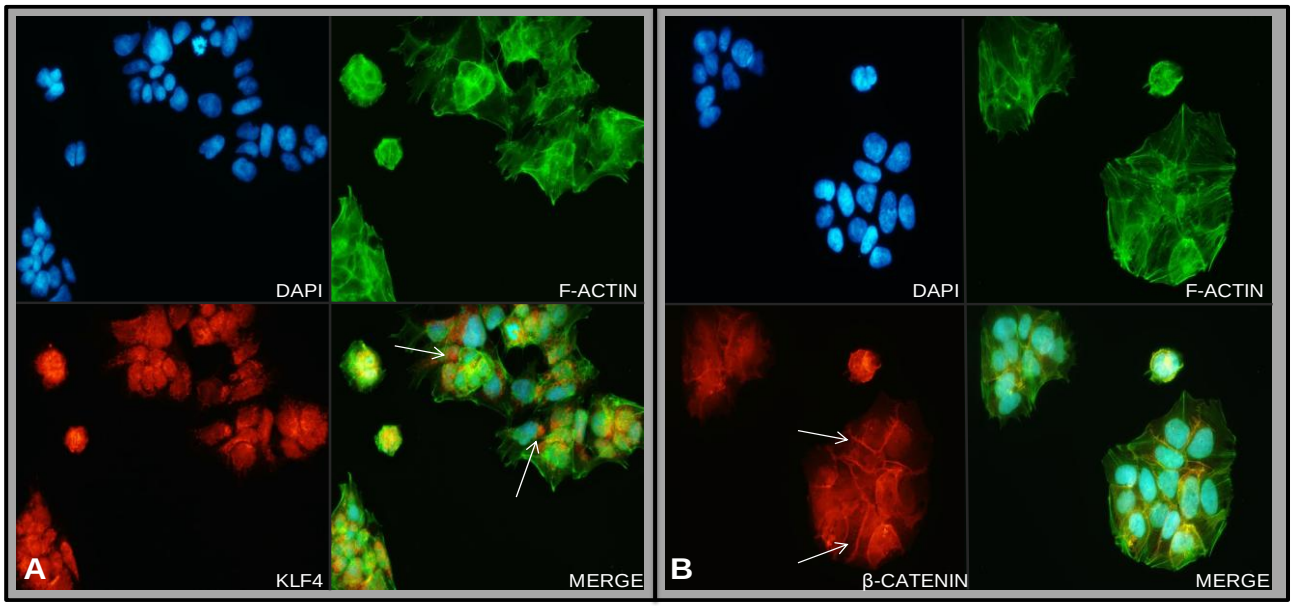


Figure A6.2 Microscopy images of untreated DLD-1 cells representing protein localisation for [A] KLF4 (60x) and [B] β-catenin (60x). Nuclei= blue, actin filaments= green, protein= red, protein localised in nuclei= pink. [A] KLF4 protein is localised within Golgi bodies or ER at the nuclear periphery, as denoted by arrows. [B] β-catenin is found at high intensity at the cell membrane, as indicated by the arrows.

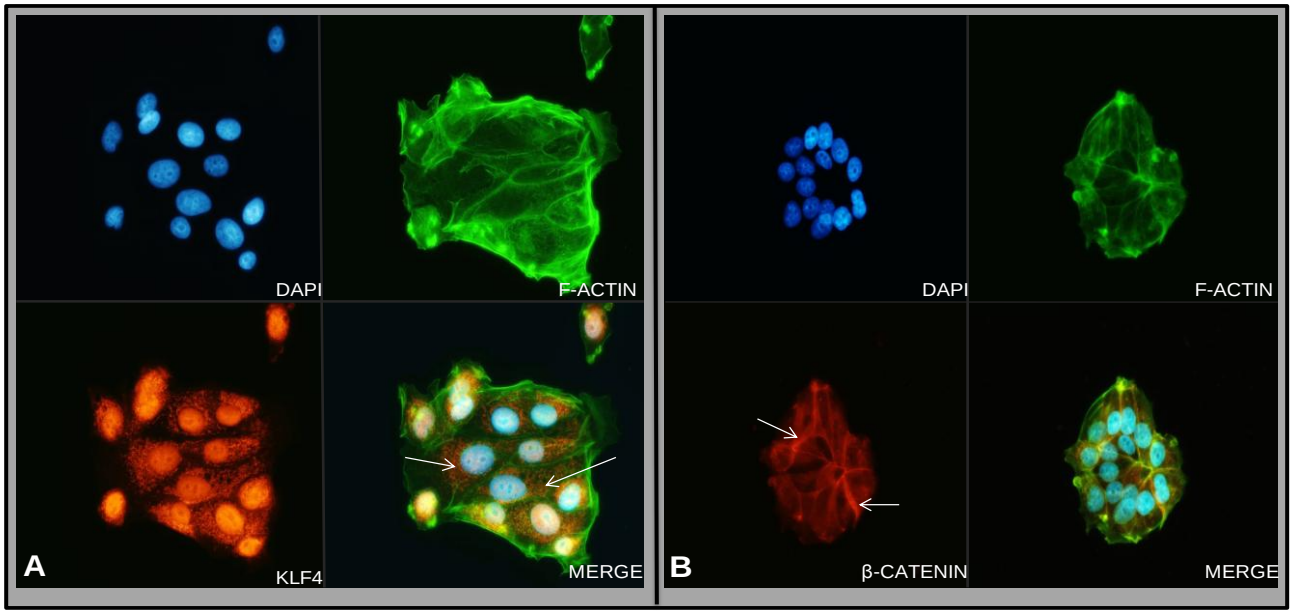


Figure A6.3 Microscopy images of untreated MCF-7 cells representing protein localisation for [A] KLF4 (63x) and [B] β-catenin (63x). Nuclei= blue, actin filaments= green, protein= red, protein localised in nuclei= pink. [A] KLF4 protein is intensely localised within the nucleus, as well as throughout the cytoplasm, as indicated by arrows. [B] β-catenin is found at high levels at the cell membrane, as denoted by the arrows.

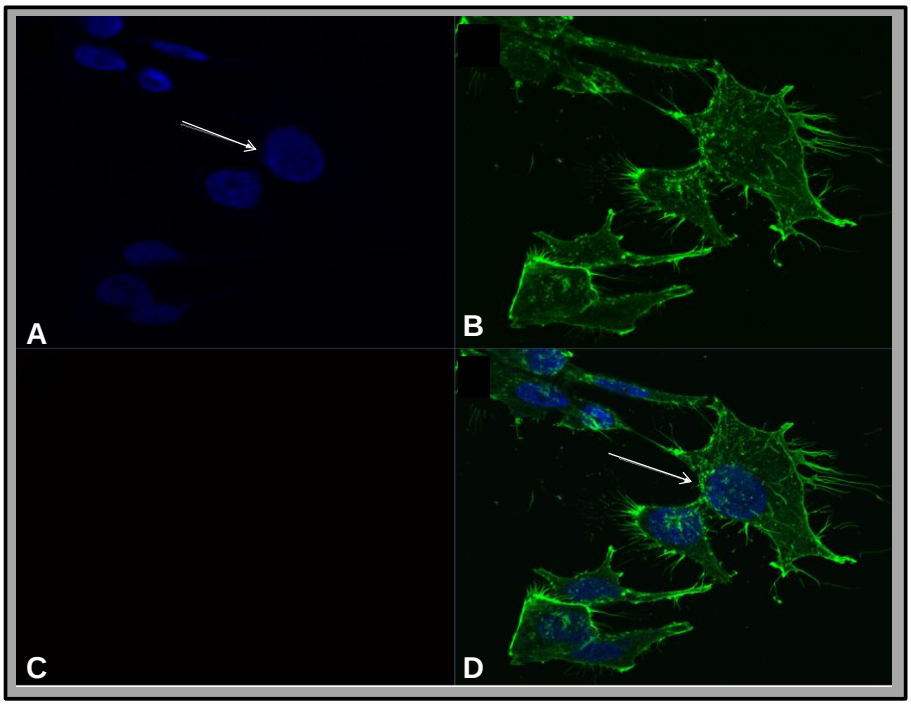


Figure A6.4 Fluorescent images depicting negative control DLD-1 cells in which the secondary antibody is omitted. [A] Represents the blue channel (DAPI), [B] represents the green channel (Phalloidin), [C] represents the red channel (Alexa Fluor® 568) and [D] is the composite image of the three channels. The blue fluorescent DAPI stain shows the presence of the nuclei. The Alexa Fluor® 488 Phalloidin (green) conjugate stains the F-actin filaments. The lack of red fluorescence (Alexa Fluor® 568) (C and D) shows the specificity of the primary antibody to β-catenin; and similarly, primary antibody to KLF4 also detected with a secondary antibody conjugated to Alexa Fluor® 568 was specific. The white arrow (A, D) indicates a nucleus present in one of the cells.

A7 Methylator results for *KLF4* (Red indicates methylated cytosines)

1	actcctctgg	ccttctcttg	aggctcccag	ttcacgctgc	acagtgctgg	gcactgcctc	ctctccacac	ccctagcgcc	ccccaccccc	cagcagaagg	100
101	gcccgcgagg	aaccgtgcga	ggtcaggccg	agcgccggca	ccgccaccgg	cactggcgct	gagcgacgag	agcggactcc	tgcgagcgca	gagagggagg	200
201	gggagatgga	gggctggatg	agtcacgcgg	ataatcgcgc	tcttctccag	cgcgcagaca	gcgcggcaag	cgcgtatgct	agcaggggtg	cggacgcgtg	300
301	accgtgccgc	ccgctgaccc	caccagtctt	cgcgggcttc	gaacccaggg	agccgacaat	ggcgggcagt	ttcccgacca	gagagaacga	acgtgtctgc	400
401	gggcgcgcgg	ggagcagagg	cggtggcggg	cggcggcggc	accgggagcc	gccgagtgac	cctccccgc	ccctctggcc	ccccaccctc	ccaccgccc	500
501	gtggcccgcg	cccatggccg	cgcgcgctcc	acacaactca	ccggagtccg	cgccttgcgc	cgccgaccag	ttcgcagctc	cgcgccacgg	cagccagtct	600
601	cacctggcgg	caccgccccgc	ccaccgcccc	ggccacagcc	cctgcgccca	cggcagcact	cgaggcgacc	gcgacagtgg	tgggggacgc	tgctgagtgg	700
701	aagagagcgc	agcccggcca	ccggacctac	ttactcgcct	tgctgattgt	ctatttttgc	gtttacaact	tttctaagaa	cttttgtata	caaaggaact	800
801	ttttaaaaaa	gacgcttcca	agttatattt	aatccaaaga	agaaggatct	cggccaattt	ggggttttgg	gttttggctt	cgtttcttct	cttcgttgac	900
901	tttggggttc	aggtgcccca	gctgcttcgg	gctgccgagg	accttctggg	cccccacatt	aatgaggagg	acggtggga	cgcgccggaa	cgacggccga	1000
1001	aagccgcccc	tgactctcct	gtctccgctc	cctgccttgc	tcgcaggcag	ccacctggcg	agtctgacat	ggctgtcagc	gacgcgctgc	tcccatcttt	1100
1101	ctccacgttc	gcgtctggcc	cggcgggaag	ggagaagaca	ctgcgtcaag	caggtgcccc	gaataacttc	ttcgaccggg	gagtgggcgg	agattgcagc	1200
1201	gctggcgccc	tgggttccgg	ggtgcttcct	gcctgaccag	tccccatgtc	tgggcggtgc	agtcgcgcgt	ggcccgccag	cacgtcagta	tgtcgggtgg	1300
1301	caacagggga	ccaccactga	caggtctctc	ccgccctgtc	cccgcagcgc	tggcgggagg	agctctccca	catgaagcga	cttcccccag	tgcttccggg	1400
1401	cgcgcccctat	gacctggcgg	cggcgaccgt	ggccacagac	ctggagagcg	gcggagccgg	tgcggcttgc	ggcggtagca	acctggcgcc	cctacctcgg	1500
1501	agagagaccg	aggagttcaa	cgatctcctg	gacctggact	ttattctctc	caatttcgctg	acccatcctc	cggagtcagt	ggccgccacc	gtgtcctcgt	1600
1601	cagcgtcagc	ctcctcttcg	tcgtcgccgt	cgagcagcgg	ccctgccagc	gcgccctcca	cctgcagctt	cacctatccg	atccgggccg	ggaacgaccc	1700
1701	gggcgtggcg	ccgggcggca	cgggcggagg	cctcctctat	ggcagggagt	ccgctccccc	tccgacggct	cccttcaacc	tggcggacat	caacgacgtg	1800
1801	agcccctcgg	gcggcttcgt	ggccgagctc	ctgcggccag	aattggaccc	ggtgtacatt	ccgccgcagc	agccgcagcc	gccaggtggc	gggctgatgg	1900
1901	gcaagttcgt	gctgaaggcg	tcgctgagcg	cccctggcag	cgagtacggc	agcccgtcgg	tcatcagcgt	cagcaaaggc	agccctgacg	gcagccaccc	2000
2001	ggtggtggtg	gcgccctaca	acggcgggcc	gccgcgcacg	tgccccaaga	tcaagcagga	ggcggtctct	tcgtgcaccc	acttgggcgc	tggacccct	2100
2101	ctcagcaatg	gccaccggcc	ggctgcacac	gacttccccc	tgggggcggca	gctccccagc	aggactaccc	cgaccctggg	tcttgaggaa	gtgctgagca	2200
2201	gcagggactg	tcaccctgcc	ctgccgcttc	ctcccggctt	ccatccccac	cggggcccca	attacccatc	cttcctgccc	gatcagatgc	agccgcaagt	2300
2301	ccgccgctc	cattaccaag	gtcagtcccg	gggatttgta	gctcgggctg	gggagccctg	tgtgtgctgg	ccccacttcg	ggacacacgg	gatgatgctc	2400
2401	accccacctt	cttcacccct	agagctcatg	ccaccggttt	cctgcatgcc	agaggagccc	aagccaaaga	ggggaagacg	atcgtggccc	cggaaaagga	2500
2501	cgccaccca	cacttgtgat	tacgcgggct	gcggcaaaac	ctacacaaag	agttcccatc	tcaaggcaca	cctgcgaacc	cacacaggtg	agaaacctta	2600
2601	ccactgtgac	tgggacggct	gtggatggaa	attcgcccgc	tcagatgaac	tgaccaggca	ctaccgtaaa	cacacggggc	accgccgtt	ccagtgccaa	2700
2701	aaatgcgacc	gagcattttc	caggtcggac	cacctcgcct	tacacatgaa	gaggcatttt	taaatcccag	acagtggata	tgacccacac	tgccagaaga	2800
2801	gaattcagta	ttttttactt	ttcacactgt	cttccgatg	agggaaggag	cccagccaga	aagcactaca	atcatggtca	agttcccaac	tgagtcatct	2900
2901	tgtgagtgga	taatcaggaa	aaatgaggaa	tccaaaagac	aaaaatcaaa	gaacagatgg	ggtctgtgac	tggatcttct	atcattccaa	ttctaaatcc	3000
3001	gacttgaata	ttcctggact	tacaaaatgc	caaggggtg	actggaagtt	gtggatatca	gggtataaat	tatatccgtg	agttgggga	gggaagacca	3100
3101	gaattccctt	gaattgtgta	ttgatgcaat	ataagcataa	aagatcacct	tgtattctct	ttaccttcta	aaagccatta	ttatgatgtt	agaagaagag	3200
3201	gaagaaattc	aggtacagaa	aacatgttta	aatagcctaa	atgatggtgc	ttggtgagtc	ttggttctaa	aggtaccaaa	caaggaagcc	aaagttttca	3300
3301	aactgctgca	tactttgaca	aggaaaatct	atatttgtct	tccgatcaac	atttatgacc	taagtcaggt	aatatacctg	gtttacttct	ttagcatttt	3400
3401	tatgcagaca	gtctgttatg	cactgtggtt	tcagatgtgc	aataatttgt	acaatggttt	attcccaagt	atgccttaag	cagaacaaat	gtgtttttct	3500

3501 atatagttcc ttgccttaat aaatatgtaa tataaattta agcaaa**c**gtc tattttgtat atttgtaaac tacaaagtaa aatgaacatt ttgtggagtt **3600**

3601 tgtattttgc atactcaagg tgagaattaa gttttaaata aacctataat attttatctg aa **3662**

A8 Methylator results for *CTNNB1* (Red indicates methylated cytosines)

1	agcaaagaat	caccccacac	aaagatggcg	cgtgcagaat	ttgtgaaagc	gaaaaagaag	acgaaggaga	agcaaagagg	gacggaatac	tgcagtgcta	100
101	gggtgacata	atttttttgtt	taagatccag	taagactccc	tgtttttaat	acatataaag	caacagacat	gtatatgtcg	ataaactgag	ggtttgcgtc	200
201	cctattgcct	ggtgcaagct	acagcaaaaa	acggtgata	tcacatctac	aaatctcaat	ggattcaaaa	acaatatgaa	aatttttagc	tgacaagaac	300
301	atgtctgctg	cctgcagtcc	ctgcaatagc	tcaccatgtt	gcctactaac	caaaagatca	aaaattatcg	atttcatggc	gctgcgaggt	ctggaaagaa	400
401	aagctacttt	aaaatttgca	ttgtttaaga	aatgacttaa	aagaaaagaa	tcatttttt	ttctgaatac	tttggaaggt	gaaaatggct	tgttttaatc	500
501	ttatccatga	tttactataa	ttctattatt	tttagcagct	ggagtccaga	aatgattttt	tcgatgaatt	taggattttg	ccgcagtata	catctgcagt	600
601	cccagaatcc	tccgaggtac	tcctaaggac	ttgttgaatt	gcgggcttgg	cgcccgttct	acggagagtt	cacagccttc	gtgagtgggg	acagaaggcg	700
701	gctcggcccg	gtgattcagg	tcgaaattca	agctgaacag	cctgctgaga	ggctgcgccg	gtggcggcag	gatacagcgg	cttctgcgcg	acttataaga	800
801	gctccttgtg	cggcgccatt	ttaagcctct	cggtctgtgg	cagcagcgtt	ggcccggccc	cgggagcgga	gagcgagggg	aggcggagac	ggaggaaggt	900
901	ctgaggagca	gcttcagtcc	ccgccgagcc	gccaccgcag	gtcgaggacg	gtcggactcc	cgcggcggga	ggagcctgtt	cccctgagag	ttggggttcg	1000
1001	ggcgctgagg	cagagacgcc	accctaagtc	ccatcagtcc	tggggatcgg	accagtggac	tttctcttaa	gatttcctct	ttcattctta	agaatagaag	1100
1101	tgttattatt	ttttttaatg	ccctggctat	gtgagtttga	atcgaagcaa	ctttaaacct	tagagcaact	aaactctaag	tgcagcgggt	gcgatgcgtc	1200
1201	agtagggtga	gcacataaaa	aatccatgtc	ttgcacctgt	attttagcgt	actatgcaga	aaattttcct	gaagtgattg	gtaagttttg	gctaattggg	1300
1301	agcactagaa	ttgggcccttt	aatggttggc	agggtgtggt	ggaggagaga	cagcccttag	tccaaaggct	caggccagaa	aaagaaagag	gaaggctttc	1400
1401	cttttccttt	ccggagcagg	gttctgccct	aggtcttgct	tggcagtcta	tttgatttct	ttagcagtta	atgctcagtt	ttttggcata	tgtggatctg	1500
1501	cctccagagc	aggtacaagg	gtatttgaag	tataccatac	aactgttttg	aaaatccagc	gtggacaatg	gctactcaag	gctacctttt	gctccatttt	1600
1601	ctgctcactc	ctcctaatgg	cttggtgaaa	tagcaaacaa	gccaccagca	ggaatctagt	ctggatgact	gcttctggag	cctggatgca	gtaccattct	1700
1701	tccactgatt	cattctaaaa	atatttcaat	gggtcatatc	acagattctt	tttttttaaa	ttaaagtaac	atttccaatc	tactaatgct	aatactgttt	1800
1801	cgtatttata	gctgatttga	tggagttgga	catggccatg	gaaccagaca	gaaaagcggc	tgttagtcac	tggcagcaac	agtcttacct	ggactctgga	1900
1901	atccattctg	gtgccactac	cacagctcct	tctctgagtg	gtaaaggcaa	tcctgaggaa	gaggatgtgg	atacctccca	agtcctgtat	gagtgggaac	2000
2001	agggatttttc	tcagtccttc	actcaagaac	aagtagctga	tattgatgga	cagtatgcaa	tgactcgagc	tcagagggta	cgagctgcta	tgttccctga	2100
2101	gacattagat	gagggcatgc	agatcccatc	tacacagttt	gatgctgctc	atcccactaa	tgtccagcgt	ttggctgaac	catcacagat	gctgaaacat	2200
2201	gcagttgtaa	acttgattaa	ctatcaagat	gatgcagaac	ttgccacacg	tgcaatccct	gaactgacaa	aactgctaaa	tgacgaggac	caggtggtgg	2300
2301	ttaataaggc	tgcagttatg	gtccatcagc	tttctaaaaa	ggaagcttcc	agacacgcta	tcatgcgttc	tcctcagatg	gtgtctgcta	ttgtacgtac	2400
2401	catgcagaat	acaaatgatg	tagaaacagc	tcgttgtacc	gctgggacct	tgcataacct	ttcccatcat	cgtgagggct	tactggccat	ctttaagtct	2500
2501	ggaggcattc	ctgccctggt	gaaaatgctt	ggttcaccag	tggattctgt	gttgttttat	gccattacaa	ctctccacaa	ccttttatta	catcaagaag	2600
2601	gagctaaaat	ggcagtgcgt	ttagctggtg	ggctgcagaa	aatggttgcc	ttgctcaaca	aaacaaatgt	taaattcttg	gctattacga	cagactgcct	2700
2701	tcaaatttta	gcttatggca	accaagaaag	caagctcatc	atactggcta	gtggtggacc	ccaagcttta	gtaaatataa	tgaggaccta	tacttacgaa	2800
2801	aaactactgt	ggaccacaag	cagagtgctg	aaggtgctat	ctgtctgctc	tagtaataag	ccggctattg	tagaagctgg	tggaatgcaa	gctttaggac	2900
2901	ttcacctgac	agatccaagt	caacgtcttg	ttcagaactg	tctttggact	ctcaggaatc	tttcagatgc	tgcaactaaa	caggaaggga	tggaaggtct	3000
3001	ccttgggact	cttgttcagc	ttctgggttc	agatgatata	aatgtggtca	cctgtgcagc	tggaattctt	tctaacctca	cttgcaataa	ttataagaac	3100
3101	aagatgatgg	tctgccaagt	gggtggtata	gaggctcttg	tgcgtactgt	ccttcgggct	ggtgacaggg	aagacatcac	tgagcctgcc	atctgtgctc	3200
3201	ttcgtcatct	gaccagccga	caccaagaag	cagagatggc	ccagaatgca	gttcgccttc	actatggact	accagttgtg	gttaagctct	tacacccacc	3300
3301	atcccactgg	cctctgataa	aggctactgt	tggattgatt	cgaaatcttg	ccctttgtcc	cgcaaatcat	gcacctttgc	gtgagcaggg	tgccattcca	3400
3401	cgactagttc	agttgcttgt	tcgtgcacat	caggataccc	agcgccgtac	gtccatgggt	gggacacagc	agcaatttgt	gcttcctgaa	ctaattgcaa	3500

3501 gttacgggga acttcgggta tataatgtaa ataattacag tctaataatt gttcctcaaa ctttacagag gagaatgccc tgtttgttaa ccatgtttct 3600
3601 tttggcagga ggggggtccgc atggaagaaa tagttgaagg ttgtaccgga gcccttcaca tcctagctcg ggatgttcac aaccgaattg ttatcagagg 3700
3701 actaaatacc attccattgt ttgtgcagct gctttattct cccattgaaa acatccaaag agtagctgca ggggtcctct gtgaacttgc tcaggacaag 3800
3801 gaagctgcag aagctattga agctgaggga gccacagctc ctctgacaga gttacttcac tctaggaatg aaggtgtggg taagtaaaaa ggaaccaaag 3900
3901 cctttagcag atgtgtacat tgaagtctca gtttttcctc aagggccttt ttctccttgt ctcttagcga catatgcagc tgctgttttg ttccgaatgt 4000
4001 ctgaggacaa gccacaagat tacaagaaac ggctttcagt tgagctgacc agctctctct tcagaacaga gccaatggct tggaatgagg tagggaaatg 4100
4101 tgagcagtta tttatctggt agtttcctag agcaggtatg gcagcttgtt ctttcctctc aaaacactta gtacacattc atttgcattg atgtttccct 4200
4201 ggcttgagta tttcttcttt atgctgtcta gcaactgctc tgaggaagaa ctataataca agctttaaag agtctgttca gaatcattac aaataagttg 4300
4301 tgttatttaa aattataatt cataagggag aaagatgaaa aatgttacca gattaaagaa gatttttcaa aaggatgtaa ggaaagaggc agtgttaaac 4400
4401 actgttaaga ggacagttta tcagtatttt ttactaaact ttaataaaac ttttctattt gaatttctgc tatgaatttt tcttcagcat ttgtcctcag 4500
4501 tacaggtggt tccttgaaac attgtttcta ataaaactag aacatcctga tattttatcc attctataga gatcattgat ggtacacaga catacagtgg 4600
4601 attatgtttg ttgagtgaat ggaaagagag attgttaggt ttacaacgat gcagctcttg agaccggagt ttaagatcag cctgggcaac atagtgaaac 4700
4701 cccatcttta gctgggcatg gagatggatg cctatagtcc tagctactgg ggagacgggg gcaggaggat tgcttgaacc caggagttaa cagactgcac 4800
4801 tcagtgacag agccagactc caacacaaaa aaaaaaaaaa aaaaaaaact gctgatcttg gacttgatat tggtgcccag ggagaacccc ttggatatcg 4900
4901 ccaggatgga tcctagctat cgttcttttc actctggtgg atatggccag gatgccttgg gtatggaccc catgatggaa catgagatgg gtggccacca 5000
5001 ccctggtgct gactatccag ttgatgggct gccagatctg gggcatgccc aggacctcat ggatgggctg cctccaggtg acagcaatca gctggcctgg 5100
5101 tttgatactg acctgtaaat catcctttag gtaagaagtt ttaaaaagcc agtttgggta aaatactttt actctgccta cagaacttca gaaagacttg 5200
5201 gttggtaggg tgggagtggt ttaggctatt tgtaaatctg ccacaaaaac aggtatatac tttgaaagga gatgtcttgg aacattggaa tgttctcaga 5300
5301 tttctggttg ttatgtgatc atgtgtggaa gttattaact ttaatgtttt ttgccacagc ttttgcaact taatactcaa atgagtaaca tttgctgttt 5400
5401 taaacattaa tagcagcctt tctctcttta tacagctgta ttgtctgaac ttgcattgtg attggcctgt agagttgctg agagggctcg aggggtgggc 5500
5501 tggtatctca gaaagtgcct gacacactaa ccaagctgag tttcctatgg gaacaattga agtaaacttt ttgttctggt ccttttggt cgaggagtaa 5600
5601 caatacaaat ggattttggg agtgactcaa gaagtgaaga atgcacaaga atggatcaca agatggaatt tatcaaaccc tagccttgct tgttaaattt 5700
5701 ttttttttt ttttttaaga atatctgtaa tggtactgac tttgcttgct ttgaagtagc tctttttttt ttttttttt ttttttgca gtaactgttt 5800
5801 tttaagtctc tcgtagtgtt aagttatagt gaatactgct acagcaattt ctaattttta agaattgagt aatggtgtag aacactaatt cataatcact 5900
5901 ctaattaatt gtaatctgaa taaagtgtaa caattgtgta gccttttgt ataaaataga caaatagaaa atggtccaat tagtttcctt tttaatatgc 6000
6001 ttaaaataag caggtggatc tatttcatgt ttttgatcaa aaactatttg ggatatgtat gggtagggta aatcagtaag aggtgttatt tggaaccttg 6100
6101 ttttggacag tttaccagtt gccttttatc ccaaagttgt tgtaacctgc tgtgatacga tgcttcaaga gaaaatgcgg ttataaaaaa tggttcagaa 6200
6201 ttaaacttttt aattcattcg attggaagta ggagtcaaag tgacccttgt ctactgtgat gctgaattca tgactaagag actattggtg aacttatcct 6300
6301 ggctgtgatt acagacgtca agagggagta ttccagcgac actaagaaaa taatgcaaga gaacgccagc gaagagtgcc caggcaacac tgacagacta 6400
6401 gaaaaaaaat atcaggagat gaagctgaca cagtgagagc agcccaggtg cttcttggtg cttgttatta cagacacaca cttcacacag gggaggatta 6500
6501 ttttaattct gtggccttca gatctcataa atacaagtaa aaacaagcag gtaactatga taactttact tcagagagtt taaatttcaa aaataaacct 6600
6601 atccatcca 6609

A9 Standard curve for MethylFlash™ methylated DNA quantification kit (colorimetric)

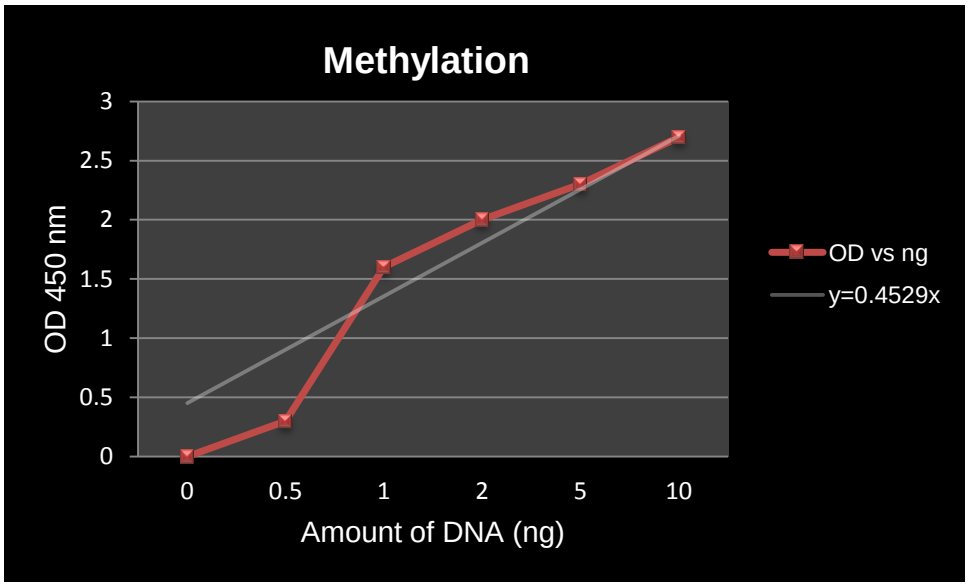


Figure A9.1 Standard curve of OD 450nm values versus the amount of ME4 buffer at each concentration point. The slope of the standard curve was calculated as y= 0.4529x.

The absolute amount and percentage of methylated DNA (5-mC) in total DNA was determined using Equation A9.1 and Equation A9.2:

$$5-mC(ng) = \frac{Sample\ OD - ME3\ OD}{Slope \times 2^{*}}$$

[Equation A9.1]

$$5-mC\ \% = \frac{5-mC \quad Amount\ (ng)}{S} \times 100\%$$

[Equation A9.2]

Where *ME3 OD* is the optical density of the negative control measured at 450nm and *S* is the amount of input sample DNA (100ng).

** 2 is a factor to normalise 5-mC in the positive control to 100%, as the positive control contains only 50% of 5-mC.*

A10 Standard curve for MethylFlash™ hydroxymethylated DNA quantification kit (colorimetric)

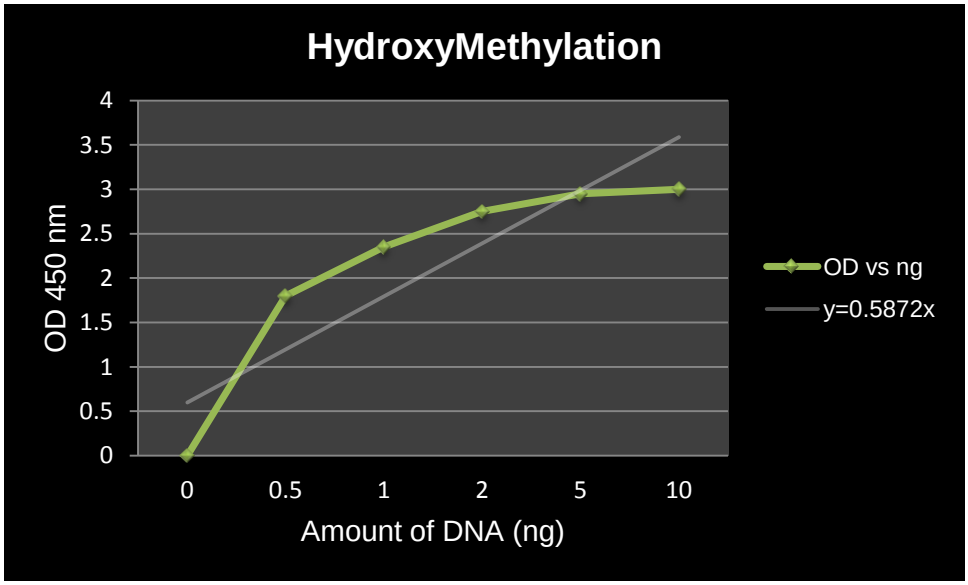


Figure A10.1 Standard curve of OD 450nm values versus the amount of HC5 buffer at each concentration point. The slope of the standard curve was calculated as y= 0.5872x.

The absolute amount and percentage of hydroxymethylated DNA (5-hmC) in total DNA was determined using Equation A10.1 and Equation A10.2:

$$5-hmC(ng) = \frac{Sample\ OD - HC4\ OD}{Slope \times 5^{*}}$$

[Equation A10.1]

$$5-hmC\ \% = \frac{5-hmC \quad Amount\ (ng)}{S} \times 100\%$$

[Equation A10.2]

Where *HC4 OD* is the optical density of the negative control measured at 450nm and *S* is the amount of input sample DNA (200ng).

** 5 is a factor to normalise 5-hmC in the positive control to 100%, as the positive control contains only 20% of 5-hmC.*

A11 Ethics Waiver

University
of the Witwatersrand,
Johannesburg

Human Research Ethics Committee (Medical)
(formerly Committee for Research on Human Subjects (Medical))

Secretariat: Research Office, Room SH10005, 10th floor, Senate House • Telephone: (27 11) 717 1234 • Fax: (27 11) 339 5709
Private Bag 3, Wits 2050, South Africa

Ref. W-CJ-100510-4

10/05/2010

TO WHOM IT MAY CONCERN:

Waiver: This certifies that the following research does not require clearance from the Human Research Ethics Committee (Medical).

Investigators: **Dr C Penny, Ms N Moodley (Student No 0505000H)**

Project title: **The induction of Klf4 by coupled epigenetic therapies; potential association with the Wnt signalling pathway in colorectal cancer cell lines.**

Reason: This is a wholly laboratory study using commercial cell lines - DLD-1, HT29, SW1116, SW480, FHC. There are no humans involved.

UNIVERSITY OF THE WITWATERSRAND
2010 -05- 10
JOHANNESBURG

Professor Peter Cleaton-Jones
Chair: Human Research Ethics Committee (Medical)

copy: Anisa Keshav, Research Office, Senate House, Wits